SPAWAR
Systems Center
San Diego

TECHNICAL REPORT 1885
July 2002

Monitoring of High-Power Microwave Tube Systems Using the Integrated Condition Assessment System (ICAS)

N. R. Joshi
North Harris College and
Prairie View A&M University

A. D. Ramirez
D. W. Brock
S. D. Russell
SSC San Diego

SSC San Diego

TECHNICAL REPORT 1885
July 2002

Monitoring of High-Power Microwave Tube Systems Using the Integrated Condition Assessment System (ICAS)

N. R. Joshi
North Harris College and
Prairie View A&M University

A. D. Ramirez
D. W. Brock
S. D. Russell
SSC San Diego

SSC San Diego
San Diego, CA 92152-5001

SSC SAN DIEGO
San Diego, California 92152-5001

T. V. Flynn, CAPT, USN
Commanding Officer

R. C. Kolb
Executive Director

ADMINISTRATIVE INFORMATION

The work described in this report summarizes research work performed under the Office of Naval Research-American Society for Engineering Education (ONR-ASEE) summer fellowship program and the Office of Naval Research in part under the auspices of Dr. Phillip Abraham (ONR-331) Automated Test Equipment and Metrology Program and in part under the auspices of Dr. Ignacio Perez (ONR-332) Discovery & Innovation program.

Released by
S. D. Russell, Head
Advanced Technology Branch

Under authority of
C. J. Sayre, Head
Electromagnetics
and Advanced
Technology Division

ACKNOWLEDGEMENTS

The lead author would like to thank Timothy Manicom, the senior program manager for the Office of Naval Research-American Society for Engineering Education (ONR-ASEE) summer fellowship program, for the financial support. The authors also thank Dr. Phillip Abraham (ONR-331) and Dr. Ignacio Perez (ONR-332) for financial support and guidance during this program. Special thanks go to Dr. Mark Roberts and Betty Aguilar for their assistance during Dr. Joshi's summer fellowship.

PS

EXECUTIVE SUMMARY

High-power microwave tube systems used on Navy radars and in communication systems are primary cost drivers as can be seen from the $100M spent yearly on replacing malfunctioning high-power microwave tubes in the Fleet. In many cases (estimated at over 25%), perfectly operating tubes are inadvertently replaced because there is insufficient in situ monitoring equipment available to diagnose specific problems within the system. High-power microwave vacuum tubes used in the fleet combat systems are equipped with only a minimum on-line component condition assessment capability with little or no built-in prognostic capability to provide advance warning of a developing failure situation. In the earlier phases of the Microwave Tube Built-In Test (MTBIT) program (1999–2001), a new advanced nondestructive testing technique was demonstrated using acoustic emission (AE) for in-situ monitoring of normal and abnormal performance of high-power radar tubes such as magnetrons, traveling wave tubes (TWTs), and klystrons. This report details the next step in transitioning the laboratory MTBIT system into a system that is compatible with condition-based maintenance systems employing the Integrated Condition Assessment System (ICAS) used by the Fleet. This report identifies the interface requirements for the sensors and ICAS, as well as accommodating limitations of the ICAS software, which currently is not configured to accommodate the sensor data rates and data sets required. Ten new electronic circuits were designed, built, and tested to interface the outputs of the current sensor and acoustic emission sensor attached to a magnetron through an OPTO22 digital and analog input/output (I/O) hardware along with its Optomux protocol and the ICAS software (Version 4.11). The ICAS software, developed by IDAX Inc., is a 32-bit Microsoft Windows NT based data analysis and integration tool currently in use by the Navy for the performance monitoring of mechanical systems on surface ships. The complete computerized system to monitor the in-situ performance of the high-power microwave tube was developed, tested, and reported here. The system could be extended to achieve the same goal with other microwave tubes such as TWTs and klystrons with minor modifications.

CONTENTS

Figures

1. MONITORING OF HIGH-POWER MICROWAVE TUBE SYSTEMS USING THE INTEGRATED CONDITION ASSESSMENT SYSTEM (ICAS)

1.1 INTRODUCTION

High-power microwave tube systems used on Navy radars and in communication systems are primary cost drivers as can be seen from the $100M spent yearly on replacing malfunctioning high-power microwave tubes in the Fleet. In many cases (estimated at over 25%), perfectly operating tubes are inadvertently replaced because there is insufficient in-situ monitoring equipment available to diagnose specific problems within the system. High-power microwave vacuum tubes used in the Fleet combat systems are equipped with only a minimum on-line component condition assessment capability with little or no built-in prognostic capability to provide advance warning of a developing failure situation.

Present microprocessor-based condition-based maintenance systems use as many as 11 sensors to monitor system performance, and could be used to provide tube protection and to record a comprehensive tube failure history. A major limitation with these systems results from the small amount of time available during the tube interpulse period for data buffering and fault analysis. These monitoring systems work well if the microwave tube is operated with 200 or less pulses per second. In typical situations, however, the tubes are operated with up to 1000 pulses per second with pulse duration of a microsecond. Increasing analog-to-digital (A/D) conversion speed will, in some cases, make the situation worse, since it will increase the amount of data that must be transferred and analyzed during the small time interval available. Therefore, there is a need to provide a system that can perform condition-based maintenance on high-power microwave tube systems that can accommodate typical operational conditions.

In the earlier phases of the Microwave Tube Built-In Test (MTBIT) program (1999-2001), a new advanced nondestructive testing technique was demonstrated using acoustic emission (AE) for in-situ monitoring of normal and abnormal performance of high-power radar tubes such as magnetrons, traveling wave tubes (TWTs), and klystrons. This report details the next step in transitioning the laboratory MTBIT system into a system that is compatible with condition-based maintenance systems employing the Integrated Condition Assessment System (ICAS) used by the Fleet.

1.2 ACOUSTIC EMISSION AND ITS SOURCES

Transient elastic stress waves can be generated in a region of a material that experiences abrupt changes in the stress field. This phenomenon is known as acoustic emission (AE). It is generally detected by means of ultrasonic transducers coupled to the material object with a suitable couplant for decreasing impedance mismatch. Among many mechanisms that produce AE activity, the principal ones are crack initiation and growth, magneto-mechanical realignment or growth of magnetic domains (Barkhausen Effect), dislocation movements, twining, phase changes, fracture of brittle inclusions, fiber breakage in composite materials, chemical activity, and cavitation. AE signals cover a wide range of energy levels and frequencies. However, two basic types of signals are often observed-burst and continuous. Some stimulus is necessary to trigger acoustic emissions. Stress, a major type of stimuli, may be mechanically applied, thermally generated, or caused by changing magnetic field. These observations raised a question in connection with microwave radar tubes operating under normal conditions. Would they be able to generate AE signals? If they could not

generate AE signals, then we cannot use the technique. However, if they generate AE activity, what could be the mechanism?

A literature survey led us to two research papers on the topics indirectly related to the subject of our research. Sakoda and Nieda (reference 1) measured the characteristics of AE signals generated due to a single pulse corona discharge as a diagnostic tool to estimate insulation deterioration in oil immersed pole transformers. Tomasz Boczar (references 2 and 3) used frequency analysis of AE signals generated by partial discharges in order to distinguish them from AE signals generated by corona discharges. Theobald et al. (reference 4) pointed out the difference between the AE event energy (AE_{energy}) and the AE energy descriptor (E_{AE}). Generally, AE stress waves disperse throughout the medium until an interaction with an interface or boundary leading to the production of reverberating field. Although this energy will be mostly absorbed by the medium, some of the energy can be detected by the use of a high frequency piezoelectric ceramic transducer. Assuming all mechanisms of energy loss in the structure and measurement system are constant, then the measured electrical signal energy from the transducer could be said to be proportional to the AE event energy,

$$AE_{energy} \propto \int_0^t v(t)^2 \, dt \tag{1}$$

where AE_{energy} is the AE event energy, t is the time length of transient signal produced, and V(t) is the transient voltage. It is often referred to as the AE energy descriptor and written as

$$E_{AE} \propto (1/R) \int_0^t v(t)^2 \, dt \tag{2}$$

where E_{AE} refers to the AE energy measured in the transducer and R is the impedance of the complete measuring circuit. The power of the acoustic emission signal of detected event is thus proportional to the power of the source event.

However, we still did not know whether high-power microwave radar tubes would produce the AE signals during normal operation. It was clear, though, that AE signal may arise if arcing takes place inside the microwave tube similar to the AE activity observed in corona discharges and partial discharges. In the earlier stages of the MTBIT project, we evaluated the suitability of numerous sensors and techniques for the performance monitoring of the high-power microwave radar tubes. We decided, therefore, to also try the AE technique that is non-invasive in nature and needed simple equipment for preliminary evaluation.

1.3 AE TECHNIQUE APPLIED TO MICROWAVE TUBES

1.3.1 Application to a Pulsed Magnetron

In 1999, the AE technique was applied to the performance monitoring of a high-power pulsed magnetron radar tube. The single channel acoustic emission system coupled with the fast digital oscilloscope was used to monitor acoustic emission signal spectra from the magnetron operating under normal and abnormal conditions. The details of the experimental setup can be found in Space and Naval Warfare Systems Center, San Diego (SSC San Diego) Technical Note 1810 published in

August 2000.[1] Four different AE transducers, two narrow band and two broad band, were coupled in turn to the cylindrical anode of the magnetron having internal resonating cavities to pick up acoustic emission signals generated by the pulsing RF output of the tube. The microwave frequency generated was about 9.650 GHz. The input pulsed power typically was 240 kilowatt and output power 50 kilowatt. The pulse rate was varied from 100 pps to 1000 pps with pulse width of 1μs. The tube generated acoustic emission activity correlated with every RF pulse. The exact mechanism behind the conversion of RF energy into acoustic energy is not understood at present. However, some rapid heating and cooling process of the magnetron walls may be the cause of the AE activity or RF coupling to the waveguide producing an electron-phonon coupling resulting in the AE signature. The next step was to stress the magnetron by creating abnormal operating conditions and see the effect on the corresponding AE activity. Figure 1 shows the AE activity associated with normal functioning of the magnetron at the low pulse rate of 100 pps. The normal pulse voltage was 15 kV. Channel 3 (denoted by Ch3 in the figure) shows the AE signal. The channel B (denoted by ChB) shows the zoomed display of the current pulse set inside the mask of channel D (ChD). The channel A (ChA) shows the magnitude fast Fourier transform (FFT) of the AE signal from Ch3. The vertical sensitivity on Ch3 was chosen to be 0.1V/div. Figure 2 shows the decreased amplitude of AE signal on Ch3 as the result of the bad current pulse (ChB) produced due to the increased pulse voltage about 5 volts above the normal value. The decreased AE activity was observed as the result of the production of the abnormal current pulses when the magnetron was stressed by deviating the parameters like the oscillator filament voltage, the high voltage pulse rate, the VSWR values, and the high pulse voltage from their normal operating values. It was thus pointed out that the nondestructive technique of acoustic emission can be used to monitor the performance of the high-power microwave radar tubes like the magnetron.

1.3.2 Application to the Pulsed Traveling Wave Tube

In 2000, the AE technique was extended to the performance monitoring of a pulsed traveling wave tube (TWT). The TWT-amplifier (TWT-A) unit when operated in continuous wave (CW) mode did not produce any AE activity. When it was operated in pulsed mode, the AE signals were generated in step with the pulsed RF input power. Figure 3 shows the AE signal (Ch3) produced at the end of "RF ON" interval (on the second vertical division from the left end) and again at the end of "RF OFF" interval (on the ninth vertical division). Ch2 shows the detected RF (inverted) signal. The horizontal time scale chosen was 0.1s per division. Figure 4 shows the same plot with horizontal scale expanded to 0.5 ms per division. Here we see the expanded AE signal starting at the second vertical division from the left on the Ch3 masked by the zoom trace D. It was observed that during the CW mode of operation, whenever there was change (increase or decrease) in the RF input power, the AE activity was generated. In short, the changes in the RF output power either due to irregular changes or due to regular changes in the RF input power caused AE signals to appear. The information on the details of the experimental setup are available in SSC San Diego Technical Note 1816 published in September 2001.[1]

1.3.3 Application to the AN/SPS-49 Pulsed Klystron

The acoustic emission technique was then evaluated on a klystron associated with the transmitter of an AN/SPS-49 long-range radar. Figure 5 shows the AE activity on the zoom trace A of the

---

[1] Space and Naval Warfare Systems Center, San Diego (SSC San Diego) Technical Notes (TNs) are working documents and do not represent an official policy statement of SSC San Diego. For further information, contact the author.

oscilloscope in step with the beam current sensor signal (Ch2) having two pairs of pulses and with the RF drive signal (Ch1) having two pair of pulses. The acoustic emission transducer was located on the waveguide terminated with dummy load. Similar data were obtained by shifting the location of the AE transducer to different locations on the waveguide. The 5-cavity klystron amplifier unit was operated at a frequency of 942 MHz. The details of the klystron tube and the experimental arrangement are also available in SSC San Diego Technical Note 1816.

1.3.4 Repeated Experiments on the AN/SPS-49 Pulsed Klystron

Figure 6 shows AE activity (ChC) in step with the klystron current pulses (ChB). Three pair of pulses are seen in Figure 6. The acoustic emission transducer was located on the waveguide. The RF frequency used was 902.999 MHz. Similar data was obtained by shifting the AE transducer to different locations on the waveguide. Next a threshold amplifier circuit coupled with appropriate filter was used to catch a bad current pulse during the abnormal operation of the klystron unit. The normal operating high voltage was 40 kV. It was increased gradually beyond 40 kV. The current showed slight increase beyond 1A when a pulse was recorded on Ch4 (Figure 7) connected to the output of the threshold amplifier.

1.3.5 Integrated Condition Assessment System (ICAS)

The next step to transition the non-destructive performance monitoring technology was to identify Navy systems with which we could integrate the laboratory test set-up. The Navy is currently using ICAS version 4.11 (from IDAX Inc. of Norfolk, VA) for the performance monitoring of mechanical pumps on surface ships. The Integrated Condition Assessment System (ICAS) is a 32-bit Microsoft Windows NT based plant data analysis and integration tool. It is the predictive maintenance program that combines state-of-the-art performance monitoring techniques with computerized maintenance management. The system provides user-defined performance alarms that alert the operator to machine problems. It provides Hybrid Diagnostic System (HDS) diagnostic advisories that assist in diagnosing approaching failures and initiating the restoring process. The Hybrid Intelligent System is a fault-modeling environment that comprises both crisp logic and fuzzy logic rules. The ICAS software consists of five basic components:

1. ICAS Shell – the main shell provides the primary user interface;
2. Analysis Engine – the engine monitors sensor data and performs HDS evaluation;
3. Router – the router distributes data between ICAS applications and workstation;
4. CDS – the Configuration Data Set (CDS) contains site-specific configuration data; and
5. Databases – the databases contain files where recorded data is stored for subsequent retrieval and analysis.

Therefore, ICAS was selected to read and analyze the acoustic emission and current signals from the normal and abnormal functioning of the high-power microwave radar tubes.

1.3.6 Sensors

ICAS uses both on-line sensor data and data collected manually from off-line sensors to perform its analysis. It can be connected to a variety of physical sensors and calculated or pseudo-sensors. Measured and calculated sensor data is used to monitor performance limits, to trigger alarms, or to record trend information. For low-speed data acquisition environment, the sensors could be interfaced with the ICAS workstation using a standard Data Acquisition Unit (DAU). The DAU

provides power supply, signal conditioning, A/D signal conversion, signal multiplexing, and data transmission to the host computer. ICAS supports a multiple of low-speed DAU's with direct interface. The maximum sampling frequency for these units is 1 Hz.

1.3.7 The Host Computer System

The host computer used in this project has a Pentium II, 450 MHz CPU although the recommended minimum required for ICAS is 133 MHz Pentium processor. It carried 2.4 GB hard drive storage capacity, and 132 MB of RAM. Microsoft Windows NT Workstation 4.0 was installed as the OS. The ICAS software took about 146 MB of the hard drive memory.

1.4 DATA ACQUISITION UNIT

An intermediate unit that will take raw data from the current and AE sensors monitoring the microwave tube performance and transfer it to the ICAS software installed on the host computer was needed. Since the Navy was using an OPTO22 Interface to get data from mechanical pumps, we decided to use the same unit. Unfortunately, the OPTO22 hardware previously used was no longer available or supported, so a new interface unit, called OPTO22 SNAP B3000 BRAIN was selected. The B3000 unit can be used with either an OPTO22 controller or a host computer. We decided to use it with the host computer to facilitate the interface with ICAS. The B3000 communicates with a host computer serially over RS485 twisted pair wiring. It supports the advanced Mistic protocol and the industry-standard Optomux protocol. We decided to use the second, the Optomux protocol. Both protocols support high-speed communication (115 kBaud).

The AC37 adapter card is installed in one of the ISA slots inside the computer to facilitate a RS-485 two or four wire communications link between the computer and the OPTO22 remote I/O bus. The remote bus is a standard RS-485 half-duplex (2 wire) serial communications link. The AC37 is designed to appear as a standard IBM serial "COM" port to user software. The AC37 has two operating modes, the Mode 0 and Mode 1. While in mode 0, the AC37 will operate very much like a standard serial COM port. Mode 0 is selected by removing the OPTO jumper on the card. Figure 8 shows the schematic arrangement of the B3000 Optomux System Architecture.

The OPTO22 SNAP B3000 brain is connected to a SNAP B series I/O rack capable of holding eight SNAP modules as shown in Figure 9a. The actual photograph of the equipment is shown in Figure 9b. In this work, only one analog voltage (-10 VDC to +10 VDC) input SNAP-AIV module (2 Channels) was used in the position "Module0" next to the B3000 Brain. The analog input module is transformer isolated as well as optically isolated from all other modules and from the SNAP brain. Transformer isolation prevents ground loop currents from flowing between field devices and causing noise that produces erroneous readings. Optical isolation provides 4000 volts of transient protection for sensitive control electronics from real-world industrial field signals. However the two channels of the analog input module use a common reference and are not isolated from each other. The SNAP analog input module has an on-board microprocessor to provide module-level intelligence.

The SNAP-PS5 power supplies takes 120 VAC input from the power line and it can provide 5 VDC power for loads up to 4 amps. It was used to power B3000 brain and SNAP I/O module through the connector strip mounted on the rack. The power supply module is normally positioned near the rack for operational testing.

The connectors and jumpers were selected from the top of the B3000 brain to adjust the baud rate of 19.2 kBaud, Optomux communication protocol, and the analog address 02. Each rack has an

address like 0, 1, 2, etc. Since we are using one rack, its address is 0 (zero). I/O on B3000 is divided into four addresses of I/O (two digital I/O and two analog I/O). The digital addresses are base+0 and base+1. The analog addresses are base+2 and base+3. So, the analog module snapped onto the rack has the total address of 0+2. The B3000 brain is connected to the Adapter card inside the computer.

Optomux is a protocol used by a family of intelligent digital and analog I/O (input/output) units that operate as slave devices to a host computer. The Optomux can communicate at eight different baud rates but we selected 19.2 kBaud because it was recommended for ICAS. In order to read data from the computer, the software Optoscan (OptoDriver Toolkit) is provided. One needs to enter the baud rate (19.2 kBaud), COM port (3), and the address (02) to see the table showing the voltage values (between 0 and 10 volts DC) from the two channels of the analog input module. The voltage values between 0 and 10 volts DC are the values of the two outputs of the electronic circuits interposed between the sensor signals (from the current sensor and the AE sensor) and the analog input module on the rack. ICAS software provided by IDAX is different from Optoscan (OptoDriver Toolkit) software provided by OPTO22.

1.5 INTERFACE CIRCUITS

1.5.1 Faulty Current Pulses

The aim of the experiment was to distinguish bad current pulses from the good or normal current pulses and the corresponding weak AE signals from the strong AE signals during the operation of the high-power microwave radar tubes. A 5 volt TTL-compatible output pulse needs to be generated corresponding to a bad current pulse, while no output is provided for the good current pulses. Figure 10 indicates the block diagram of the electronic circuits that could achieve this aim. The circuits are identified with the numbers included in square parenthesis [1C] to [5C] where the suffix "C" stands for "Current." Figures 11a and 11b show the current sensor. The microwave pulse input to the Magnetron Amplifier comes from P25 Pulse Generator (Interstate Electronic Corporation, USA). The pulse generator is triggered in this work with the help of Trigger box (Figure 11c). Current pulses are generated at the rate of 60 pulses per second, synchronized to the power line.

It was found that good cathode current pulses from the magnetron have very little spectral content above about 8 MHz in frequency while bad pulses have much greater content above 8 MHz. Thus, the 8 Mz high pass filter (Figure 12) may produce a much greater output for bad pulses relative to that for good pulses. The signal is then filtered by 15 MHz low pass filter (Figure 13) that cleans up the spectral content of the pulses and smoothes the pulses. As a result, the output of the 15 MHz filter is relatively small for good pulses and much larger for bad pulses. The threshold amplifier has a comparator (Figure 14) with an adjustable threshold that can be set so that it will not respond to good pulses but will generate a 5 volts TTL-compatible output pulse when a bad current pulse occurs.

Next, methods were needed to count faulty current pulse signals from the threshold amplifier. Two methods were designed, fabricated, and tested to count faulty pulse signals from the threshold amplifier. A digital method was developed for use when reset pulses were available, and an analog method was developed for use in the absence of reset pulses. These two counting methods are represented in the circuit diagram "Defective Current Pulse Counter," (Figure 15) with the upper part of the drawing showing the digital section and the lower part of the drawing showing the analog section. The digital method used two TTL count-by-ten circuits, giving the counter the ability to count up to 100 pulses between reset pulses. The output of the TTL counters was fed into a digital-to-

analog converter, since the ICAS system is set up to use only analog inputs. After each reset pulse the TTL counters would begin counting pulses again from zero.

The analog pulse counter circuit is shown in the lower part of the diagram. One problem with counting pulses from the threshold amplifier is that the lengths of the pulses vary from 1 to 3 microseconds. This problem was solved by sending the input pulses to the base of a high gain, high current transistor Q1. The transistor fully charges a 1 microfarad capacitor, C2, connected to its emitter in less that 1 microsecond, so that if the pulses are longer that 1 microsecond, there will be no effect on the charge on the capacitor. The capacitor then discharges through resistors R3 and R4 over a time of approximately 1 millisecond. During this discharge period, most of the current passes through the 1-kiloohm resistor, R4, and diode, D1, into a second 1-microfarad capacitor, C3. This capacitor serves as a charge accumulator and analog counter of the number of faulty pulses. The counter capacitor is connected to a high input impedance JFET input operational amplifier that measures and amplifies its voltage while not discharging the capacitor. A method must be provided to discharge capacitor C3. Without a discharge, the voltage on capacitor C3 would quickly reach a maximum value and it would stop accumulating charge and stop counting. The discharge method used is to continuously discharge the capacitor through a 1-megohm resistor, R5, which results in a 1-second time constant for the discharge time. This results in an exponentially decaying signal, which may not be suitable for some applications.

1.5.2 Faulty Acoustic Emission Pulses

Figure 16 indicates the block diagram of the electronic circuits for faulty acoustic emission pulses similar to the one of Figure 10 for faulty current pulses. The circuits are identified with the numbers [1A] to [9A] where the suffix "A" stands for "Acoustic." The AE signal generated during the operation of the pulsed Magnetron was picked up by the AE transducer. It was experientially determined, in the case of the magnetron, that the total pulse energy of faulty pulses was significantly less than that of good pulses. The total energy of acoustic pulses coming from the acoustic energy amplifier was determined by passing the output of the post-amplifier (Figure 17) into an acoustic energy integrator (Figure 18), which rectified the acoustic signal, then used the rectified output to charge a capacitor. The output of the capacitor was then sent through a 10 KHz low pass filter (Figure 19) to clean up the output pulses. The output from the low pass filter was then sent into a circuit containing a time delay, amplifier, and sample-and-hold (Figure 20). The amplifier, U3, increased the voltage of the pulses by a factor of 33. The time delay, generated by U1, allowed the acoustic pulse integrator time to fully integrate the energy of the acoustic pulses. Its delay time could be adjusted from 0 to 3 milliseconds, and would typically be set for about 1 millisecond. At the end of the delay period, U2 would send a 100-microsecond pulse to sample-and-hold U4, which would sample the output from amplifier U3. Also, shown in the diagram is a 50-ohm output driver circuit, which amplified the output of U4. The output of the circuit was then sent through a second 10 KHz low pass filter (Figure 21), which removed unwanted voltage spikes from its output.

Next, methods were needed to count faulty acoustic pulse signals and two methods were developed. A digital method was developed for usage when reset pulses were available, and an analog method was developed for usage in the absence of reset pulses. These two counting methods are represented in the circuit diagram "Defective Acoustic Pulse Counter" (Figure 22), with the upper part of the drawing showing the digital section and the lower part of the drawing showing the analog section. The digital method used two TTL count-by-ten circuits, giving the counter the ability to count up to 100 pulses between reset pulses. The output of the TTL counters was fed into a digital-to-analog converter, since the ICAS system is set up to use only analog inputs. After each reset pulse, the TTL counters would begin counting pulses again from zero.

The analog pulse counter circuit is shown in the lower part of the diagram. The input from the faulty pulse detector circuit is fed through capacitor C1. The input voltage is always positive; however, when faulty pulses occur, the positive voltage is reduced. The amount of voltage reduction varies from one faulty pulse to the next, so that the circuit has to compensate for these variations. Capacitor C1 introduces DC blockage, so that the inverting input of operational amplifier U1 will receive negative input pulses when a faulty pulse occurs. Potentiometer R3 provides an adjustable positive bias on the inverting input of U1. During good pulses, the output of U1 will be negative. Diode D1 limits this voltage to negative 0.15 volts. When a faulty pulse occurs, the negative voltage from C1 will overcome the positive bias from R3, at the inverting input of U1, so that the output of U1 will become positive. The gain of U1 is adjusted so that every faulty pulse will drive its output to the maximum positive limiting value. Some of the output current of U1 will flow through 1-megohm resistor R7 and diode D2 into 1-microfarad capacitor, C2. This capacitor serves as a charge accumulator and analog counter of the number of faulty pulses. The counter capacitor is connected to a high input impedance JFET input operational amplifier, U2, which measures and amplifies its voltage while not discharging the capacitor. A method must be provided to discharge capacitor C2. Without a discharge, the voltage on capacitor C2 would quickly reach a maximum value and it would stop accumulating charge and stop counting. The discharge method used is to continuously discharge the capacitor through a 1-megohm resistor, R8, which results in a 1-second time constant for the discharge time. This results in an exponentially decaying signal, which may not be suitable for some applications.

1.5.3 OPTO22 and ICAS Interface Circuit

For our application, ICAS has limitations in that it checks data only once every second and there is no reset pulse available. Therefore, it was necessary to develop a circuit with timer, sample-and-hold, and amplifier to provide once-per-second data sampling from the faulty current and acoustic pulse counters, and provide reset pulses for the counters. The circuit called "One-Second Data Sample and Reset" is shown in Figure 23. This corresponds to block [9A] of the Figure 16 common to both current and acoustic data. This serves as the OPTO22 interface circuit. The timer consists of four LM555 timer integrated circuits. The first timer, U1, provides a 1-second period of time for counting the pulses. Its time period is adjustable with a 1-megohm potentiometer. The second timer, U2, provides a 100-microsecond output pulse, which is fed to the inputs of two sample-and-hold circuits, U5 and U6. The U5 samples-and-holds the output of the faulty current pulse counter, while the U6 samples-and-holds the output of the faulty acoustic pulse counter. Timer U3 provides a waiting period of 25 microseconds to ensure that U5 and U6 have passed beyond their aperture times before resetting the counters. This is to prevent a change on the input voltages from affecting the output voltages. Timer U4 next provides a 25-microsecond voltage pulse to the reset inputs of the faulty current and acoustic pulse counters. Timer U1 then resumes the counts of faulty current and acoustic pulses. The outputs of the U5 and the U6 are fed to the amplifiers U7 and U8, respectively. The outputs of the amplifiers U7 and U8 are fed to the OPTO22 Analog Input Module on the rack.

1.5.4 OPTO22 Software and ICAS Software

The OptoDriver Toolkit of the OPTO22 equipment can be used for direct communication from the host computer to the B3000 Brain. The toolkit is included with the 32-bit Windows driver. Within the OPTOSCAN (for 32-bit Windows Version A4.0b) window, one can see the values of the two sensor outputs (current and acoustic emission) listed in the table of sensors. However, this software is extremely limited and was not used in this work.

Figure 24 shows the Sensor Editor Window of the ICAS software. The Sensor Editor translates the raw data from an external source into an ICAS sensor value. This process allows ICAS to merge a variety of input types into a single, homogeneous "virtual" type. When ICAS receives inputs and converts them to virtual data, all sensors values are alike, regardless of where they originate. Since all sensor values have a common unit once inside ICAS, operations between dissimilar devices are possible. The sensor definition elements describe the properties associated with a sensor, all of which can be edited using the Sensor Editor. These properties include data acquision source, display units, background scan rate, sensor value calibration, and many others. The sensor definition window is also shown in Figure 24.

1.6 EXPERIMENTAL PROCEDURE

Testing OPTO22 Hardware, OPTODriver Toolkit and ICAS Software

Testing was performed using the various softwares and the OPTO22 Analog Module installed on the rack next to the OPTO B3000 Brain, which in turn was connected to the AC37 Adapter card installed in the PC. Two DC voltages were fed into the two inputs of the Analog Module from two separate HP6216A Power Supply units to simulate sensor input. All units were turned on, and the software accurately acquired the simulated sensor voltages.

1.6.1 Testing of Electronic Circuits

Testing was performed to ensure functionality of the various electronic circuits before connecting them in chains as shown in Figures 10 and 16. The inputs and outputs of the chosen circuits were connected to the various channels of the LeCroy 9354AM 500 MHz Digital oscilloscope. The oscilloscope has four regular channels (Ch1, Ch2, Ch3, and Ch4) and four zoom channels (A, B, C, and D). The sampling rate is 2 Gs/s (1 million points) if one channel is used and 500 Ms/s (250 kilosamples) if four channels are used. The pulsed magnetron was turned on. The AE transducer (S9208-Physical Acoustics) was coupled to the magnetron cylinder with a couplant and then held in position with a thick aluminum block as shown in Figure 17. The AE signal picked up by the transducer during the pulsed operation of the magnetron was fed to the preamplifier of high input impedance and 50 ohm output impedance. The useful frequency range of the preamplifier was 100 KHz to 1 MHz. The signal was amplified by the post-amplifier (input and out impedance 50 ohm) and then fed to the circuit of the acoustic energy integrator (Figure 18). It was observed from the research work of the past 2 years that it takes a really bad worn-out high-power microwave radar tube (magnetron, TWT, or klystron) to generate defective (faulty) current pulses. However, these tubes may generate defective current pulses at startup before they stabilize. In the present research work, the procedure of restarting the magnetron was used to generate the defective current pulses. The faulty current pulses and the corresponding faulty acoustic emission pulses were displayed by the oscilloscope along with related outputs from the other electronic circuits. The results of the research work include the oscilloscope displays showing the various signals. A total of 63 oscilloscope screen displays were saved on discs and were later printed out for further analysis. The selected ones are listed below in order to highlight the performance of the various electronic circuits and finally the performance of the whole system. The remaining data is included in the Appendix.

1.7 EXPERIMENTAL RESULTS

All of the 63 oscilloscope screen displays were identified with numbers like Data No.1, 2, etc., on the top left hand corner of the display. The numbers next to them like D000, D001, D002, etc., were

file numbers on the discs. They repeat with the use of a new disc and hence can be ignored. The selected displays are used here to discuss the experimental results. The rest are included in the Appendix.

DATA NO.1

The output of the acoustic energy integrator, after taking it through the 10 kHz low pass filter, was connected to Ch3 and to the input of the Time Delay Amplifier and the Sample-and-Hold circuit [6A]. The output of the same circuit was connected to Ch4. Defective current pulses were generated by triggering and retriggering the pulsed magnetron. Ch3 recorded one defective acoustic energy pulse on the second vertical division and the corresponding TTL output is shown on the Ch4. See Figure 25.

DATA NO.8

The screen display shows simultaneously the defective current pulse (Ch2), the defective acoustic energy pulse (Ch3), and the TTL output pulse from the output of the second 10 kHz low-pass filter [7A]. All three arrived at the same showing the satisfactory performance of the electronic circuits. See Figure 26.

DATA NO.12

The purpose of this data set was to check the two counter circuits [5C] and [8A], the outputs of which were connected to Ch3 and Ch4. The three signals from Ch2, Ch3, and Ch4 appeared on the second vertical division coinciding in time. The three circuits [4C], [5C], and [8A] performed as expected, as shown in Figure 27.

DATA NO.13

This data clearly shows a defective current pulse (Ch2) from the Threshold Amplifier, Comparator Circuit [4C] and the corresponding output (Ch3) from the defective current pulse counter [5C]. Note that no count from the output of the defective acoustic pulse counter [8A] was recorded on the Ch4. See Figure 28.

DATA NO.14

This data shows three characteristic signals, a defective current pulse (Ch2) from the Threshold Amplifier, Comparator Circuit [4C], the corresponding output (Ch3) from the defective current pulse counter [5C], and output of the defective acoustic pulse counter [8A] was recorded on the Ch4 appearing at the same time noted by the second vertical division. See Figure 29.

DATA NO.18

Here Ch2 and Ch3 were connected to the input and output of the defective current pulse counter [5C] and Ch4 to the defective acoustic pulse counter [8A]. All three outputs coincide indicating good performance of the electronic circuits involved. See Figure 30.

DATA NO.26

This data set demonstrates the functioning of the reset pulses. The reset pulses are separated by 1s. The output of the defective acoustic pulse counter [8A] is connected to Ch2. The output of the defective current pulse counter [5C] is connected to Ch4. The reset for both counters is the same. The Ch3 was connected to Reset from 1-second data sample and reset circuit [9A]. The Ch3 shows two reset pulses separated by 1s. Both counters showed their output counts in step

with the reset pulses as expected. The cursor is present close to the 6^{th} vertical division on all three channels. See Figure 31.

DATA NO.28

This oscilloscope display is similar to that of Data No.26. It shows again the counting of defective pulses between the two reset pulses. See Figure 32.

DATA NO.33

This data set demonstrates the functioning of the circuit 1-second data sample and reset [9A]. The maximum output of the circuit for each of the two defective pulse counts is 10 volts, which is the limit to the DC voltage that the Analog Module [10] can take in. The reset is adjusted to repeat after 99 pulses (99 pulses X 0.1 volt/pulse = 9.99 volts). First, we checked the functioning with respect to defective current pulses. The output of the defective current pulse counter [5C] was connected to Ch4 and to the input of the 1-second data sample and reset circuit [9A]. It therefore shows the counts in the form of increasing step. The output of the 1-second data sample and reset circuit [9A] is connected to Ch2. The reset pulses are present on Ch3. The cursor appears on three channels between the 5^{th} and 6^{th} vertical divisions. Next, the cursor was moved to the right in order to effect the data transfer. The result of the data transfer is shown in the next display. See Figure 33.

DATA NO.34

Here the signal value on Ch4 is changed to 31 mV from 609 mV (Data No.33) and the similar transfer occurred on Ch2 from 31 mV (Data No.33) to 625 mV. As before, Ch3 shows the two reset pulses. See Figure 34.

DATA NO.41

The data display is similar to that of Data No.33 but it is now obtained for defective acoustic pulse count and corresponding DC voltage output before transfer. See Figure 35.

DATA NO.42

This data set shows the cursor is moved to the right (with respect to data set No.41) to execute the data transfer. See Figure 36.

DATA NO.56

After verifying the functioning of the 1-second data sample and reset circuit [9A] for both defective current pulses and also separately for defective acoustic pulses, we also examined operation of the circuit for simultaneous current and acoustic inputs and studied the outputs with successive data transfers. Two inputs to the circuit [9A] were connected to Ch1 and Ch3. The outputs were connected to Ch2 and Ch4. Using the special feature of the LeCroy oscilloscope, two cursors were set on each of the four channels in order to see the sequence of the data transfer to the next circuit of OPTO22 Analog Input Module [10] in the chain. See Figure 37.

DATA NO.57

The first data transfer was executed when the cursors were moved to the right (with respect to data set 56). See Figure 38.

DATA NO.58

The second data transfer was executed when the cursors were moved to the right (with respect to data set 57). The signal values corresponding to the cursors are printed below each of the Data displays 56, 57, and 58. See Figure 39.

1.8 CONCLUSIONS

Between 1999 and 2000, we demonstrated experimentally that the advanced acoustic emission technique can be used as a nondestructive testing method for in-situ performance monitoring of high-power microwave radar tubes like a pulsed magnetron, a pulsed TWT, and a pulsed klystron. It was shown that the changes in the amplitude and frequency contents of current pulses of the operating microwave tubes were accompanied by the changes in the acoustic emission pulse energy. The next step was to interface the outputs of the current sensor and acoustic emission sensor with the computer installed with ICAS (Integrated Condition Assessment System) currently used by the U.S. Navy. The interfacing was completed using the hardware of OPTO22 intelligent digital and analog I/O (input and output) units. The OPTO22 Analog Input Module can take 0 to 10 volts for its two inputs. The challenge was to develop the electronic circuitry to convert the outputs of the current and acoustic emission sensors into DC voltages compatible with the inputs of the OPTO22 Analog Input Module. This task was successfully completed as circuits were designed, fabricated, and tested at each successive stage. Finally, the sensors, interface circuits, OPTO22 modules, and ICAS were integrated and used to detect defective AE and current pulses from a "stressed" magnetron. The converted outputs from these sensors were finally received in the Sensor Editor Window of the ICAS software on the computer. In short, the total functioning of the high-power microwave monitoring system of sensors, Acoustic Emission Equipment, OPTO22 B3000 Intelligent Processor, and ICAS was demonstrated.

1.9 RECOMMENDATIONS FOR FUTURE RESEARCH

ICAS monitors equipment performance and identifies equipment failure by comparing the sensor data to established engineering performance criteria. If a machine's actual performance (as compared to its design performance) violates a designated limit, an alarm is activated. In order to utilize this ability of ICAS to monitor performance of high-power microwave tubes, data generated at specific intervals of time must be stored in ICAS database, and trend analysis performed. The task of storing the data, comparing the data, displaying the trend indicator graphs, and setting alarm activation guidelines is the next step in the development of a prognostic system for microwave tube condition-based maintenance.

Since ICAS has the ability to take data inputs from multiple sensors, it is recommended to use a multi-sensor multi-channel acoustic emission system in place of the present single sensor system. ICAS has the ability to use calculated or pseudo-sensors in addition to the physical sensors. This ability can be exploited to generate virtual sensor outputs obtained by performing appropriate mathematical operations on the real data from physical sensors.

REFERENCES

1. Sakoda, T. and H. Nieda. 2001. "Characteristic of Elastic Waves Caused by Corona Discharges in an Oil-immersed Pole Transformer," *IEEE Transactions on Dielectrics and Electrical Insulation*, vol. 8, no.2.

2. Boczar, Tomasz. 2001. "Frequency Analysis of Disturbing Signals Generated by Corona Discharges in Overhead Power Lines," Inter-Noise 2001, sponsored by Acoustical Society of The Netherlands (NAG) and the Bond voor Materialenkennis, in cooperation with I-INCE, the International Institute of Noise Control Engineering, The Hague, Holland, Session C7-1, Paper number 66, August.

3. Boczar, Tomasz. 1999. "Identification of Fundamental Forms of Partial Discharges based on the Results of Frequency Analysis of their Acoustic Emission," *Journal of Acoustic Emission*, vol. 17, no. 3-4, pp. S7-S12. July-December, Los Angeles, USA.

4. Theobald, P. et al. 2001. "Reference Source for the Calibration of Acoustic Emission Measurement," *IEEE Instrumentation and Measurement Technology Conference*, pp. 412–416, 21–23 May, Budapest, Hungary.

FIGURES

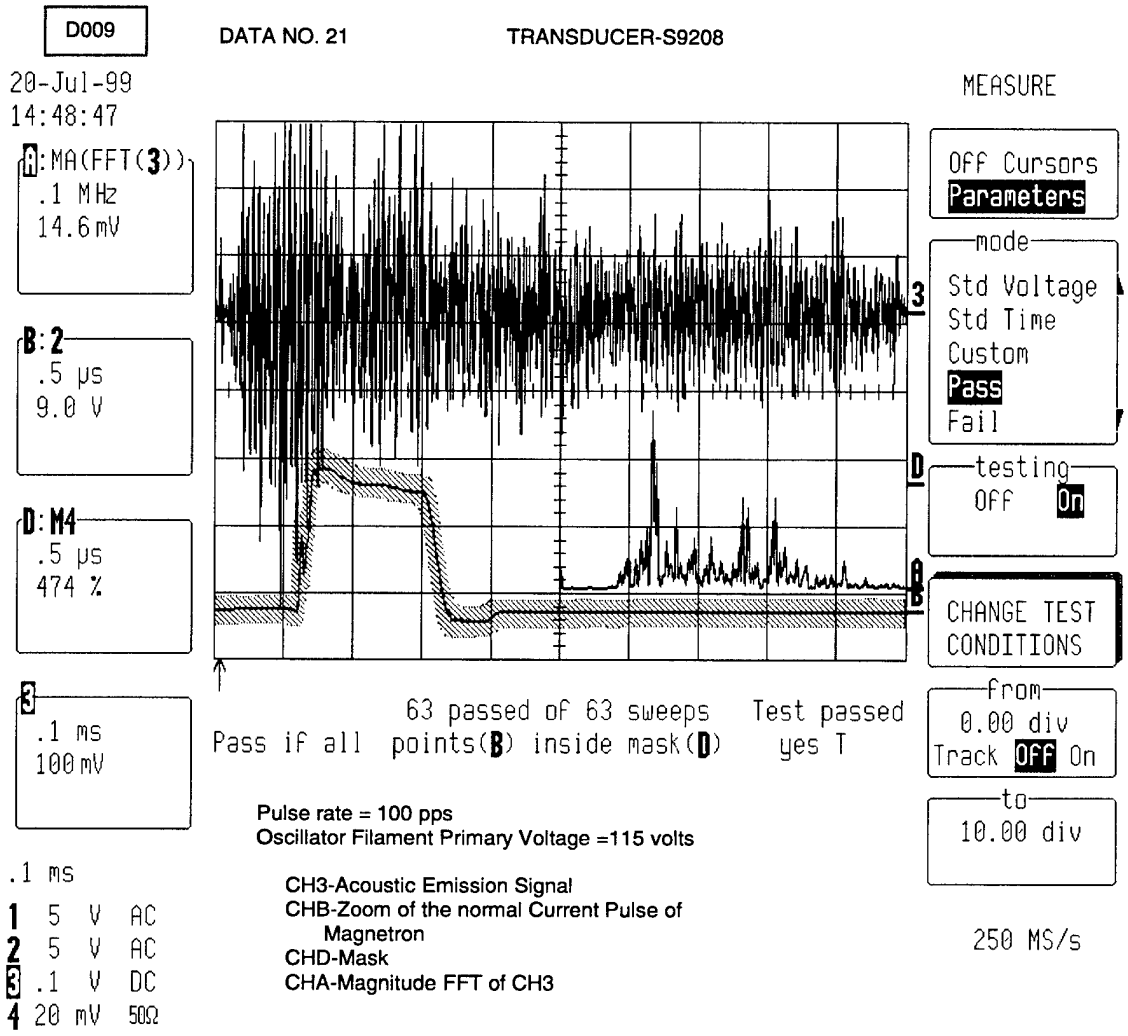

Pulse rate = 100 pps
Oscillator Filament Primary Voltage =115 volts

CH3-Acoustic Emission Signal
CHB-Zoom of the normal Current Pulse of Magnetron
CHD-Mask
CHA-Magnitude FFT of CH3

Figure 1. Normal operation of magnetron.

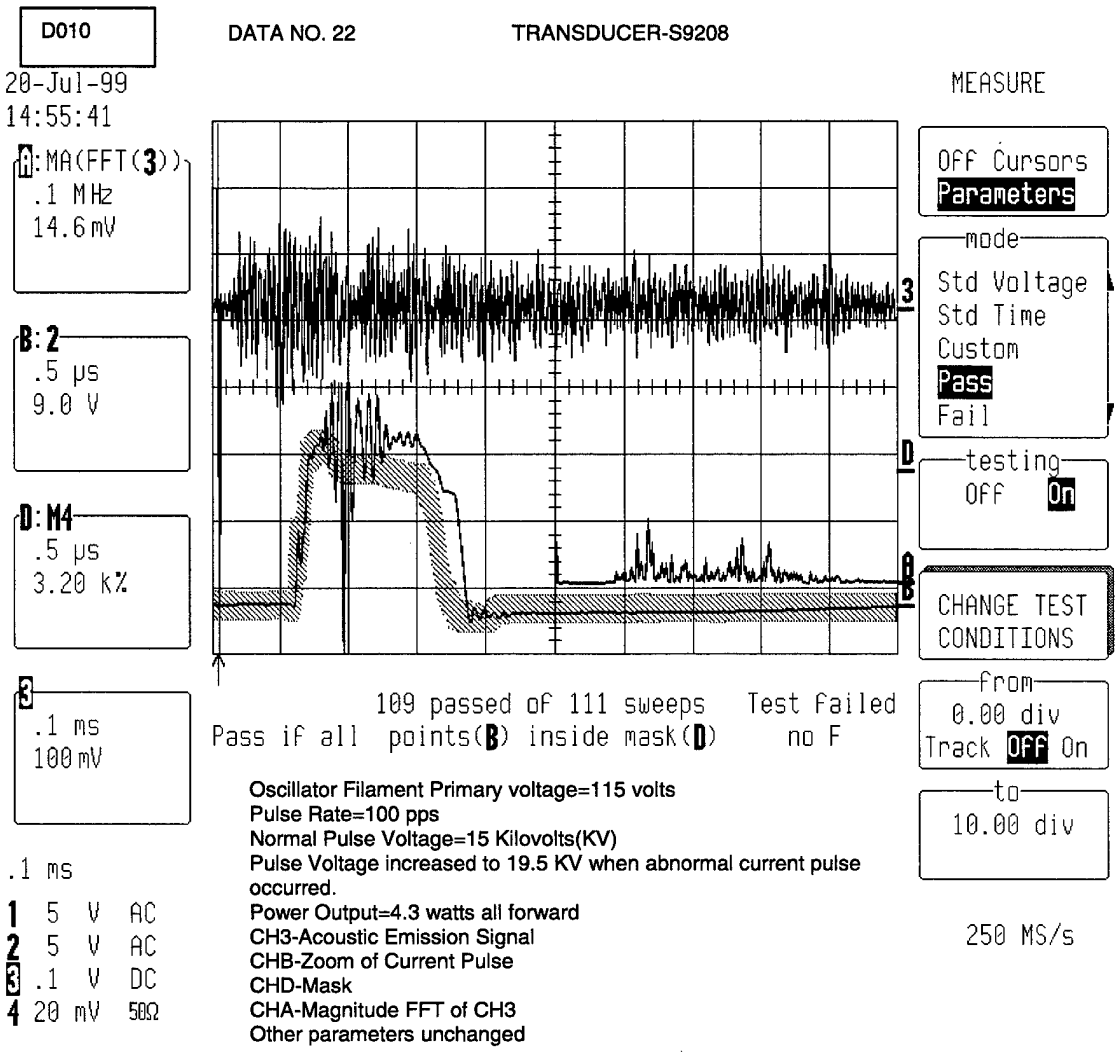

Oscillator Filament Primary voltage=115 volts
Pulse Rate=100 pps
Normal Pulse Voltage=15 Kilovolts(KV)
Pulse Voltage increased to 19.5 KV when abnormal current pulse occurred.
Power Output=4.3 watts all forward
CH3-Acoustic Emission Signal
CHB-Zoom of Current Pulse
CHD-Mask
CHA-Magnitude FFT of CH3
Other parameters unchanged

Figure 2. Abnormal current pulse with decreased acoustic emission signal amplitude.

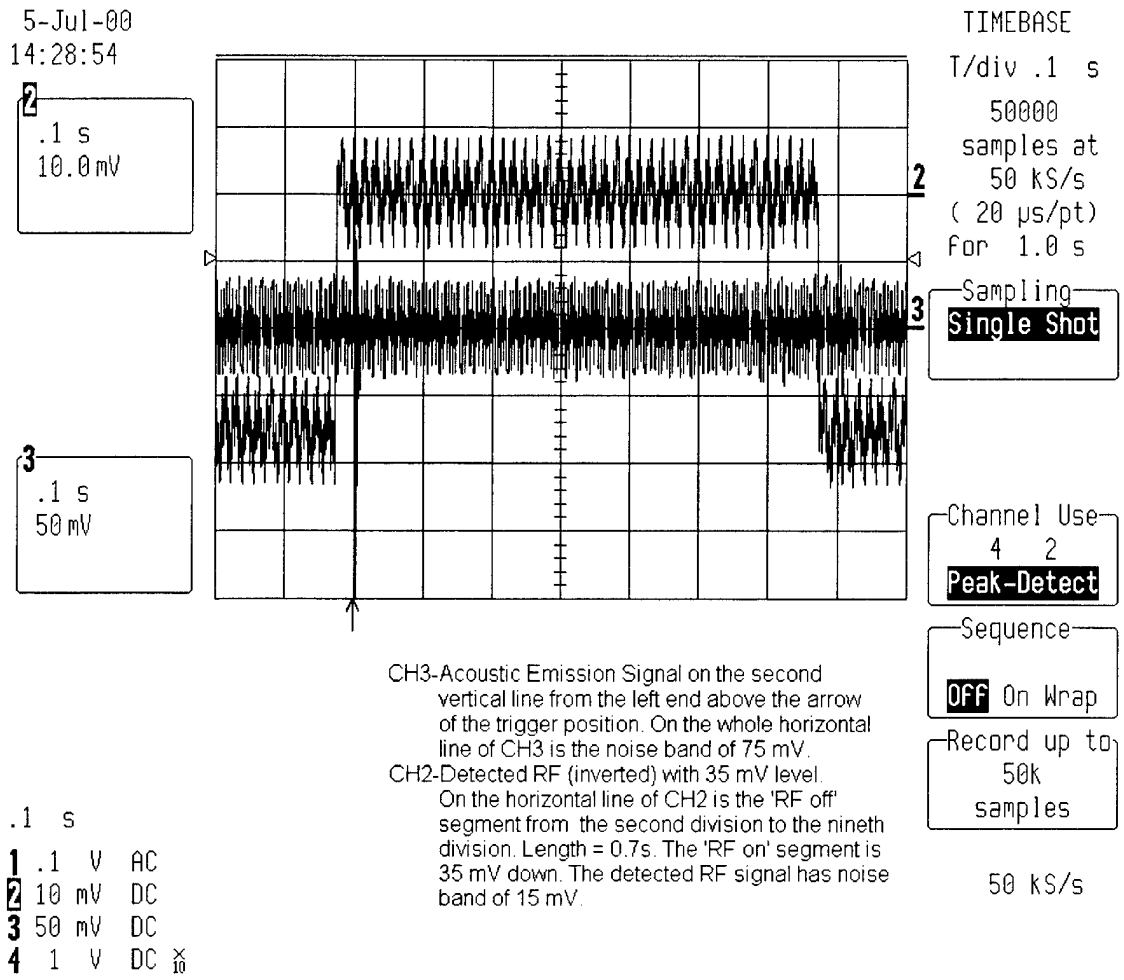

Figure 3. Acoustic emission during normal operation of TWT.

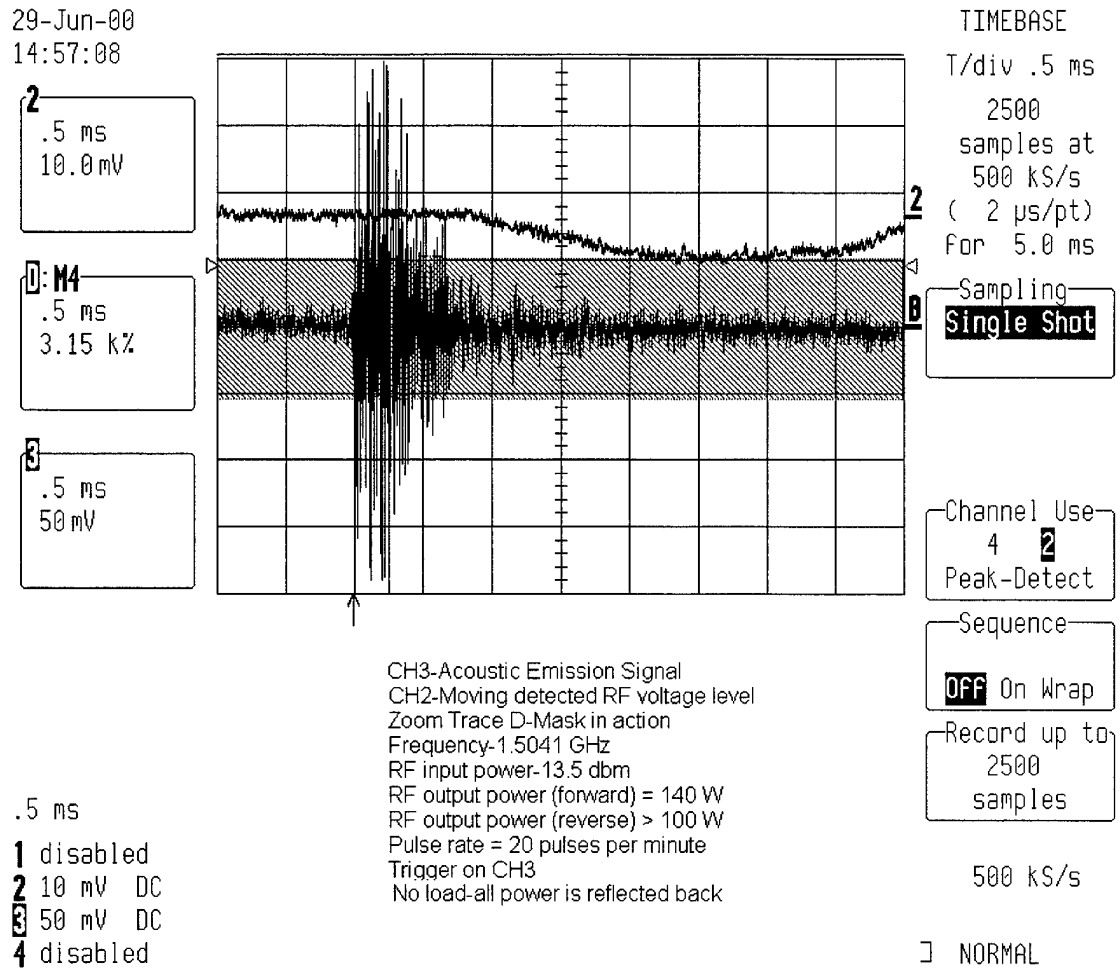

Figure 4. This is the same display as Figure 3 with horizontal time scale expanded to show AE signal starting at the change of RF signal on Ch2.

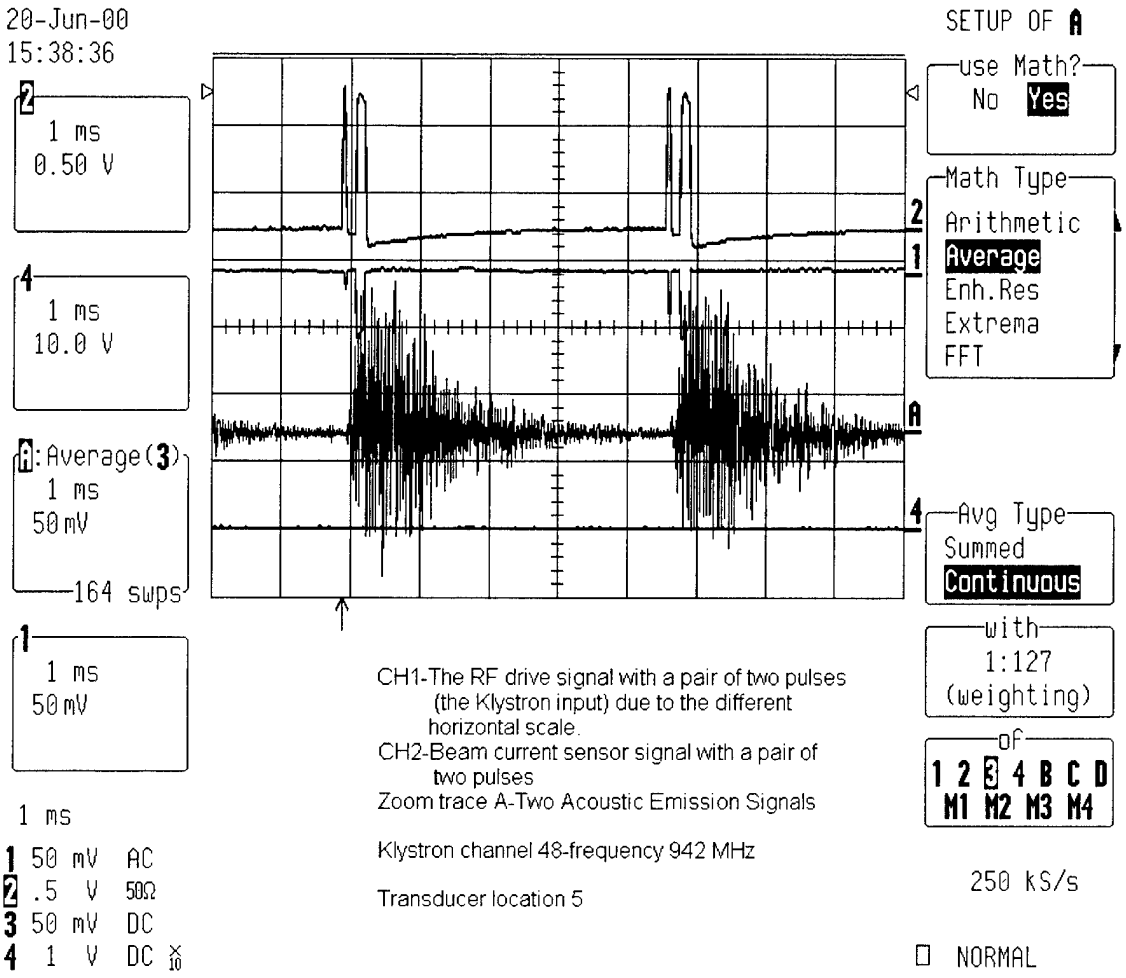

Figure 5. Acoustic emission signals correlated with the beam current sensor signals on Ch2 from klystron of AN/SPS-49 radar transmitter.

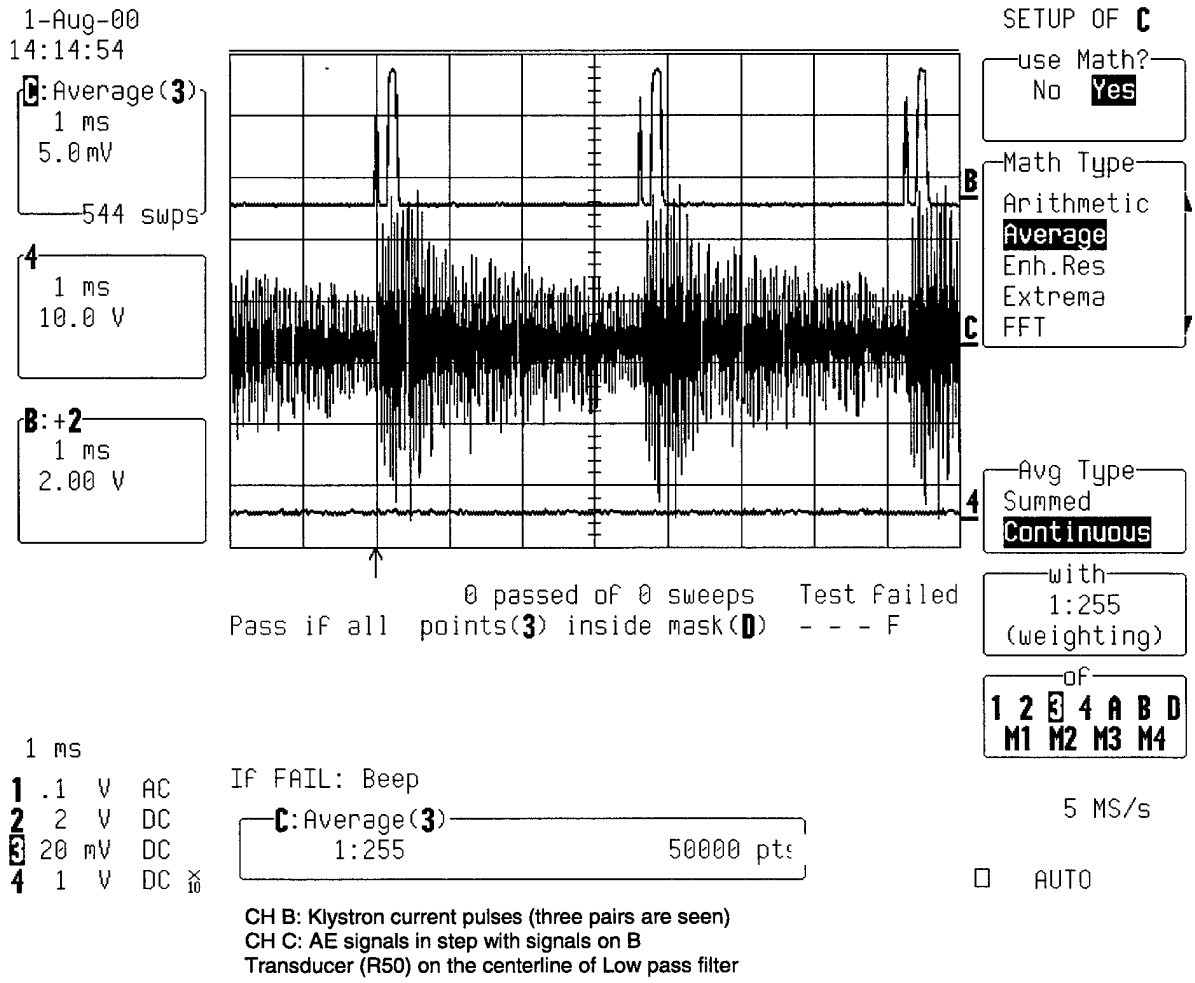

CH B: Klystron current pulses (three pairs are seen)
CH C: AE signals in step with signals on B
Transducer (R50) on the centerline of Low pass filter

Figure 6. AE activity in step with the beam current pulses from an AN/SPS-49 klystron at NSWC PHD Dam Neck.

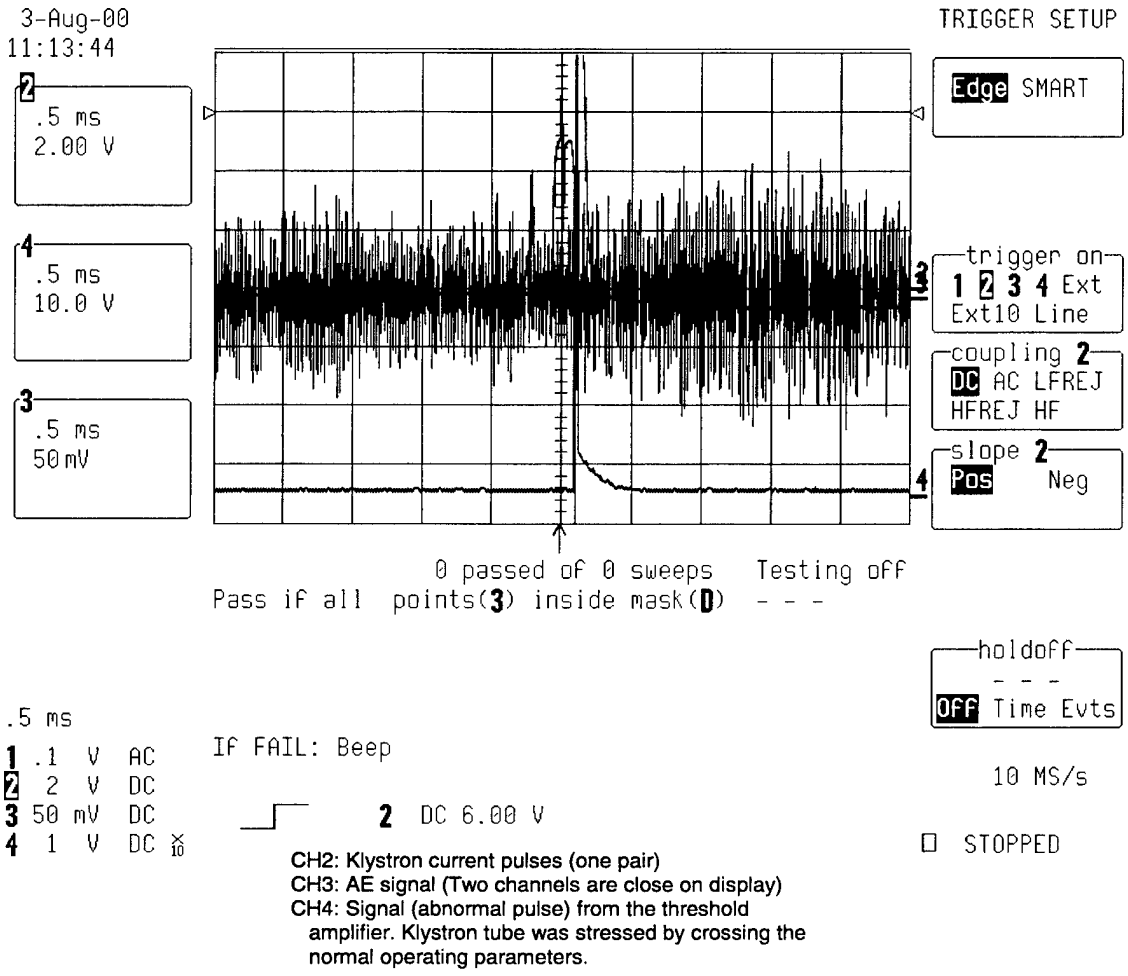

CH2: Klystron current pulses (one pair)
CH3: AE signal (Two channels are close on display)
CH4: Signal (abnormal pulse) from the threshold amplifier. Klystron tube was stressed by crossing the normal operating parameters.

Figure 7. Abnormal current pulse is caught on Ch4 AN/SPS-49 radar klystron unit at NSWC PHD Dam Neck.

B3000 Optomux System Architecture

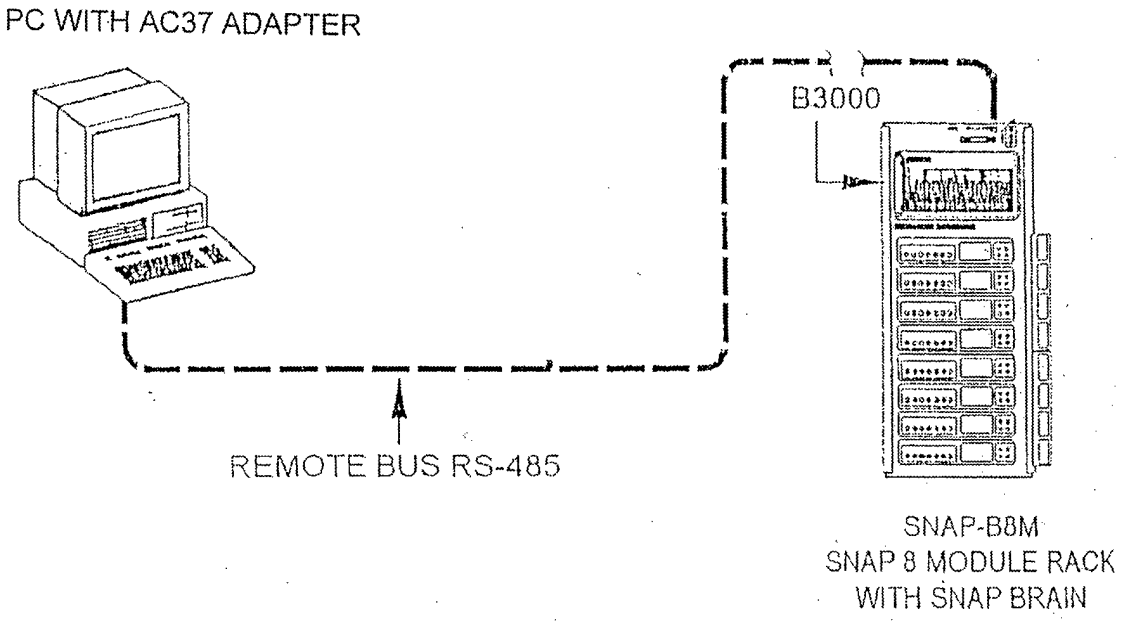

Figure 8. Schematic arrangement of the B3000 Optomux System Architecture.

SNAP-B8MC 8-Module Position I/O Mounting Rack
with SNAP B3000 Brain

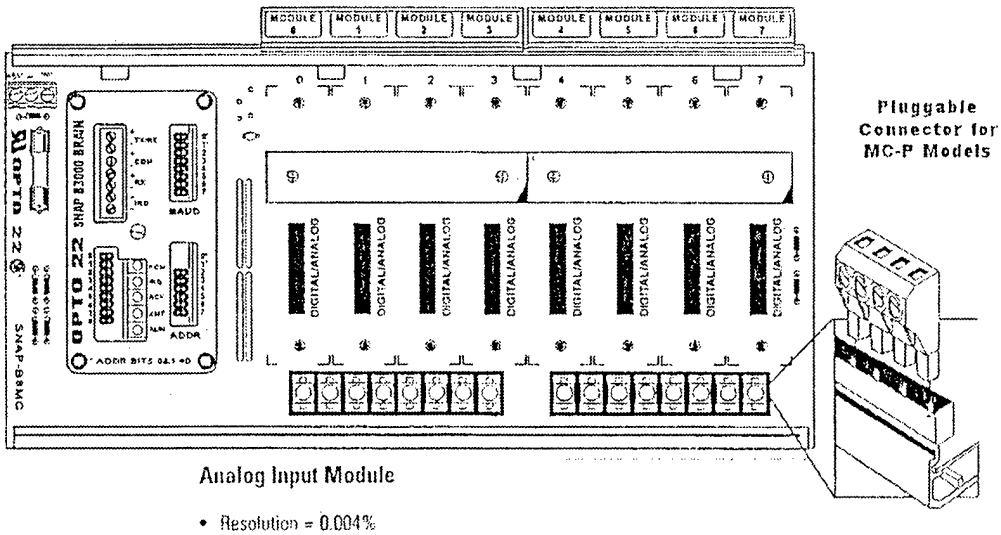

Analog Input Module

- Resolution = 0.004% of nominal range
- Two or four single-ended inputs per module

Features

- Rugged packaging
- Convenient pluggable wiring
- Powered by a single 5-volt supply
- Out-of-range indication
- Operating temperature 0° to 70° C
- Accepts up to 14 AWG wire.
- Factory calibrated, no user adjustment necessary

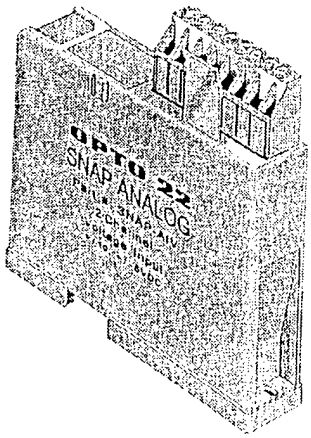

Figure 9a. SNAP B series I/O Rack with B3000 mounted on left side.

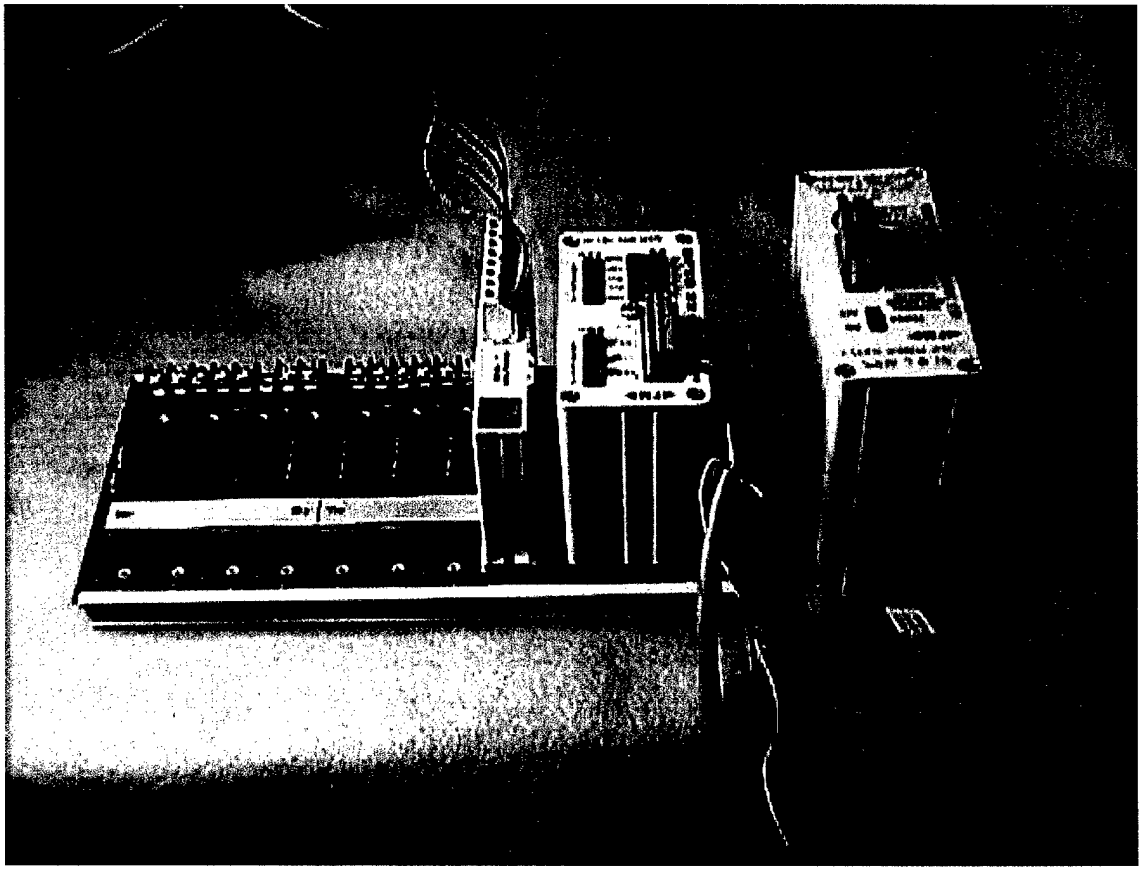

Figure 9b. Photograph of the (from right to left) power supply, OPTO22 SNAP3000 Brain, OPTO22 SNAP Analog Input Module, and SNAP B series of I/O rack.

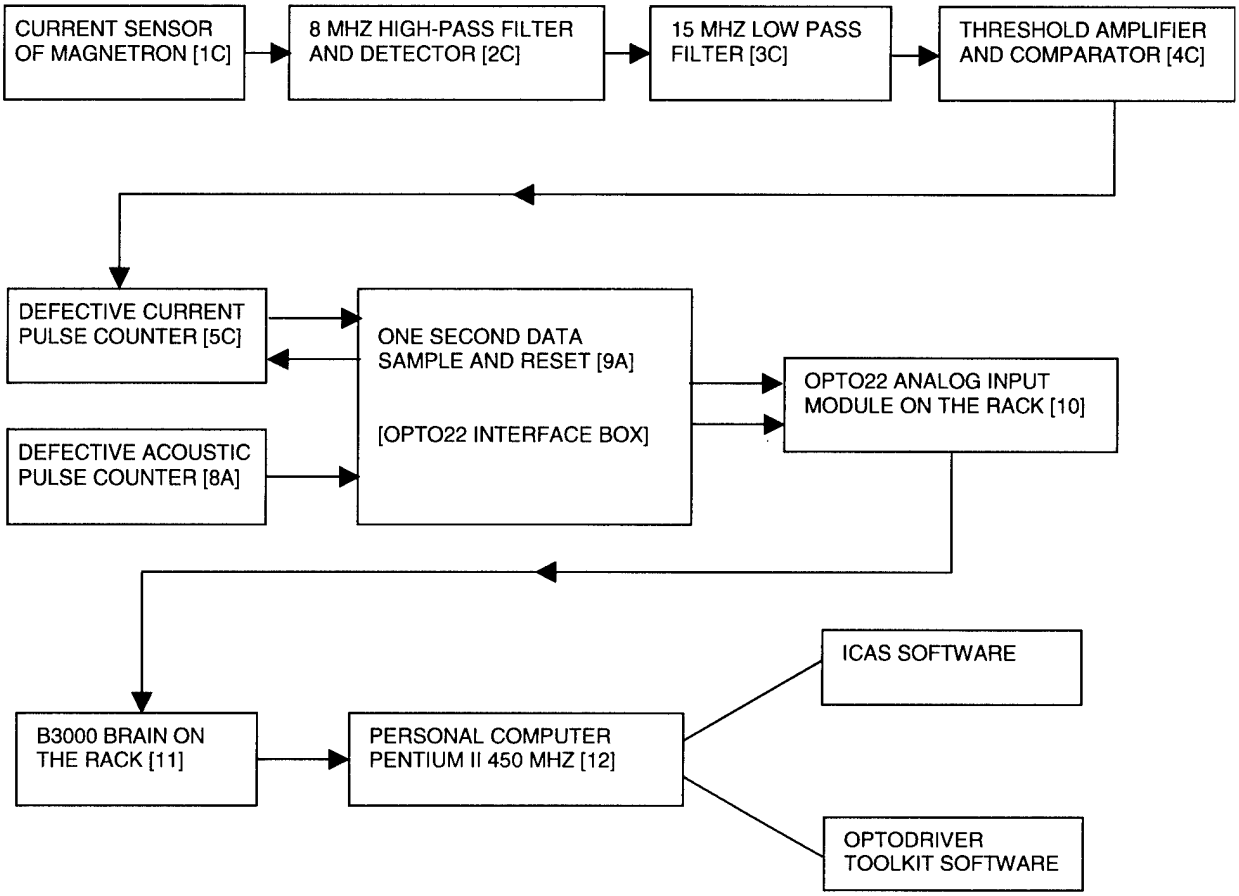

Figure 10. Electronic circuits between current sensor and OPT022 interface box for detecting and counting defective current pulses.

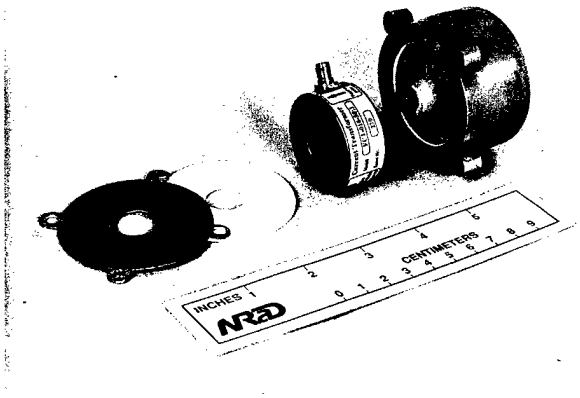

Figure 11a. Photo of current sensor.

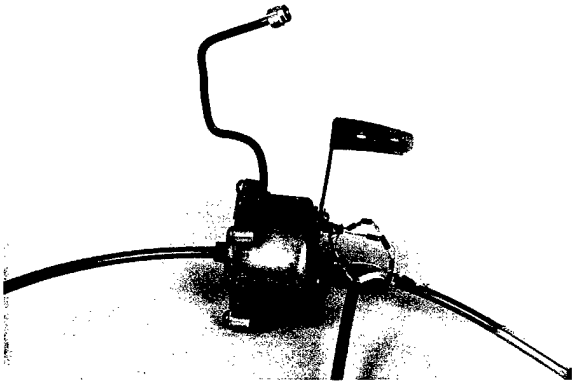

Figure 11b. Photo of current sensor.

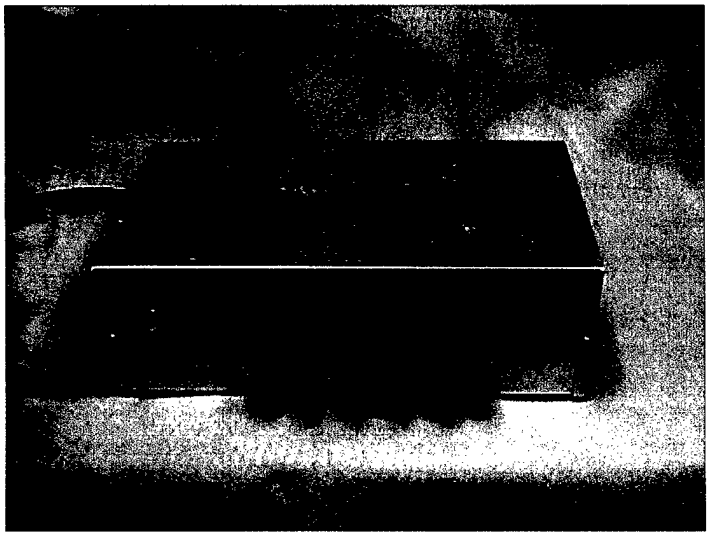

Figure 11c. Power line trigger box.

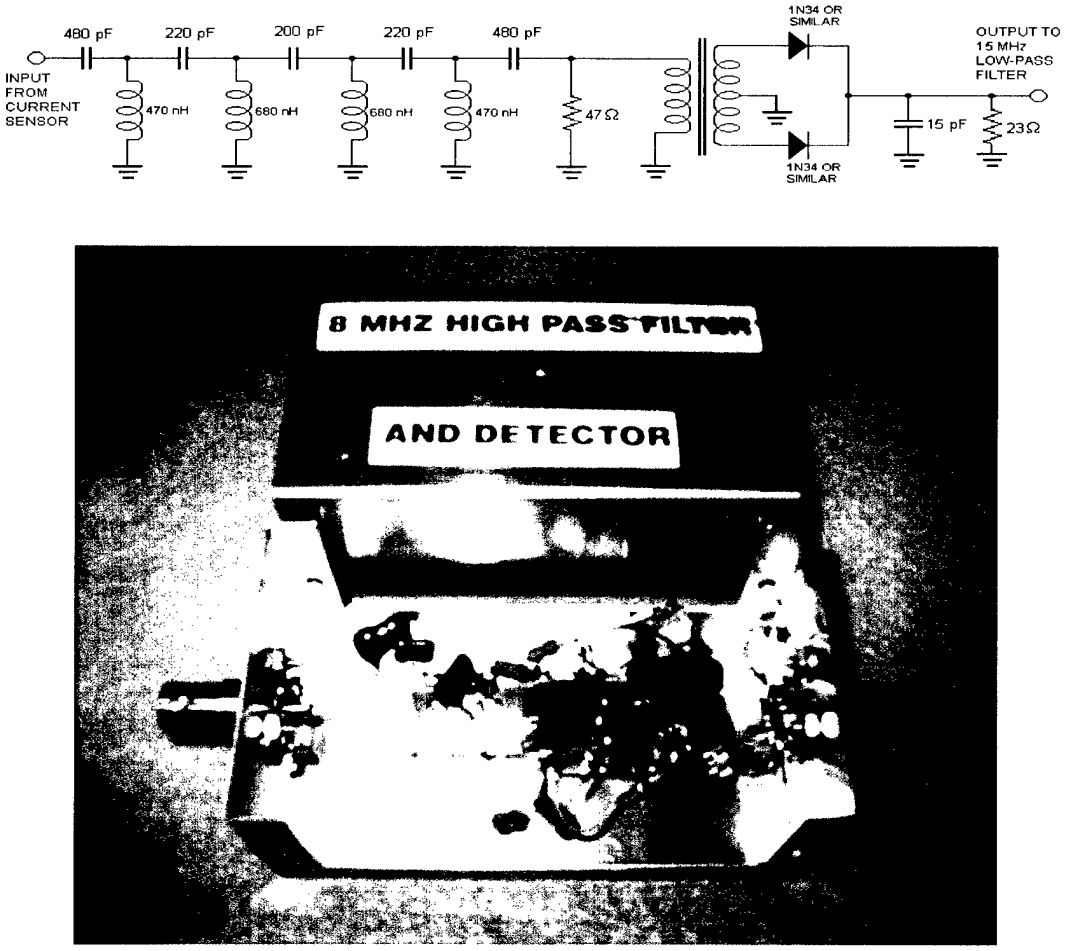

Figure 12. 8 MHz High-Pass Filter and Detector [2C] with photo.

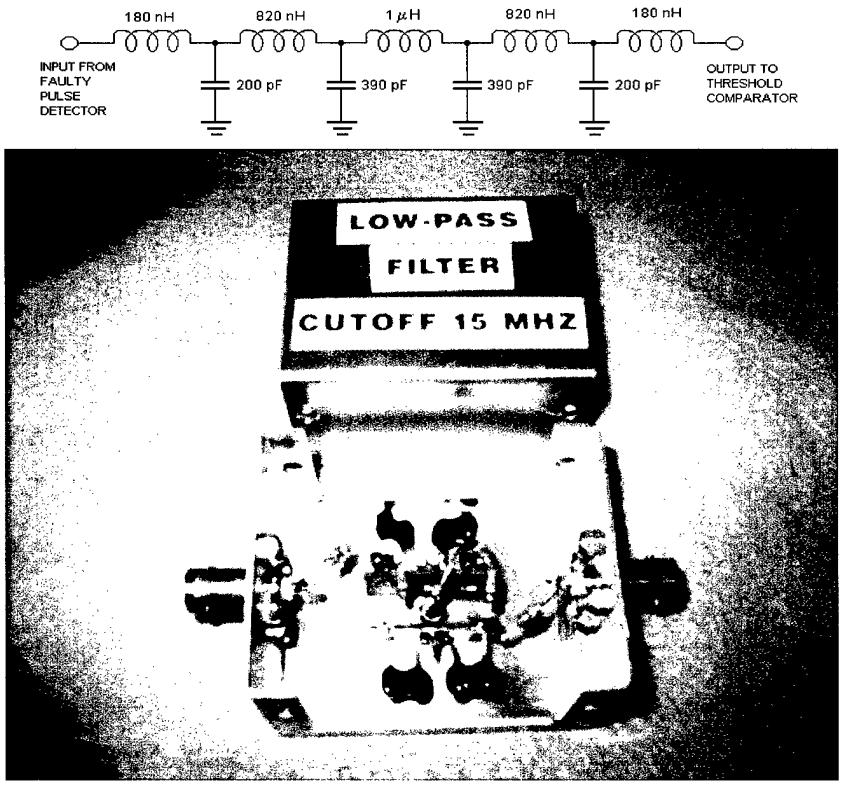

Figure 13. Low-Pass Filter (cutoff 15 MHz) circuit [3C] and photo.

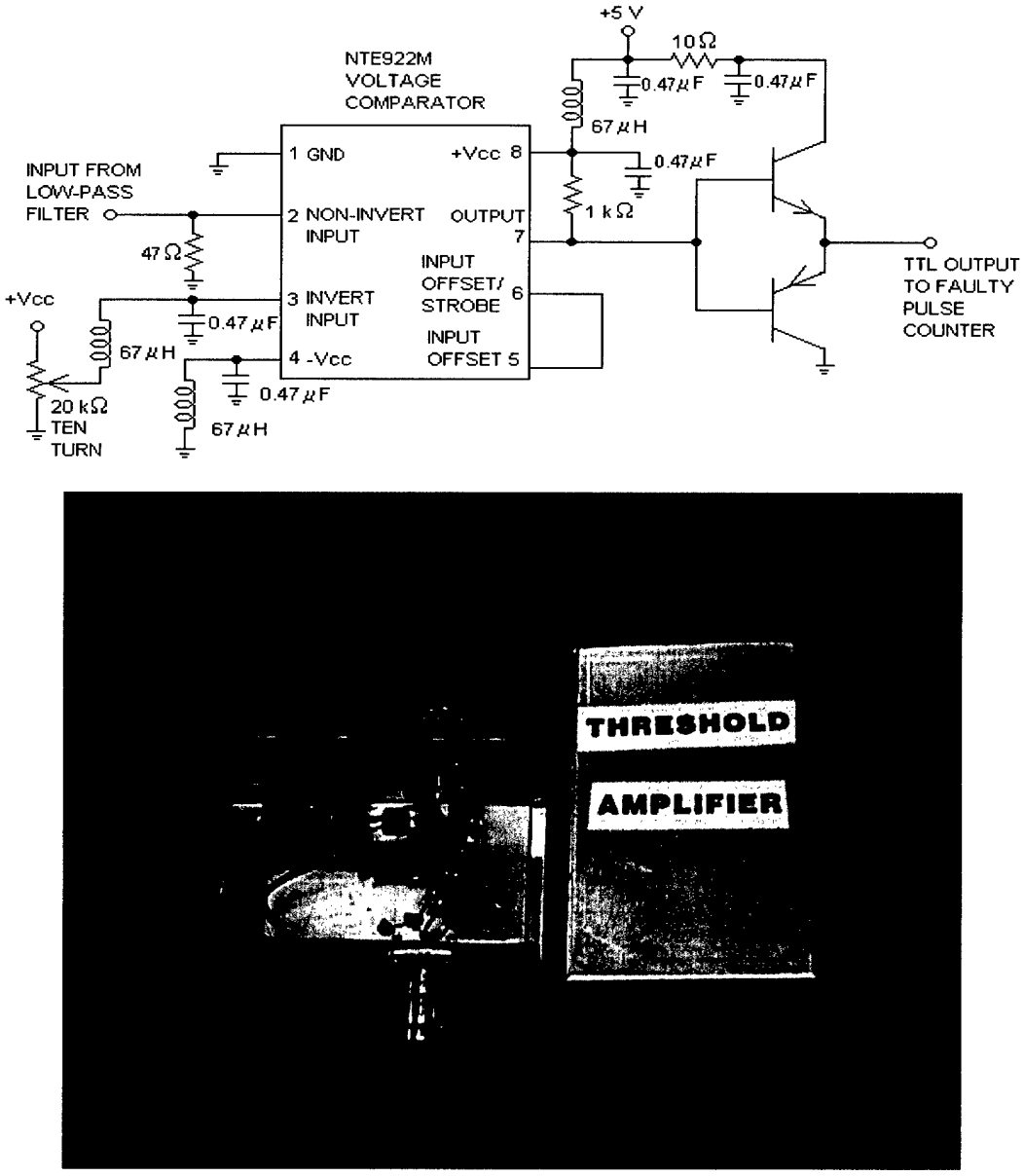

Figure 14. Threshold Amplifier and Comparator circuit [4C] and photo.

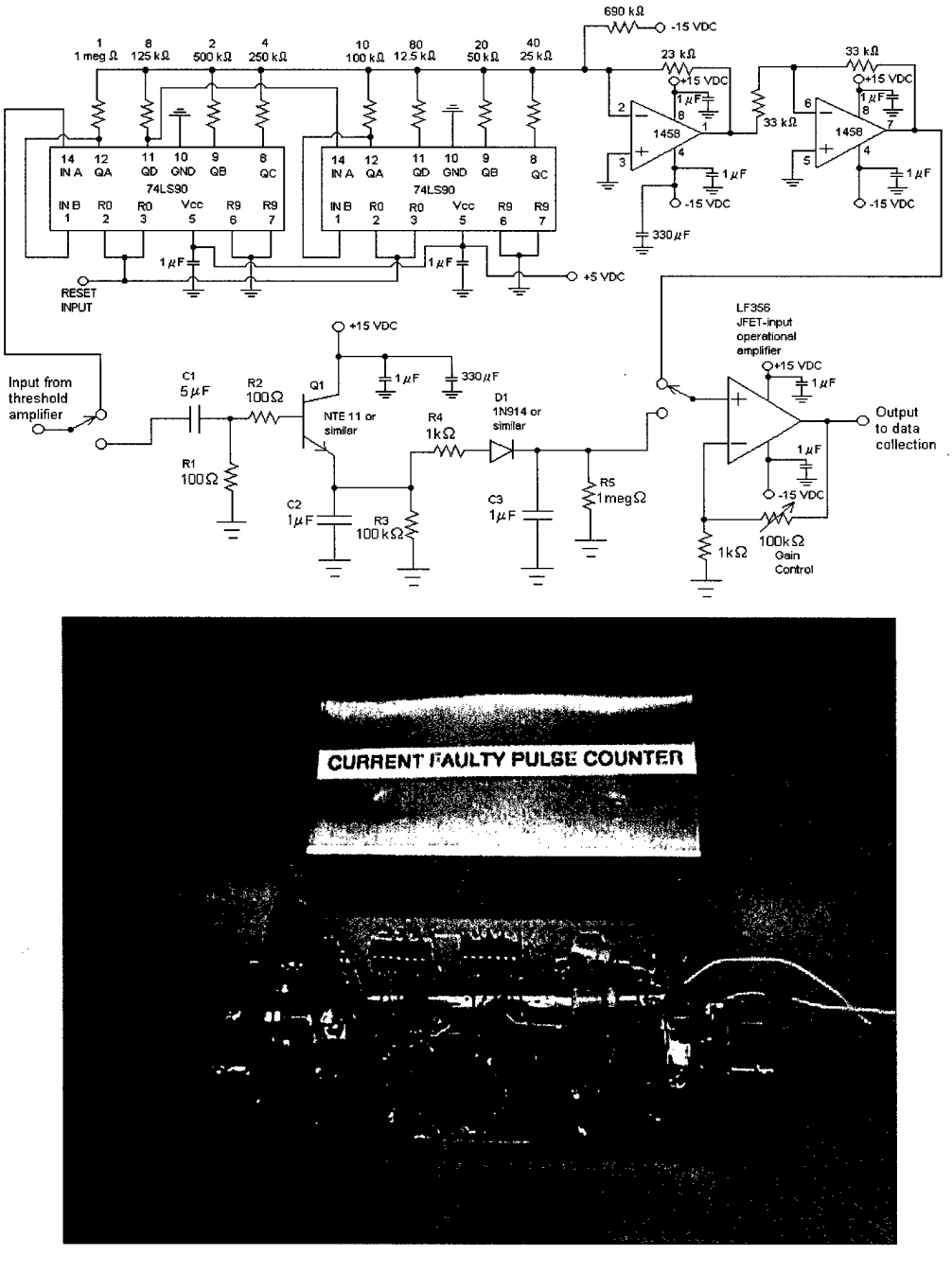

Figure 15. Defective Current Pulse Counter circuit [5C] and photo.

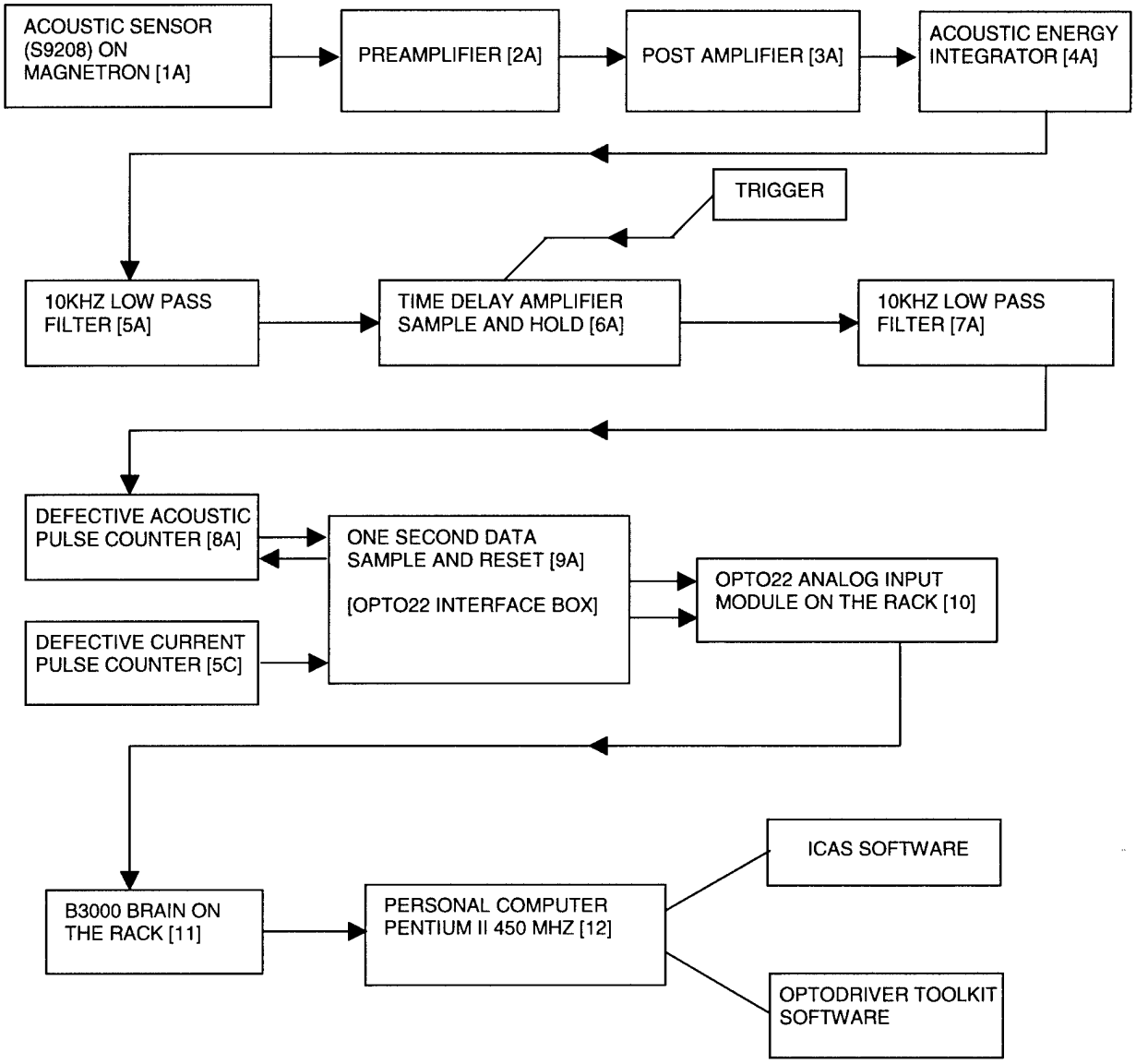

Figure 16. Electronic circuits between AE Sensor and OPTO22 interface box for detecting and counting defective acoustic pulses.

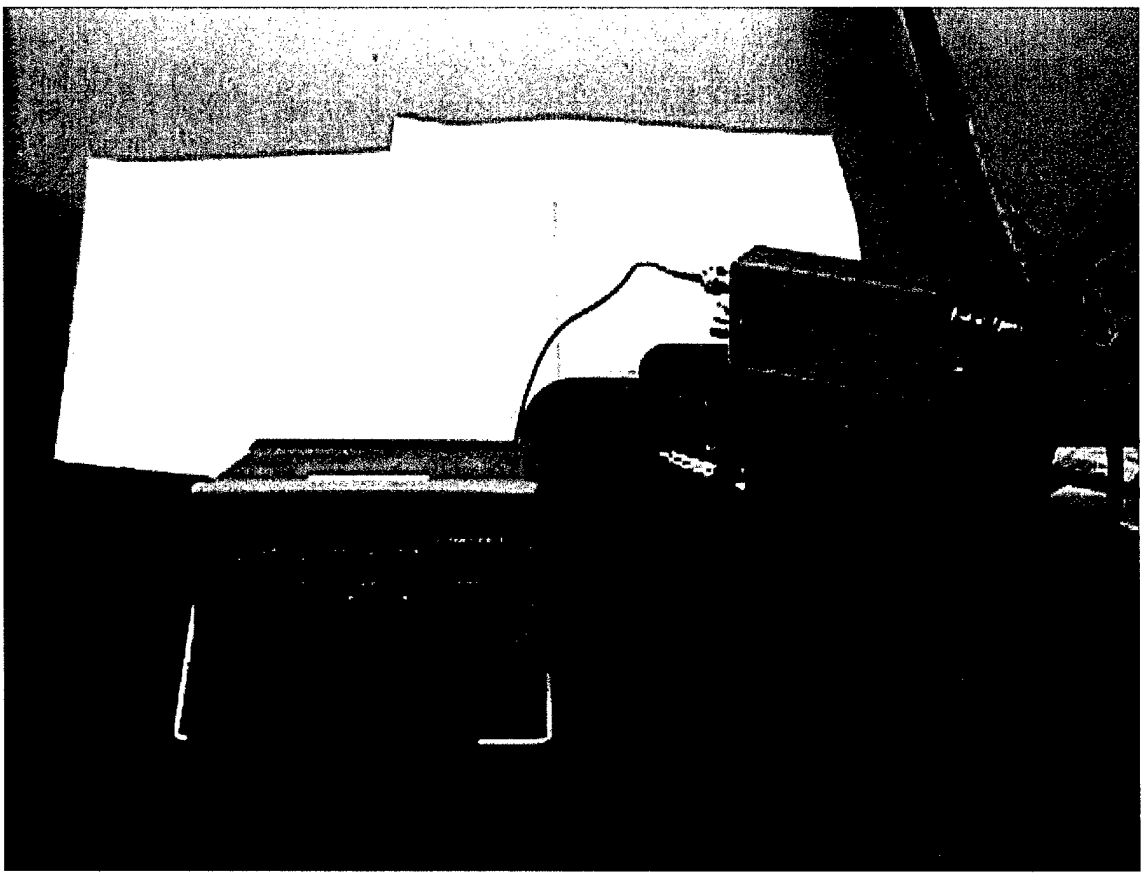

Figure 17. Photo of Post-amplifier (left), Pre-amplifier (right), and Acoustic Emission Transducer (middle) coupled to the cylinder of the pulsed magnetron.

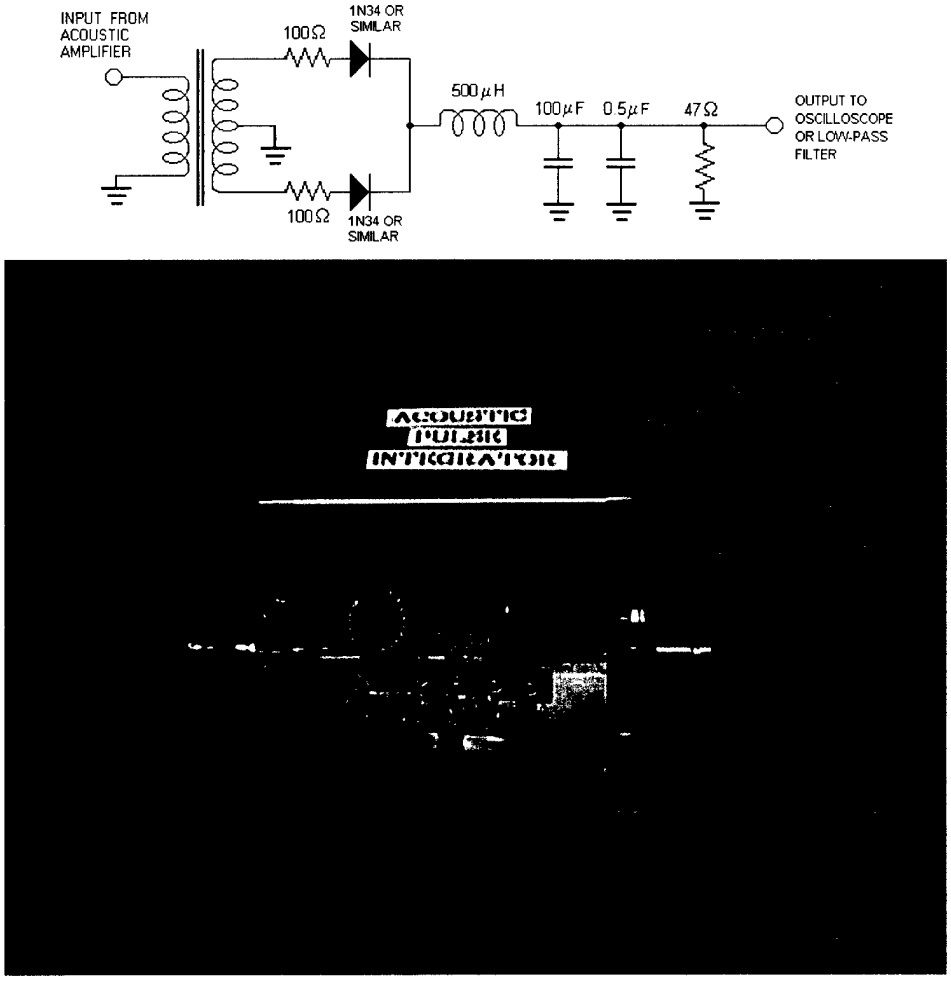

Figure 18. Acoustic Pulse Energy Integrator circuit [4A] and photo.

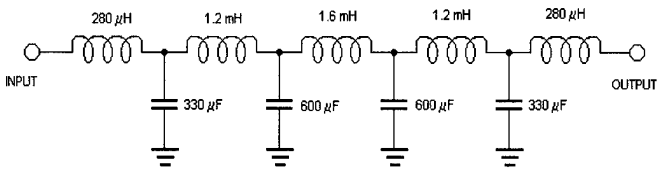

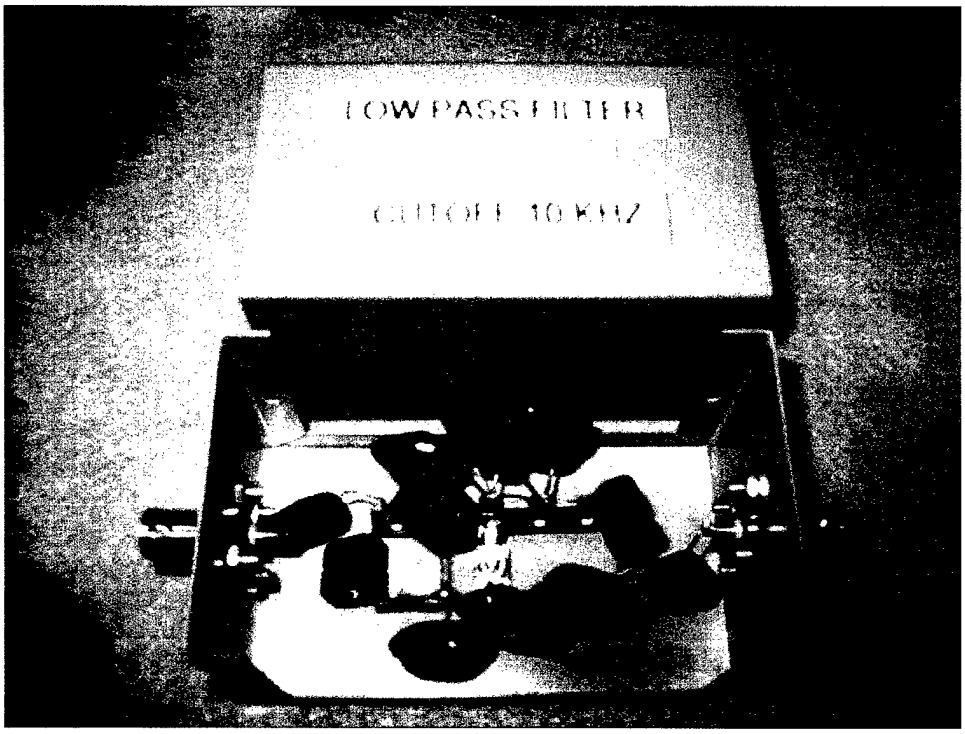

Figure 19. Low-Pass Filter (10 kHz cutoff) circuit [5A] and photo.

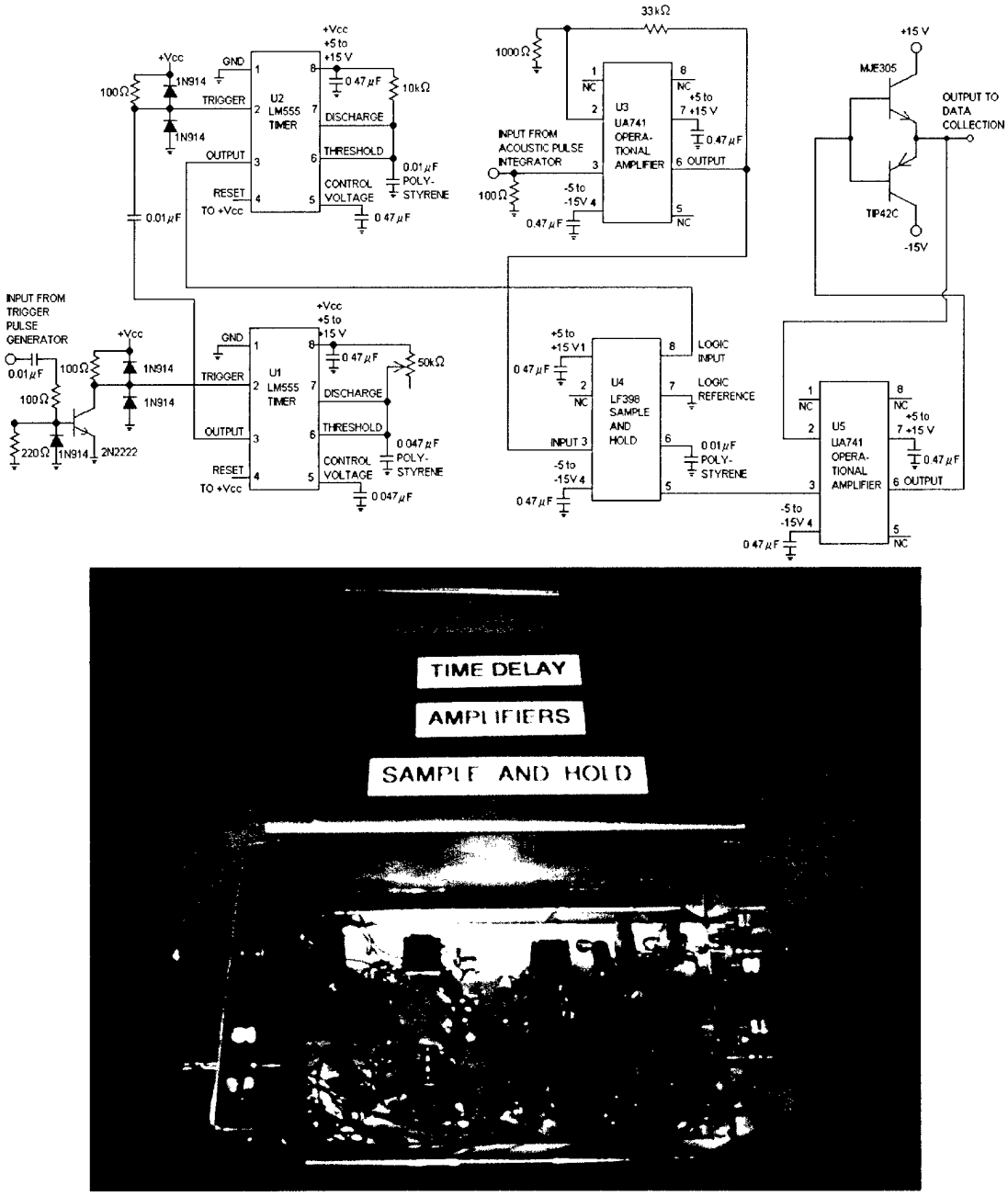

Figure 20. Time Delay, Amplifier, Sample-and-Hold circuit [6A], and photo.

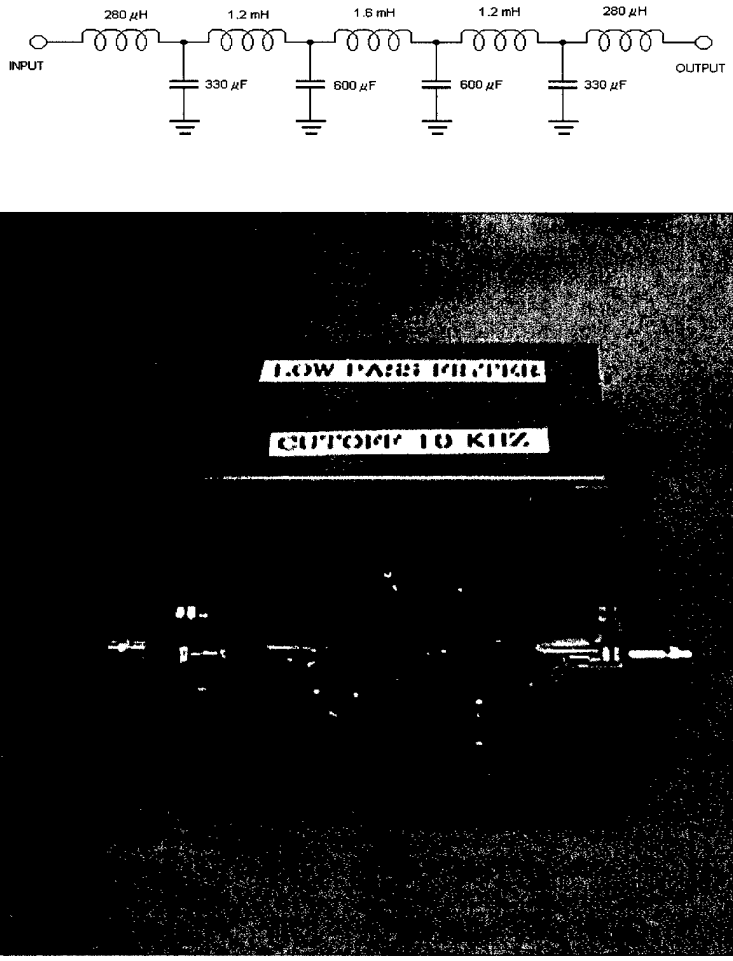

Figure 21. Low-Pass Filter (10 kHz cutoff) circuit [7A] and photo.

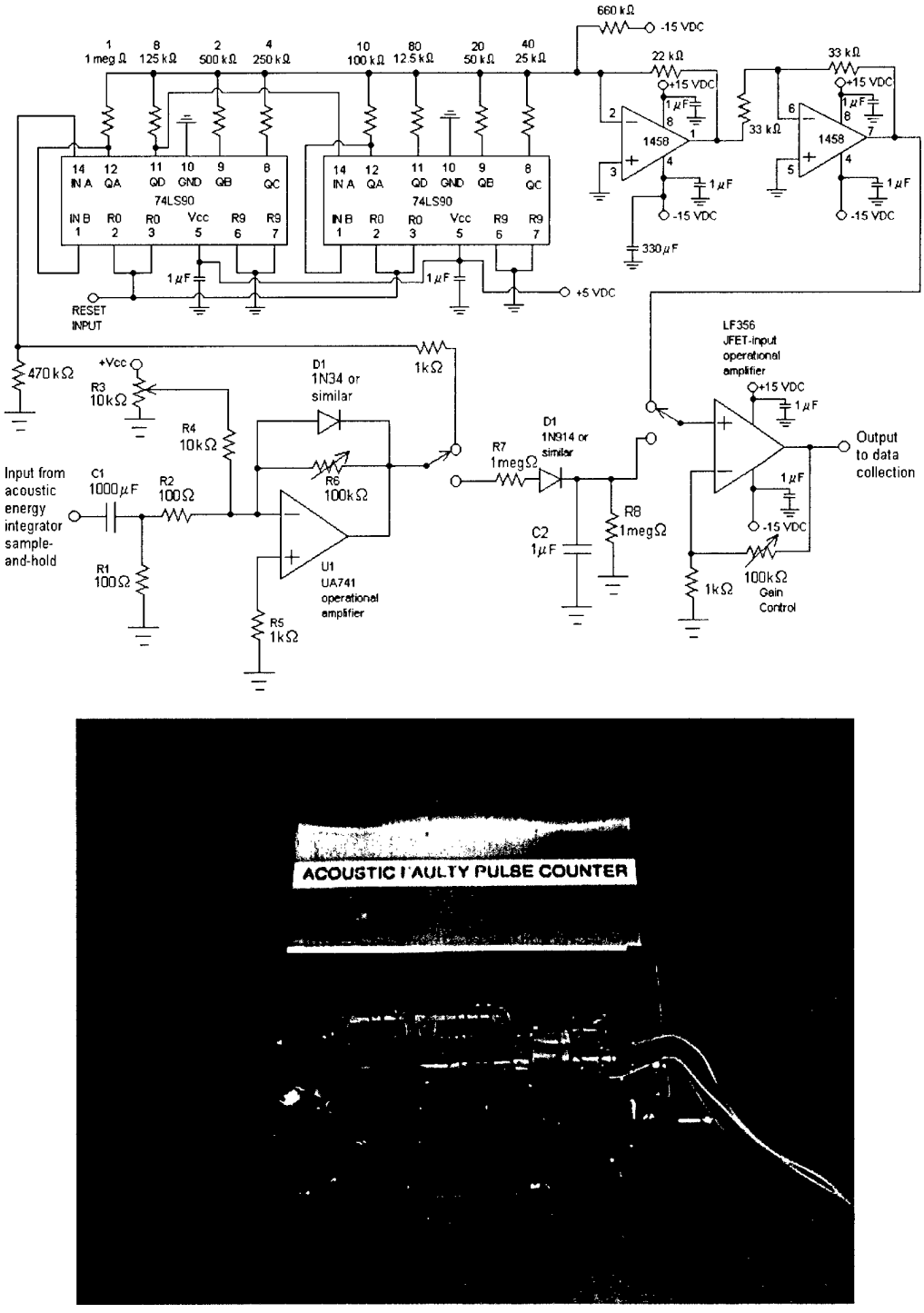

Figure 22. Defective Acoustic Pulse Counter circuit [8A] and photo.

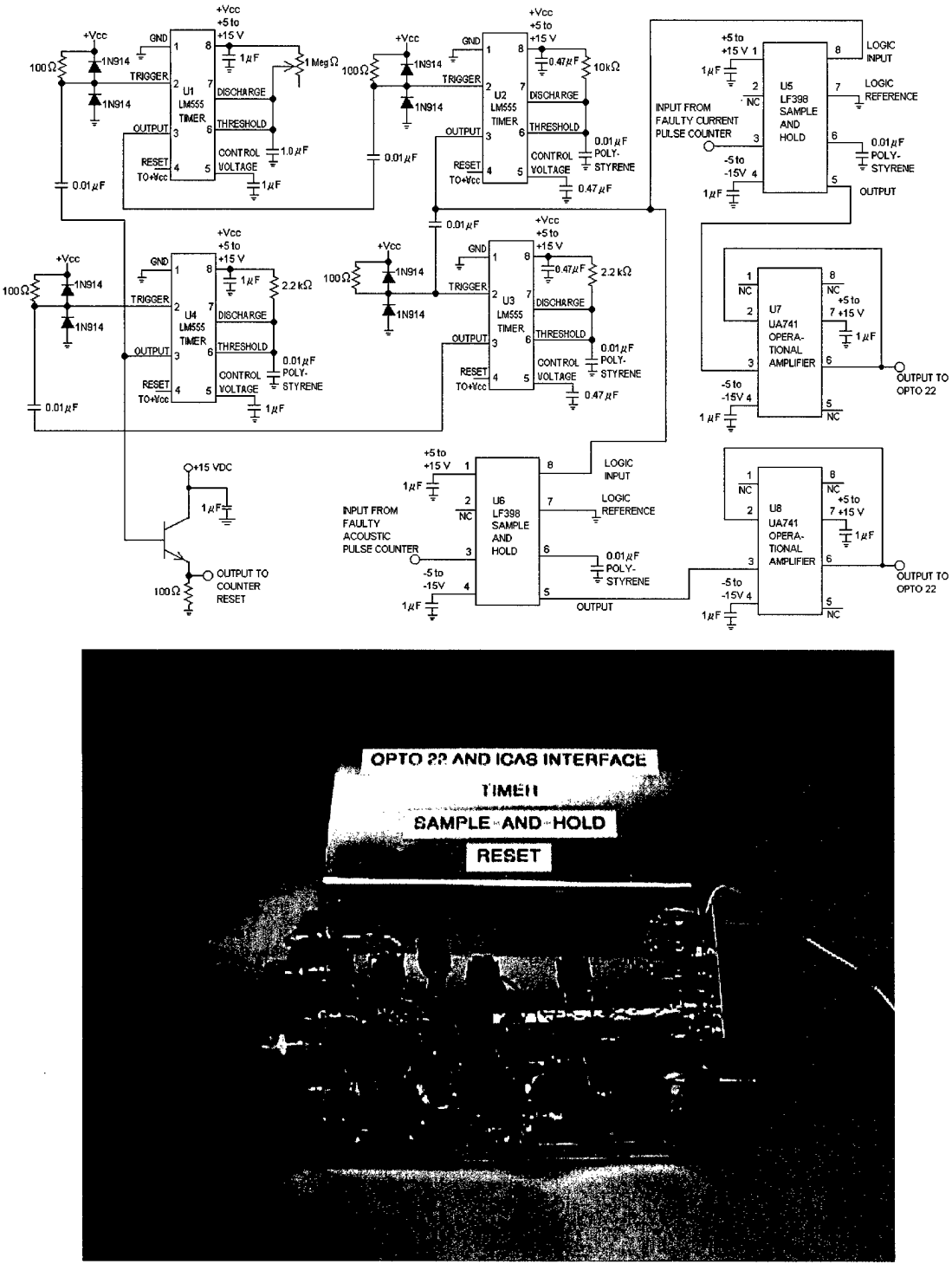

Figure 23. One-Second Data Sample and Reset circuit [9A] and photo.

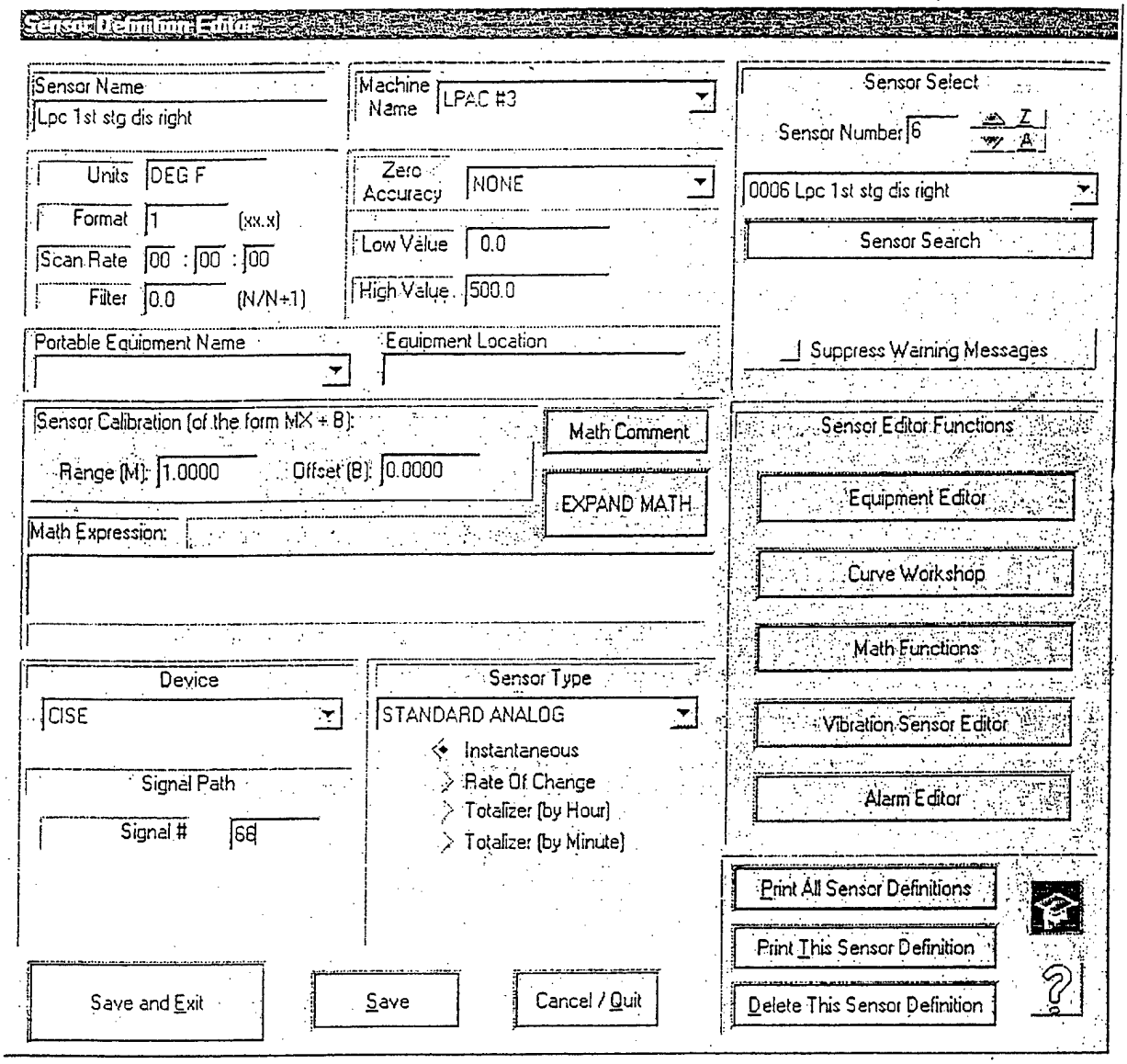

Figure 24. The Sensor Editor Window of the ICAS Software.

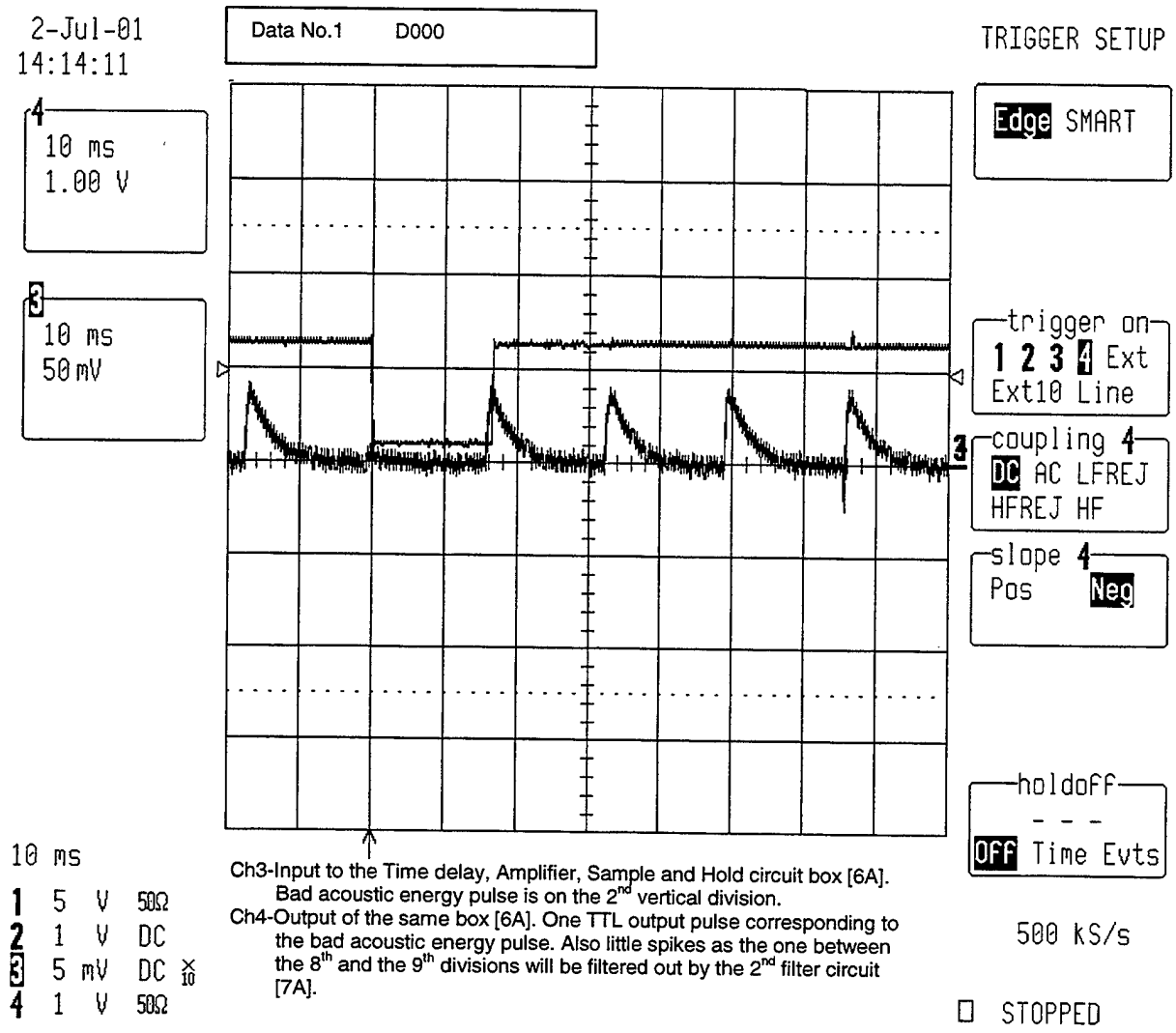

Ch3-Input to the Time delay, Amplifier, Sample and Hold circuit box [6A]. Bad acoustic energy pulse is on the 2nd vertical division.

Ch4-Output of the same box [6A]. One TTL output pulse corresponding to the bad acoustic energy pulse. Also little spikes as the one between the 8th and the 9th divisions will be filtered out by the 2nd filter circuit [7A].

Figure 25. Defective current and acoustic pulses and single TTL output at the same time as expected.

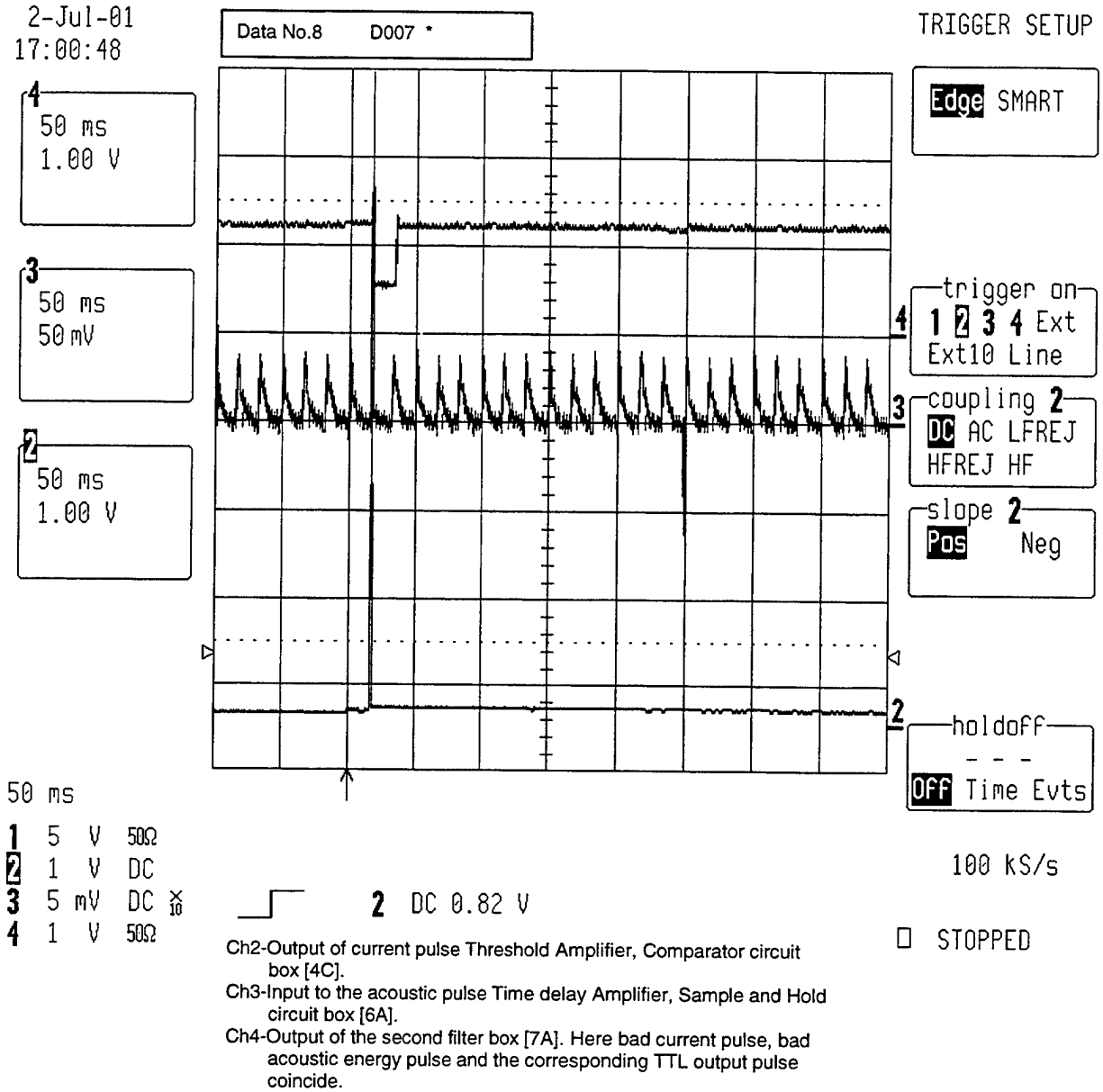

Ch2-Output of current pulse Threshold Amplifier, Comparator circuit box [4C].
Ch3-Input to the acoustic pulse Time delay Amplifier, Sample and Hold circuit box [6A].
Ch4-Output of the second filter box [7A]. Here bad current pulse, bad acoustic energy pulse and the corresponding TTL output pulse coincide.

Figure 26. Defective current and acoustic pulses and single TTL output at the same time as expected.

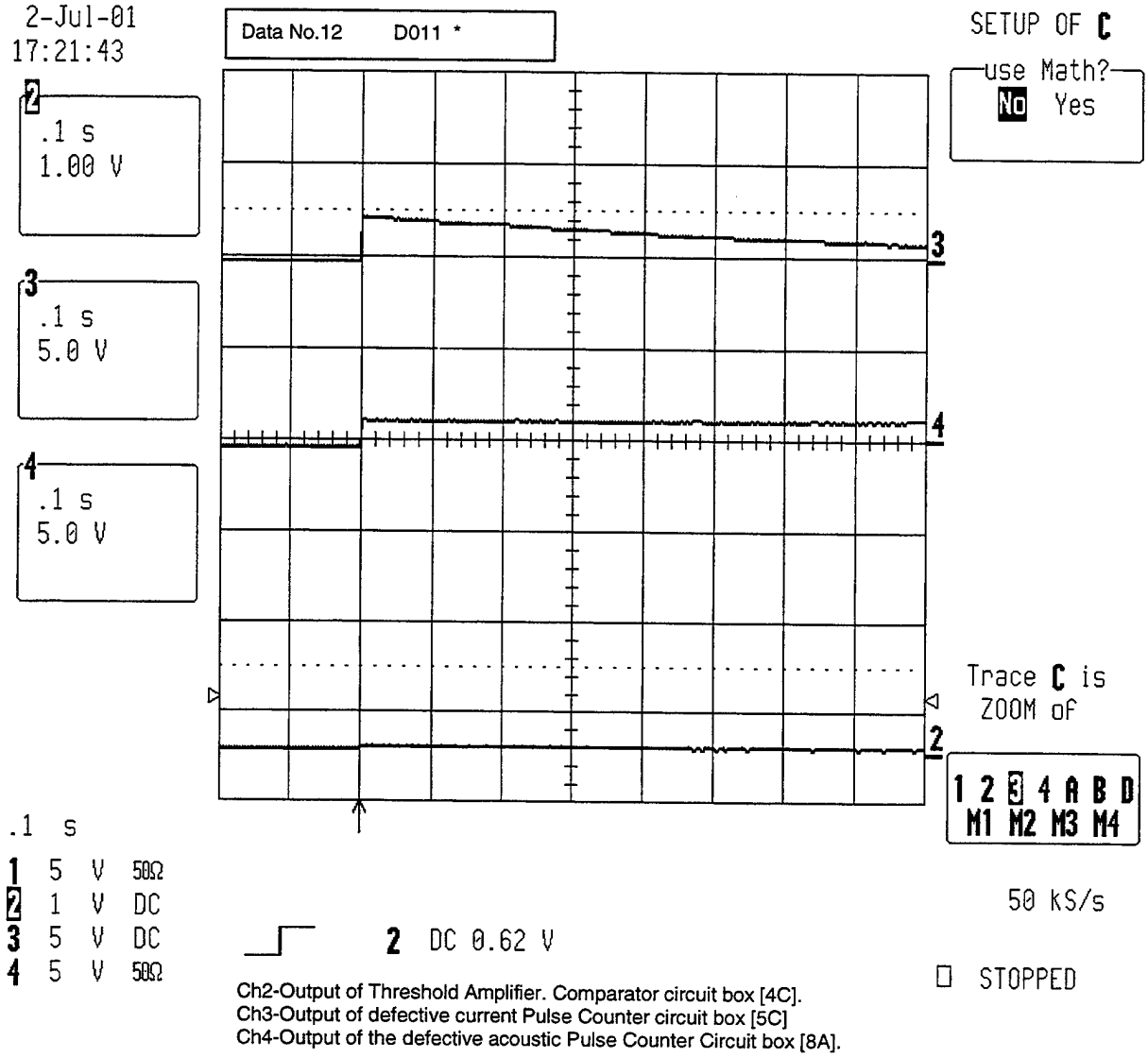

Ch2-Output of Threshold Amplifier. Comparator circuit box [4C].
Ch3-Output of defective current Pulse Counter circuit box [5C]
Ch4-Output of the defective acoustic Pulse Counter Circuit box [8A].

Figure 27. Outputs from two counters and Threshold Amplifier-Comparator coincide as expected.

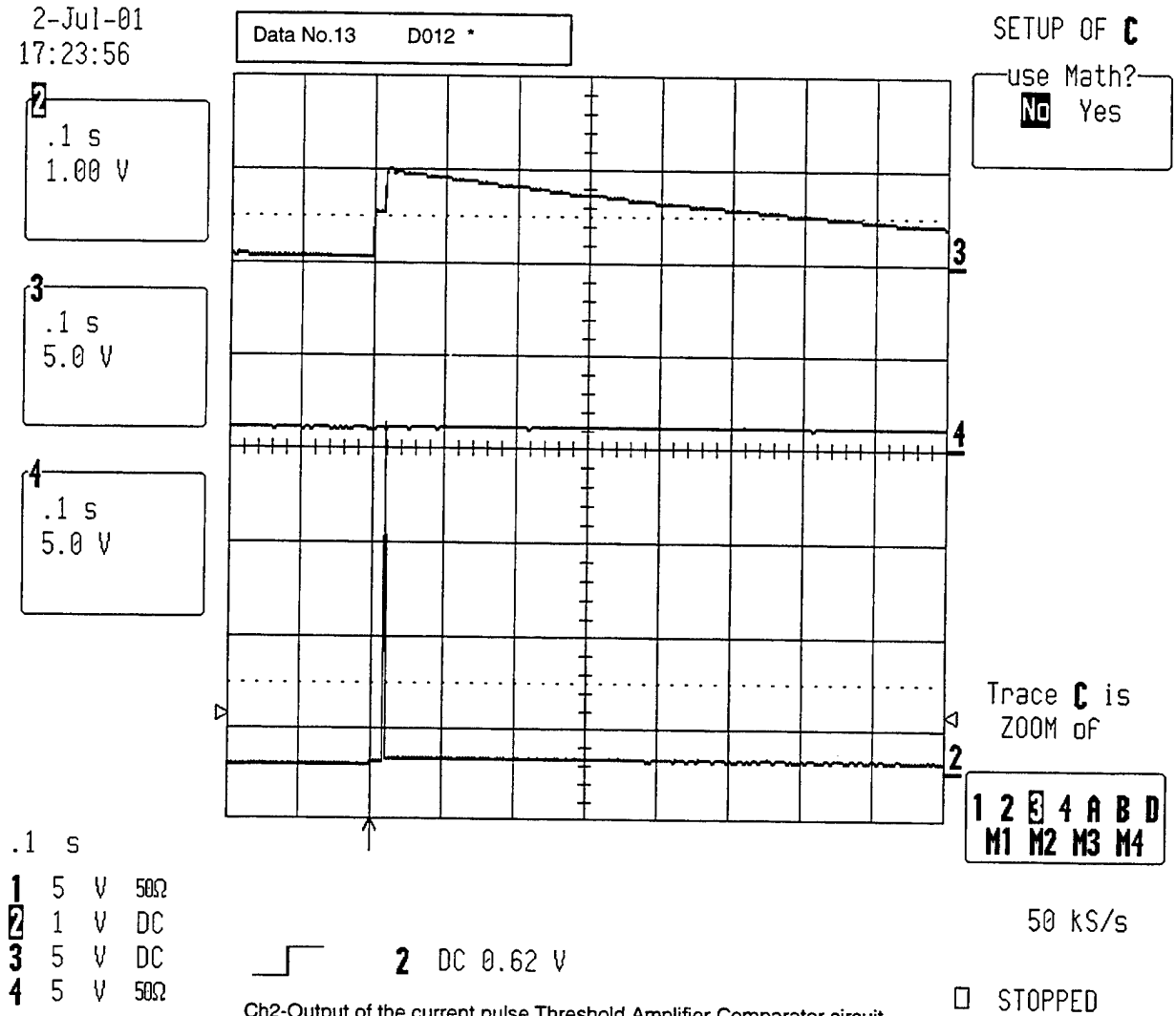

Ch2-Output of the current pulse Threshold Amplifier,Comparator circuit box [4C].
Ch3-Output of the defective current Pulse Counter circuit box [5C].
Ch4-Output of the defective acoustic Pulse Counter circuit box [8A]. Here events on Ch2 and Ch3 coincided but somehow no bad acoustic pulse on Ch4.

Figure 28. Output from one counter and Threshold Amplifier-Comparator coincide.

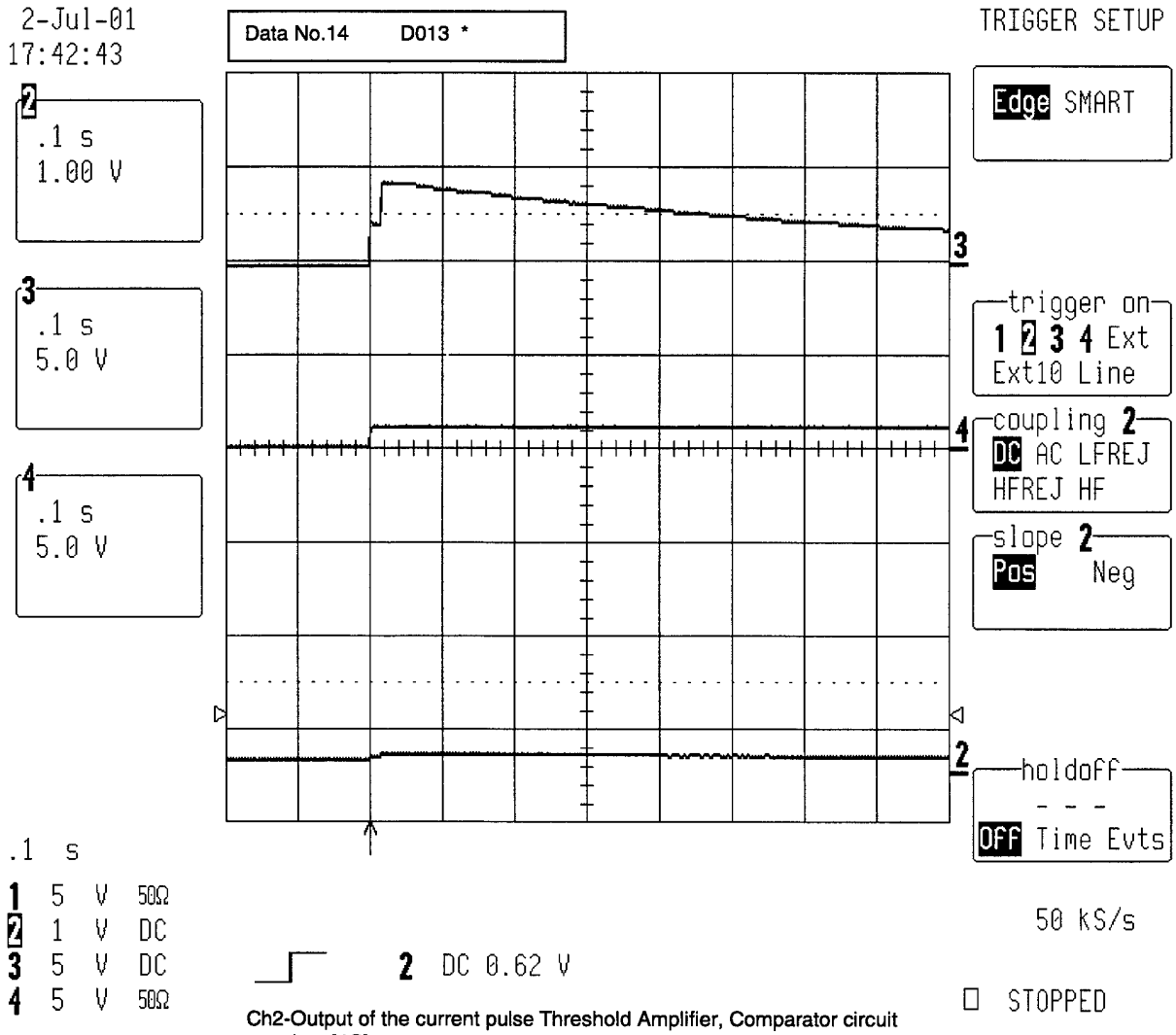

Ch2-Output of the current pulse Threshold Amplifier, Comparator circuit box [4C].
Ch3-Output of the defective current Pulse Counter circuit box [5C].
Ch4-Output of the defective acoustic Pulse Counter circuit box [8A].
Here the Ch3 shows the steps at the 2nd vertical division due to the double bad current pulses. Also the display shows the coincidence of the events on all 3 channels as expected.

Figure 29. Defective Current Pulse Counter (Ch3) shows steps for successive counts as expected.

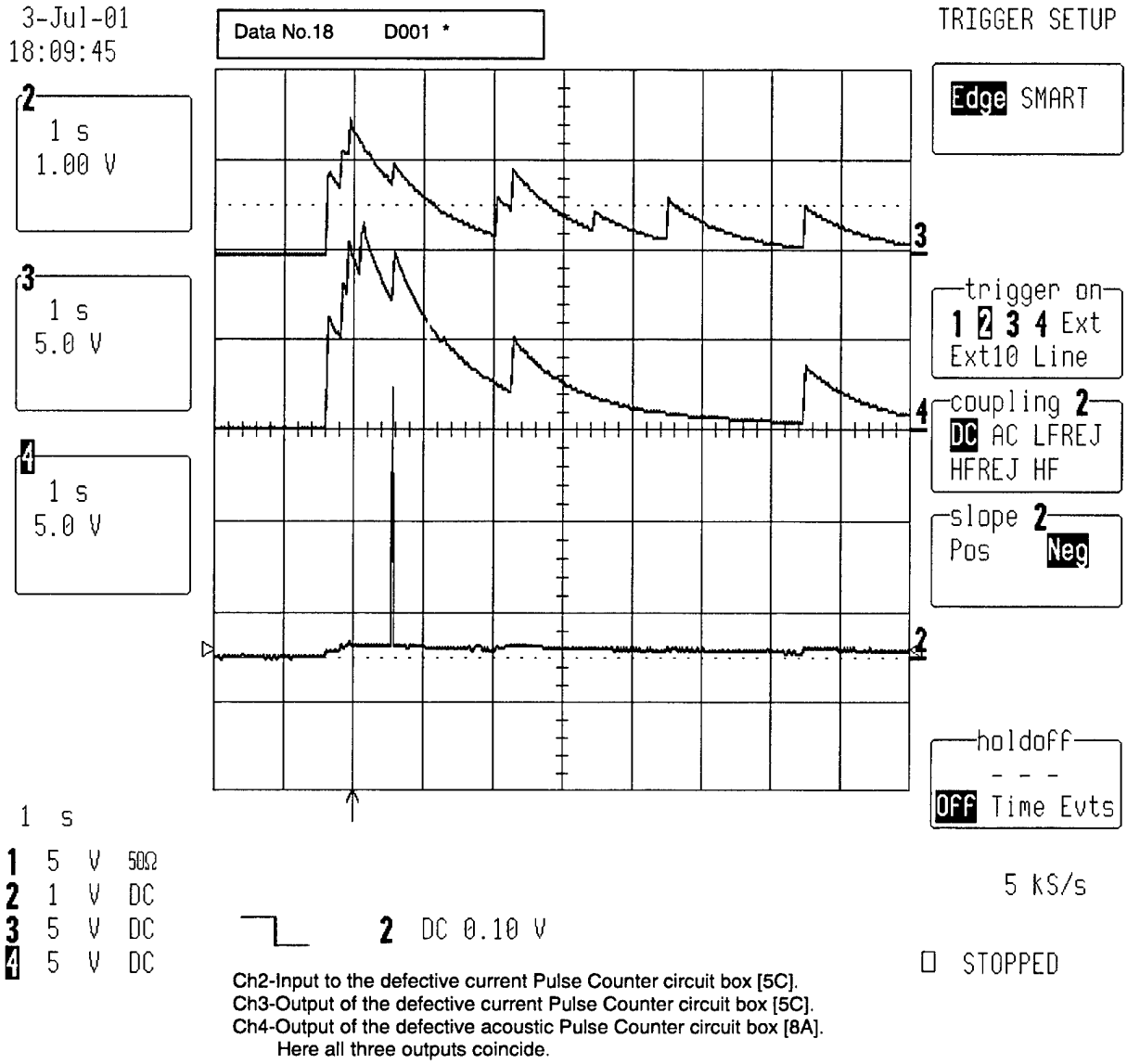

Ch2-Input to the defective current Pulse Counter circuit box [5C].
Ch3-Output of the defective current Pulse Counter circuit box [5C].
Ch4-Output of the defective acoustic Pulse Counter circuit box [8A].
Here all three outputs coincide.

Figure 30. Output of two counters with input to the Current Pulse Counter.

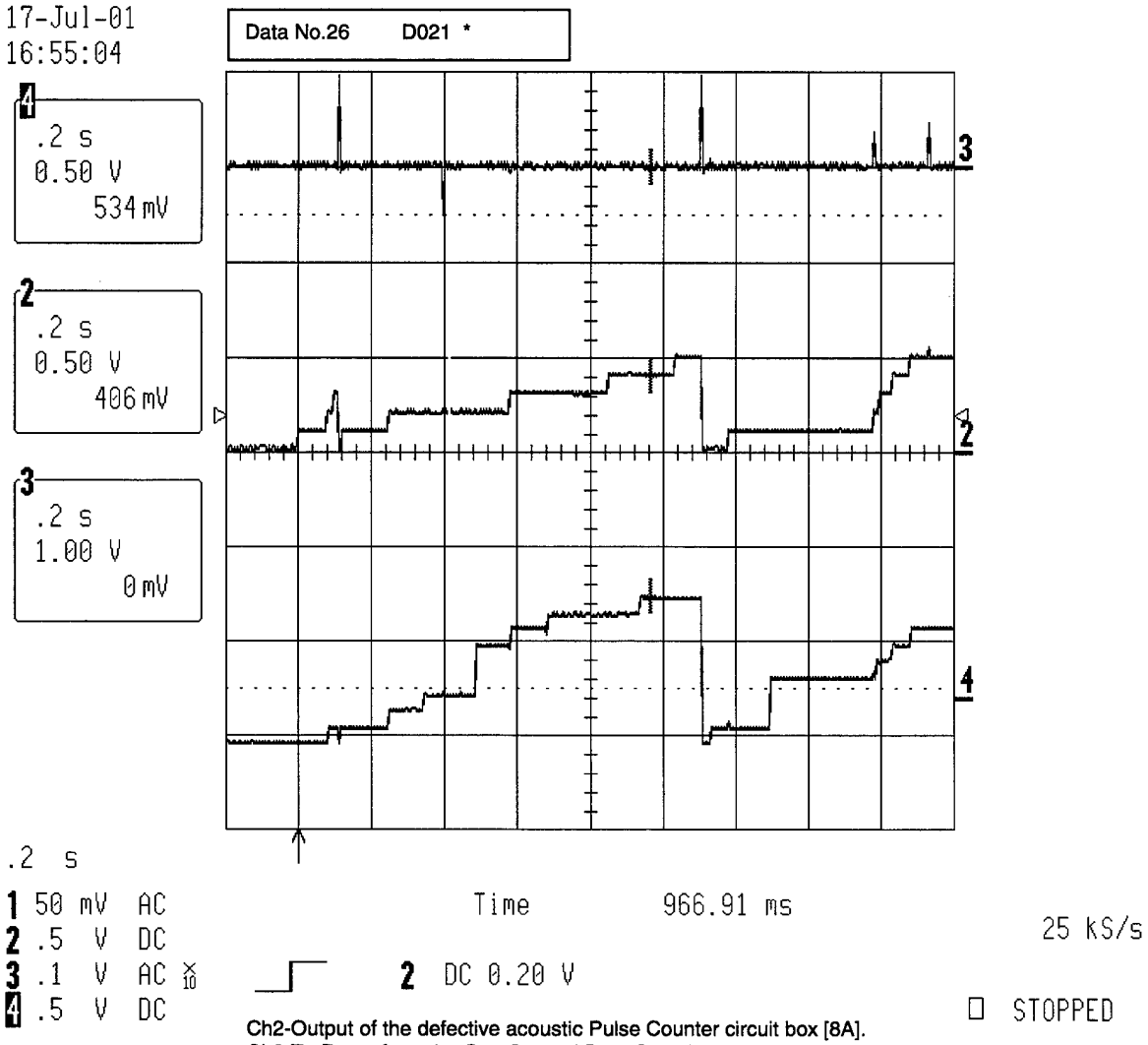

Ch2-Output of the defective acoustic Pulse Counter circuit box [8A].
Ch3-To Reset from the One Second Data Sample and Reset circuit box [9A].
Ch4-Output of the defective current Pulse Counter circuit box [5C].
Here two reset pulses are present separated by one second time interval on Ch3.
Ch2 and Ch4 show nice counts of bad pulses.

Figure 31. Outputs from two counters coincide with reset pulses as expected.

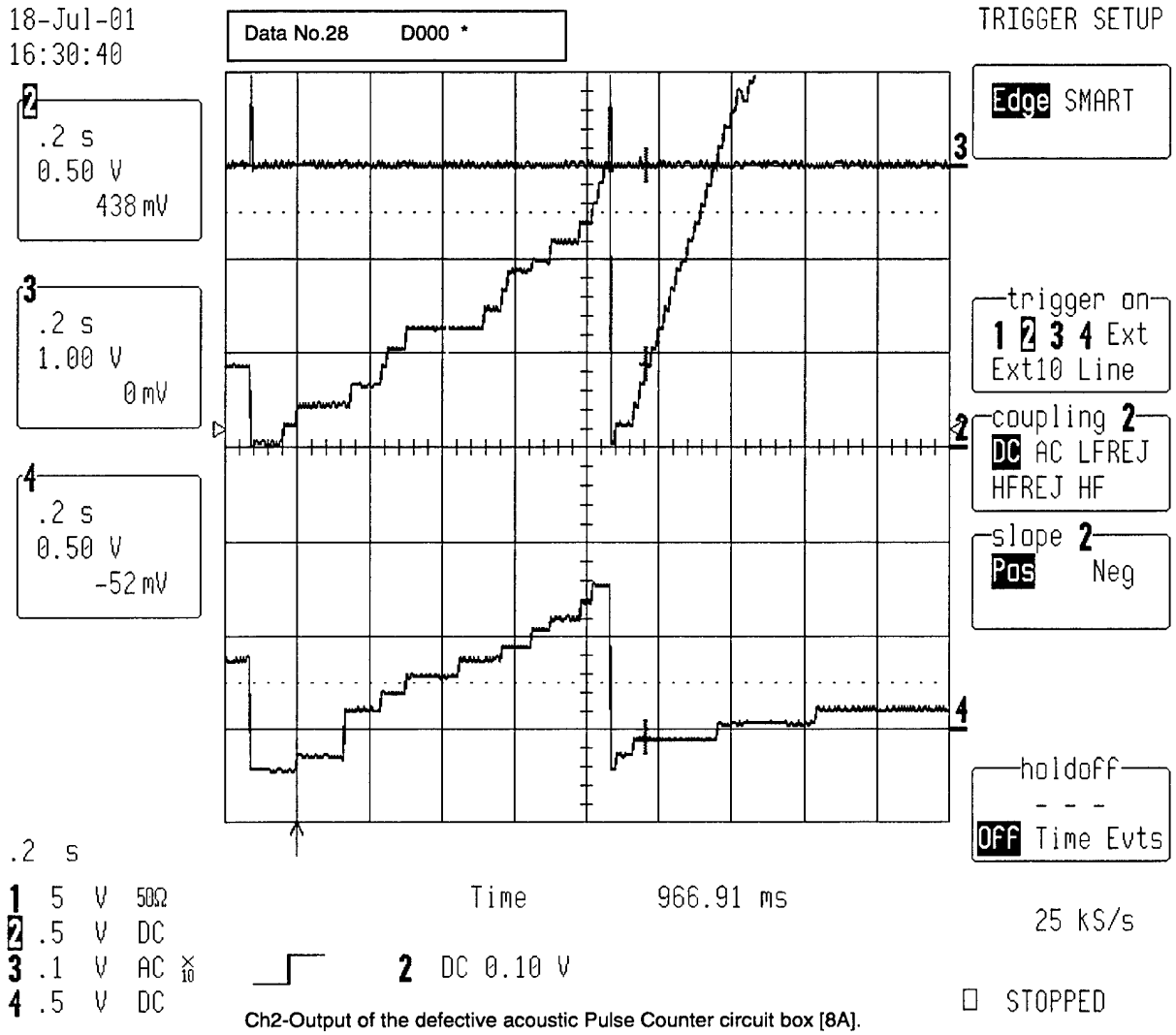

Ch2-Output of the defective acoustic Pulse Counter circuit box [8A].
Ch3-To Reset from the One Second Data Sample and Reset circuit box [9A].
Ch4-Output of the defective current Pulse Counter circuit box [5C].
Here Ch2 and Ch4 show nice counts of bad acoustic and current pulses between two reset pulses (before 1st vertical division and after 5th vertical division) on Ch3.

Figure 32. Step outputs from two counters between two reset pulses.

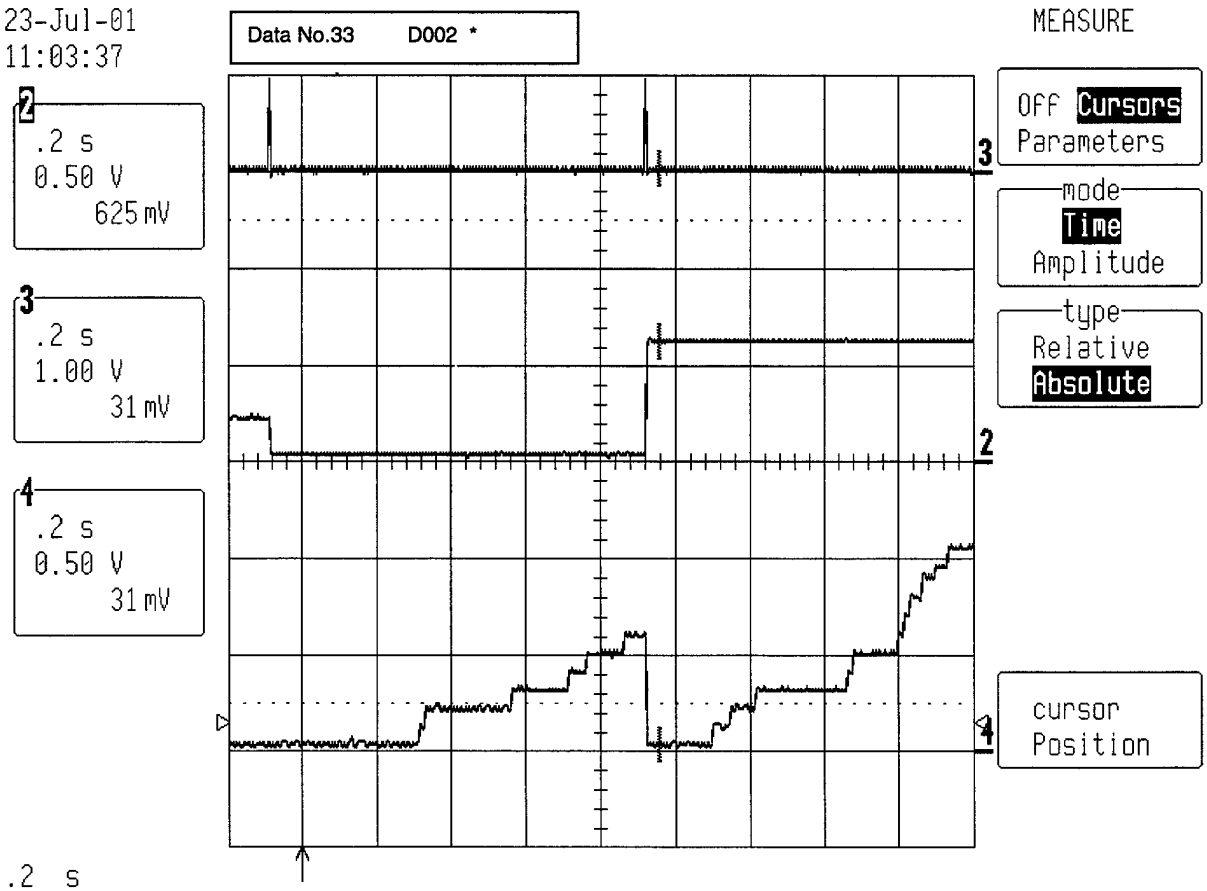

Ch2-Current pulses output of the One second Data Sample and Reset circuit box [9A].
Ch3-To Reset from the One Second Data Sample and Reset circuit box [9A].
Ch4-Current pulses input to the One second Data Sample and Reset circuit box [9A].
Two reset pulses are present on Ch3.
The value of the signal on Ch4 at the cursor is 609 mV and that on Ch2 at the cursor is 31mV.
Note: Compare with the next oscilloscope display.

Figure 33. Defective current pulses output transfer (before transfer).

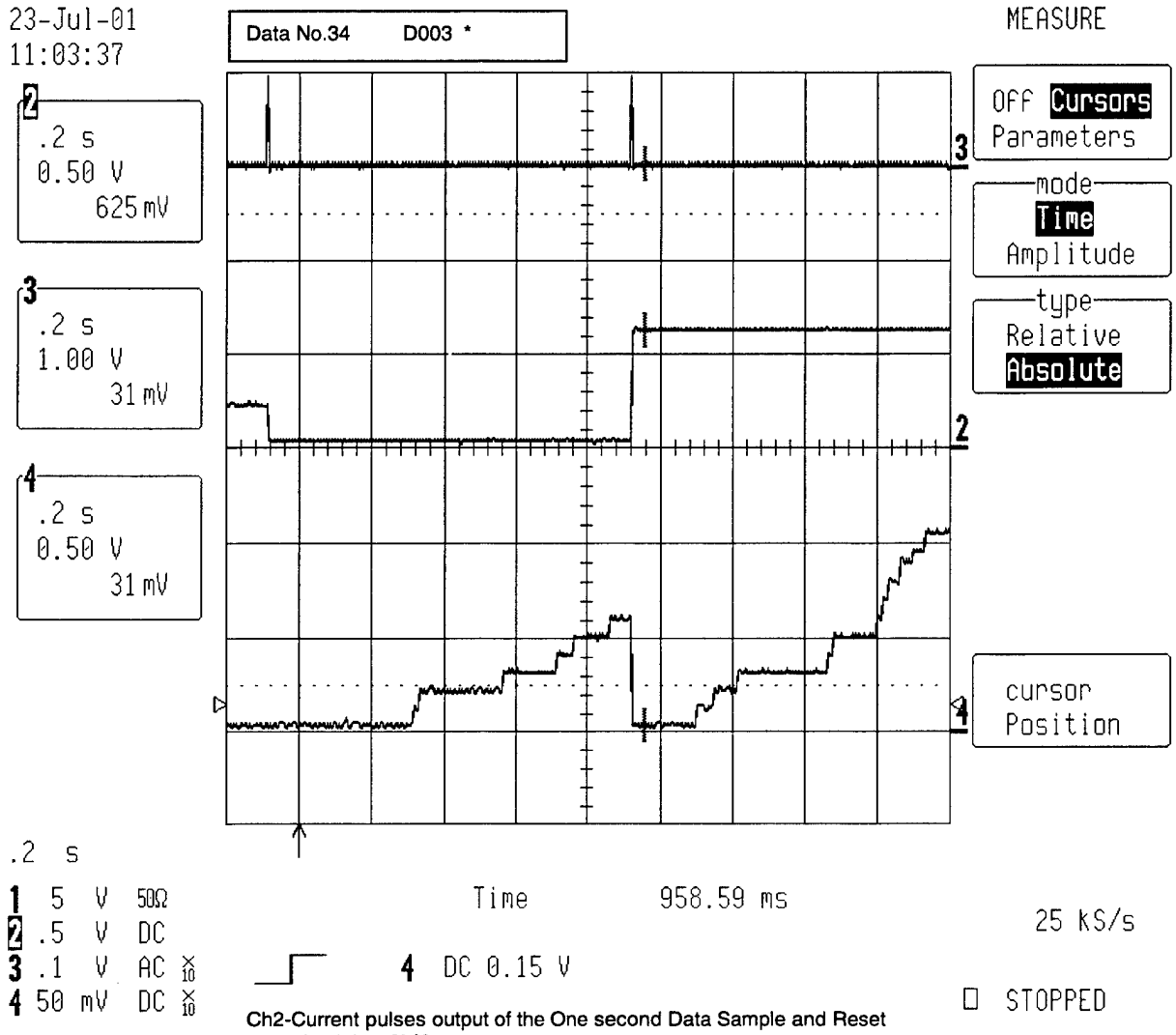

Ch2-Current pulses output of the One second Data Sample and Reset circuit box [9A].
Ch3-To Reset from the One Second Data Sample and Reset circuit box [9A].
Ch4-Current pulses input to the One second Data Sample and Reset circuit box [9A].
Two reset pulses are present on Ch3.
The value of the signal on Ch4 at the cursor now is changed to 31 mV and that on Ch2 at the cursor is changed to 625 mV.
Note: Compare with the previous oscilloscope display.

Figure 34. Output of OPTO22 interface box [9A] after data transfer.

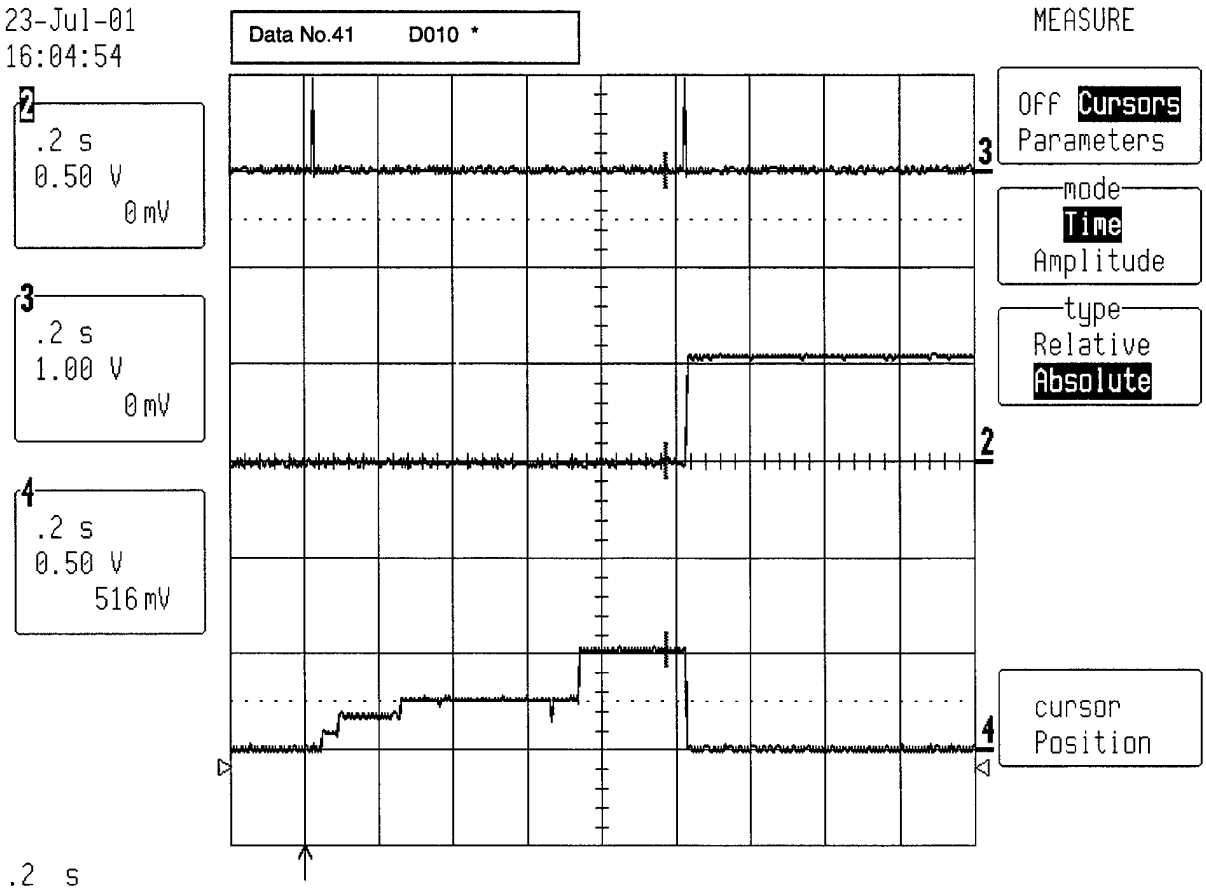

Ch2-Acoustic pulses output of the One second Data Sample and Reset circuit box [9A].
Ch3-To Reset from the One Second Data Sample and Reset circuit box [9A].
Ch4-Acoustic pulses input to the One second Data Sample and Reset circuit box [9A].
Two reset pulses are present on Ch3 on 1st and 6th vertical divisions. The value of the signal on Ch4 at the cursor is 516 mV and that on Ch2 at the cursor is 0 mV.
Note: Compare with the next oscilloscope display.

Figure 35. Defective acoustic pulses output transfer (before transfer).

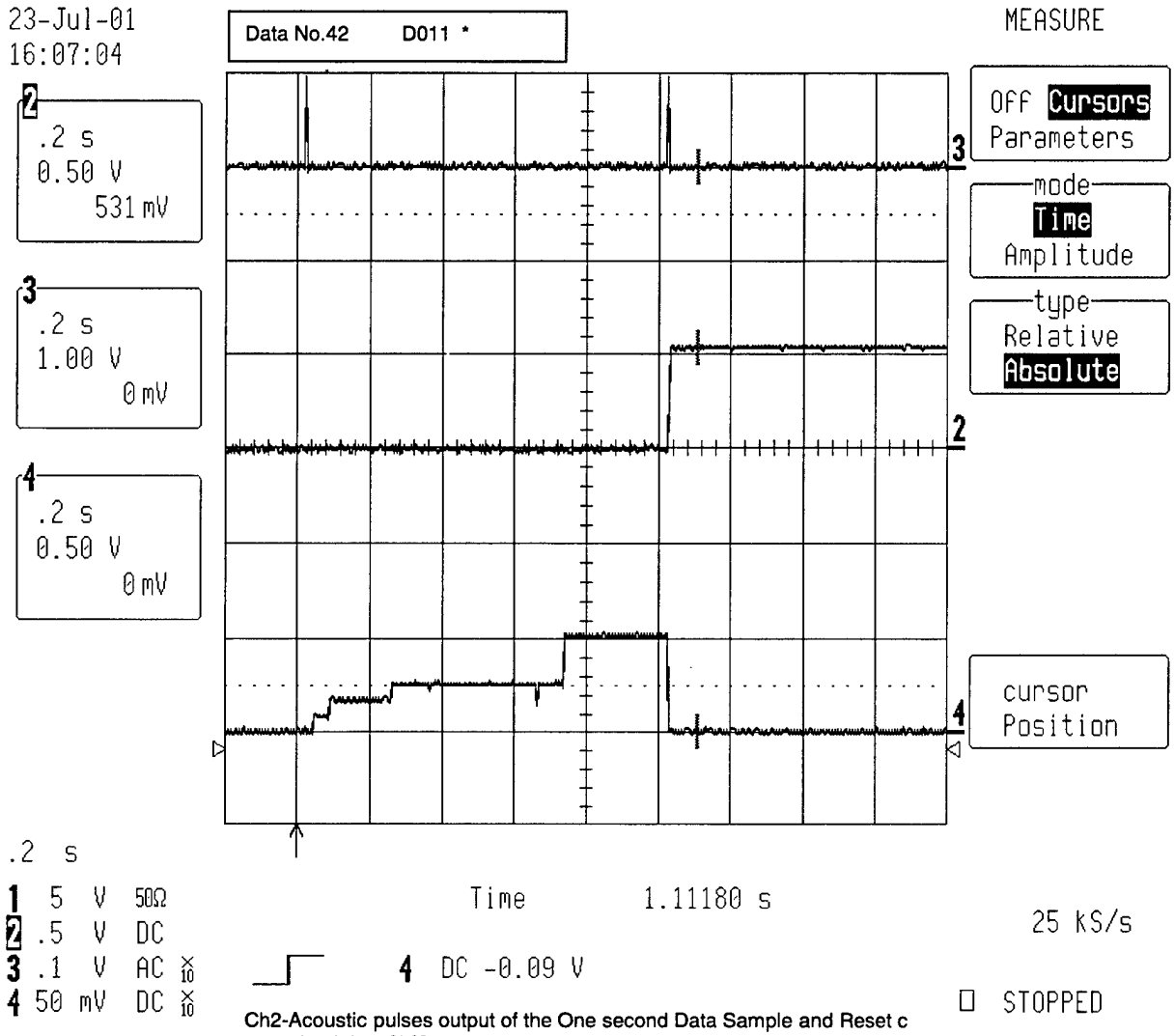

Ch2-Acoustic pulses output of the One second Data Sample and Reset c circuit box [9A].
Ch3-To Reset from the One Second Data Sample and Reset circuit box [9A].
Ch4-Acoustic pulses input to the One second Data Sample and Reset circuit box [9A].
Two reset pulses are present on Ch3 on 1st and 6th vertical divisions. The value of the signal on Ch4 at the cursor is now changed to 0 mV and that on Ch2 at the cursor to 531 mV after data transfer.
Note: Compare with the previous oscilloscope display.

Figure 36. Defective acoustic pulses output transfer (after transfer).

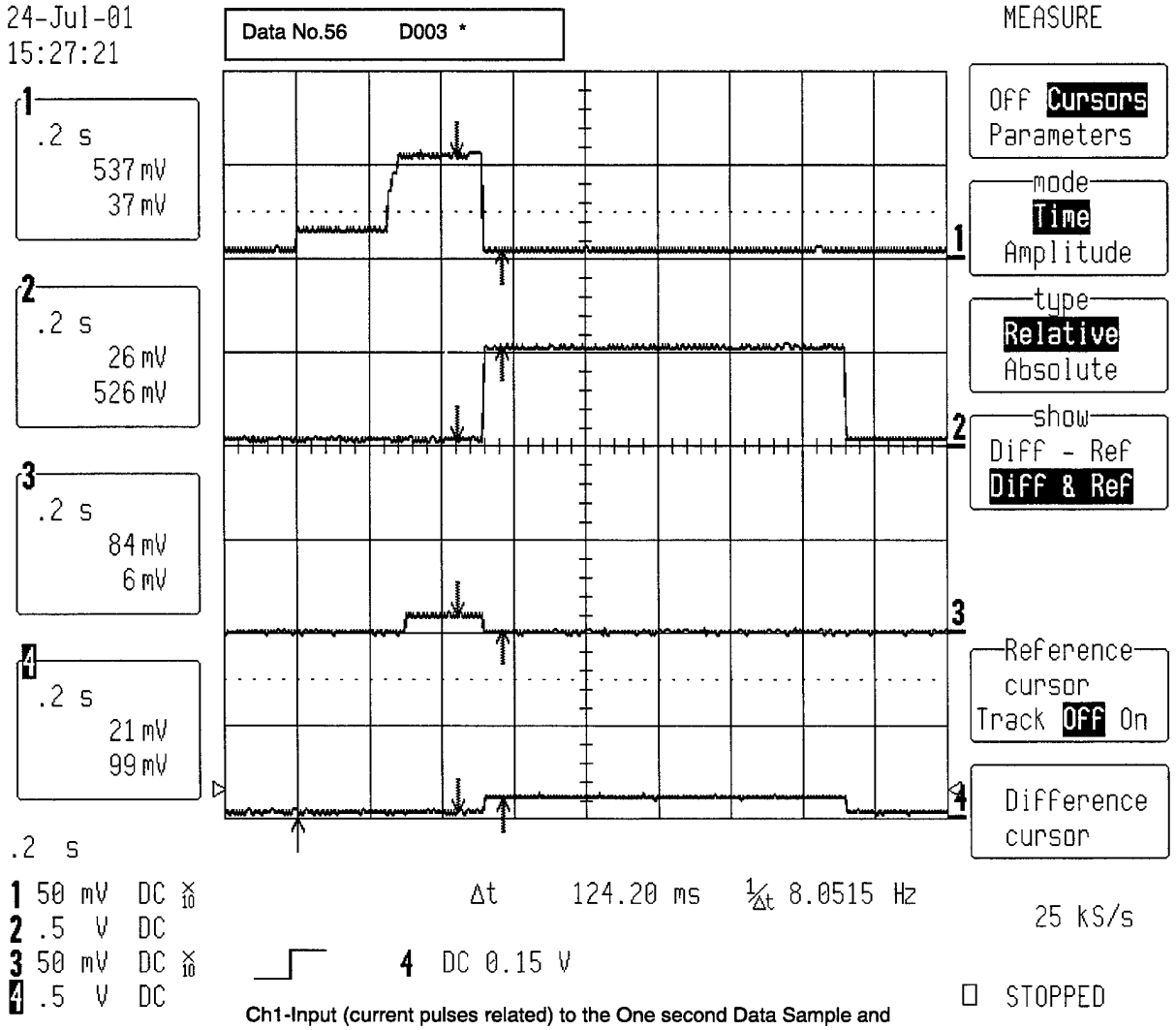

Ch1-Input (current pulses related) to the One second Data Sample and Reset circuit box [9A].
Ch2-Output (current pulses related) from the One second Data Sample and Reset circuit box [9A].
Ch3-Input (acoustic pulses related) to the One second Data Sample and Reset circuit box [9A].
Ch4- Output (acoustic pulses related) from the One second Data Sample and Reset circuit box [9A].
Note: This is a special display where both cursors (before and after data transfer)on each channel
are shown.
---Voltages corresponding to the cursor positions—

Before transfer	After Transfer
Ch1-537 mV	37 mV
Ch2-26 mV	526 mV
Ch3-84 mV	6 mV
Ch4-21 mV	99 mV

Note: Compare with the next display.

Figure 37. Inputs and outputs of the last circuit box [9A] in the chain (before transfer).

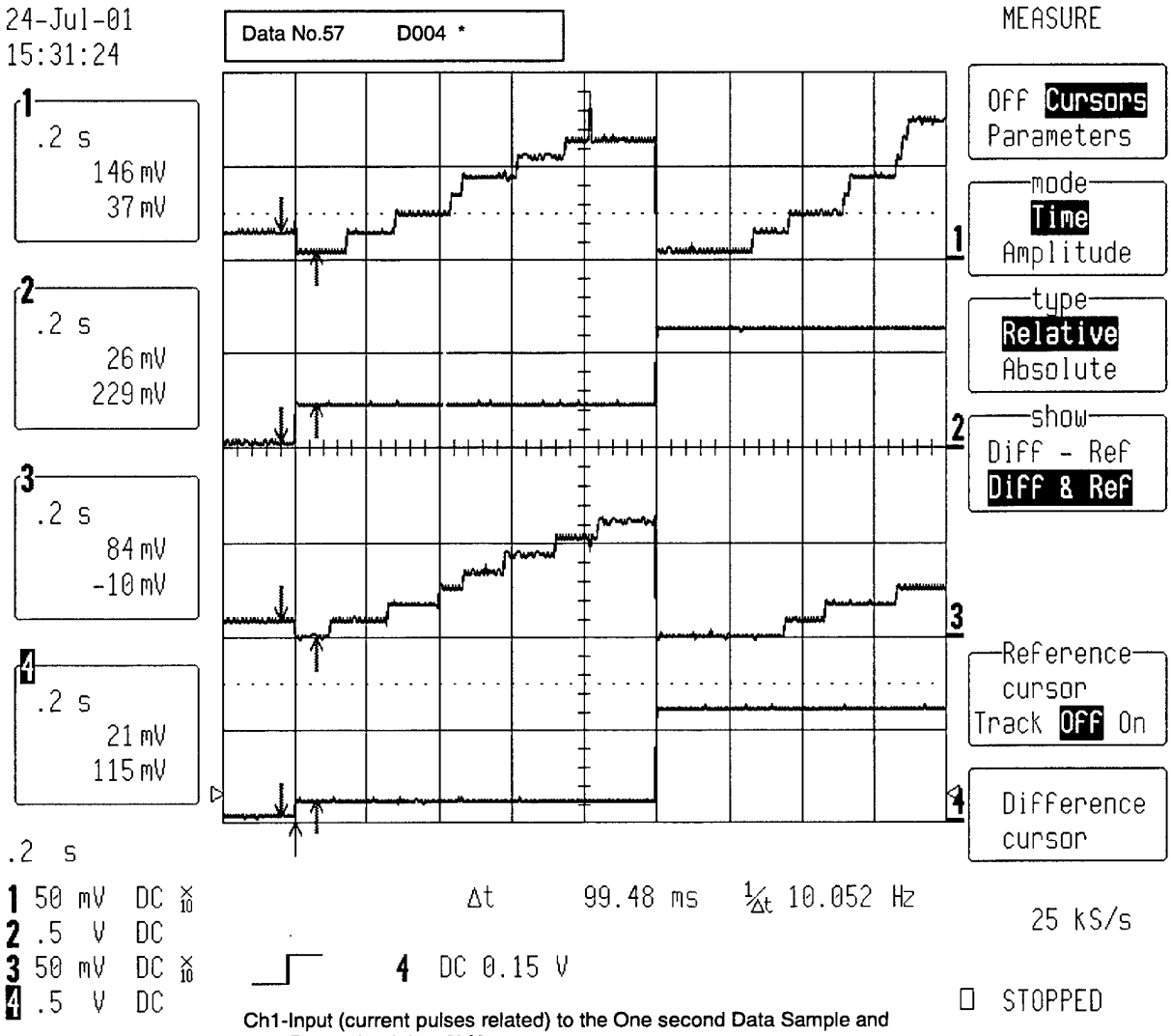

Ch1-Input (current pulses related) to the One second Data Sample and Reset circuit box [9A].
Ch2-Output (current pulses related) from the One second Data Sample and Reset circuit box [9A].
Ch3-Input (acoustic pulses related) to the One second Data Sample and Reset circuit box [9A].
Ch4- Output (acoustic pulses related) from the One second Data Sample and Reset circuit box [9A].
Note: Cursors are moved to the right to execute the first data transfer.
---Voltages corresponding to the cursor positions—

Before transfer	After Transfer
Ch1-146 mV	37 mV
Ch2-26 mV	229 mV
Ch3-84 mV	10 mV
Ch4-21 mV	115 mV

Note: Compare with the previous and next displays.

Figure 38. Inputs and outputs of the last circuit box [9A] in the chain (after transfer).

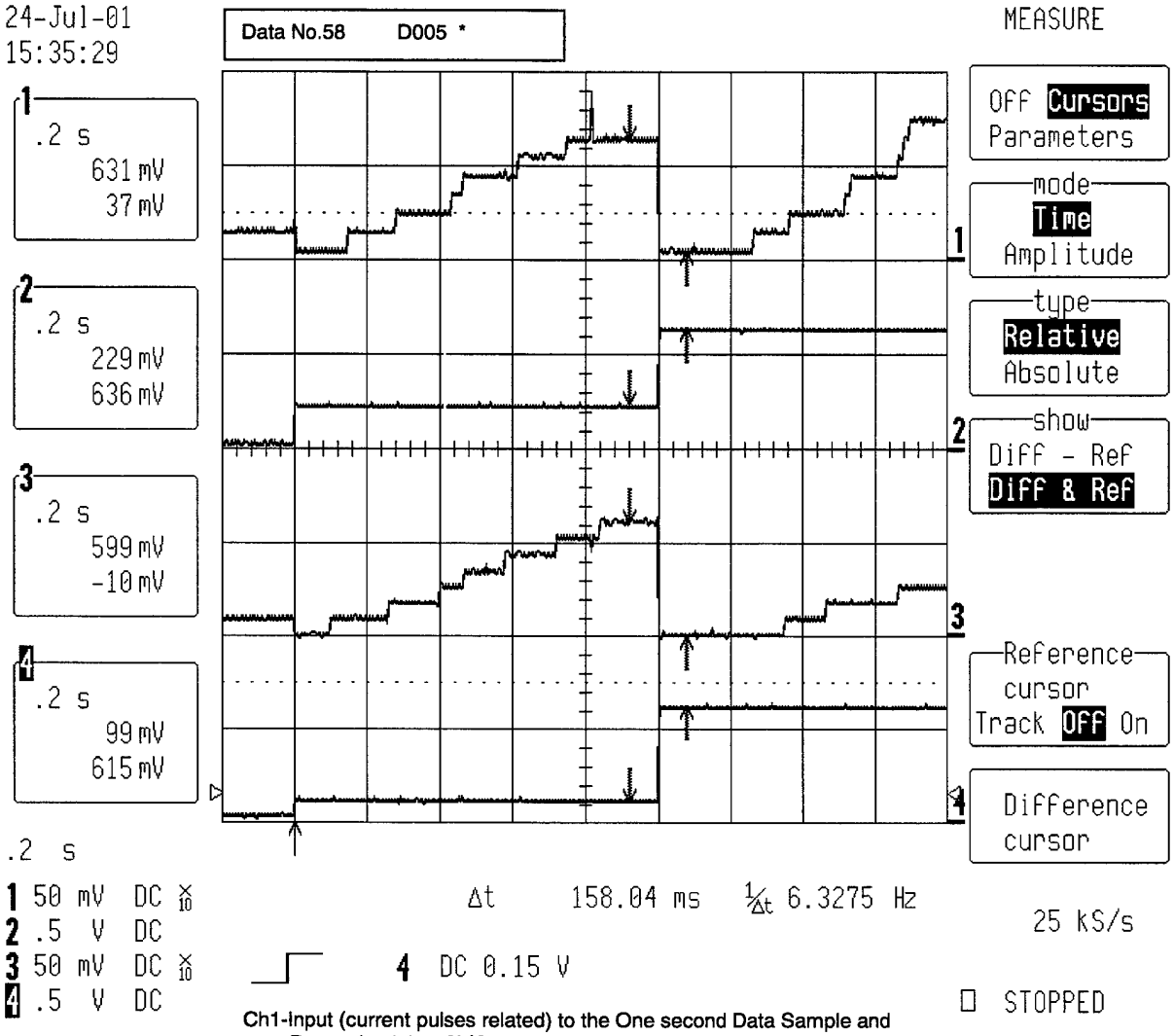

Ch1-Input (current pulses related) to the One second Data Sample and Reset circuit box [9A].
Ch2-Output (current pulses related) from the One second Data Sample and Reset circuit box [9A].
Ch3-Input (acoustic pulses related) to the One second Data Sample and Reset circuit box [9A].
Ch4- Output (acoustic pulses related) from the One second Data Sample and Reset circuit box [9A].
Note: Cursors are moved again to the right to execute the second data transfer.
---Voltages corresponding to the cursor positions—

Before transfer	After Transfer
Ch1-631mV	37 mV
Ch2-229 mV	636 mV
Ch3-599 mV	10 mV
Ch4- 99mV	615mV

Note: Compare with the two previous displays.

Figure 39. Inputs and outputs of the last circuit box [9A] in the chain (after second transfer).

APPENDIX A: RECORD OF COLLECTED DATA

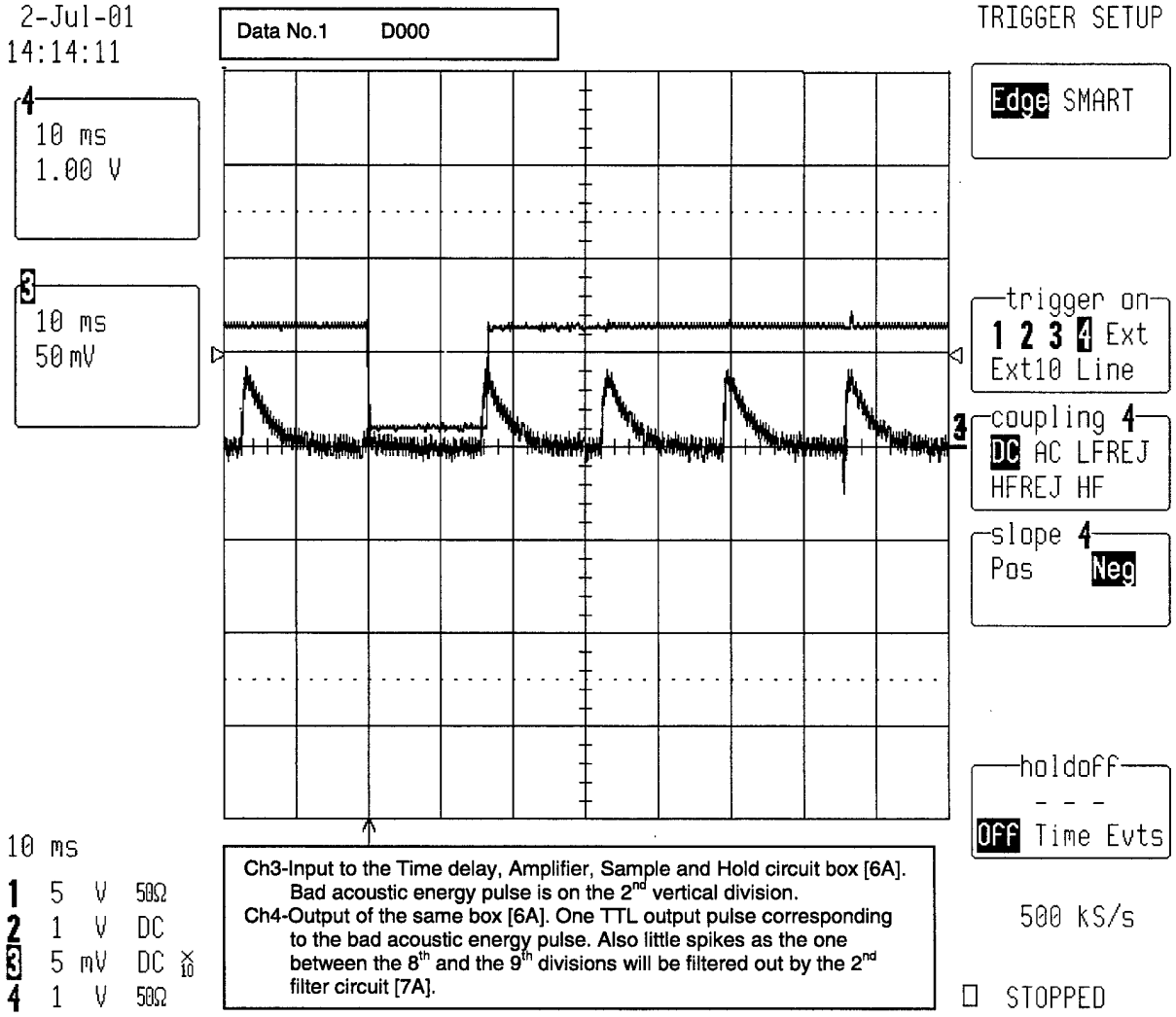

Ch3-Input to the Time delay, Amplifier, Sample and Hold circuit box [6A]. Bad acoustic energy pulse is on the 2nd vertical division.
Ch4-Output of the same box [6A]. One TTL output pulse corresponding to the bad acoustic energy pulse. Also little spikes as the one between the 8th and the 9th divisions will be filtered out by the 2nd filter circuit [7A].

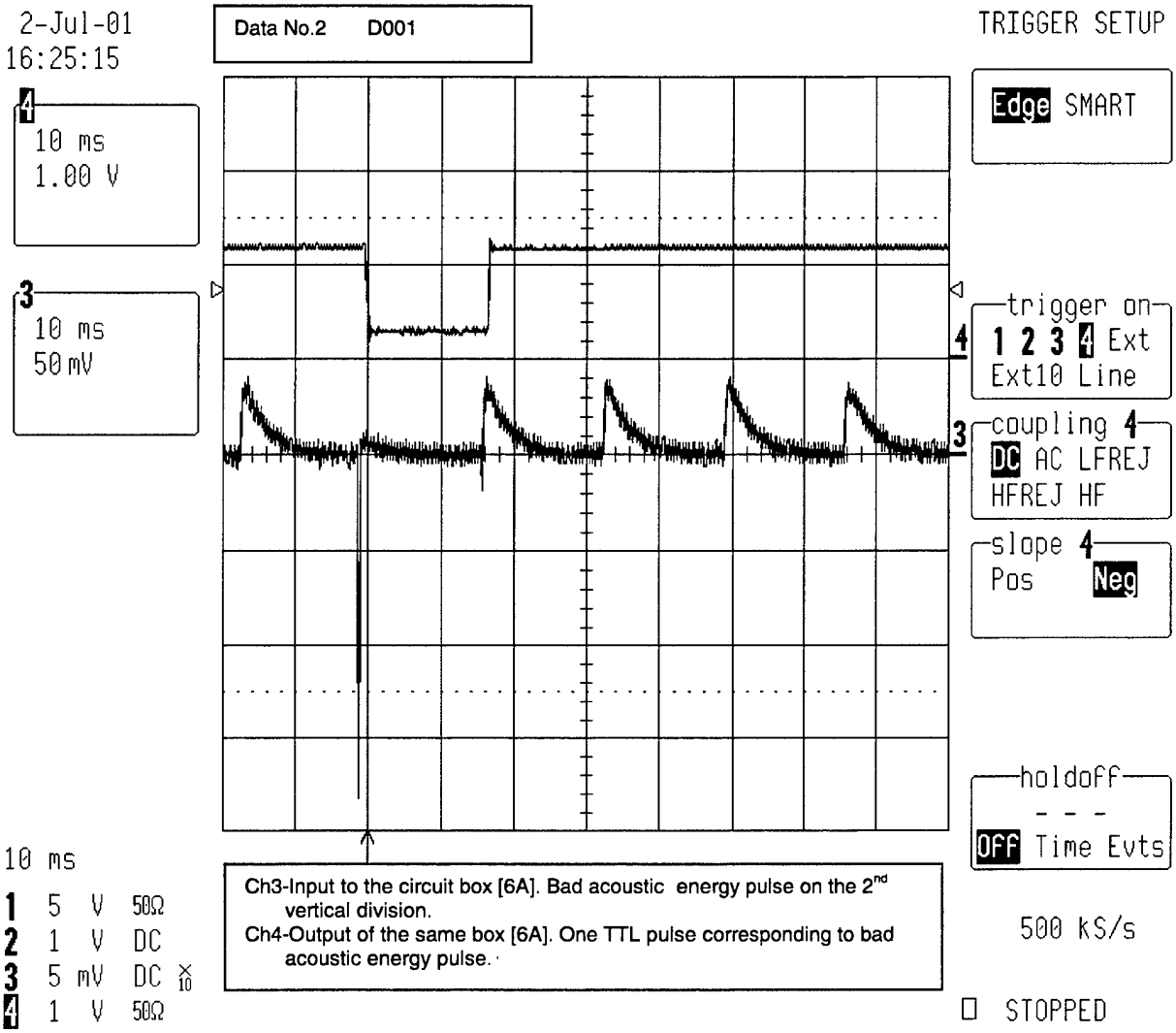

Ch3-Input to the circuit box [6A]. Bad acoustic energy pulse on the 2nd vertical division.
Ch4-Output of the same box [6A]. One TTL pulse corresponding to bad acoustic energy pulse.

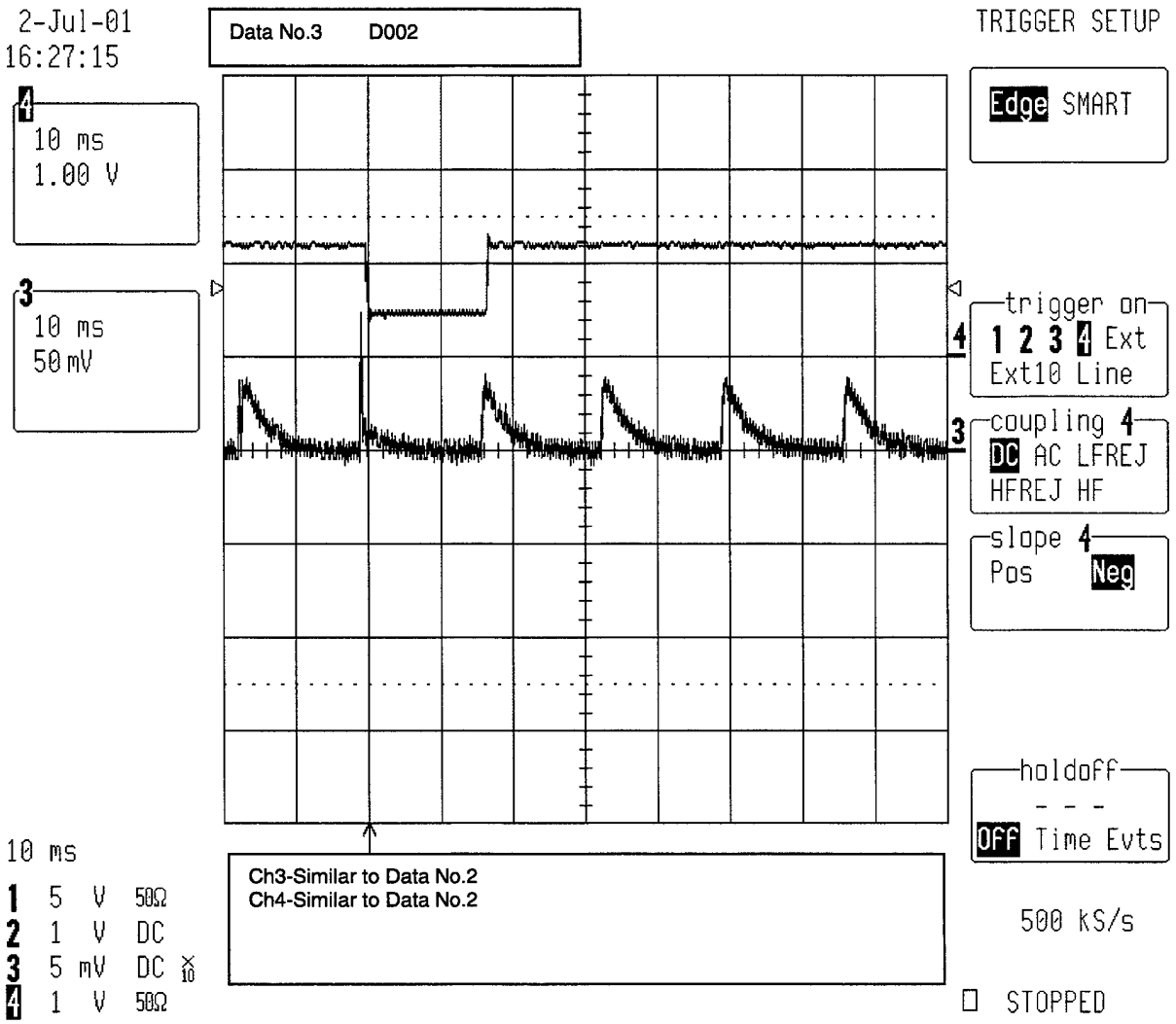
2-Jul-01
16:27:15
Data No.3 D002
TRIGGER SETUP
4
10 ms
1.00 V
3
10 ms
50 mV
Edge SMART
trigger on
4
1 2 3 4 Ext
Ext10 Line
coupling 4
3
DC AC LFREJ
HFREJ HF
slope 4
Pos Neg
holdoff
- - -
OFF Time Evts
10 ms
1 5 V 50Ω
2 1 V DC
3 5 mV DC X10
4 1 V 50Ω
Ch3-Similar to Data No.2
Ch4-Similar to Data No.2
500 kS/s
STOPPED

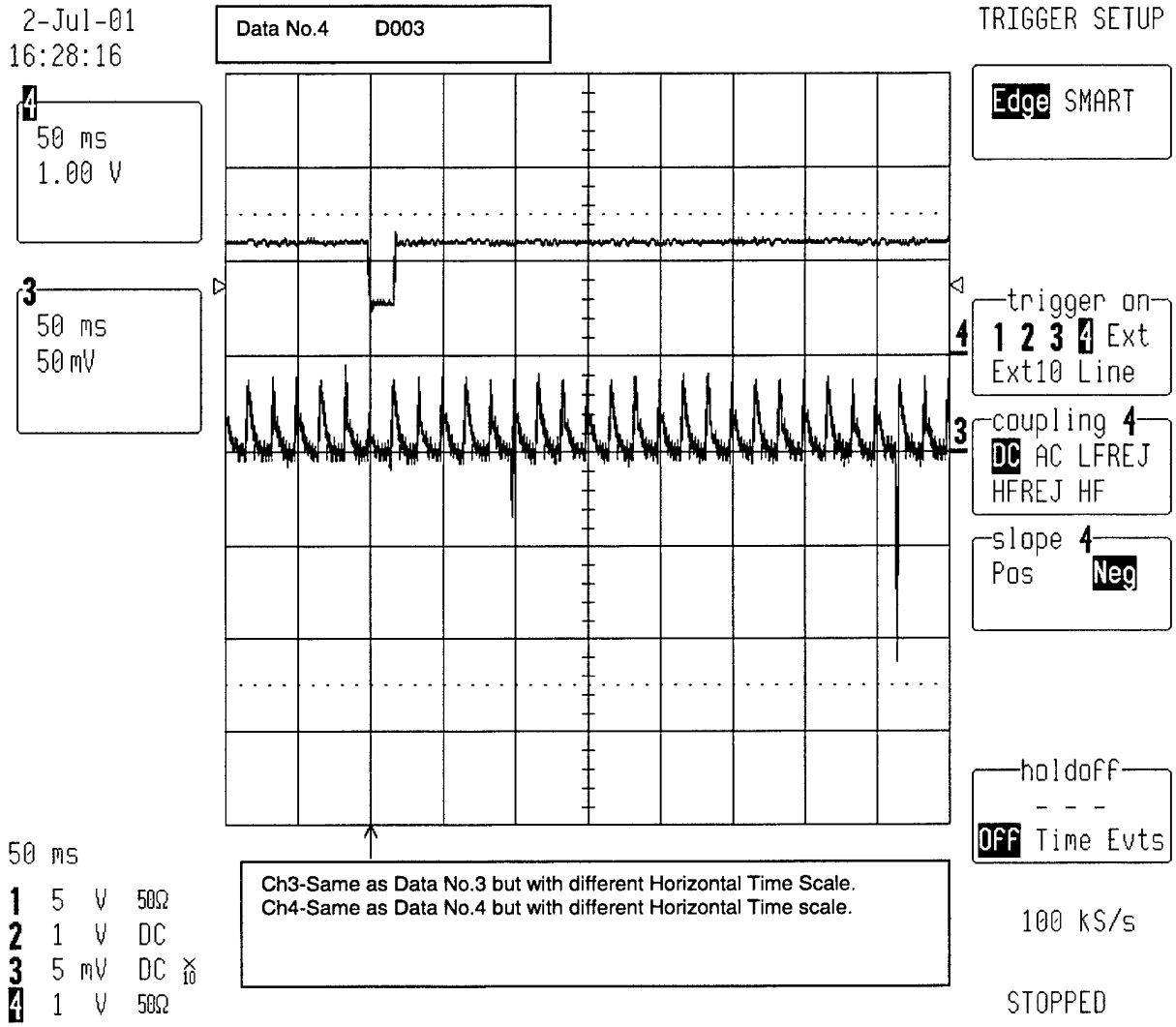
2-Jul-01
16:28:16
Data No.4 D003
TRIGGER SETUP
4
50 ms
1.00 V
3
50 ms
50 mV
Edge SMART
trigger on
1 2 3 4 Ext
Ext10 Line
coupling 4
DC AC LFREJ
HFREJ HF
slope 4
Pos Neg
holdoff
- - -
Off Time Evts
50 ms
1 5 V 50Ω
2 1 V DC
3 5 mV DC 10
4 1 V 50Ω
Ch3-Same as Data No.3 but with different Horizontal Time Scale.
Ch4-Same as Data No.4 but with different Horizontal Time scale.
100 kS/s
STOPPED

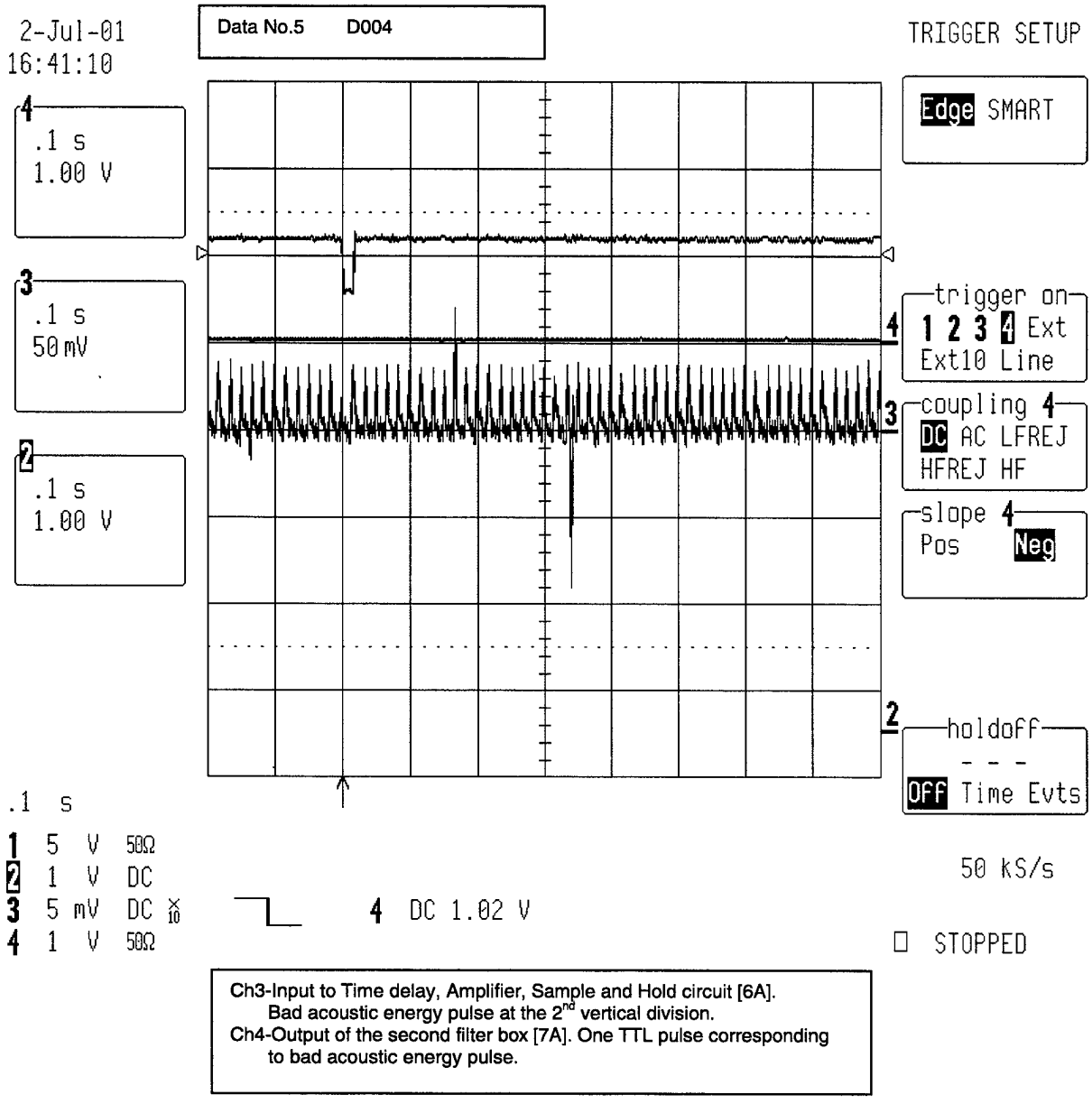

Ch3-Input to Time delay, Amplifier, Sample and Hold circuit [6A].
Bad acoustic energy pulse at the 2nd vertical division.
Ch4-Output of the second filter box [7A]. One TTL pulse corresponding to bad acoustic energy pulse.

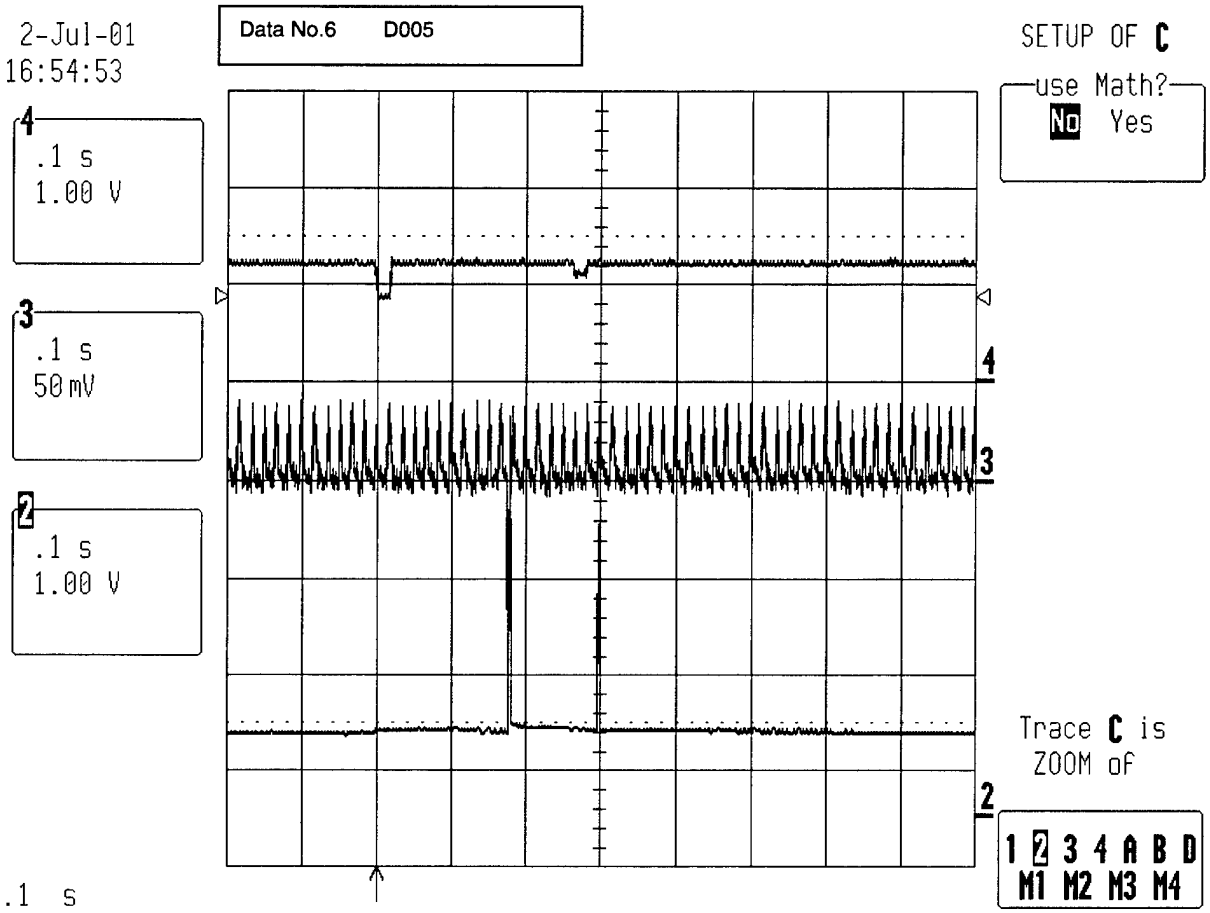

Ch2-Output of current pulseThreshold Amplifier, Comparator circuit box [4C]. Bad current pulses appeared.
Ch3-Input to the circuit box [6A].These are integrated acoustic energy pulses.
Ch4-Output of the circuit box [6A]. Two TTL outputs are present corresponding to two bad acoustic energy pulses.

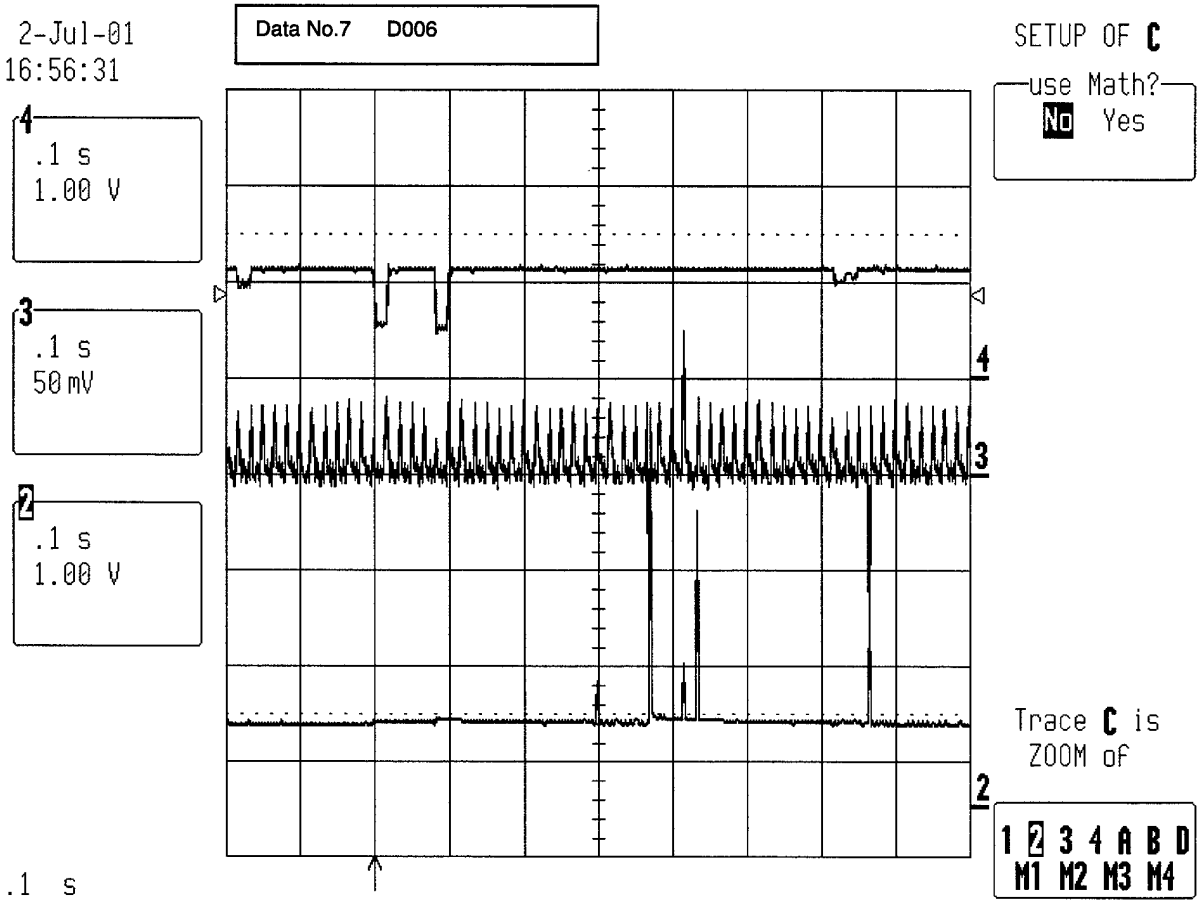

Ch2-Similar to Data No.6
Ch3-Similar to Data No.6
Ch4-Similar to Data No.6

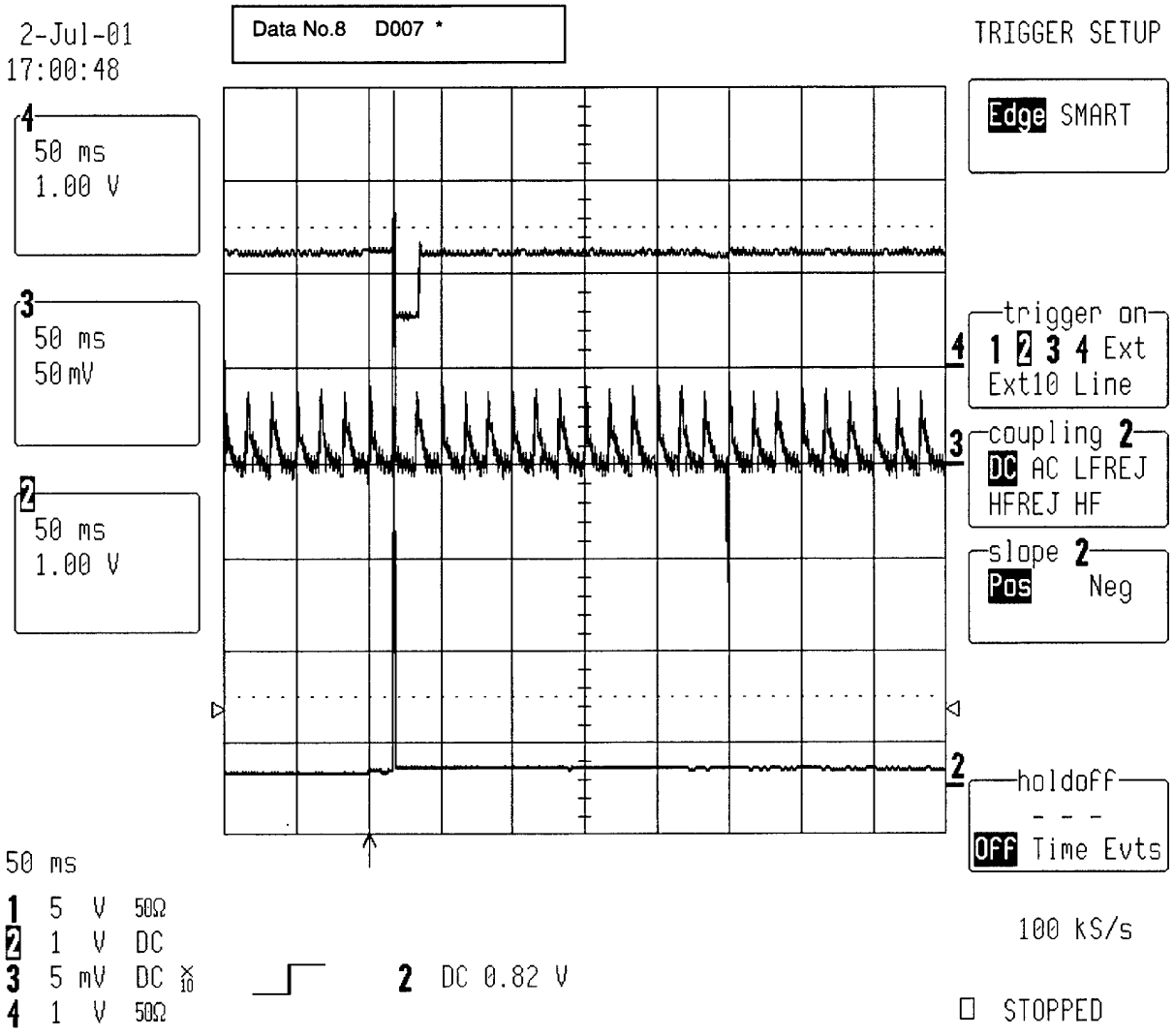

Ch2-Output of current pulse Threshold Amplifier, Comparator circuit box [4C]
Ch3-Input to the acoustic pulse Time delay Amplifier, Sample and Hold circuit box [6A]
Ch4-Output of the second filter box [7A].
Here bad current pulse, bad acoustic energy pulse and the corresponding TTL output pulse coincide

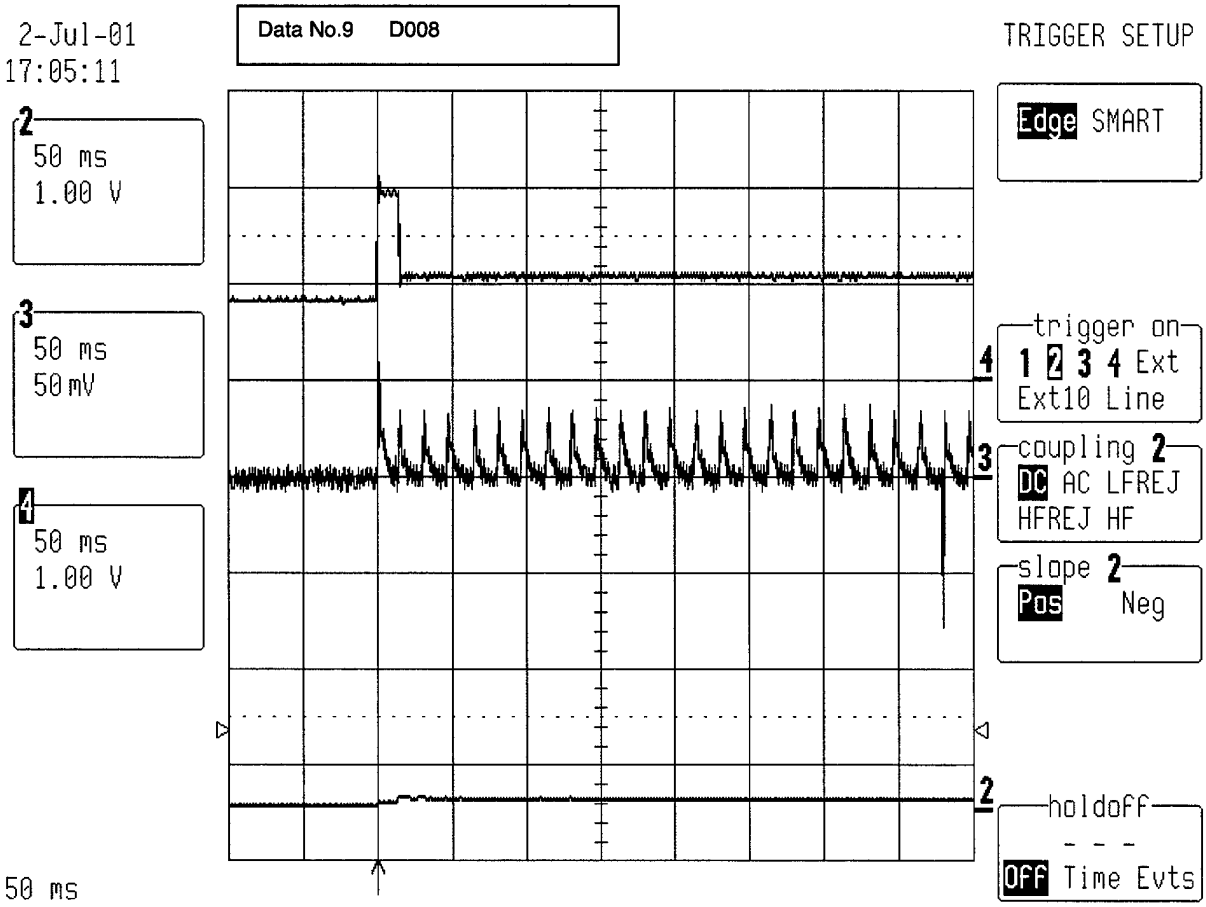

Ch2-Similar to Data No.8
Ch3-Similar to Data No.8
Ch4-Similar to Data No.8
In this case the bad acoustic pulse appears to be taller than the normal one. Hence the TTL output on the Ch 4 got reversed.

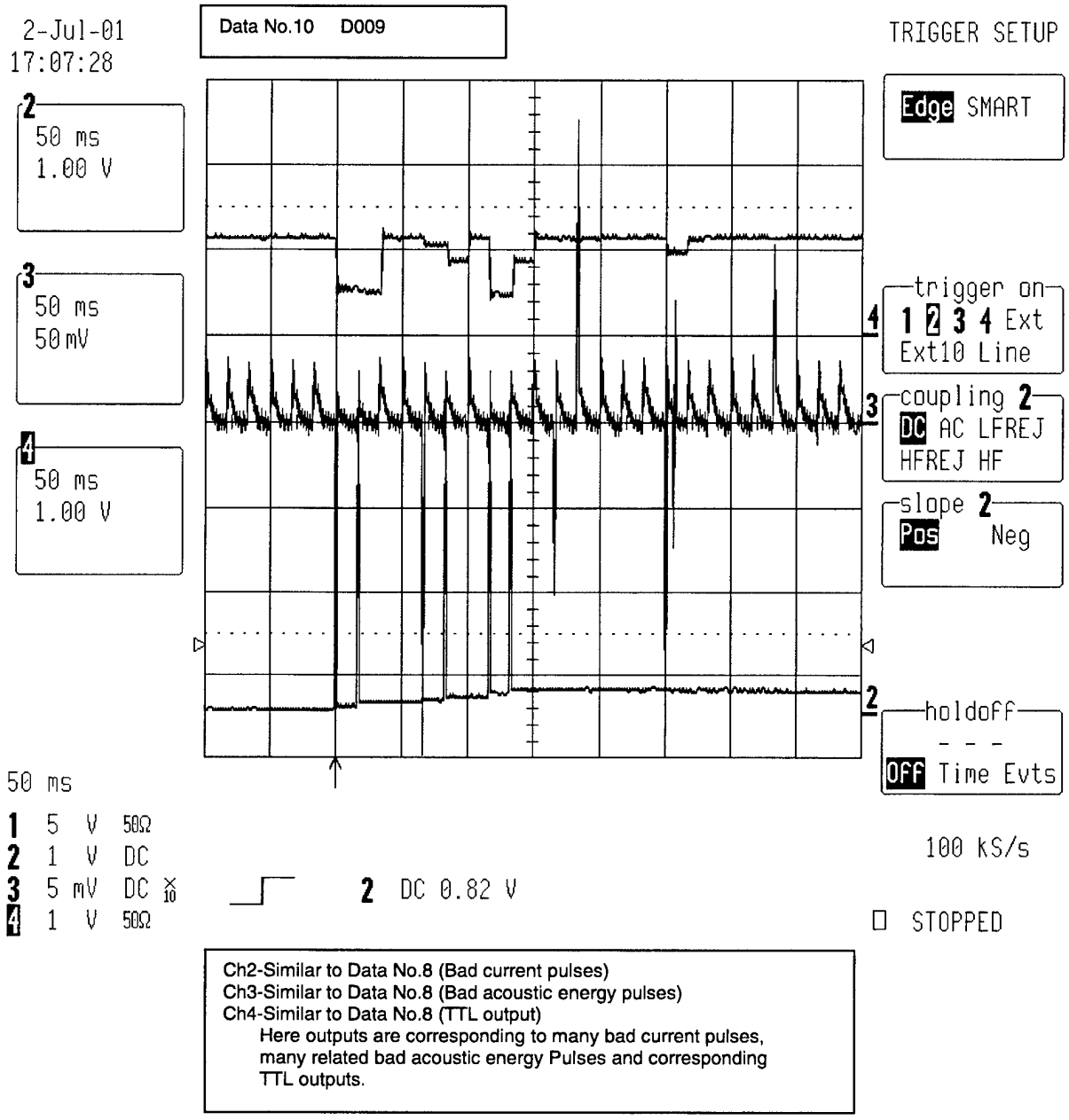

Ch2-Similar to Data No.8 (Bad current pulses)
Ch3-Similar to Data No.8 (Bad acoustic energy pulses)
Ch4-Similar to Data No.8 (TTL output)
Here outputs are corresponding to many bad current pulses, many related bad acoustic energy Pulses and corresponding TTL outputs.

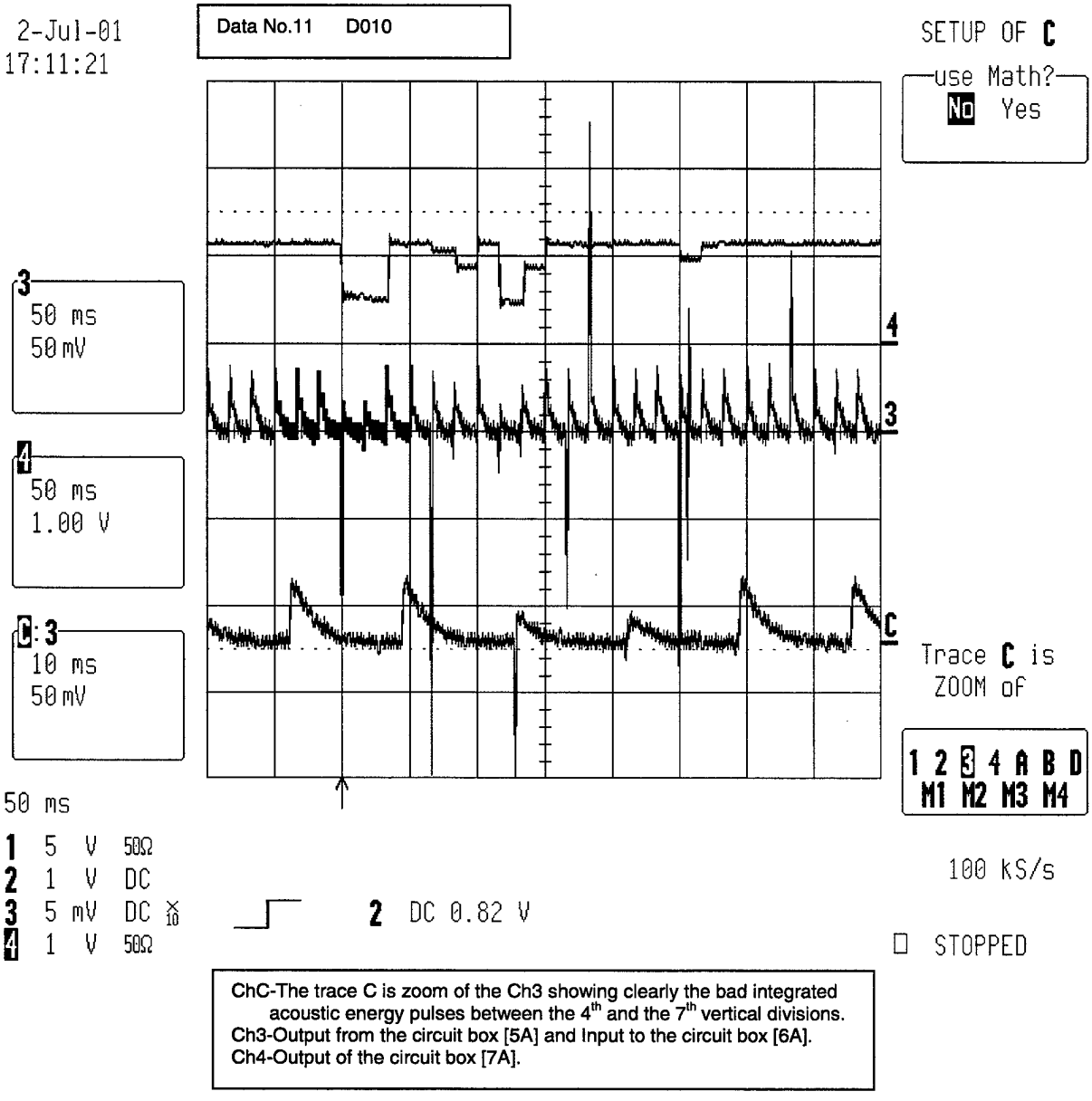

ChC-The trace C is zoom of the Ch3 showing clearly the bad integrated acoustic energy pulses between the 4th and the 7th vertical divisions.
Ch3-Output from the circuit box [5A] and Input to the circuit box [6A].
Ch4-Output of the circuit box [7A].

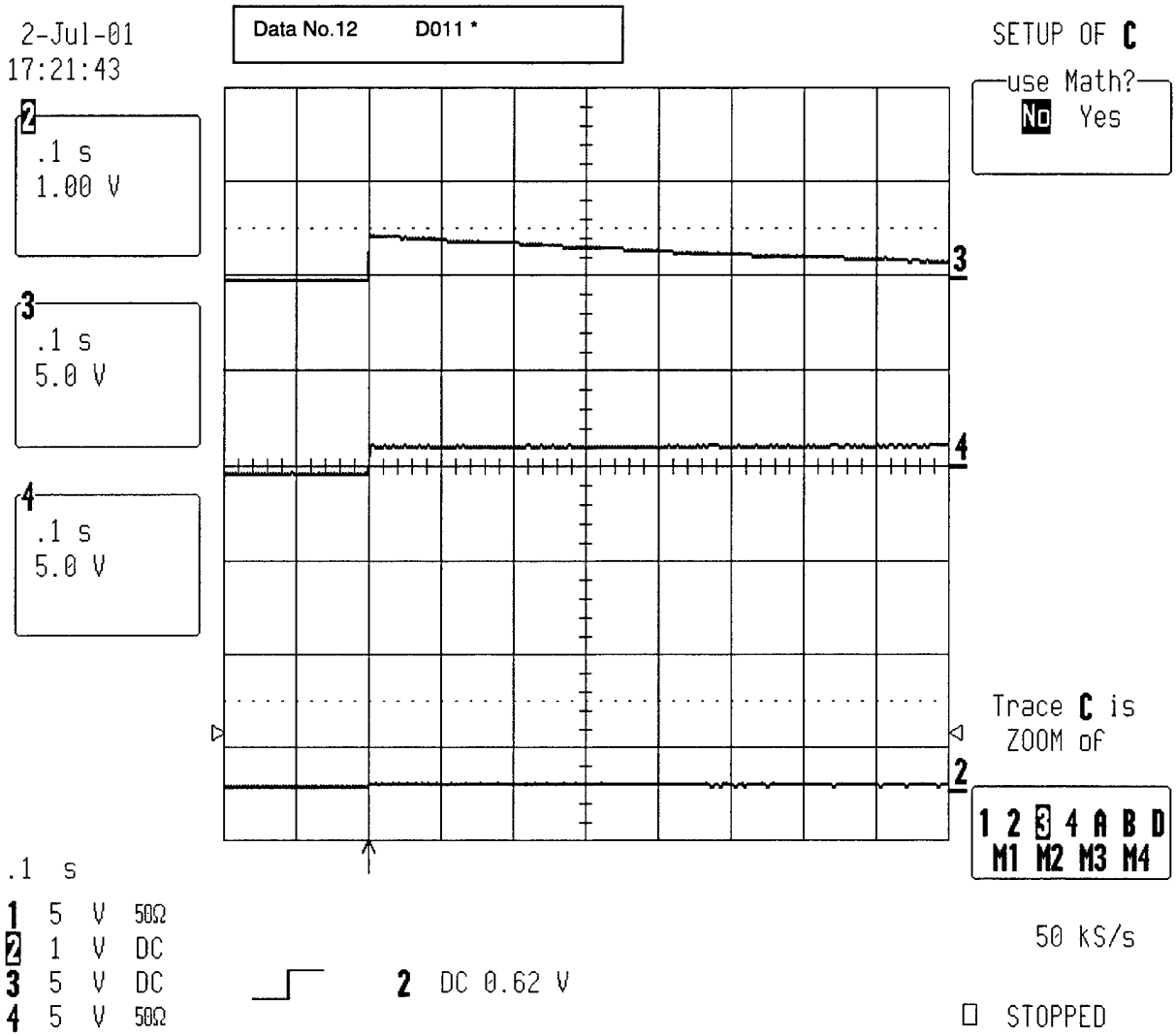

Ch2-Output of Threshold Amplifier. Comparator circuit box [4C].
Ch3-Output of defective current Pulse Counter circuit box [5C]
Ch4-Output of the defective acoustic Pulse Counter Circuit box [8A]

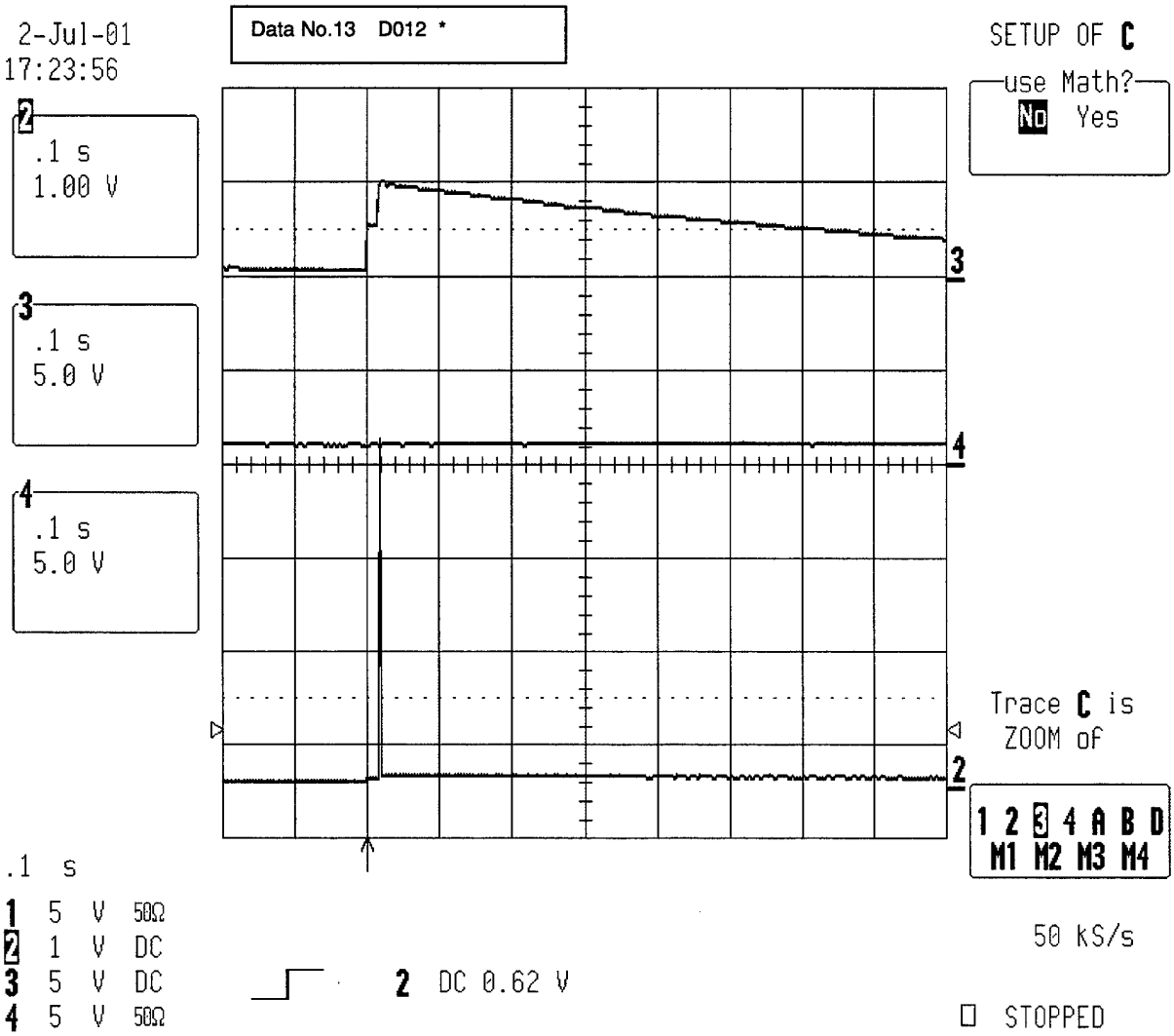

Ch2-Output of the current pulse Threshold Amplifier,Comparator circuit box [4C]
Ch3-Output of the defective current Pulse Counter circuit box [5C]
Ch4-Output of the defective acoustic Pulse Counter circuit box [8A].
Here events on Ch2 and Ch3 coincided but somehow no bad acoustic pulse on Ch4.

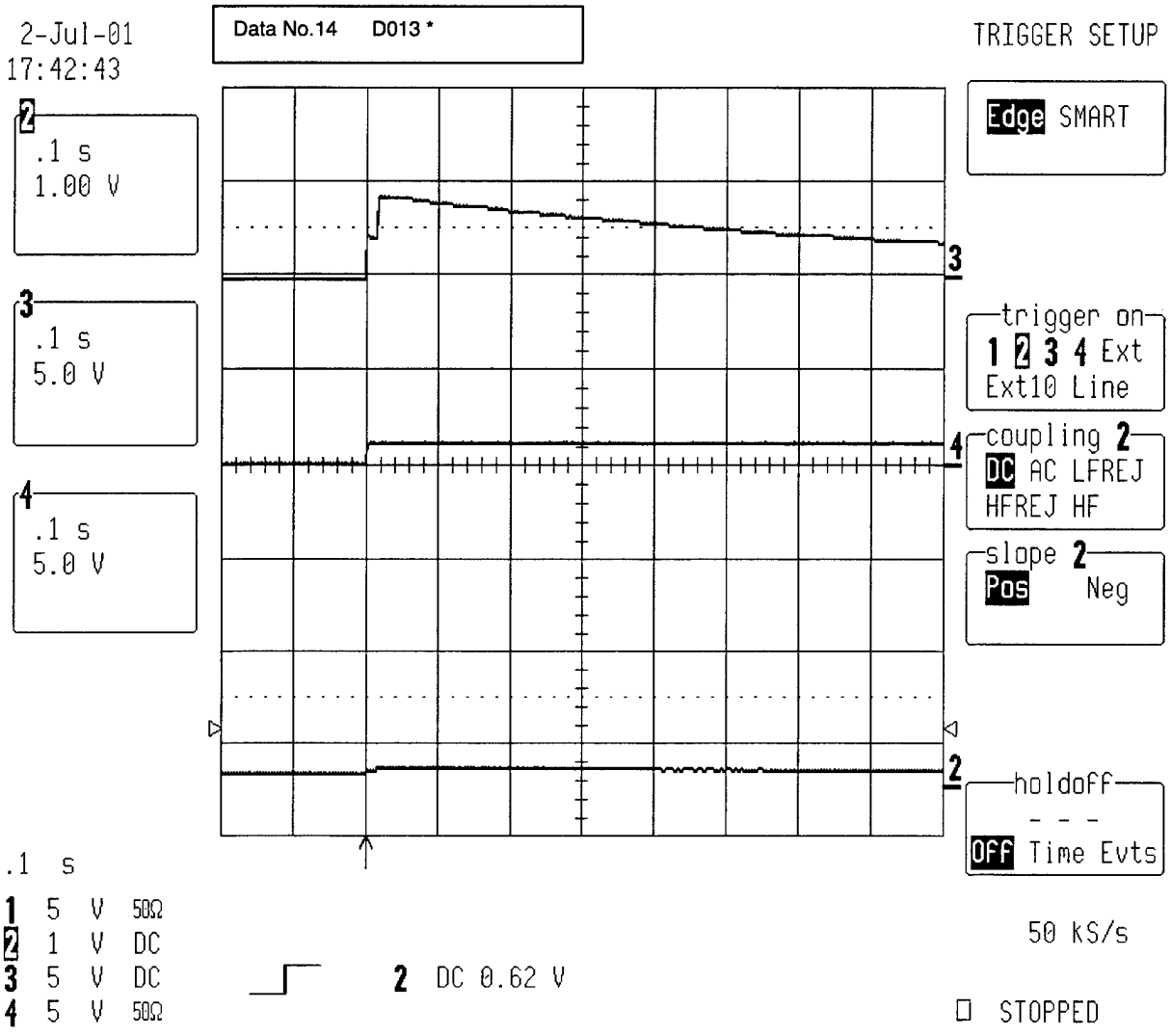

Ch2-Output of the current pulse Threshold Amplifier, Comparator circuit box [4C]
Ch3-Output of the defective current Pulse Counter circuit box [5C]
Ch4-Output of the defective acoustic Pulse Counter circuit box [8A].
Here the Ch3 shows the steps at the 2nd vertical division due to the double bad current pulses. Also the display shows the coincidence of the events on all 3 channels as expected.

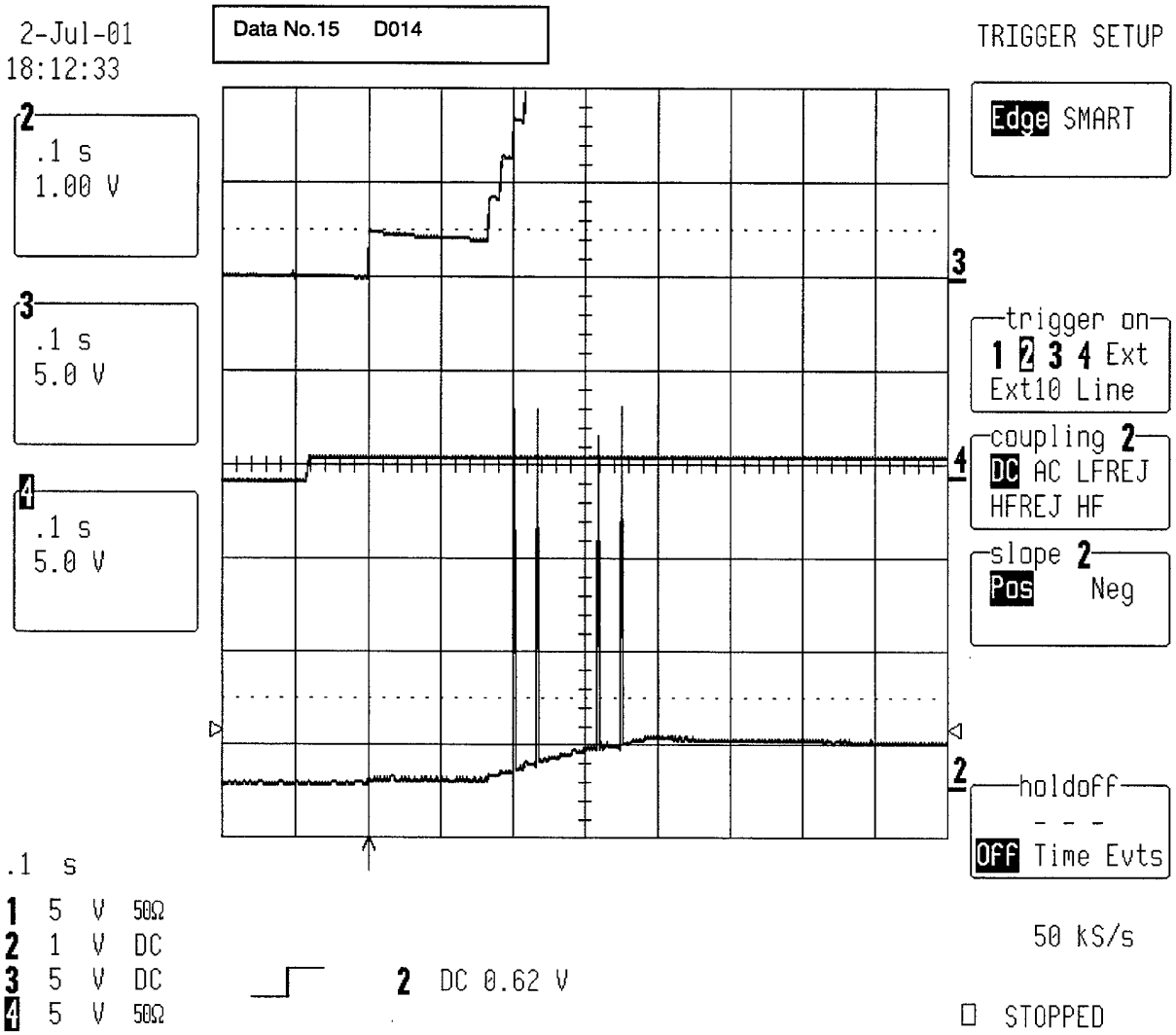

Ch2-Output from the current pulse Threshold Amplifier, Comparator circuit box [4C].
Ch3-Output from the defective current Pulse Counter circuit box [5C]. It shows the presence of many bad current pulses.
Ch4-Output from the defective acoustic Pulse Counter circuit box [8A]. It shows the presence of one defective acoustic pulse.

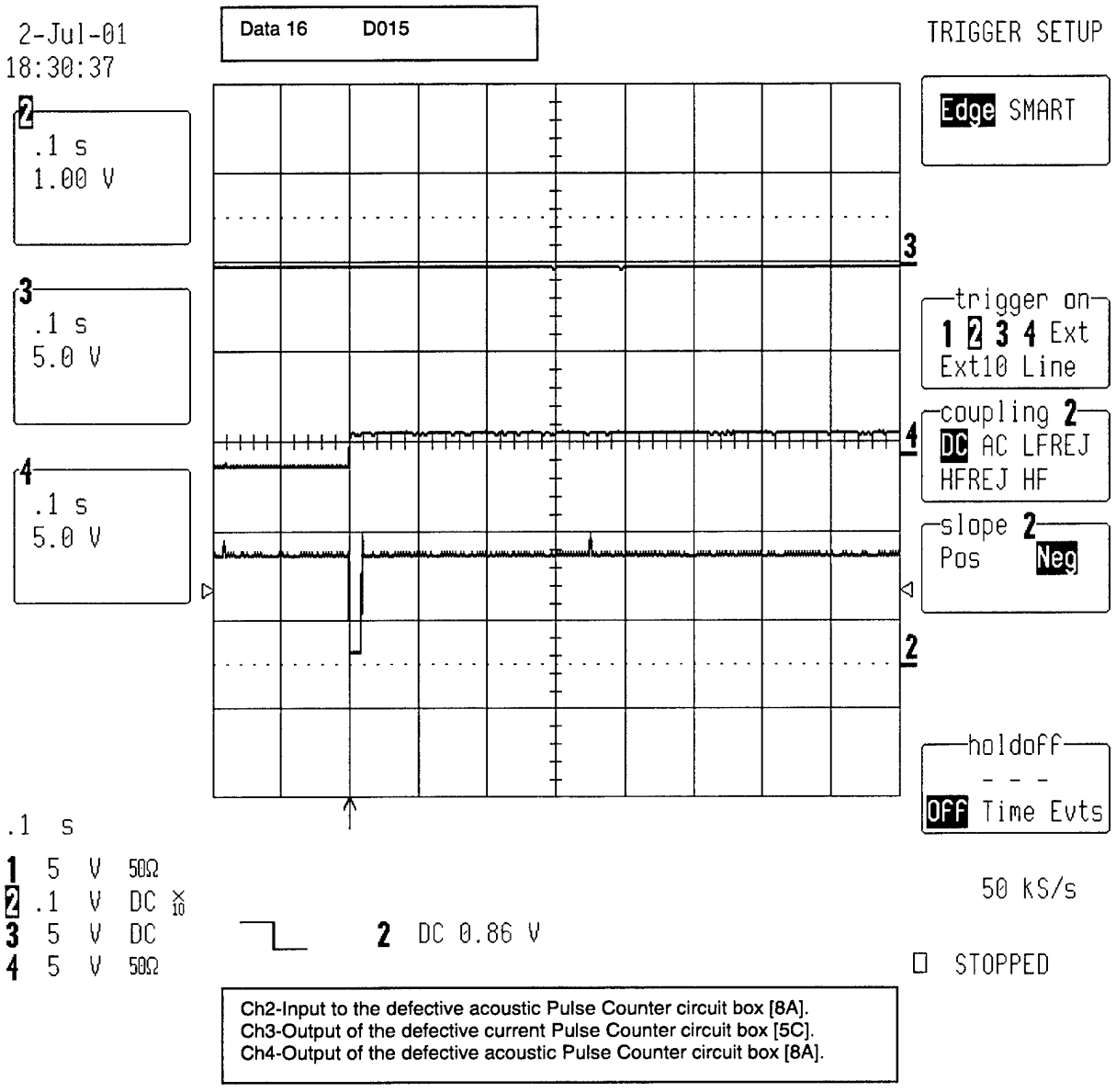

Ch2-Input to the defective acoustic Pulse Counter circuit box [8A].
Ch3-Output of the defective current Pulse Counter circuit box [5C].
Ch4-Output of the defective acoustic Pulse Counter circuit box [8A].

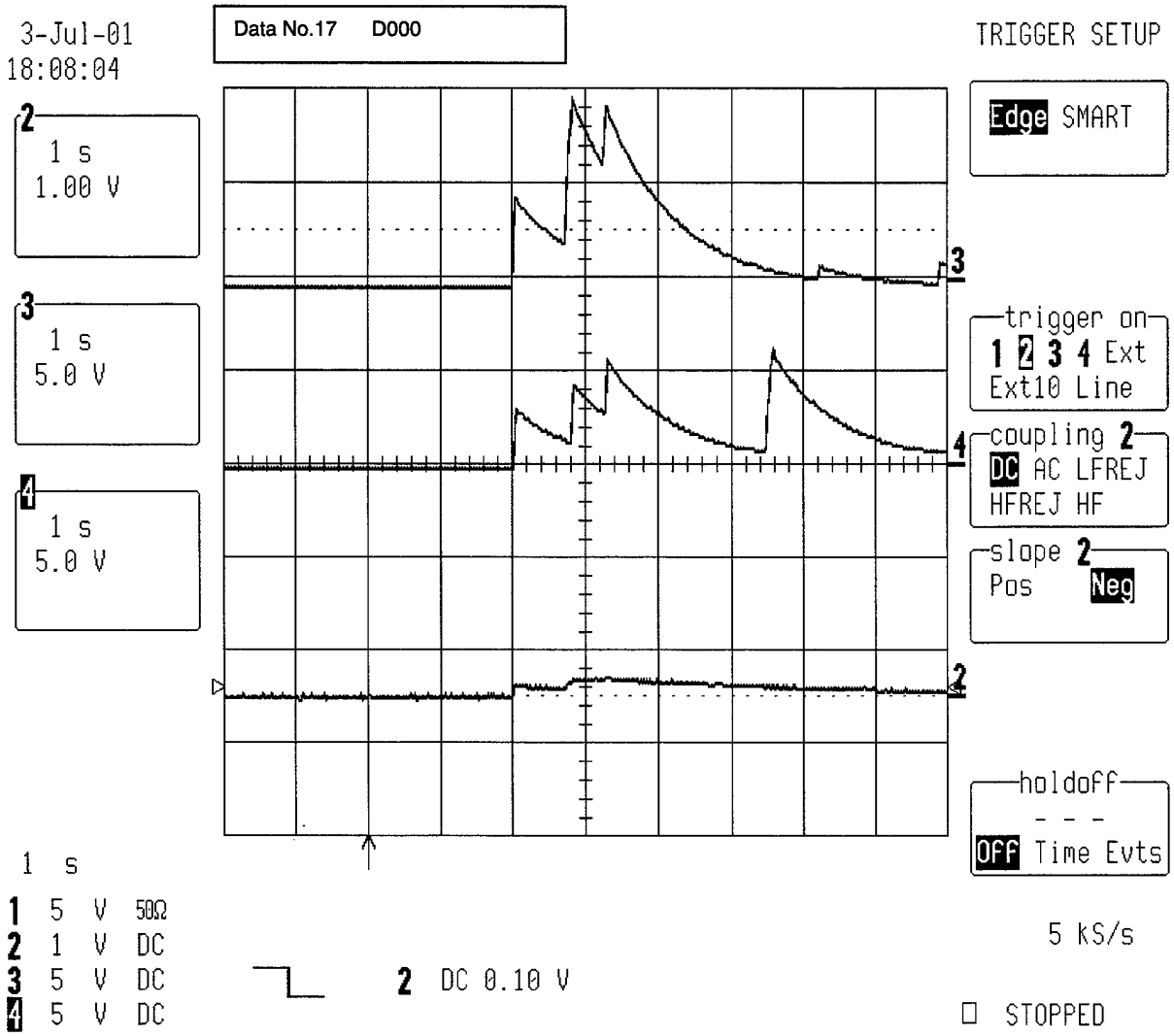

Ch2-Output of the current Threshold Amplifier and Comparator circuit box [4C] and input to the defective current Pulse Counter circuit box [5C].
Ch3-Output of the defective current Pulse Counter circuit box [5C].
Ch4-Output of the defective acoustic Pulse Counter circuit box [8A]. Here outputs from both counters coincide.

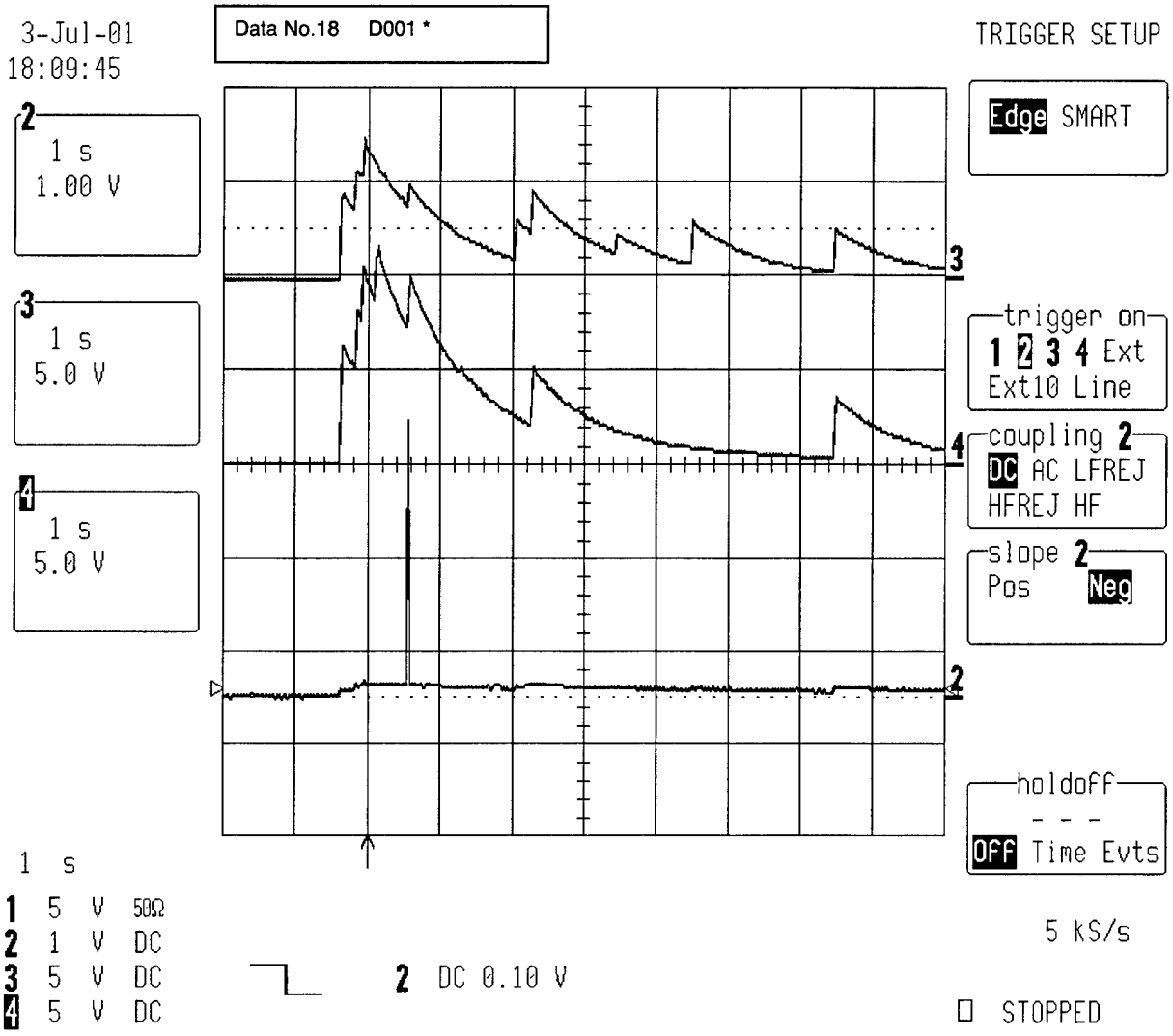

Ch2-Input to the defective current Pulse Counter circuit box [5C]
Ch3-Output of the defective current Pulse Counter circuit box [5C].
Ch4-Output of the defective acoustic Pulse Counter circuit box [8A].
Here all three outputs coincide.

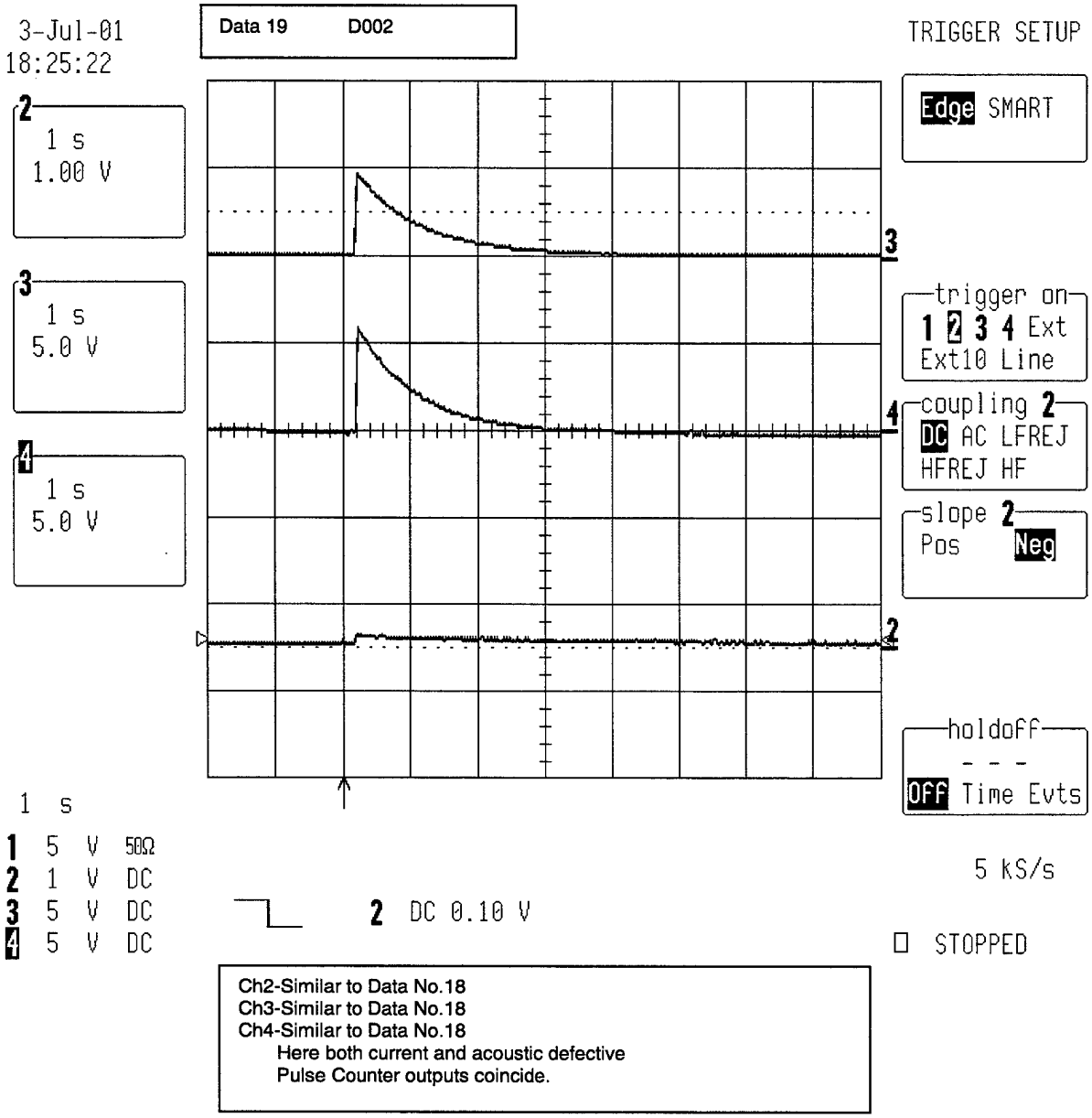

Ch2-Similar to Data No.18
Ch3-Similar to Data No.18
Ch4-Similar to Data No.18
Here both current and acoustic defective
Pulse Counter outputs coincide.

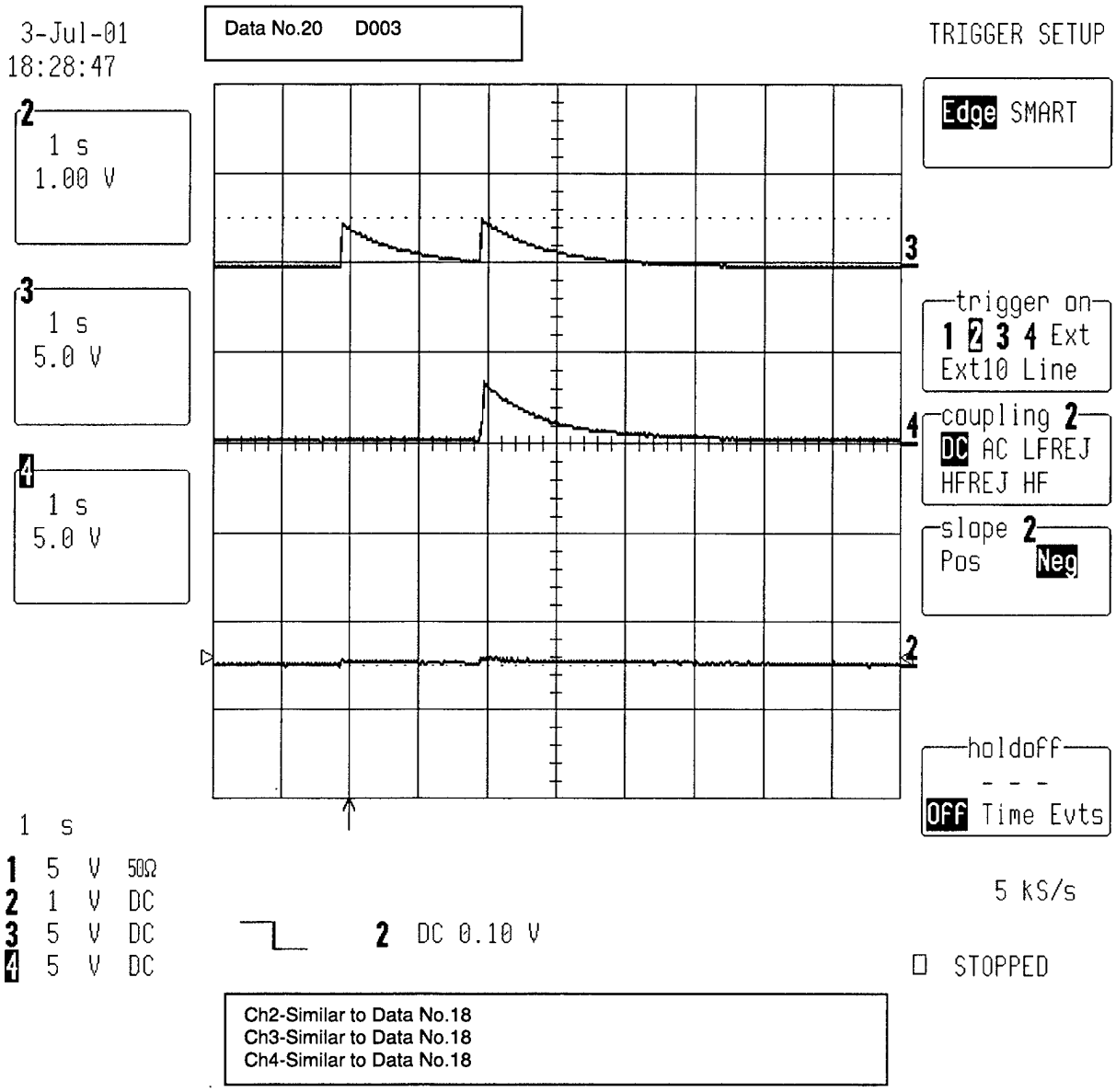

Ch2-Similar to Data No.18
Ch3-Similar to Data No.18
Ch4-Similar to Data No.18

17-Jul-01
16:38:47

Data No.21 D016

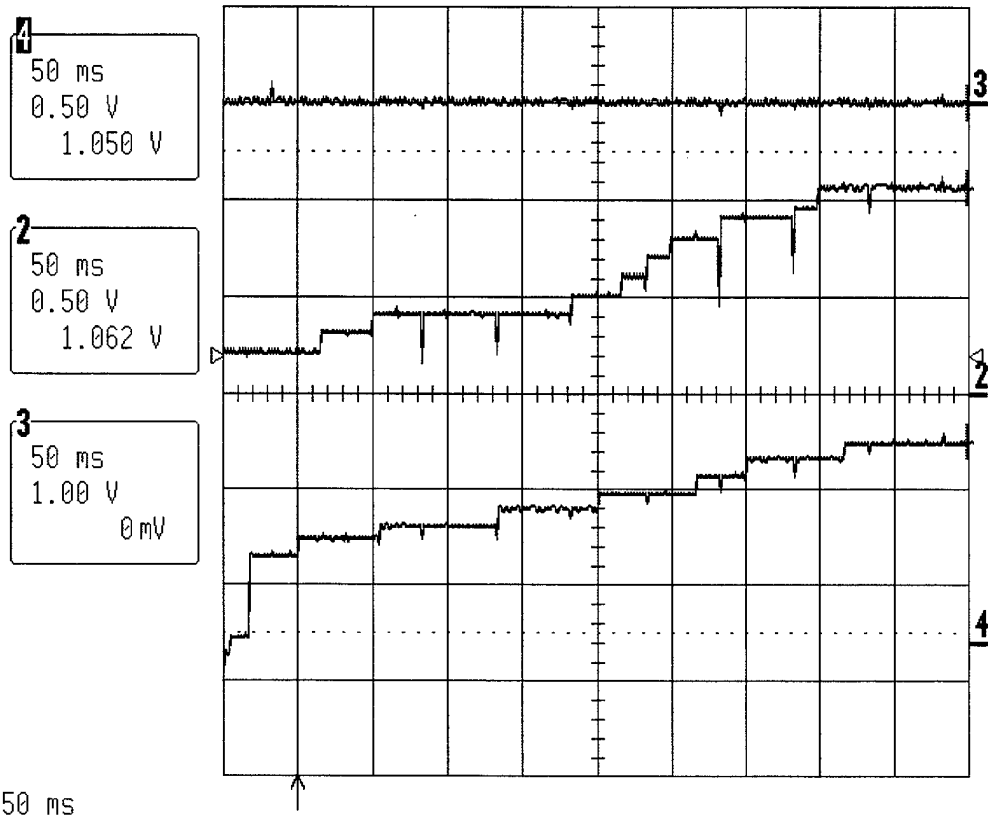

50 ms

1 50 mV AC
2 .5 V DC
3 .1 V AC X10
4 .5 V DC

Time 450.00 ms

2 DC 0.20 V

100 kS/s

STOPPED

Ch2-Output of the defective acoustic Pulse Counter circuit box [8A].
Ch3-To Reset from the One Second Data Sample and Reset circuit box [9A].
Ch4-Output of the defective current Pulse Counter circuit box [5C].
Here one reset pulse is present just before the first vertical division on Ch3 covering the time span of 0.5s (50 ms/div X 10 div) on the horizontal time axis. Ch2 and Ch4 show counts of bad pulses.

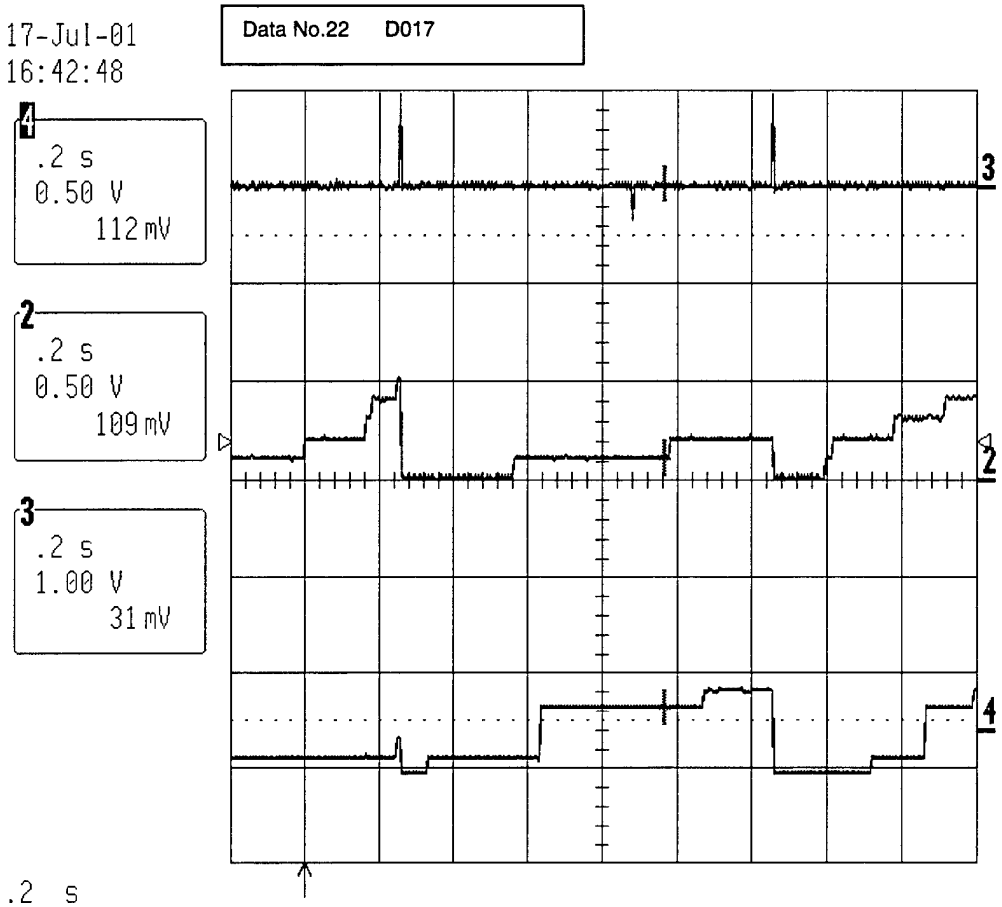

Ch2-Output of the defective acoustic Pulse Counter circuit box [8A].
Ch3-To Reset from the One Second Data Sample and Reset circuit box [9A].
Ch4-Output of the defective current Pulse Counter circuit box [5C].
Here two reset pulses are present after 2nd and after 7th division on Ch3 separated by 1s (0.2s/div X 5 div).Ch2 and Ch4 show counts of bad pulses.

17-Jul-01
16:49:15

Data No.23 D018

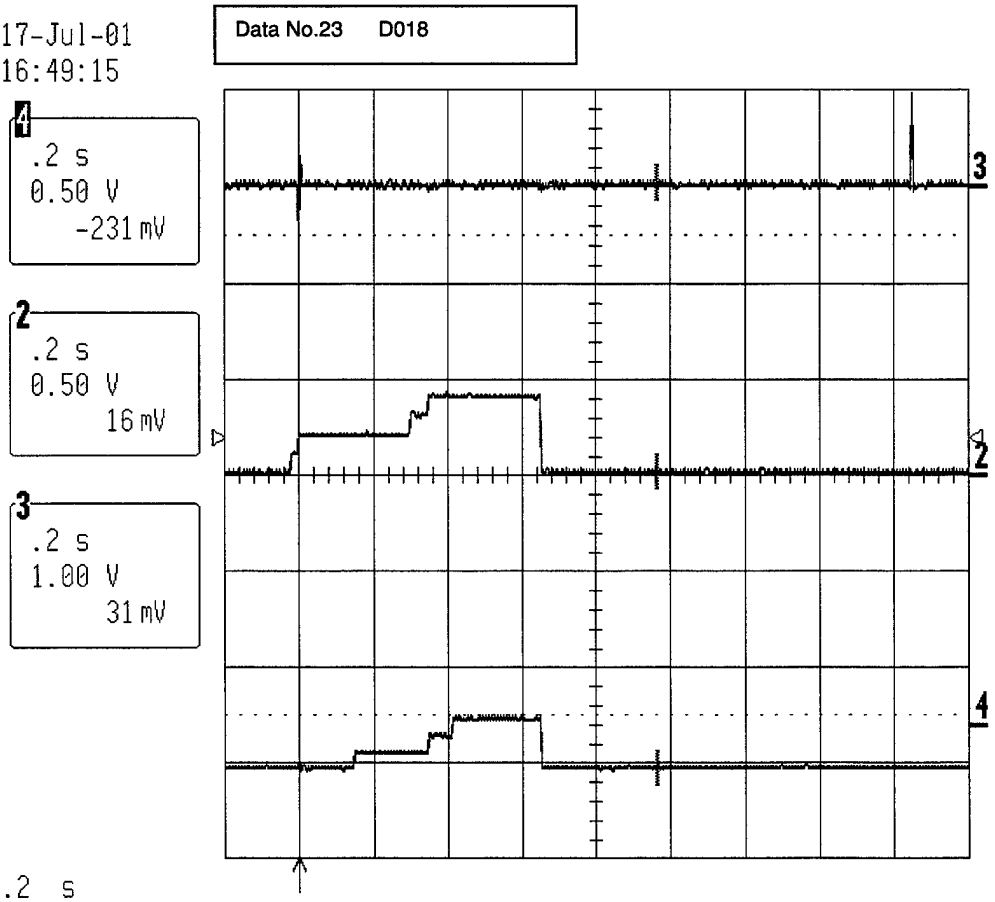

Ch2-Output of the defective acoustic Pulse Counter circuit box [8A].
Ch3-To Reset from the One Second Data Sample and Reset circuit box [9A].
Ch4-Output of the defective current Pulse Counter circuit box [5C].
Here one reset pulse is present after the 9th vertical division on Ch3. There should be the one after the 4th division. Ch2 and Ch4 show counts of bad pulses.

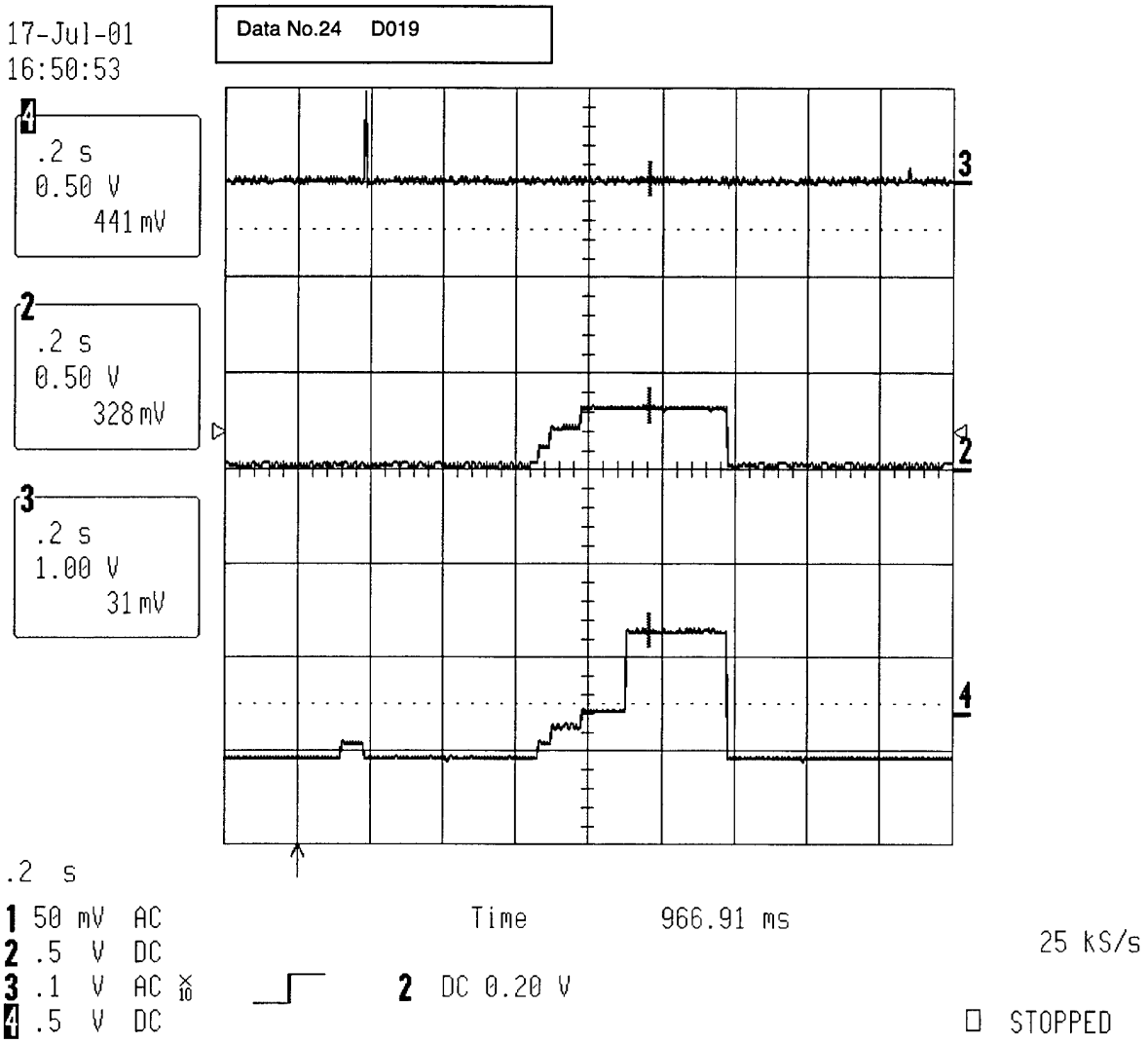

Ch2-Output of the defective acoustic Pulse Counter circuit box [8A].
Ch3-To Reset from the One Second Data Sample and Reset circuit box [9A].
Ch4-Output of the defective current Pulse Counter circuit box [5C].
Here one reset pulse is present just on the 2nd vertical division on Ch3. The 2nd should be there on the 7th division but does not show. Ch2 and Ch4 show counts of bad pulses.

Data No.25 D020

17-Jul-01
16:53:46

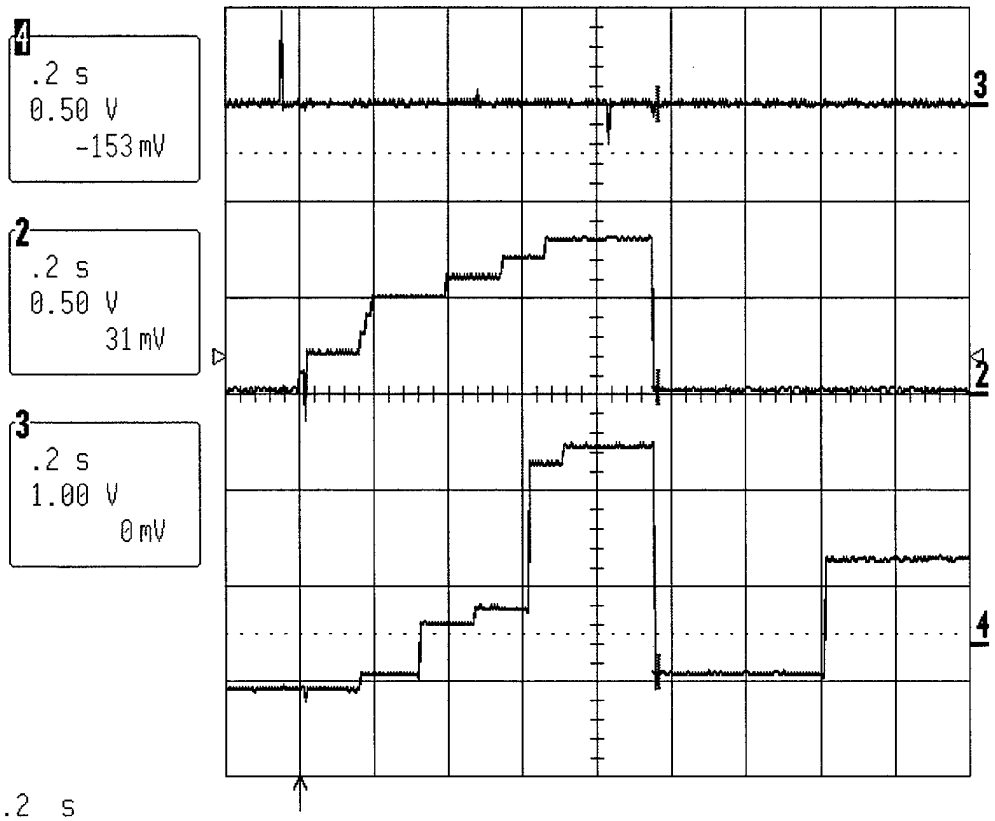

.2 s

1 50 mV AC
2 .5 V DC
3 .1 V AC X10
4 .5 V DC

Time 966.91 ms

25 kS/s

2 DC 0.20 V

STOPPED

Ch2-Output of the defective acoustic Pulse Counter circuit box [8A].
Ch3-To Reset from the One Second Data Sample and Reset circuit box [9A].
Ch4-Output of the defective current Pulse Counter circuit box [5C].
Here one reset pulse is present just before the 1st vertical division on Ch3.Timescale 0.2s/div.
Ch2 and Ch4 show nice counts of bad pulses.

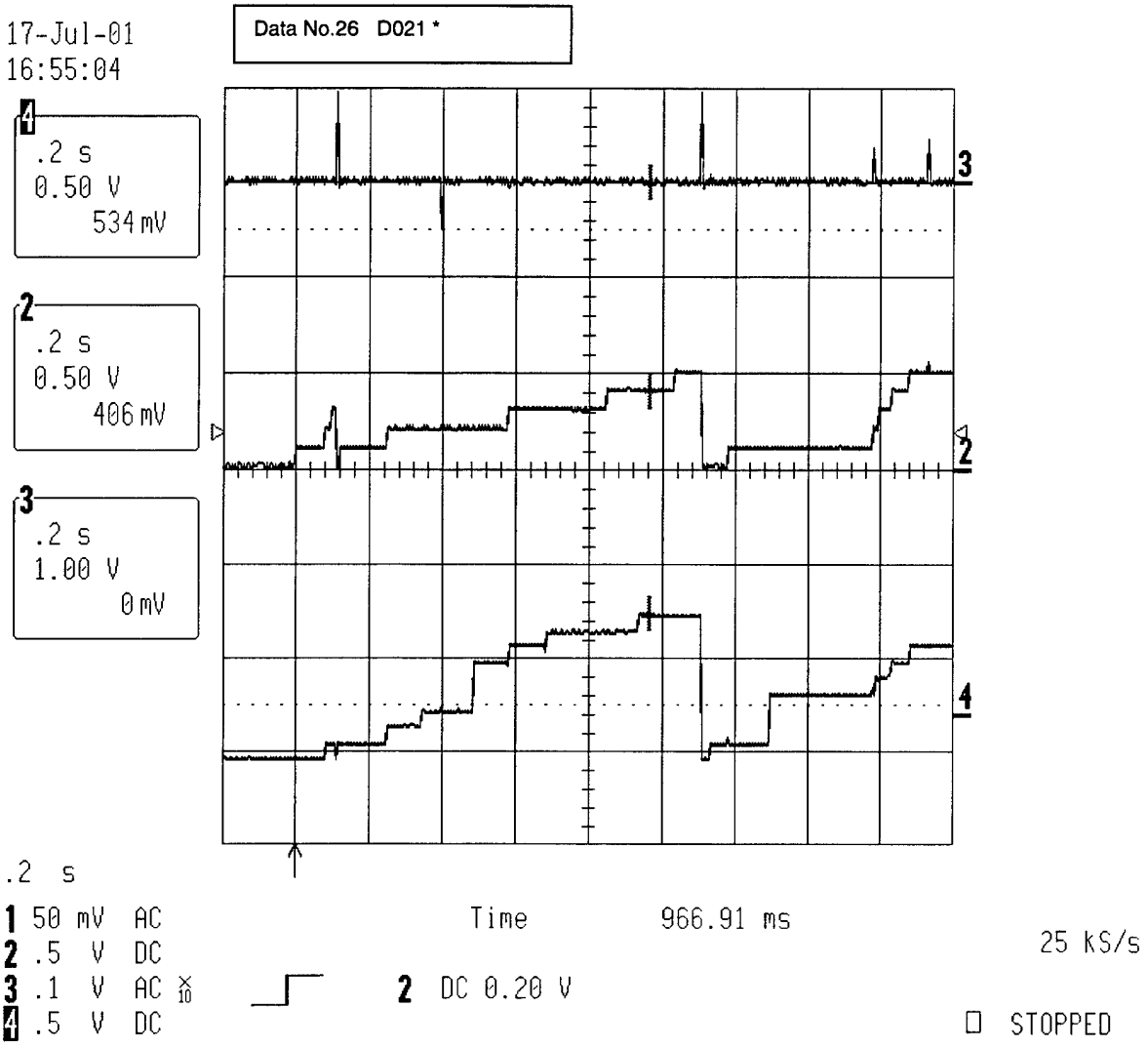

Ch2-Output of the defective acoustic Pulse Counter circuit box [8A].
Ch3-To Reset from the One Second Data Sample and Reset circuit box [9A].
Ch4-Output of the defective current Pulse Counter circuit box [5C].
Here two reset pulses are present separated by one second time interval on Ch3.
Ch2 and Ch4 show nice counts of bad pulses.

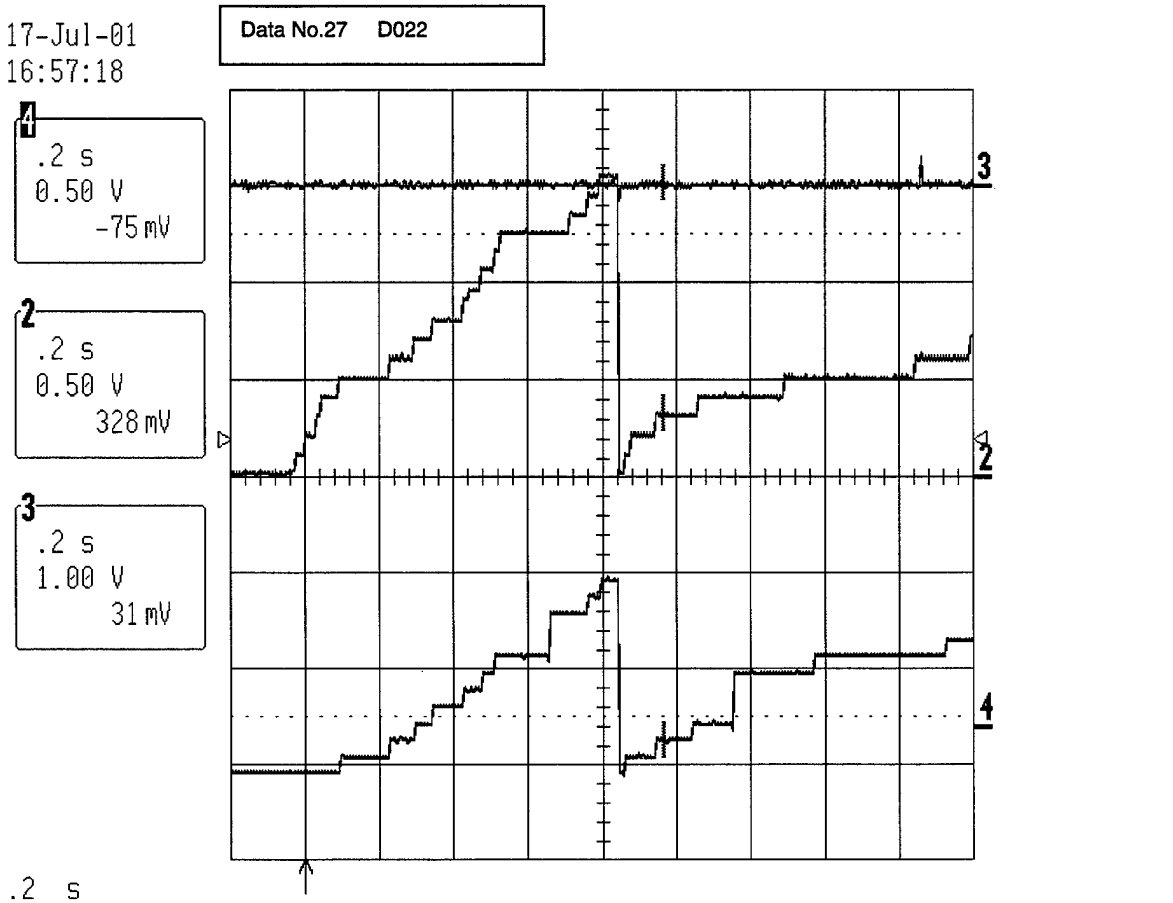

Ch2-Output of the defective acoustic Pulse Counter circuit box [8A].
Ch3-To Reset from the One Second Data Sample and Reset circuit box [9A].
Ch4-Output of the defective current Pulse Counter circuit box [5C].
Here Ch2 and Ch4 show very nice counts of bad pulses.
Sometimes reset pulses do not appear on Ch3 because they are of width 25μs or less.

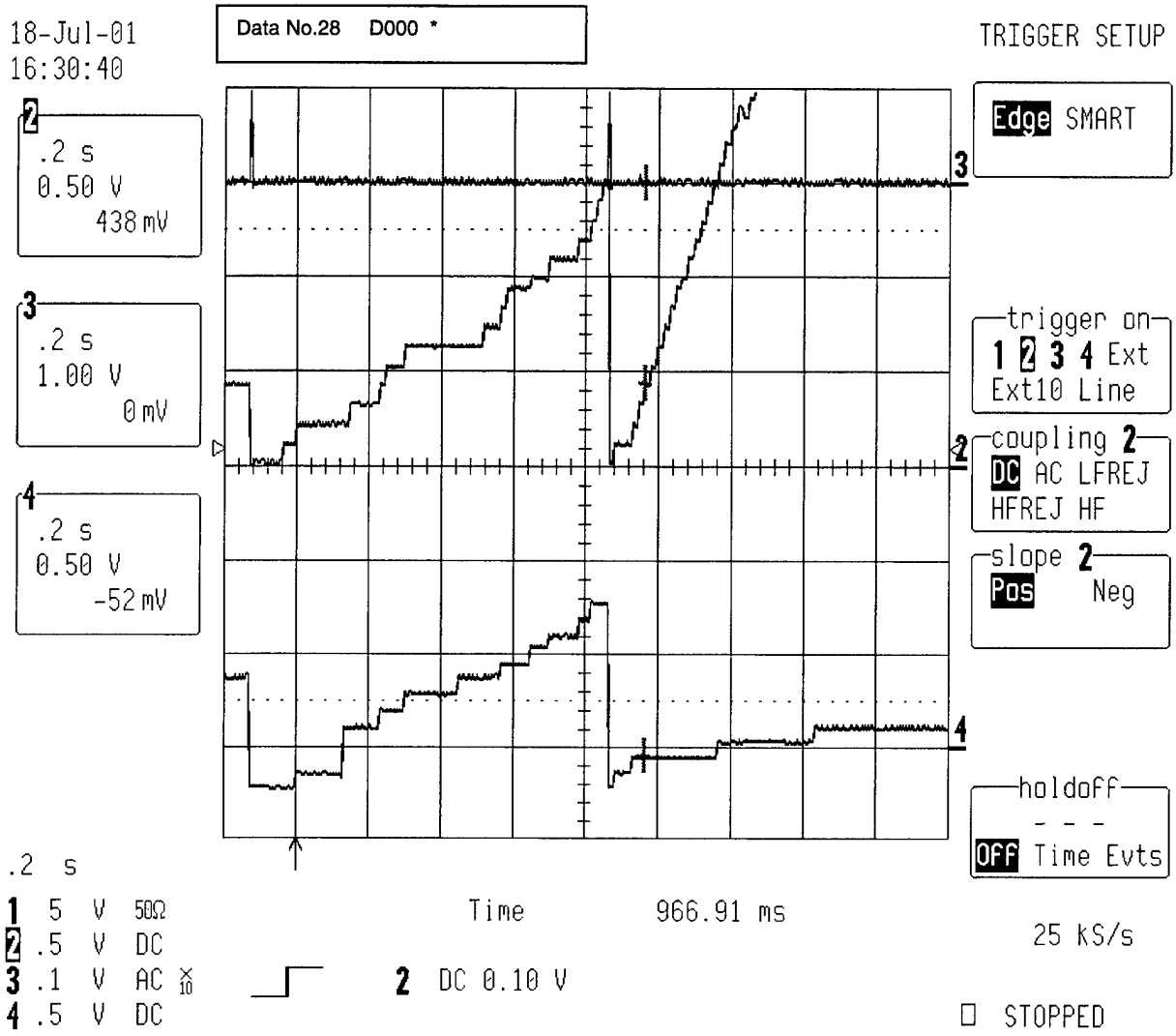

Ch2-Output of the defective acoustic Pulse Counter circuit box [8A].
Ch3-To Reset from the One Second Data Sample and Reset circuit box [9A].
Ch4-Output of the defective current Pulse Counter circuit box [5C].
Here Ch2 and Ch4 show nice counts of bad acoustic and current pulses between two reset pulses (before 1st vertical division and after 5th vertical division) on Ch3.

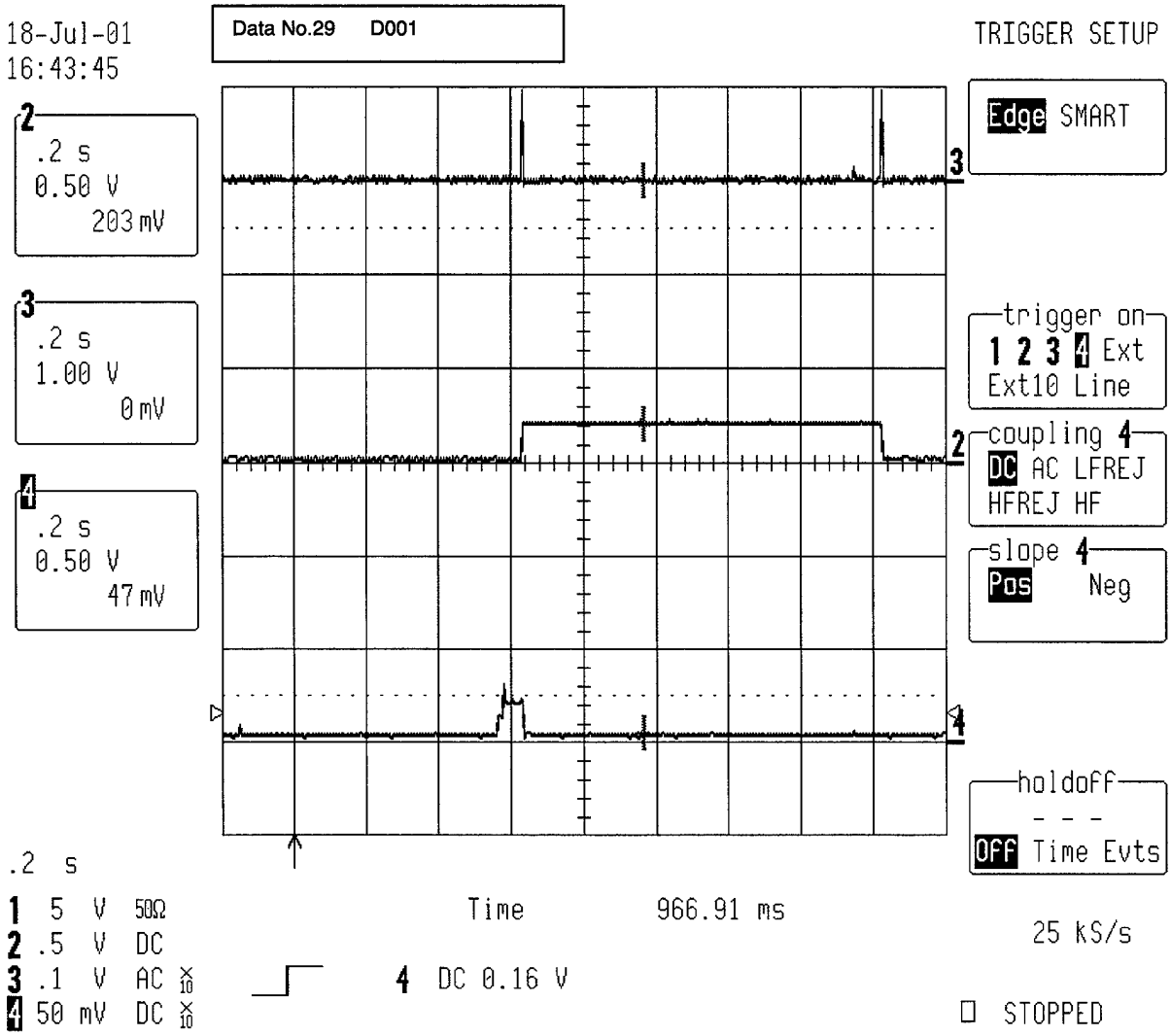

Ch2-Output of the defective acoustic Pulse Counter circuit box [8A].
Ch3-To Reset from the One Second Data Sample and Reset circuit box [9A].
Ch4-Output of the defective current Pulse Counter circuit box [5C].
Here Ch2 and Ch4 show counts of bad acoustic and current pulses between two reset pulses (next to 4th vertical division and next to 9th vertical division) on Ch3.

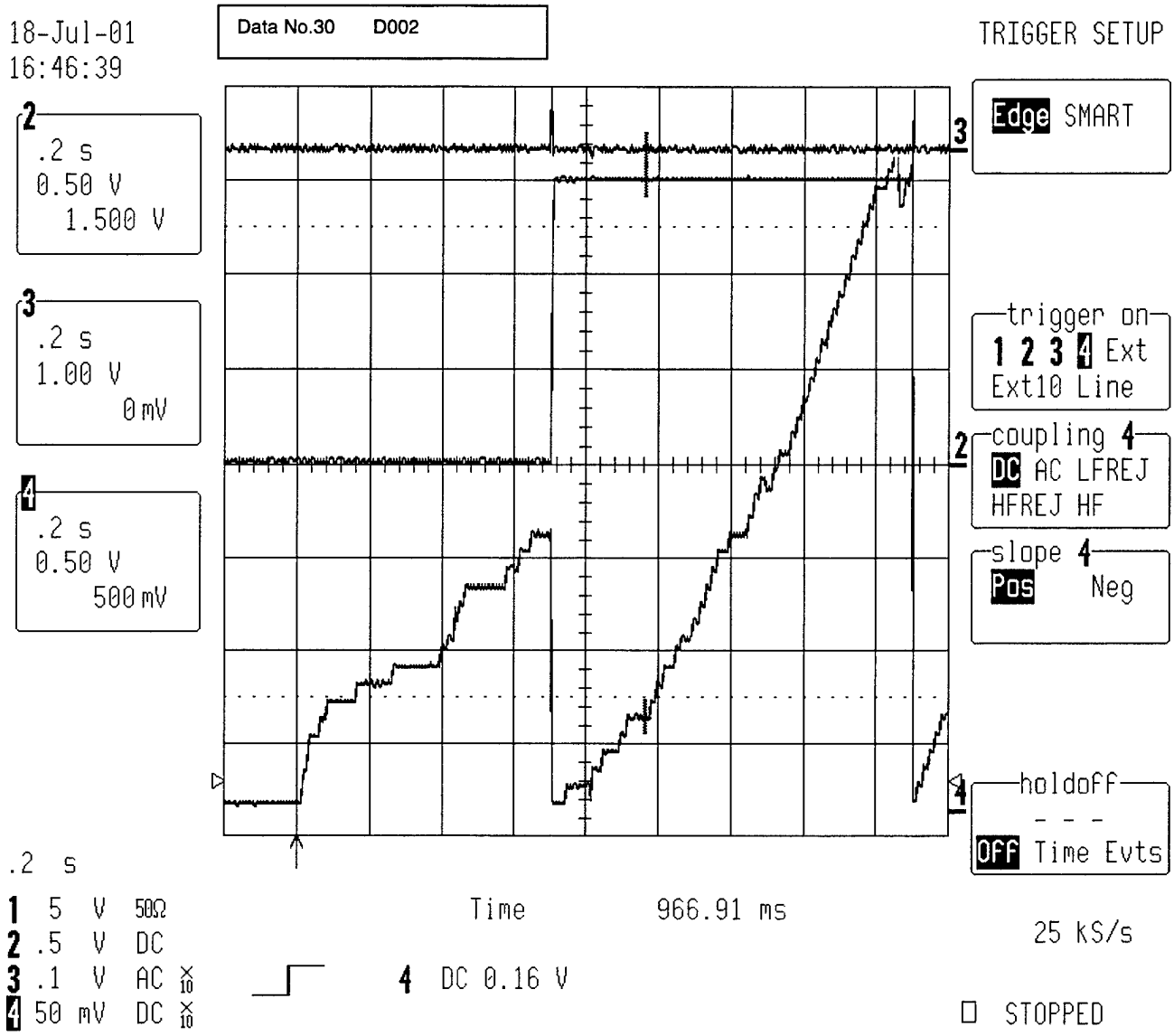

Ch2-Output of the defective acoustic Pulse Counter circuit box [8A].
Ch3-To Reset from the One Second Data Sample and Reset circuit box [9A].
Ch4-Output of the defective current Pulse Counter circuit box [5C].
Here Ch4 show nice counts of bad current pulses between two reset pulses (next to 4th vertical division and after 9th vertical division) on Ch3.

Data No.31 D000

23-Jul-01
10:50:19

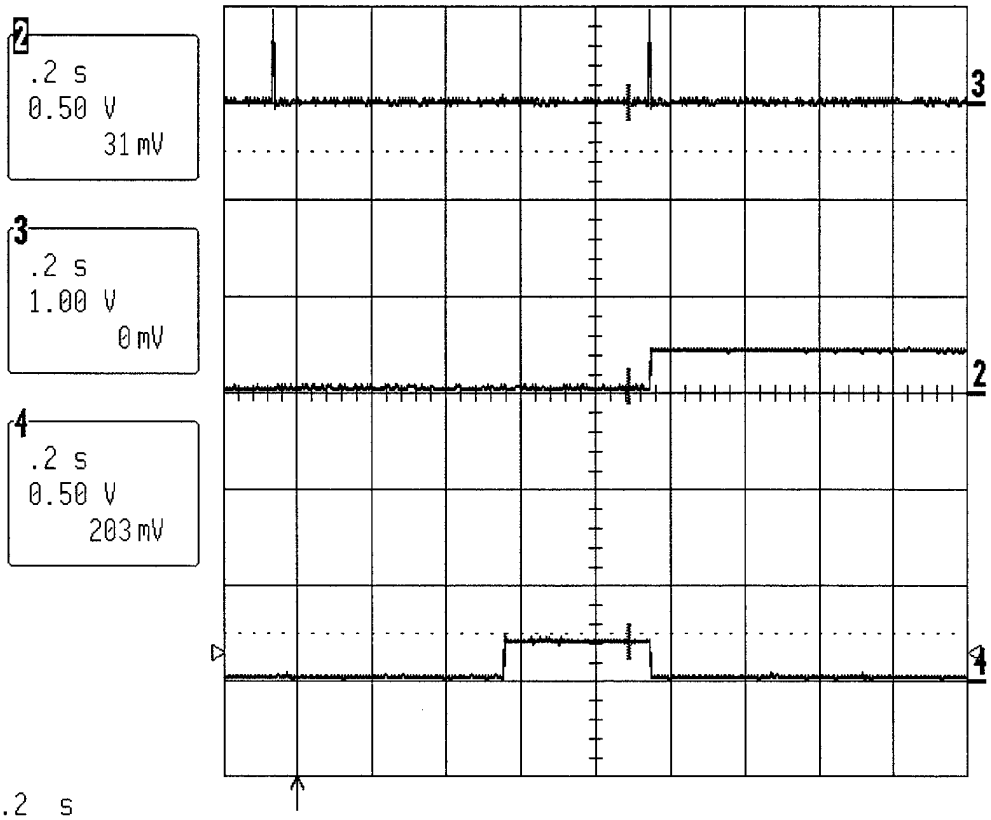

.2 s

1 5 V 50Ω
2 .5 V DC
3 .1 V AC
4 50 mV DC

Time 892.31 ms

4 DC 0.15 V

25 kS/s

STOPPED

Ch2-Current pulses output of the One second Data Sample and Reset circuit box [9A].
Ch3-To Reset from the One Second Data Sample and Reset circuit box [9A].
Ch4-Current pulses input to the One second Data Sample and Reset circuit box [9A].
Two reset pulses are present on Ch3.
The value of the signal on Ch4 at the cursor is 203 mV and that on Ch2 at the cursor is 31mV.
Note: Compare with the next oscilloscope display.

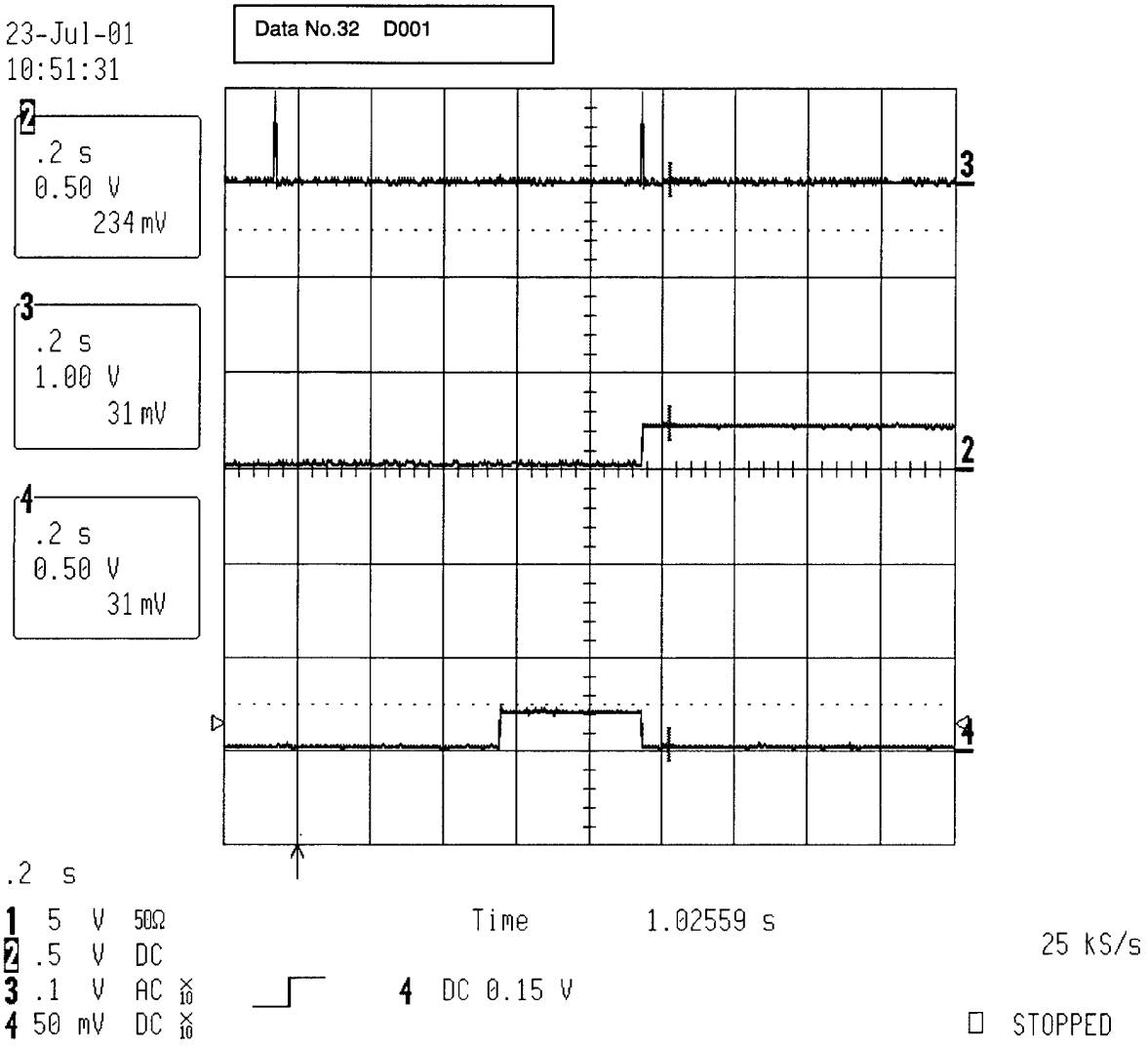

Ch2-Current pulses output of the One second Data Sample and Reset circuit box [9A].
Ch3-To Reset from the One Second Data Sample and Reset circuit box [9A].
Ch4-Current pulses input to the One second Data Sample and Reset circuit box [9A].
Two reset pulses are present on Ch3.
The value of the signal on Ch4 at the cursor now is changed to 31 mV and that on Ch2 at the cursor is changed to 234 mV.
Note: Compare with the previous oscilloscope display.

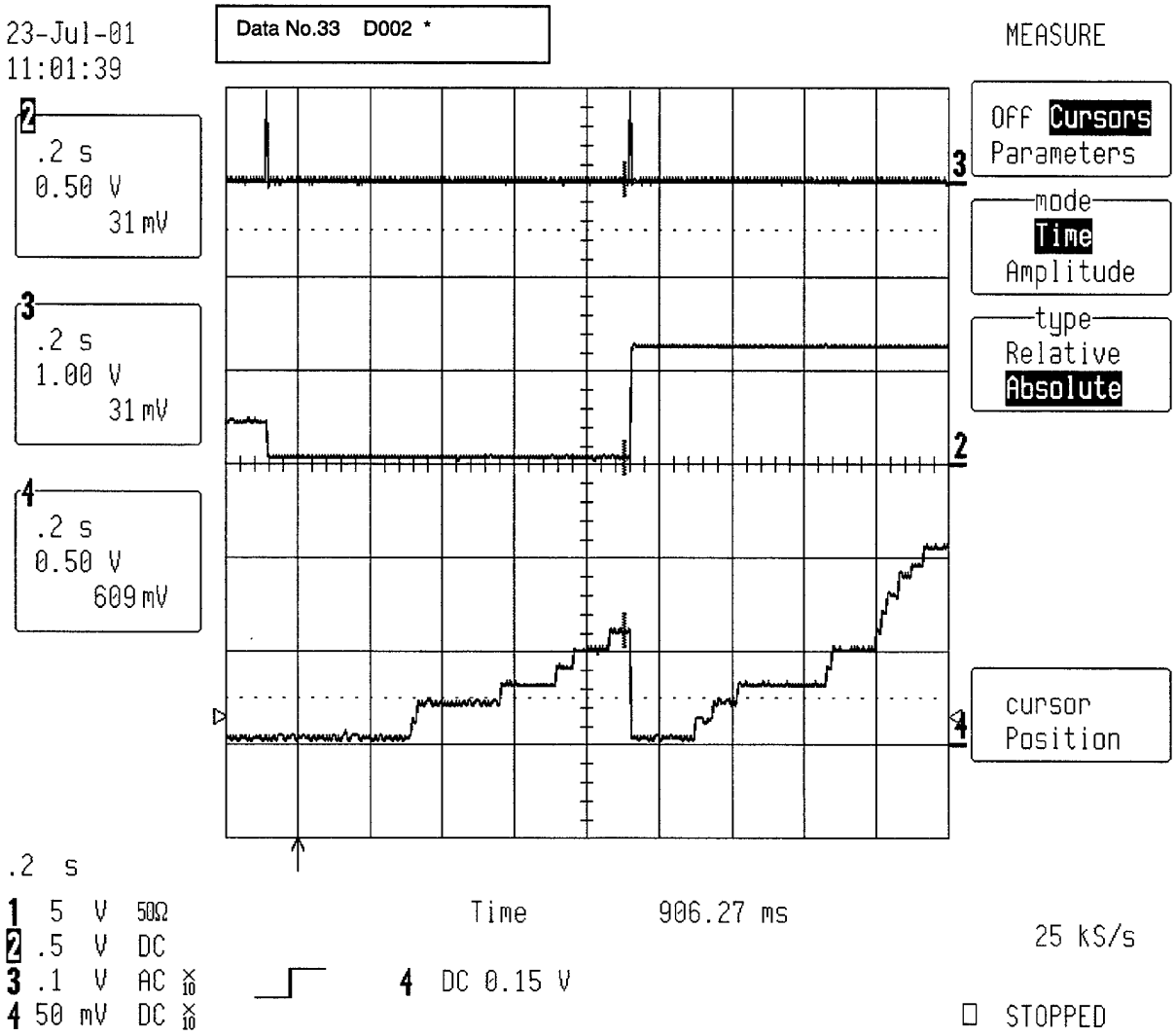

Ch2-Current pulses output of the One second Data Sample and Reset circuit box [9A].
Ch3-To Reset from the One Second Data Sample and Reset circuit box [9A].
Ch4-Current pulses input to the One second Data Sample and Reset circuit box [9A].
Two reset pulses are present on Ch3 separated by one second time interval.
The value of the signal on Ch4 at the cursor is 609 mV and that on Ch2 at the cursor is 31mV.
Note: Compare with the next oscilloscope display.

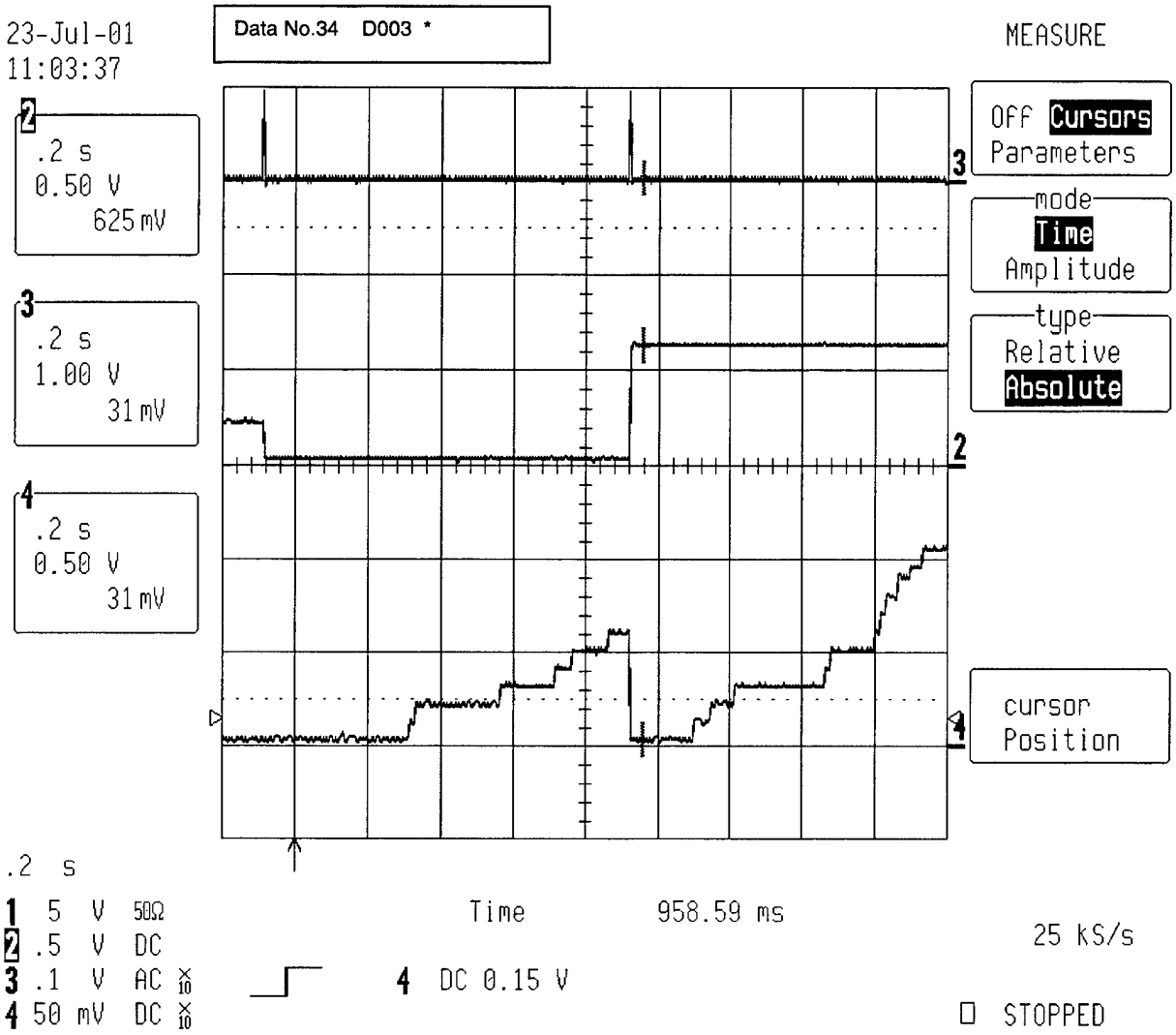

Ch2-Current pulses output of the One second Data Sample and Reset circuit box [9A].
Ch3-To Reset from the One Second Data Sample and Reset circuit box [9A].
Ch4-Current pulses input to the One second Data Sample and Reset circuit box [9A].
Two reset pulses are present on Ch3.
The value of the signal on Ch4 at the cursor now is changed to 31 mV and that on Ch2 at the cursor is changed to 625 mV.
Note: Compare with the previous oscilloscope display.

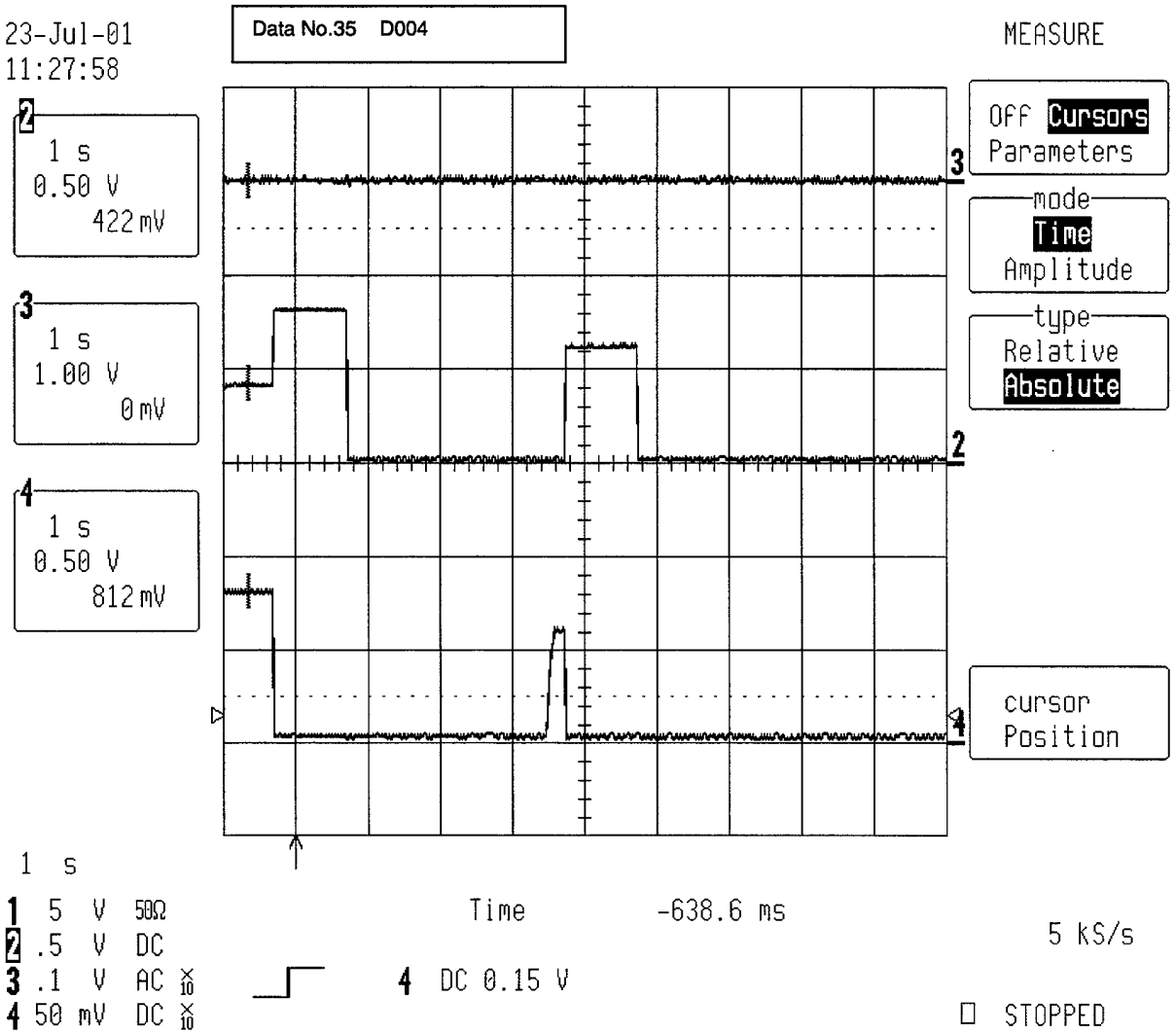

Ch2-Current pulses output of the One second Data Sample and Reset circuit box [9A].
Ch3-To Reset from the One Second Data Sample and Reset circuit box [9A].
Ch4-Current pulses input to the One second Data Sample and Reset circuit box [9A].
Two reset pulses are present on Ch3.
The value of the signal on Ch4 at the cursor is 812 mV and that on Ch2 at the cursor is 422 mV.
The high value on Ch2 is from previous storage of the transferred data
Note: Compare with the next oscilloscope display.

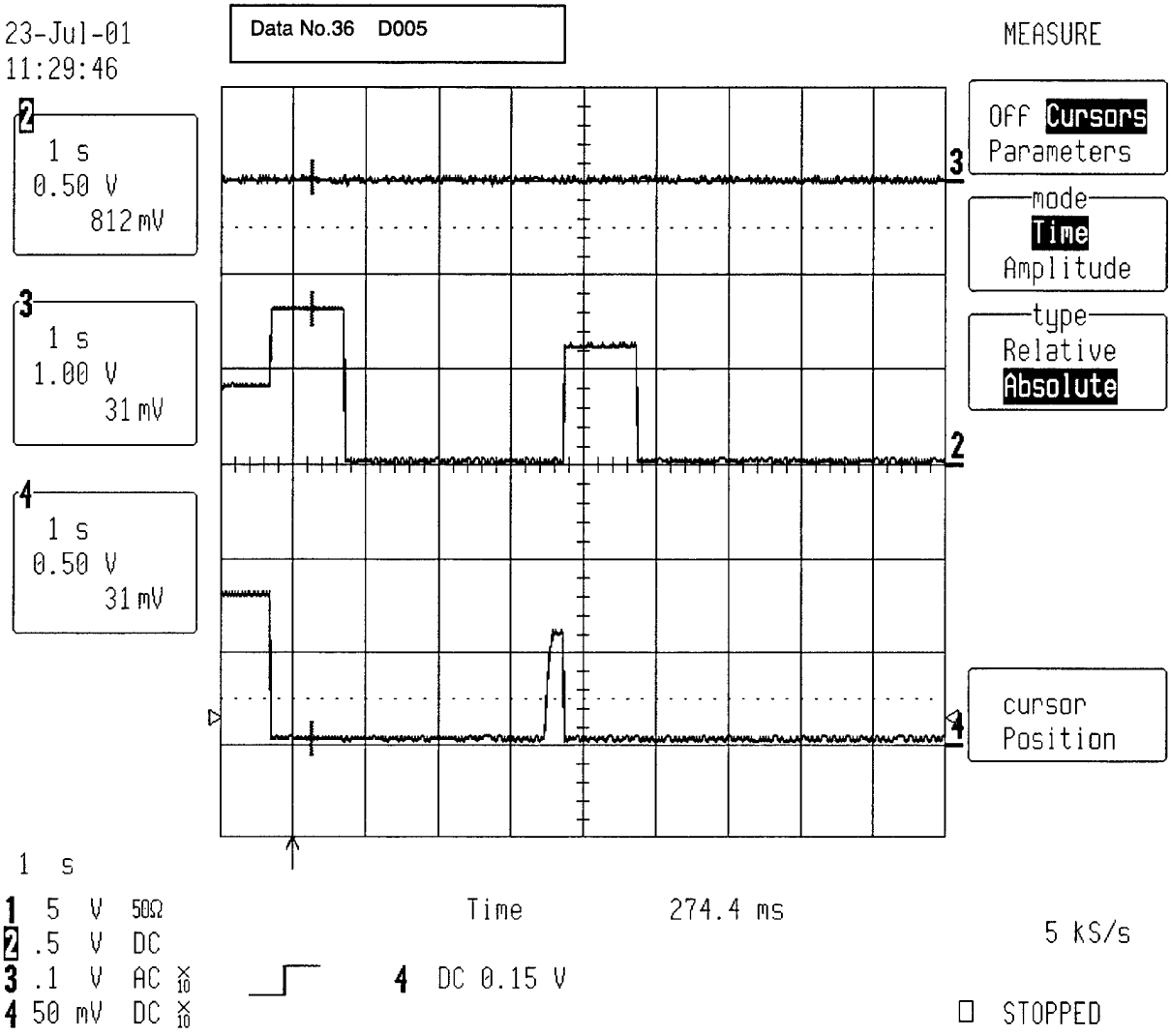

Ch2-Current pulses output of the One second Data Sample and Reset circuit box [9A].
Ch3-To Reset from the One Second Data Sample and Reset circuit box [9A].
Ch4-Current pulses input to the One second Data Sample and Reset circuit box [9A].
Two reset pulses are present on Ch3.
The value of the signal on Ch4 at the cursor now is changed to 31 mV and that on Ch2 at the cursor is changed to 812 mV.
Note: Compare with the previous oscilloscope display.

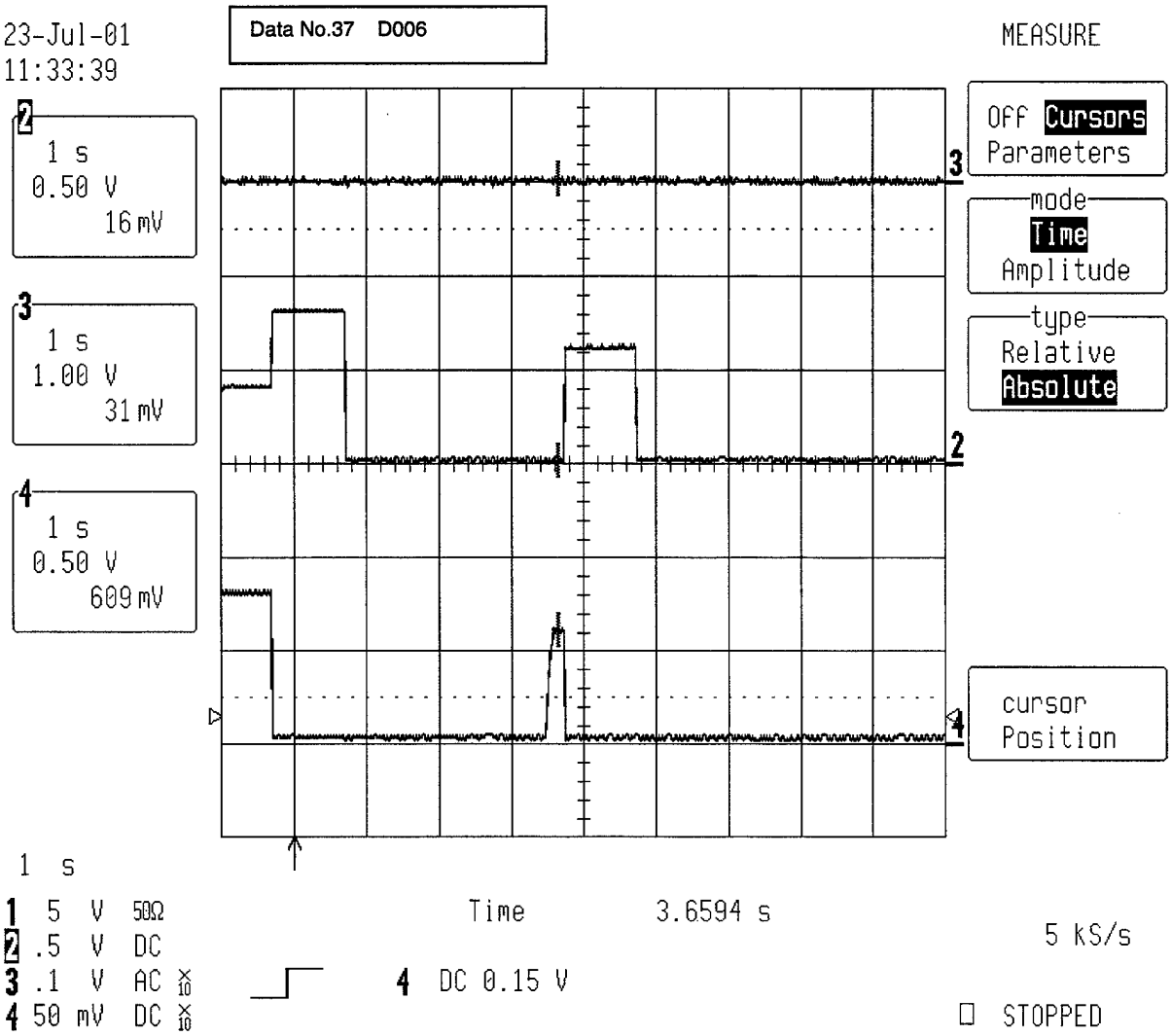

Ch2-Current pulses output of the One second Data Sample and Reset circuit box [9A].
Ch3-To Reset from the One Second Data Sample and Reset circuit box [9A].
Ch4-Current pulses input to the One second Data Sample and Reset circuit box [9A].
Two reset pulses are present on Ch3.
The value of the signal on Ch4 at the cursor is 609 mV and that on Ch2 at the cursor is 16 mV.
Note: Compare with the next oscilloscope display.

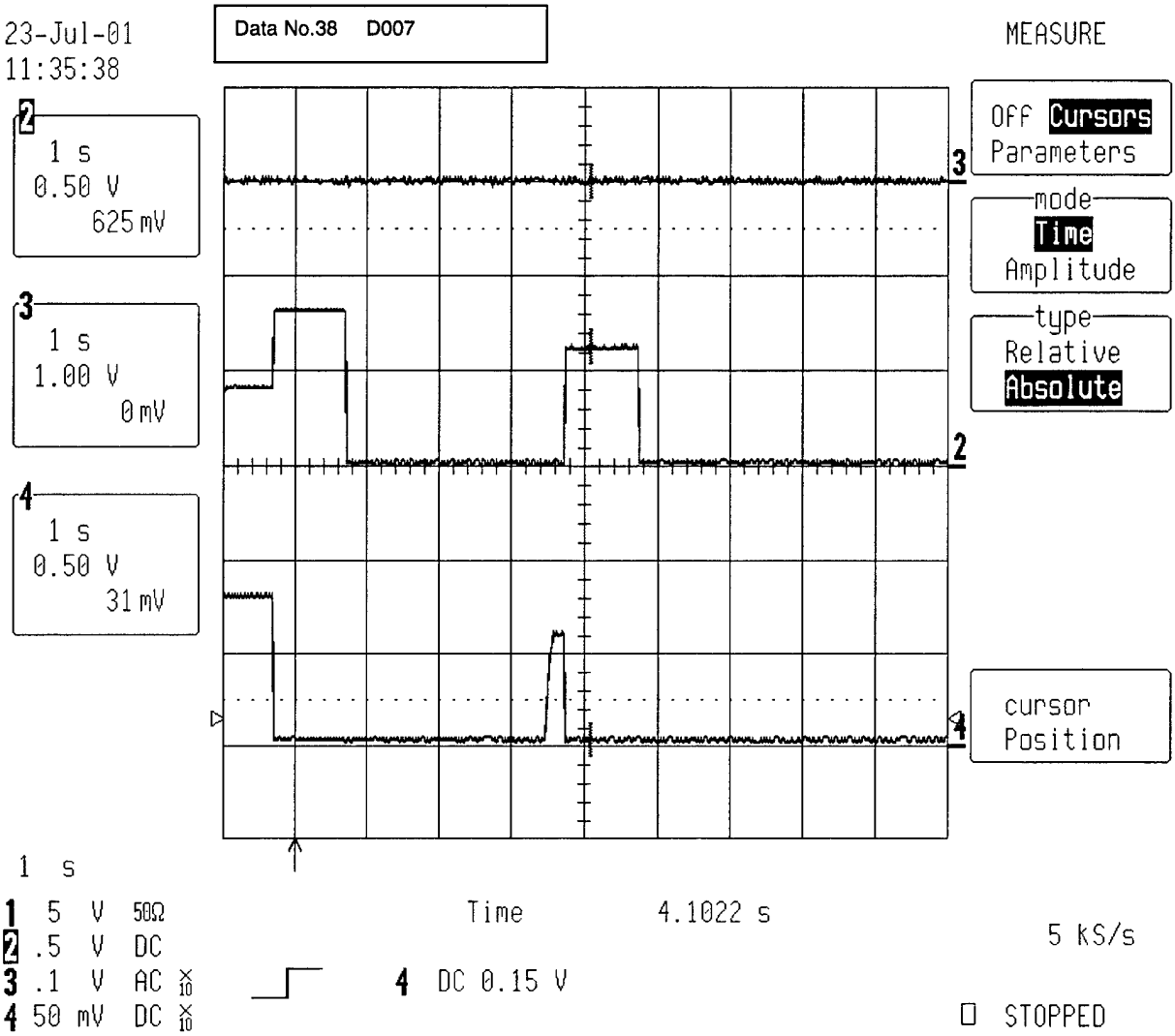

Ch2-Current pulses output of the One second Data Sample and Reset circuit box [9A].
Ch3-To Reset from the One Second Data Sample and Reset circuit box [9A].
Ch4-Current pulses input to the One second Data Sample and Reset circuit box [9A].
Two reset pulses are present on Ch3.
The value of the signal on Ch4 at the cursor now is changed to 31 mV and that on Ch2 at the cursor is changed to 625 mV.
Note: Compare with the previous oscilloscope display.

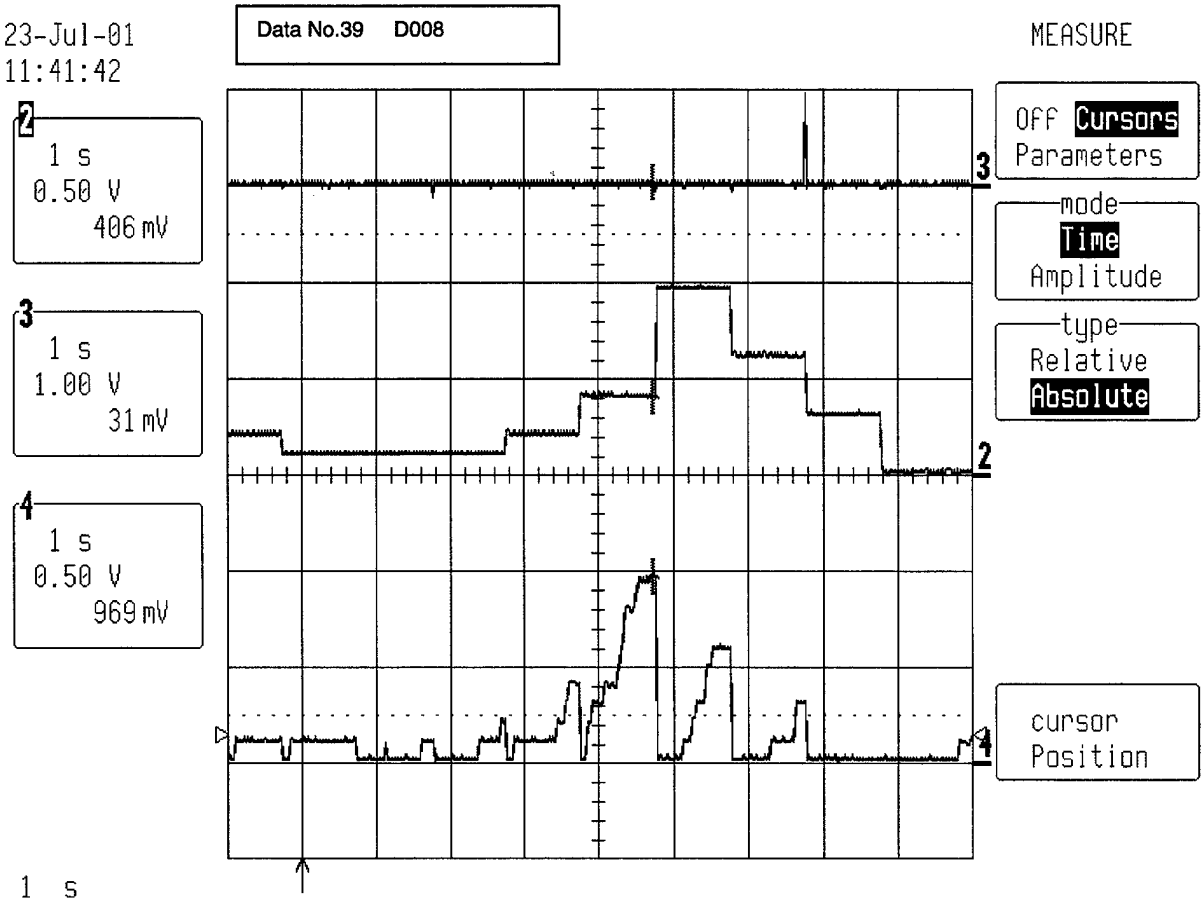

Ch2-Current pulses output of the One second Data Sample and Reset circuit box [9A].
Ch3-To Reset from the One Second Data Sample and Reset circuit box [9A].
Ch4-Current pulses input to the One second Data Sample and Reset circuit box [9A].
The value of the signal on Ch4 at the cursor is 969 mV and that on Ch2 at the cursor is 406 mV.
Note: Compare with the next oscilloscope display.

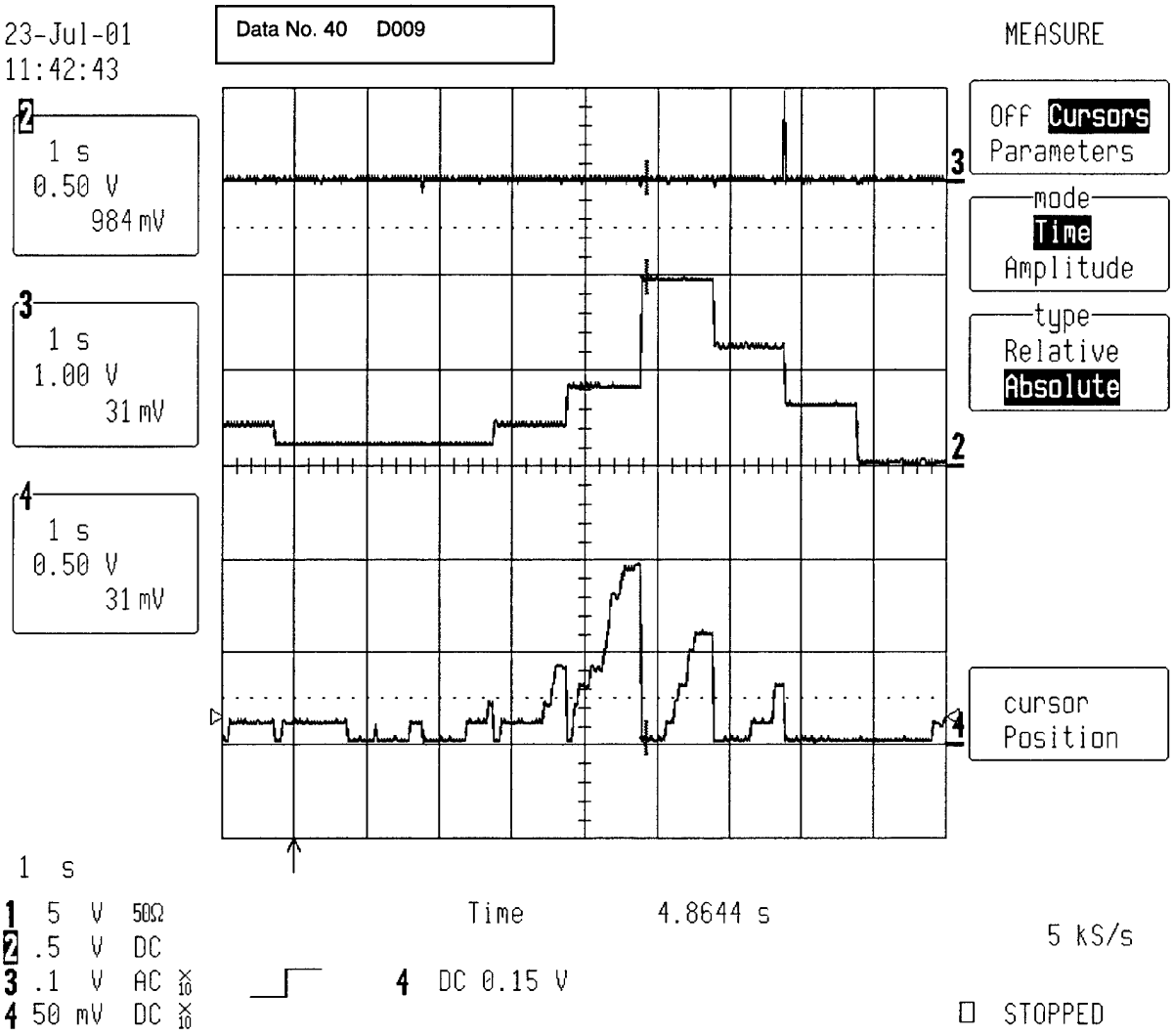

Ch2-Current pulses output of the One second Data Sample and Reset circuit box [9A].
Ch3-To Reset from the One Second Data Sample and Reset circuit box [9A].
Ch4-Current pulses input to the One second Data Sample and Reset circuit box [9A].
Two reset pulses are present on Ch3.
The value of the signal on Ch4 at the cursor now is changed to 31 mV and that on Ch2 at the cursor is changed to 984 mV.
Note: Compare with the previous oscilloscope display.

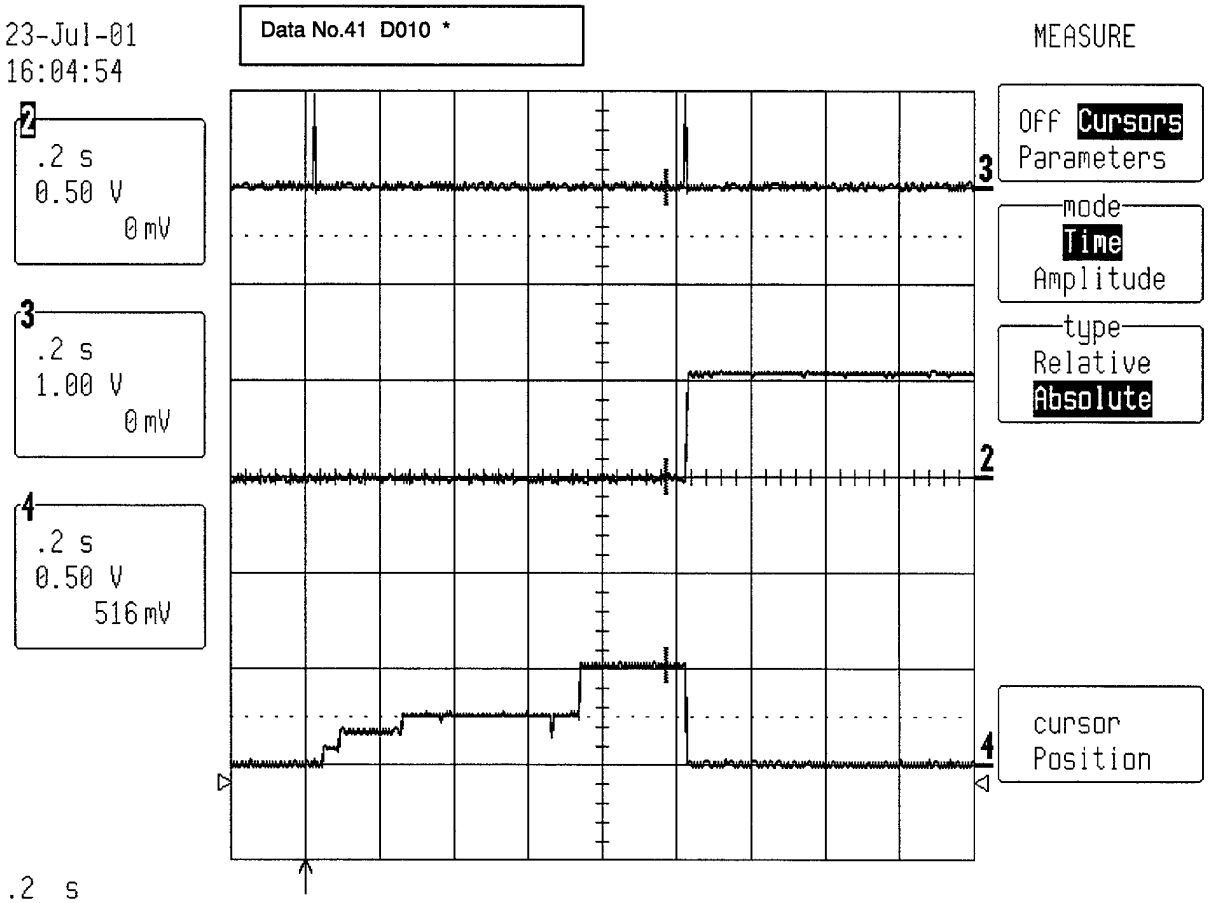

Ch2-Acoustic pulses output of the One second Data Sample and Reset circuit box [9A].
Ch3-To Reset from the One Second Data Sample and Reset circuit box [9A].
Ch4-Acoustic pulses input to the One second Data Sample and Reset circuit box [9A].
Two reset pulses are present on Ch3 on 1st and 6th vertical divisions. The value of the signal on Ch4 at the cursor is 516 mV and that on Ch2 at the cursor is 0 mV.
Note: Compare with the next oscilloscope display.

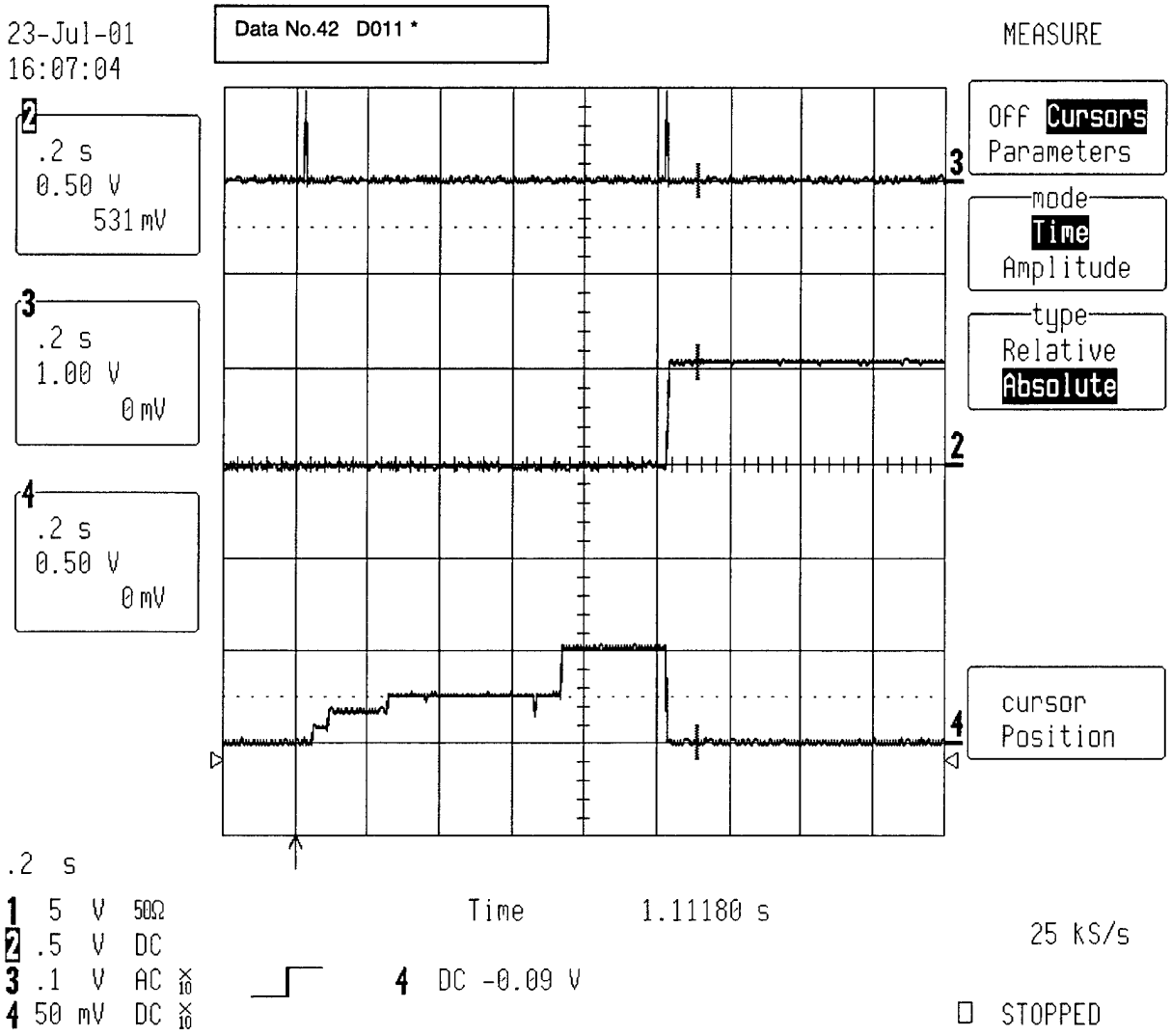

Ch2-Acoustic pulses output of the One second Data Sample and Reset circuit box [9A].
Ch3-To Reset from the One Second Data Sample and Reset circuit box [9A].
Ch4-Acoustic pulses input to the One second Data Sample and Reset circuit box [9A].
Two reset pulses are present on Ch3 on 1st and 6th vertical divisions.
The value of the signal on Ch4 at the cursor is now changed to 0 mV and that on Ch2 at the cursor to 531 mV after data transfer.
Note: Compare with the previous oscilloscope display.

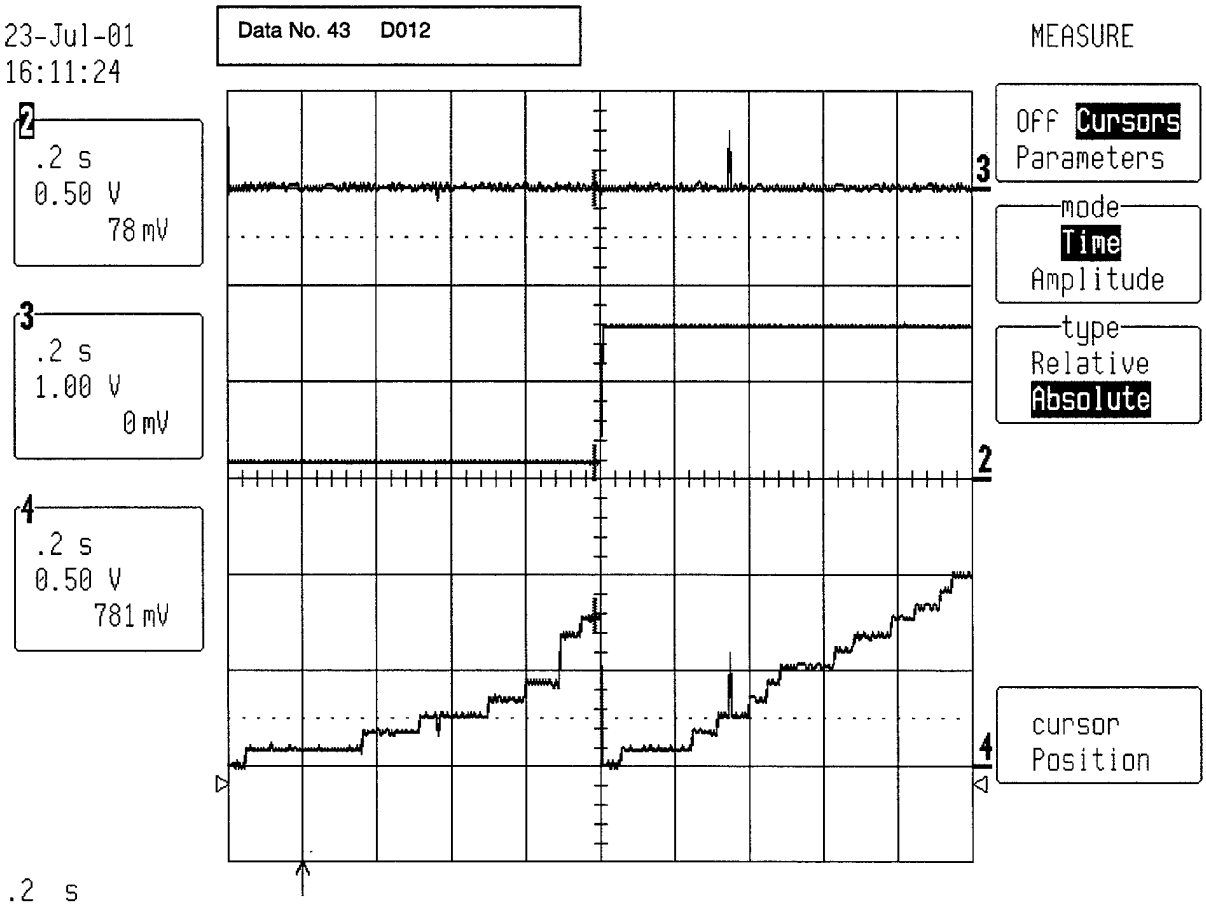

Ch2-Acoustic pulses output of the One second Data Sample and Reset circuit box [9A].
Ch3-To Reset from the One Second Data Sample and Reset circuit box [9A].
Ch4-Acoustic pulses input to the One second Data Sample and Reset circuit box [9A].
The value of the signal on Ch4 at the cursor is 781 mV and that on Ch2 at the cursor is78 mV.
Note: Compare with the next oscilloscope display.

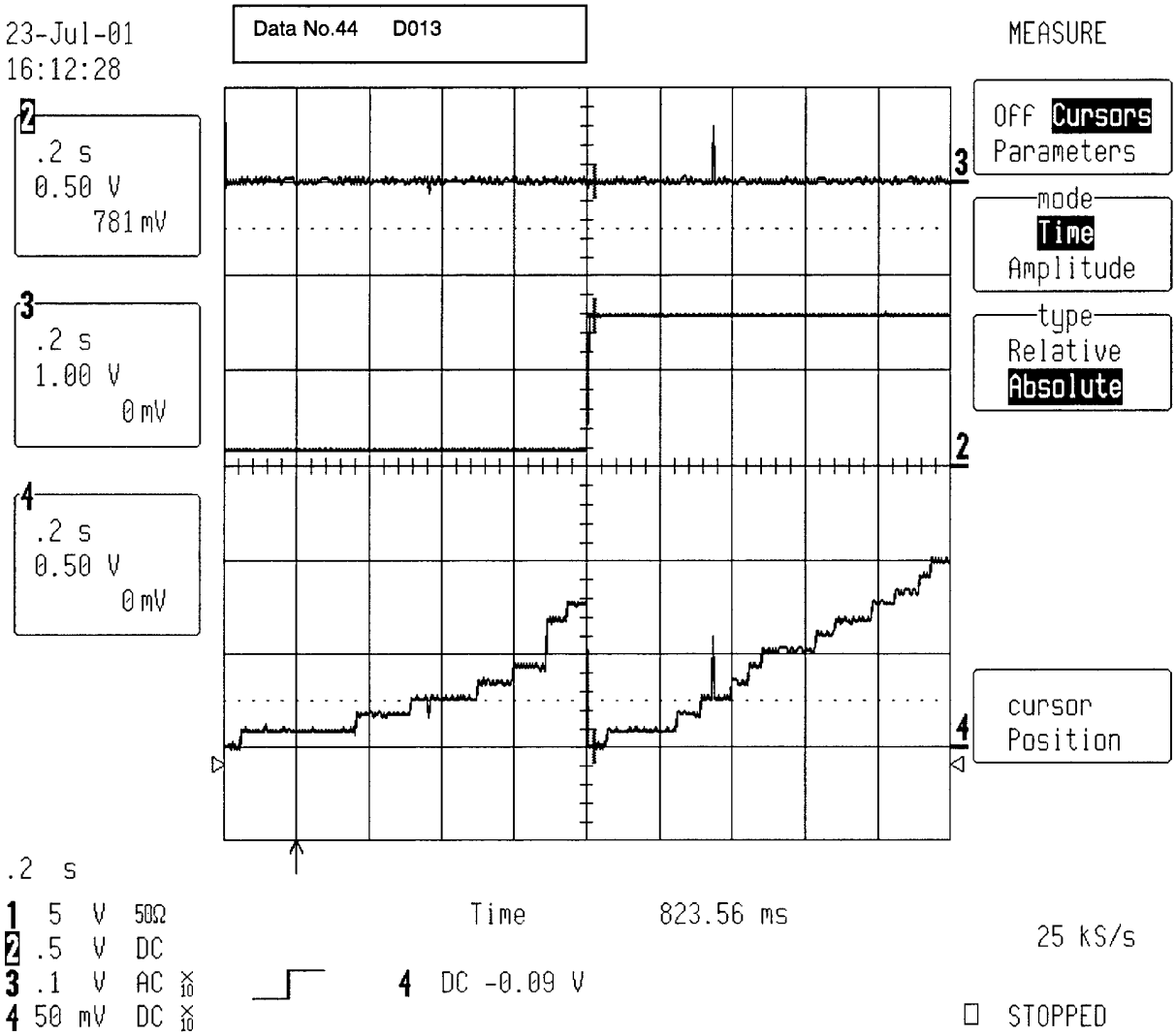

Ch2-Acoustic pulses output of the One second Data Sample and Reset circuit box [9A].
Ch3-To Reset from the One Second Data Sample and Reset circuit box [9A].
Ch4-Acoustic pulses input to the One second Data Sample and Reset circuit box [9A].
The value of the signal on Ch4 at the cursor is now changed to 0 mV and that on Ch2 at the cursor changed to 781 mV after data transfer.
Note: Compare with the previous oscilloscope. ..display.

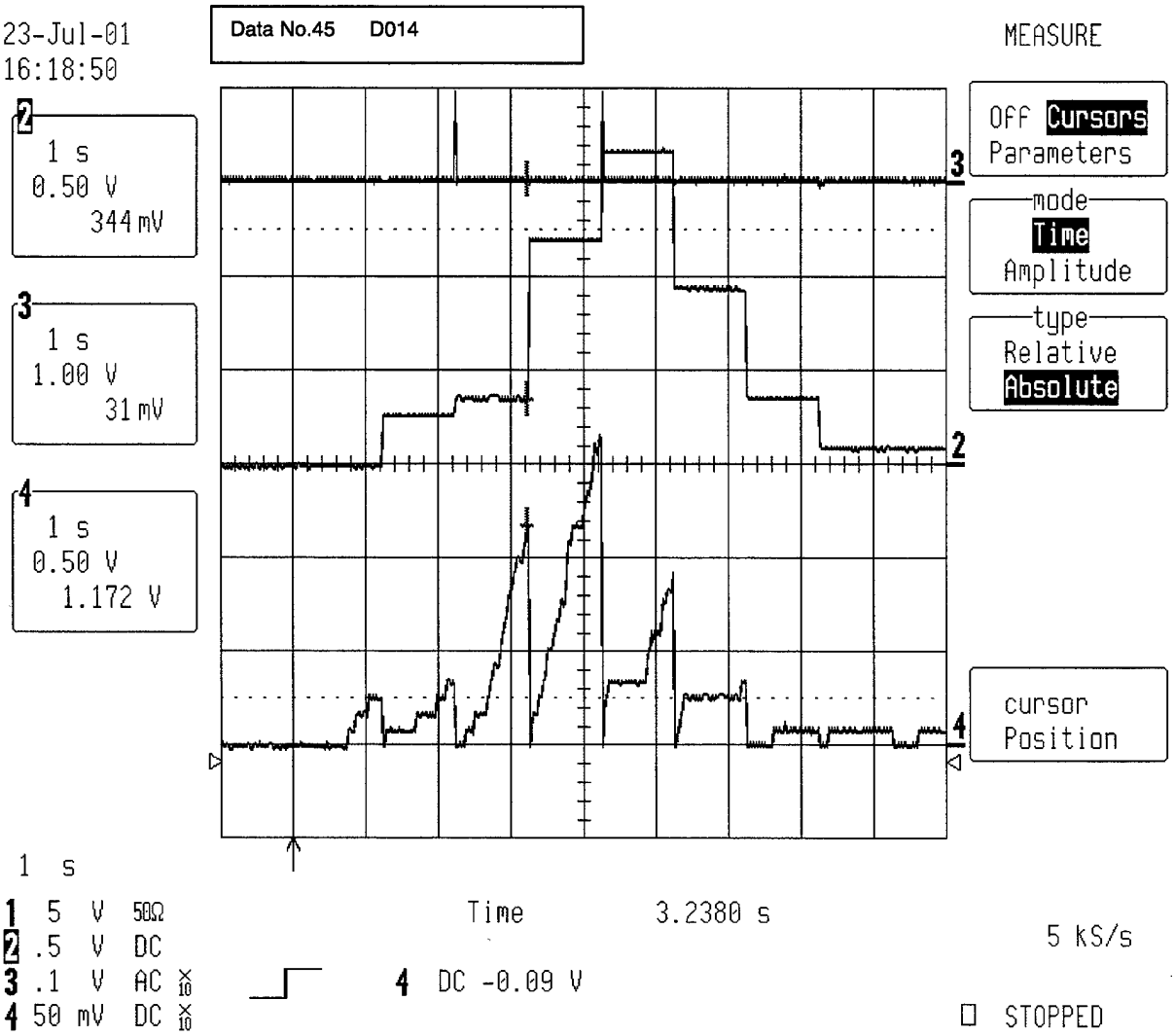

Ch2-Acoustic pulses output of the One second Data Sample and Reset circuit box [9A].
Ch3-To Reset from the One Second Data Sample and Reset circuit box [9A].
Ch4-Acoustic pulses input to the One second Data Sample and Reset circuit box [9A].
The value of the signal on Ch4 at the cursor is 1.172 V and that on Ch2 at the cursor is 344 mV.
Note: Compare with the next oscilloscope display.

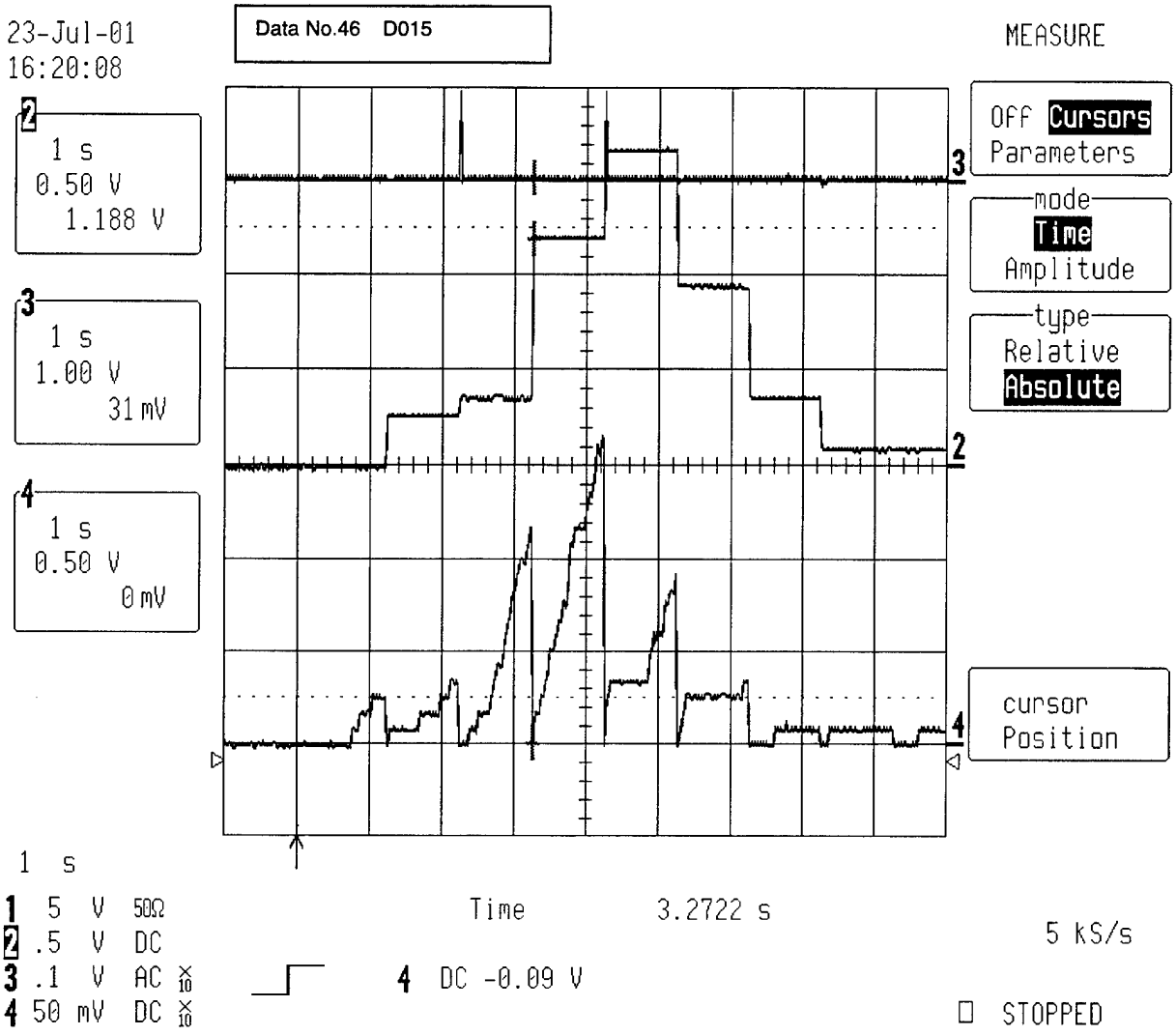

Ch2-Acoustic pulses output of the One second Data Sample and Reset circuit box [9A].
Ch3-To Reset from the One Second Data Sample and Reset circuit box [9A].
Ch4-Acoustic pulses input to the One second Data Sample and Reset circuit box [9A].
The value of the signal on Ch4 at the cursor is now changed to 0 mV and that on Ch2 at the cursor changed to 1.118 V after data transfer.
Note: Compare with the previous oscilloscope.

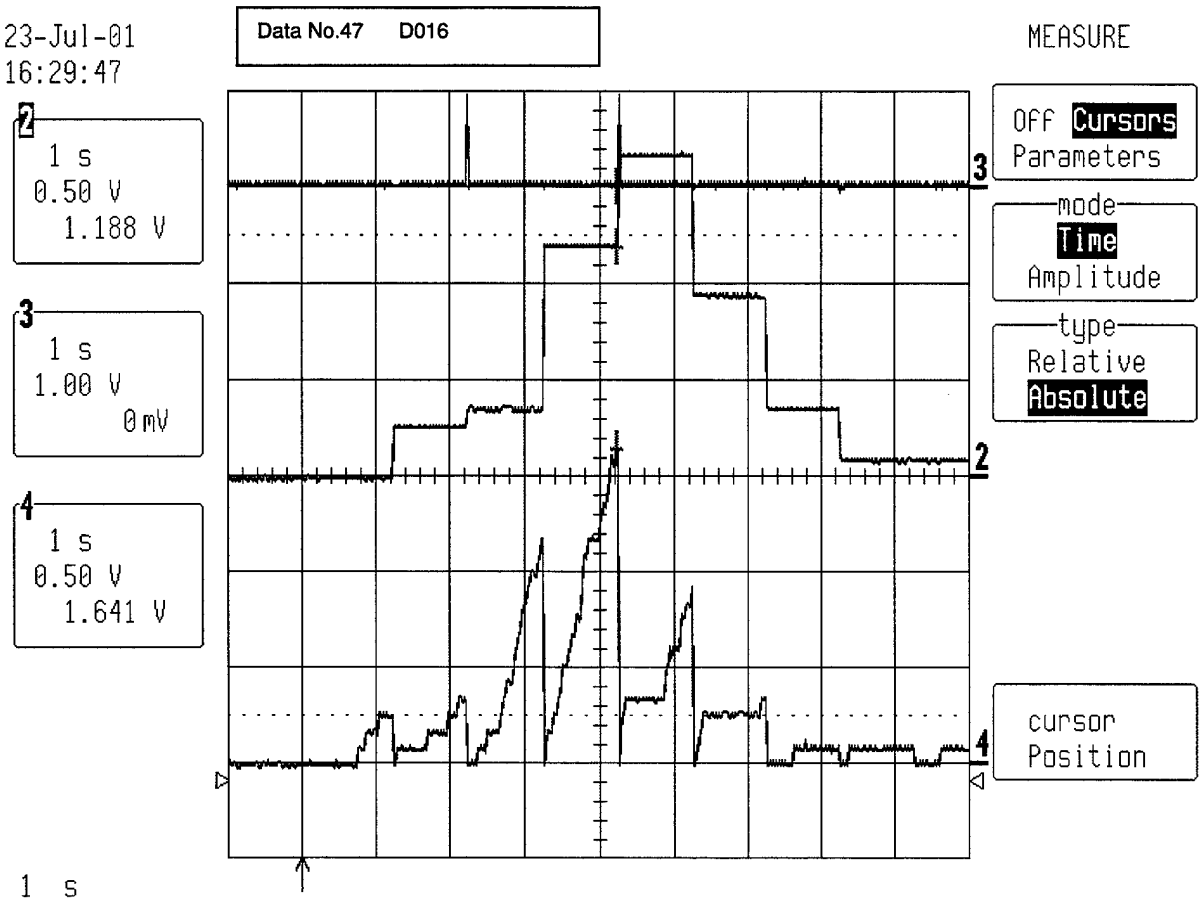

Ch2-Acoustic pulses output of the One second Data Sample and Reset circuit box [9A].
Ch3-To Reset from the One Second Data Sample and Reset circuit box [9A].
Ch4-Acoustic pulses input to the One second Data Sample and Reset circuit box [9A].
The value of the signal on Ch4 at the cursor is 1.641V and that on Ch2 at the cursor is 1.188 V.
Note: Compare with the next oscilloscope display.

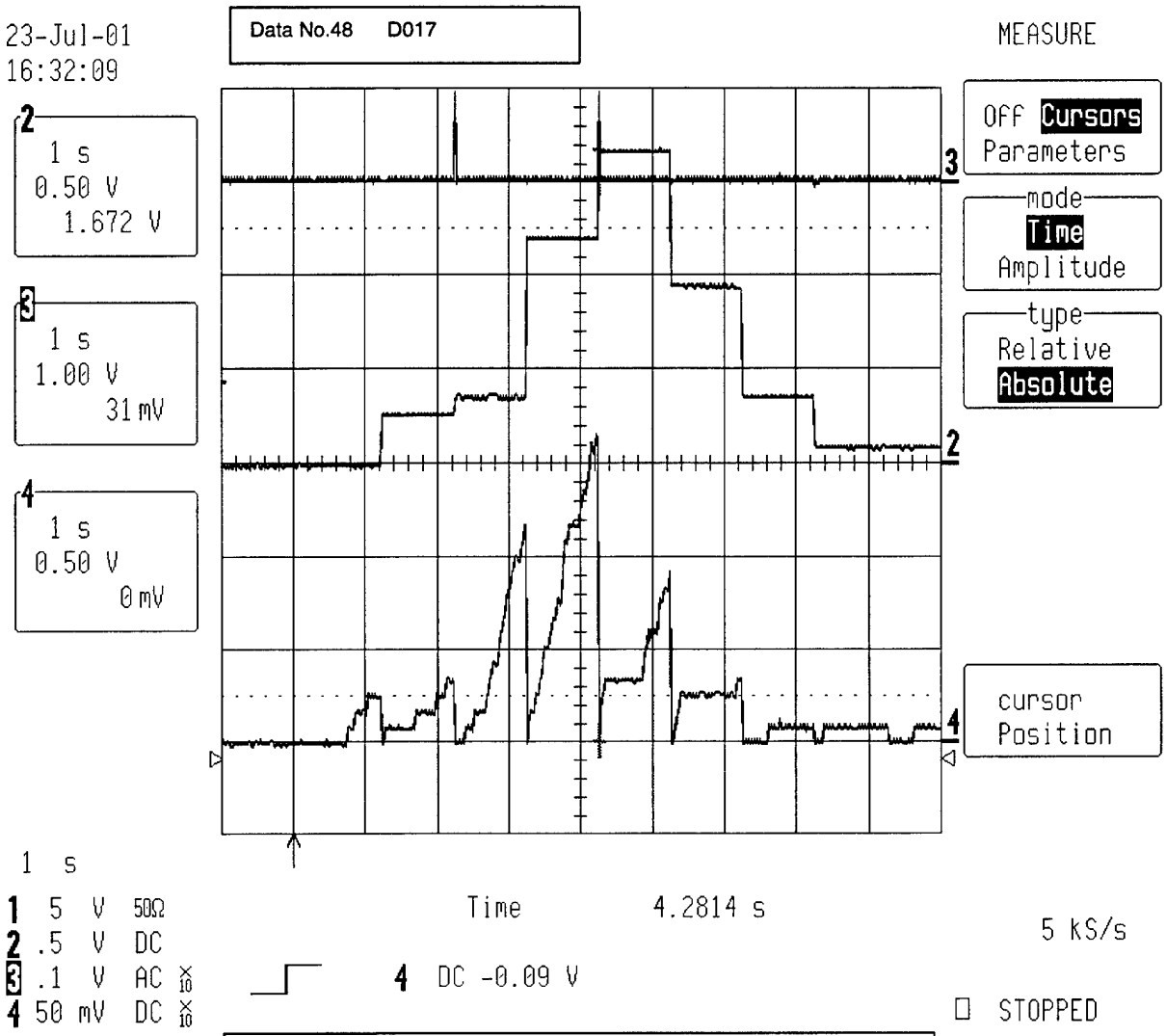

Ch2-Acoustic pulses output of the One second Data Sample and Reset circuit box [9A].
Ch3-To Reset from the One Second Data Sample and Reset circuit box [9A].
Ch4-Acoustic pulses input to the One second Data Sample and Reset circuit box [9A].
The value of the signal on Ch4 at the cursor is now changed to 0 mV and that on Ch2 at the cursor changed to 1.672 V after data transfer.
Note: Compare with the previous oscilloscope display.

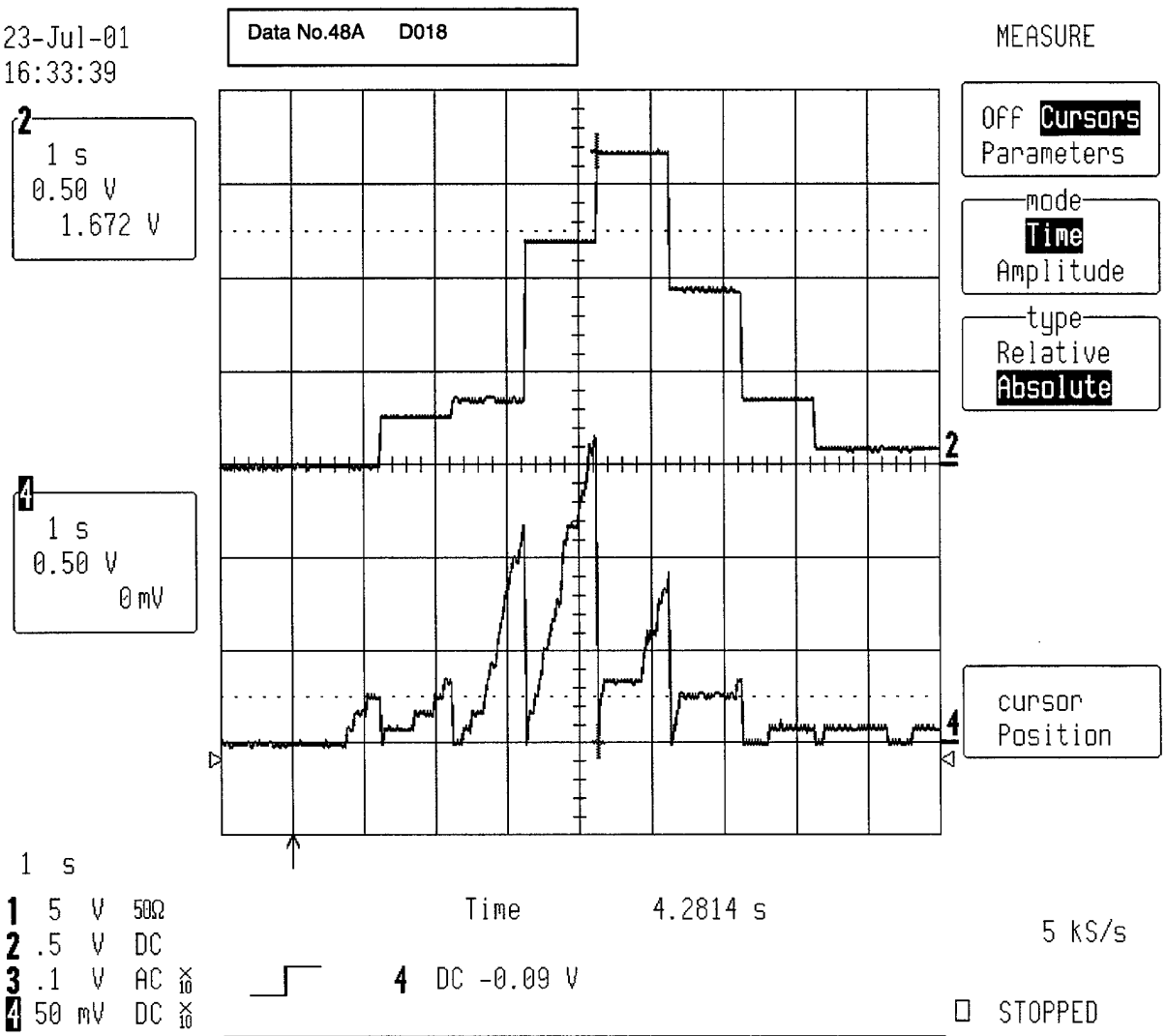

Ch2-Acoustic pulses output of the One second Data Sample and Reset circuit box [9A].
Ch3-This channel is turned off.
Ch4-Acoustic pulses input to the One second Data Sample and Reset circuit box [9A].
The value of the signal on Ch4 at the cursor is now changed to 0 mV and that on Ch2 at the cursor changed to 1.672 V after data transfer.
Note: This display is the same as Data No.48 (the previous one) except the Ch3 is turned off.

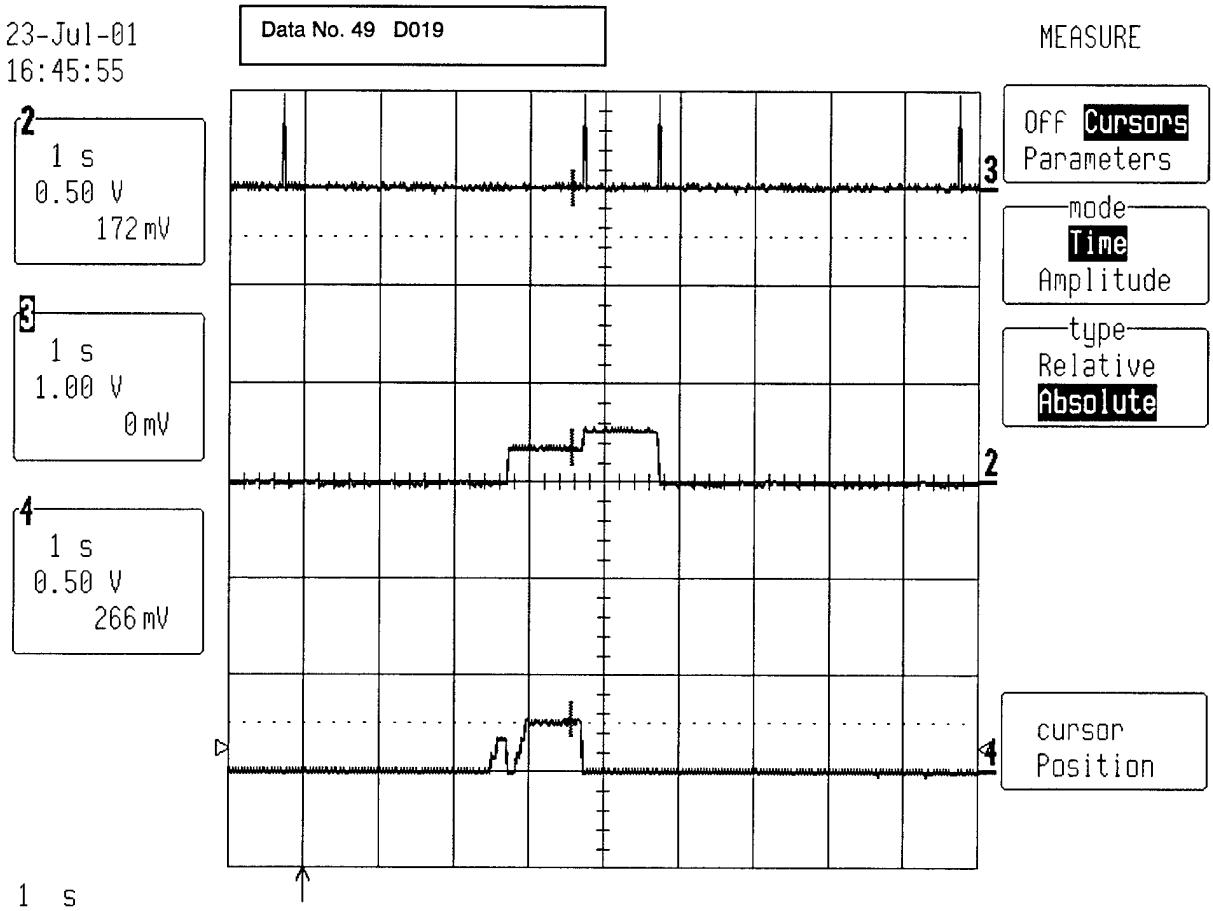

Ch2-Acoustic pulses output of the One second Data Sample and Reset circuit box [9A].
Ch3-To Reset from the One Second Data Sample and Reset circuit box [9A].
Ch4-Acoustic pulses input to the One second Data Sample and Reset circuit box [9A].
Ch3 shows 2 pairs of reset pulses.
The value of the signal on Ch4 at the cursor is 266 mV and that on Ch2 at the cursor is 172 mV.

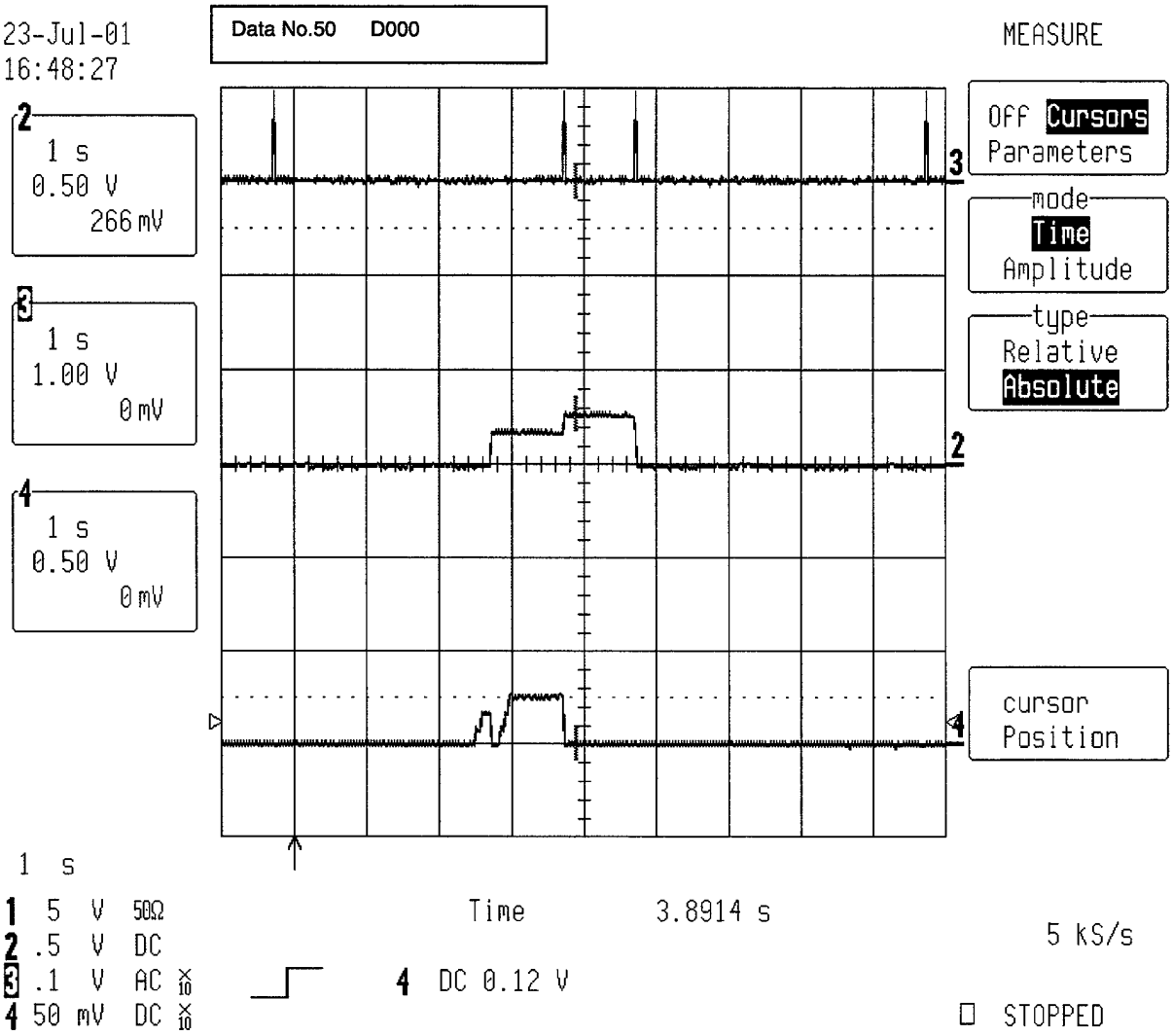

Ch2-Acoustic pulses output of the One second Data Sample and Reset circuit box [9A].
Ch3-To Reset from the One Second Data Sample and Reset circuit box [9A].
Ch4-Acoustic pulses input to the One second Data Sample and Reset circuit box [9A].
Ch3 shows 2 pairs of reset pulses.
The value of the signal on Ch4 at the cursor is now changed to 0 mV and that on Ch2 at the cursor to 266 mV.
Note: Compare with the previous oscilloscope display.

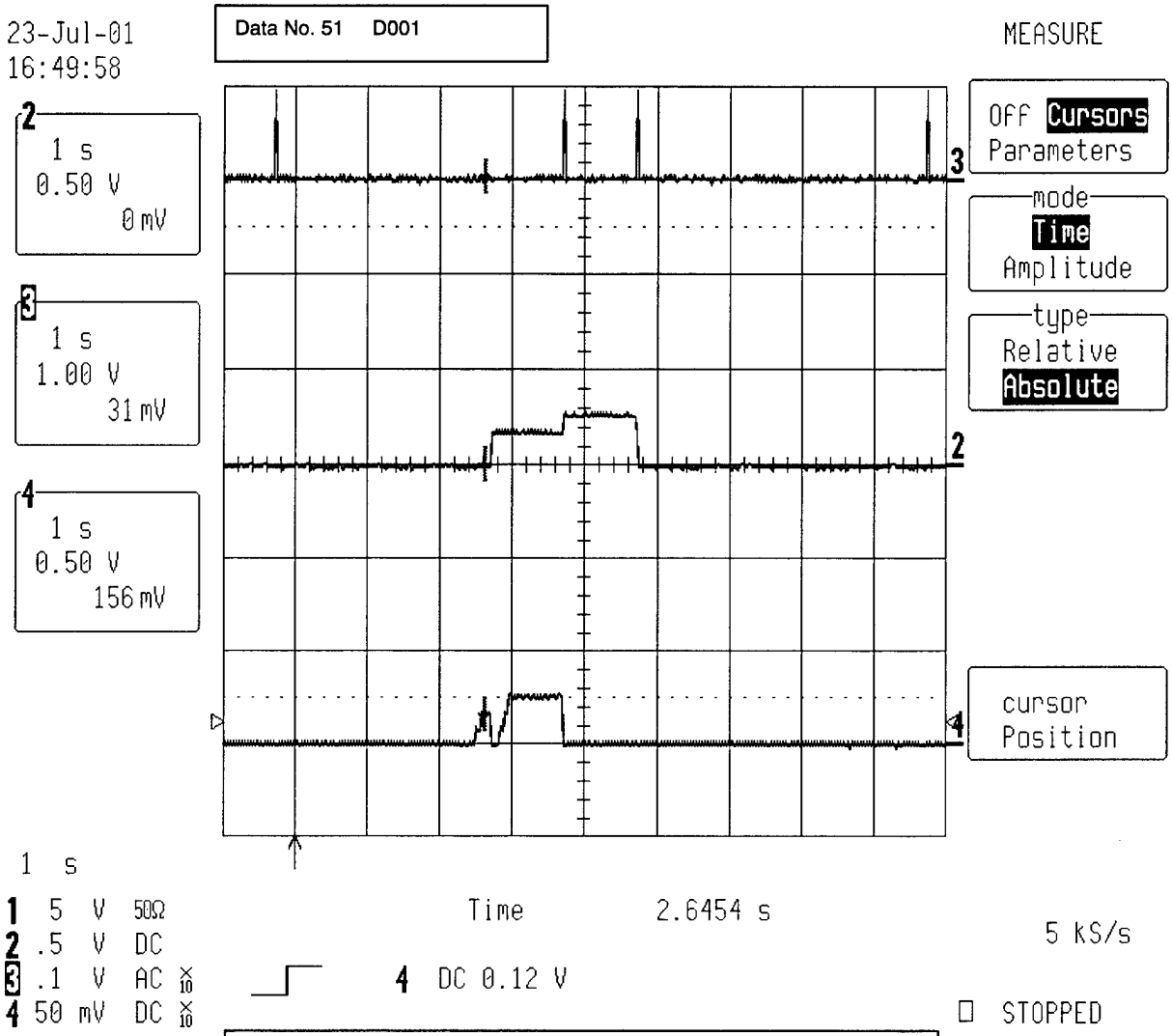

Ch2-Acoustic pulses output of the One second Data Sample and Reset circuit box [9A].
Ch3-To Reset from the One Second Data Sample and Reset circuit box [9A].
Ch4-Acoustic pulses input to the One second Data Sample and Reset circuit box [9A]. Ch3 shows 2 pairs of reset pulses.
The value of the signal on Ch4 at the cursor is 156 mV and that on Ch2 at the cursor is 0 mV.
Note: Compare with the next oscilloscope display.

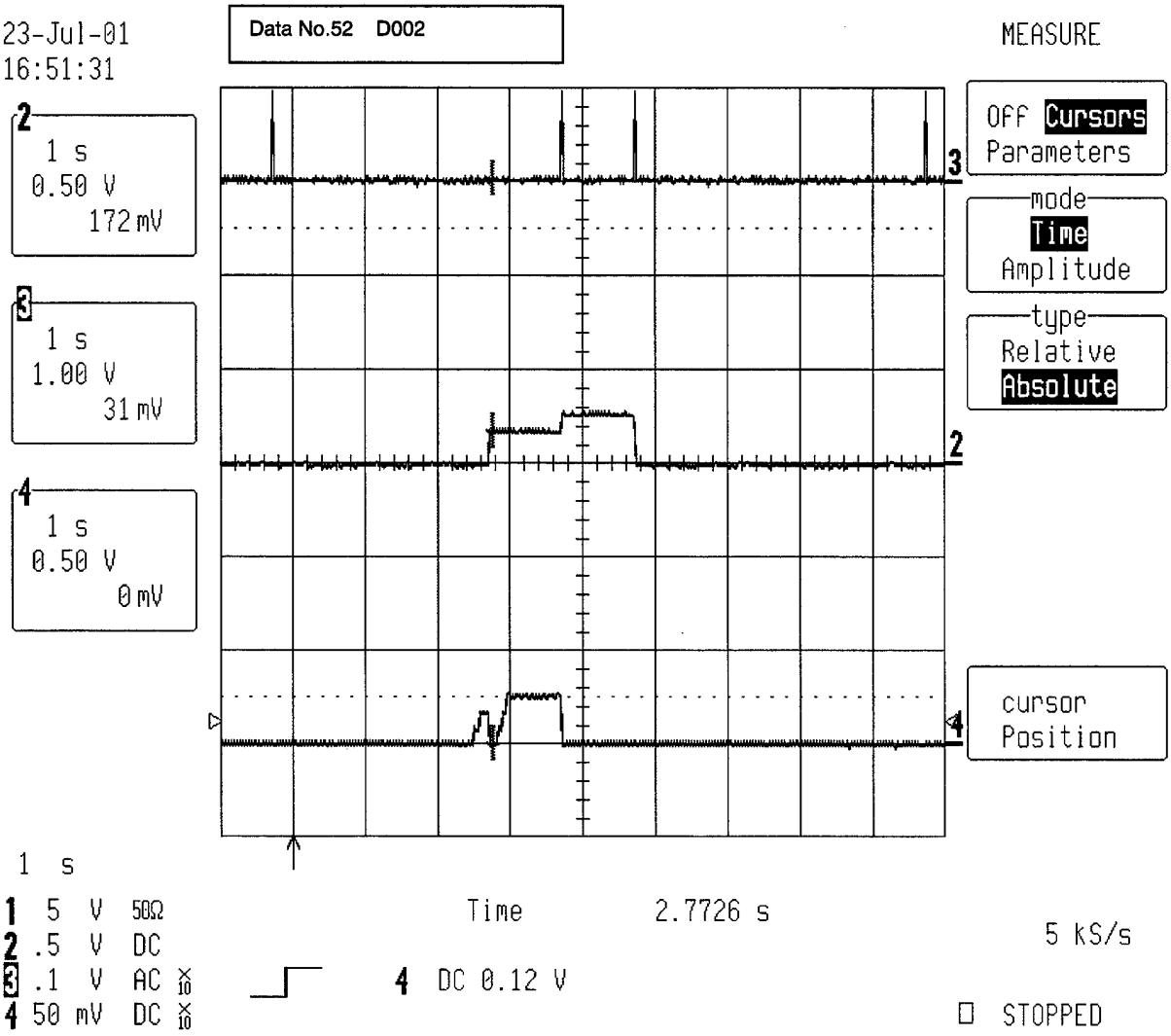

Ch2-Acoustic pulses output of the One second Data Sample and Reset circuit box [9A].
Ch3-To Reset from the One Second Data Sample and Reset circuit box [9A].
Ch4-Acoustic pulses input to the One second Data Sample and Reset circuit box [9A]. Ch3 shows 2 pairs of reset pulses.
The value of the signal on Ch4 at the cursor is now changed to 0 mV and that on Ch2 at the cursor to 172 mV after data transfer.
Note: Compare with the previous oscilloscope display.

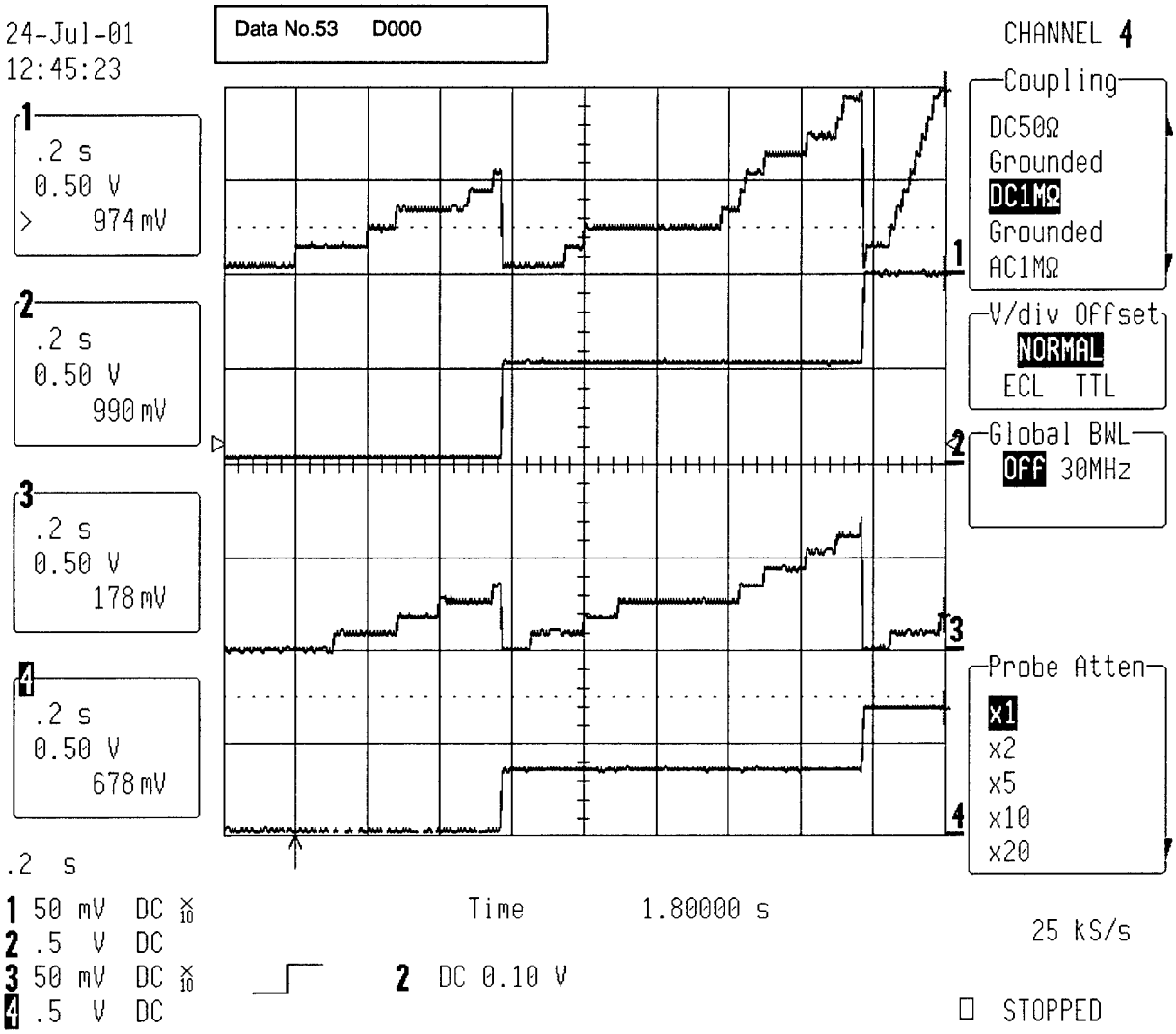

Ch1-Input (current pulses related) to the One second Data Sample and Reset circuit box [9A].
Ch2-Output (current pulses related) from the One second Data Sample and Reset circuit box [9A].
Ch3-Input (acoustic pulses related) to the One second Data Sample and Reset circuit box [9A].
Ch4- Output (acoustic pulses related) from the One second Data Sample and Reset circuit box [9A].
Note: The circuit box [9A] is the last box in the chain. The two output counts related to the defective current and corresponding acoustic pulses in terms of DC voltages in the range 0 to 10 volts are fed into OPTO22 Analog Input Module[10]. Hence the circuit box [9A] is also called OPTO22 Interface box.

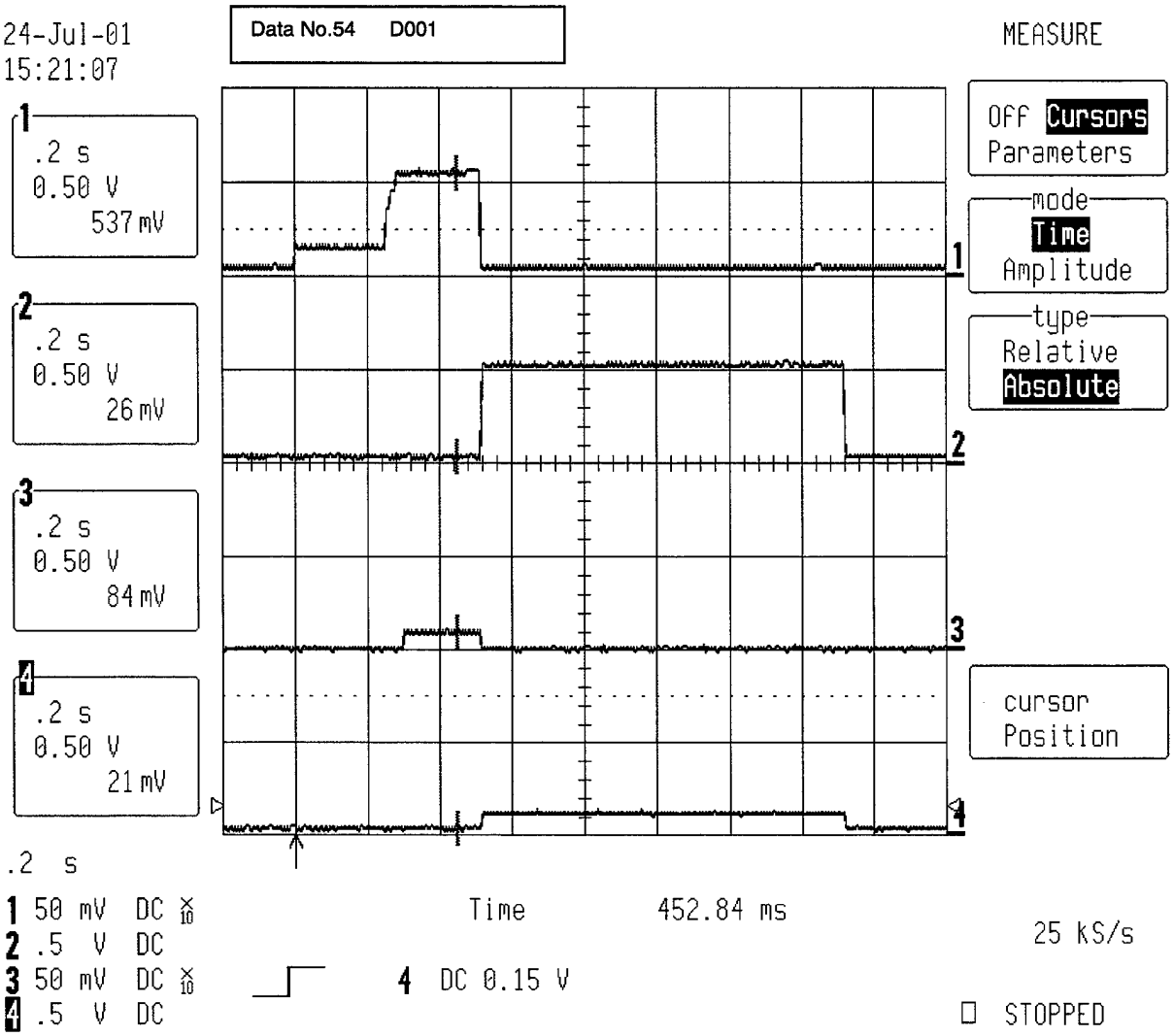

Ch1-Input (current pulses related) to the One second Data Sample and Reset circuit box [9A].
Ch2-Output (current pulses related) from the One second Data Sample and Reset circuit box [9A].
Ch3-Input (acoustic pulses related) to the One second Data Sample and Reset circuit box [9A].
Ch4- Output (acoustic pulses related) from the One second Data Sample and Reset circuit box [9A].
---Voltages corresponding to the cursor positions—
Ch1-537 mV
Ch2-26 mV
Ch3-84 mV
Ch4-21 mV
Note: Compare with the next display.

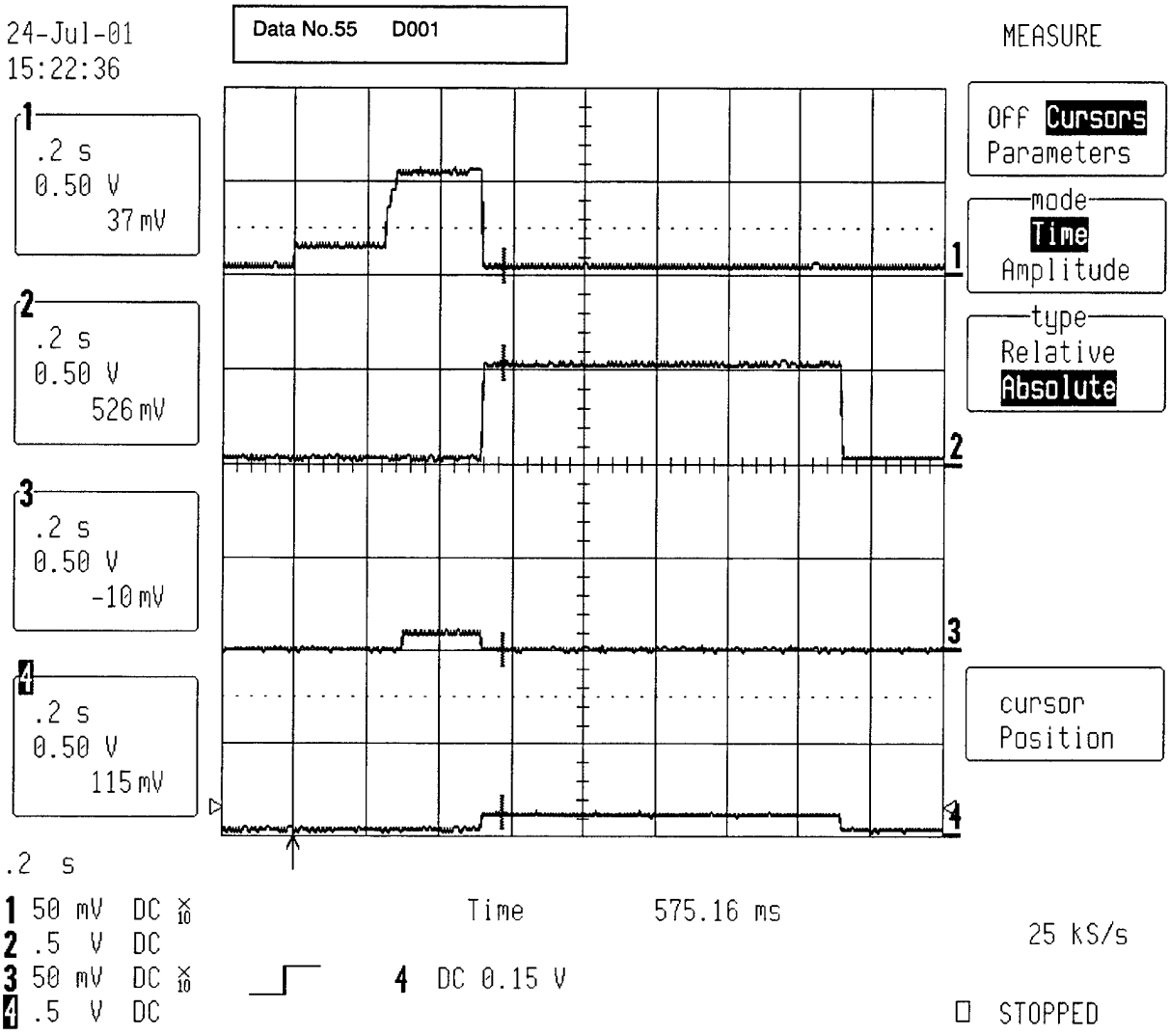
24-Jul-01
15:22:36
Data No.55 D001
MEASURE
1
.2 s
0.50 V
37 mV
2
.2 s
0.50 V
526 mV
3
.2 s
0.50 V
-10 mV
4
.2 s
0.50 V
115 mV
Off Cursors
Parameters
mode
Time
Amplitude
type
Relative
Absolute
cursor
Position
.2 s
1 50 mV DC
2 .5 V DC
3 50 mV DC
4 .5 V DC
Time 575.16 ms
4 DC 0.15 V
25 kS/s
STOPPED

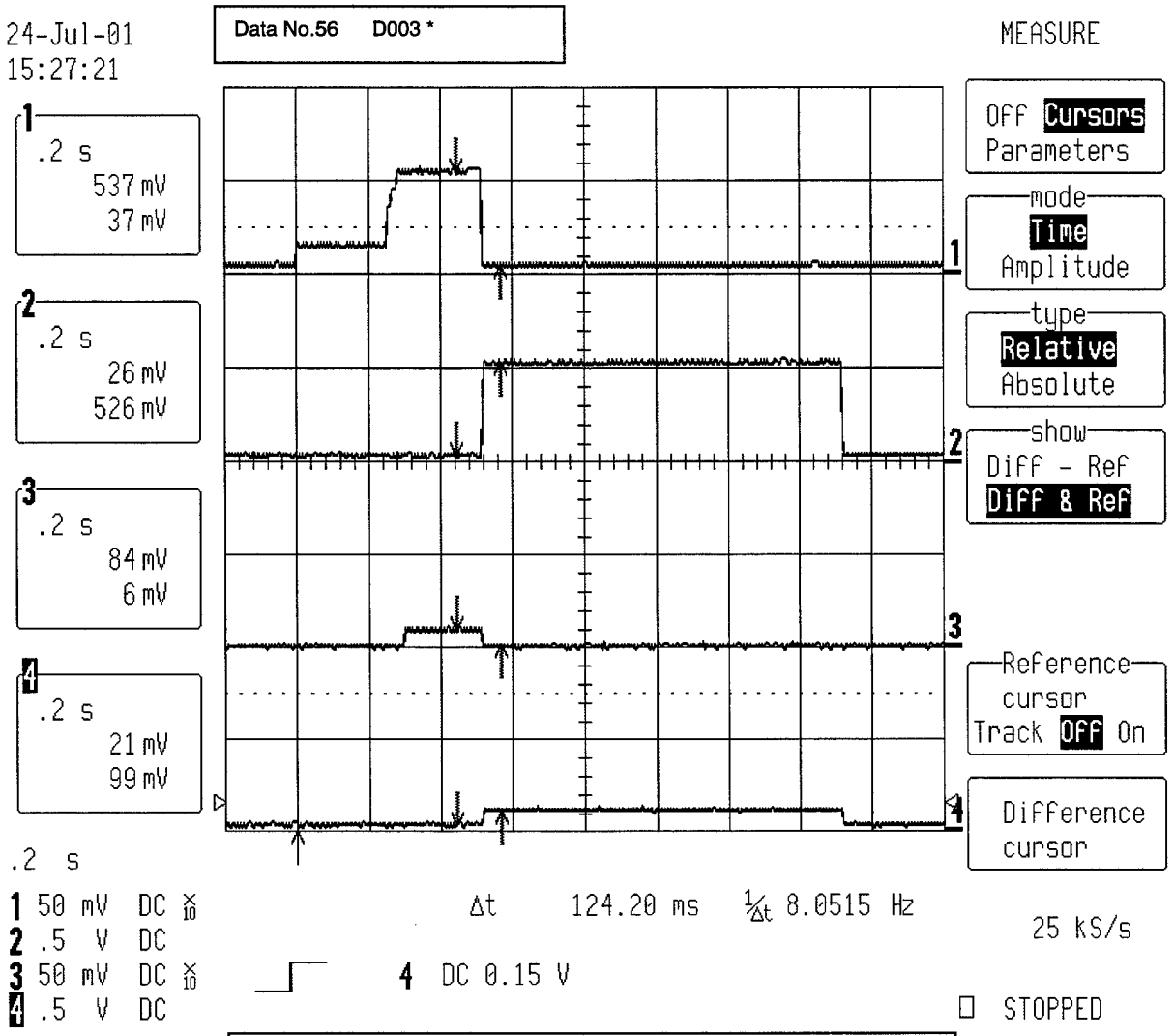

Ch1-Input (current pulses related) to the One second Data Sample and Reset circuit box [9A].
Ch2-Output (current pulses related) from the One second Data Sample and Reset circuit box [9A].
Ch3-Input (acoustic pulses related) to the One second Data Sample and Reset circuit box [9A].
Ch4- Output (acoustic pulses related) from the One second Data Sample and Reset circuit box [9A].
Note: This is a special display where both cursors (before and after data transfer)on each channel are shown.
---Voltages corresponding to the cursor positions—

	Before transfer	After Transfer
Ch1	537 mV	37 mV
Ch2	26 mV	526 mV
Ch3	84 mV	6 mV
Ch4	21 mV	99 mV

Note: Compare with the next display.

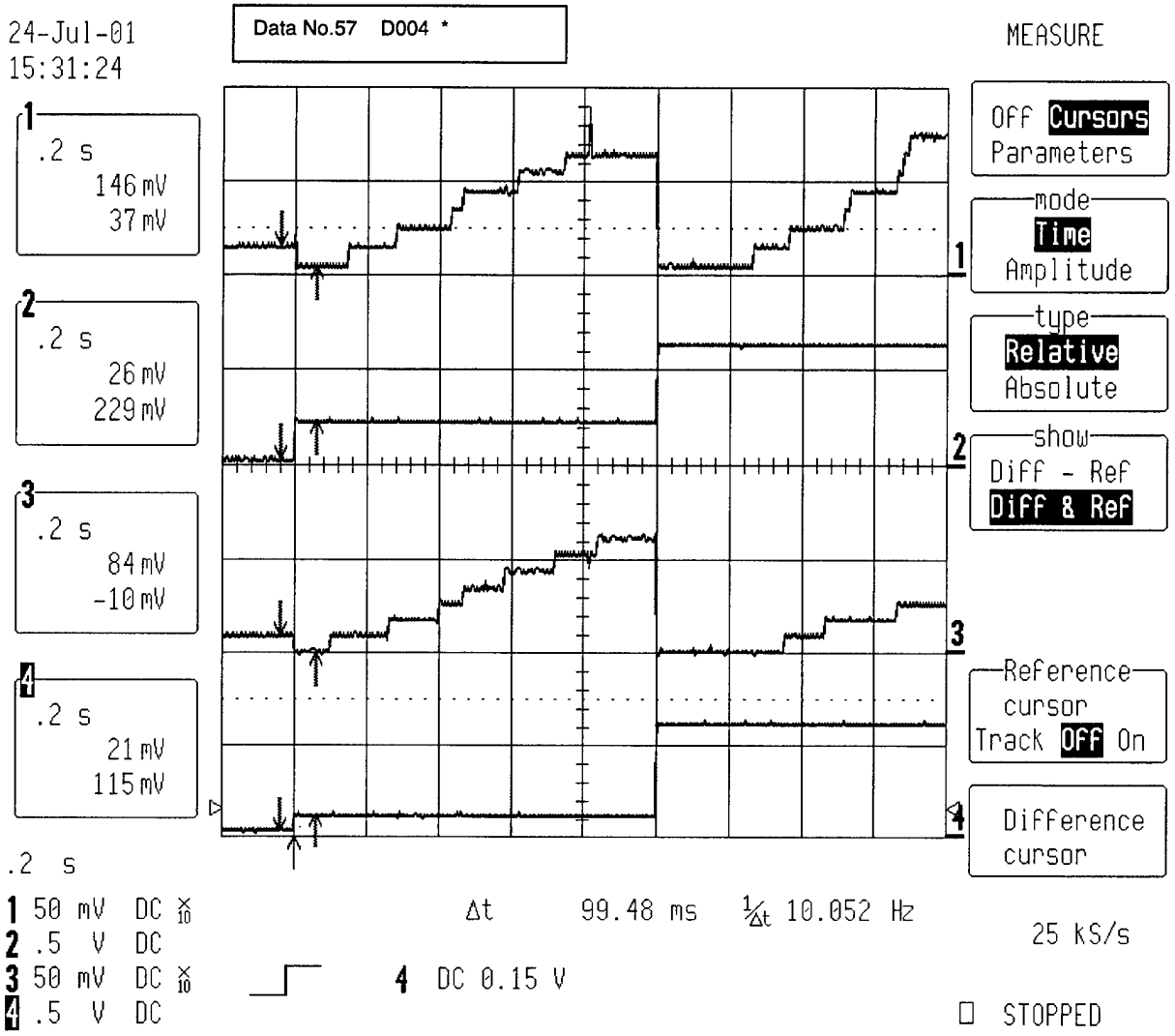

Ch1-Input (current pulses related) to the One second Data Sample and Reset circuit box [9A].
Ch2-Output (current pulses related) from the One second Data Sample and Reset circuit box [9A].
Ch3-Input (acoustic pulses related) to the One second Data Sample and Reset circuit box [9A].
Ch4- Output (acoustic pulses related) from the One second Data Sample and Reset circuit box [9A].
Note: Cursors are moved to the right to execute the first data transfer.
---Voltages corresponding to the cursor positions---

Before transfer	After Transfer
Ch1-146 mV	37 mV
Ch2-26 mV	229 mV
Ch3-84 mV	10 mV
Ch4-21 mV	115 mV

Note: Compare with the previous and next displays.

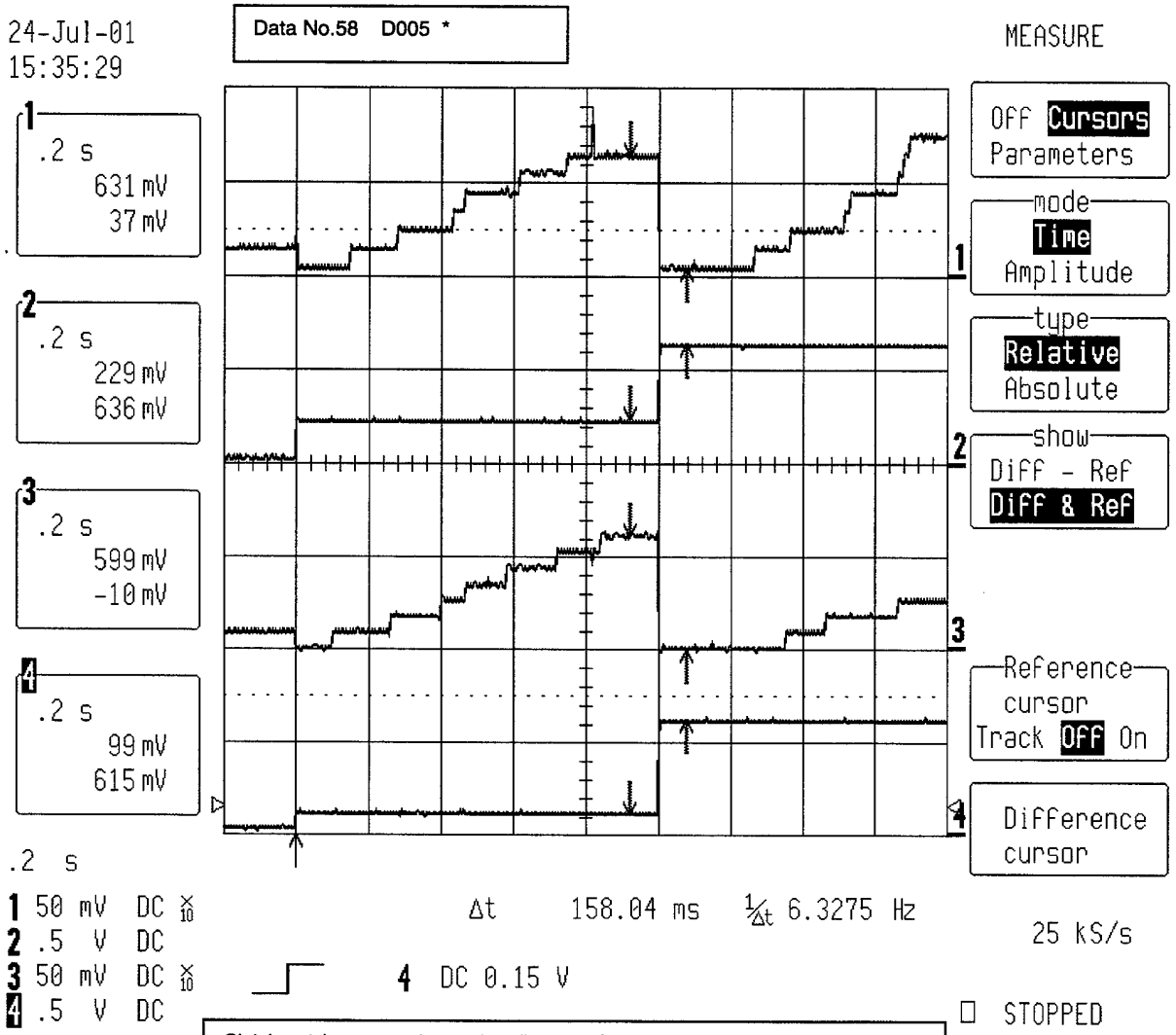

Ch1-Input (current pulses related) to the One second Data Sample and Reset
circuit box [9A].
Ch2-Output (current pulses related) from the One second Data Sample and Reset circuit box [9A].
Ch3-Input (acoustic pulses related) to the One second Data Sample and Reset circuit box [9A].
Ch4- Output (acoustic pulses related) from the One second Data Sample and Reset circuit box [9A].
Note: Cursors are moved again to the right to execute the second data transfer.
---Voltages corresponding to the cursor positions—

	Before transfer	After Transfer
Ch1	631mV	37 mV
Ch2	229 mV	636 mV
Ch3	599 mV	10 mV
Ch4	99mV	615mV

Note: Compare with the two previous displays.

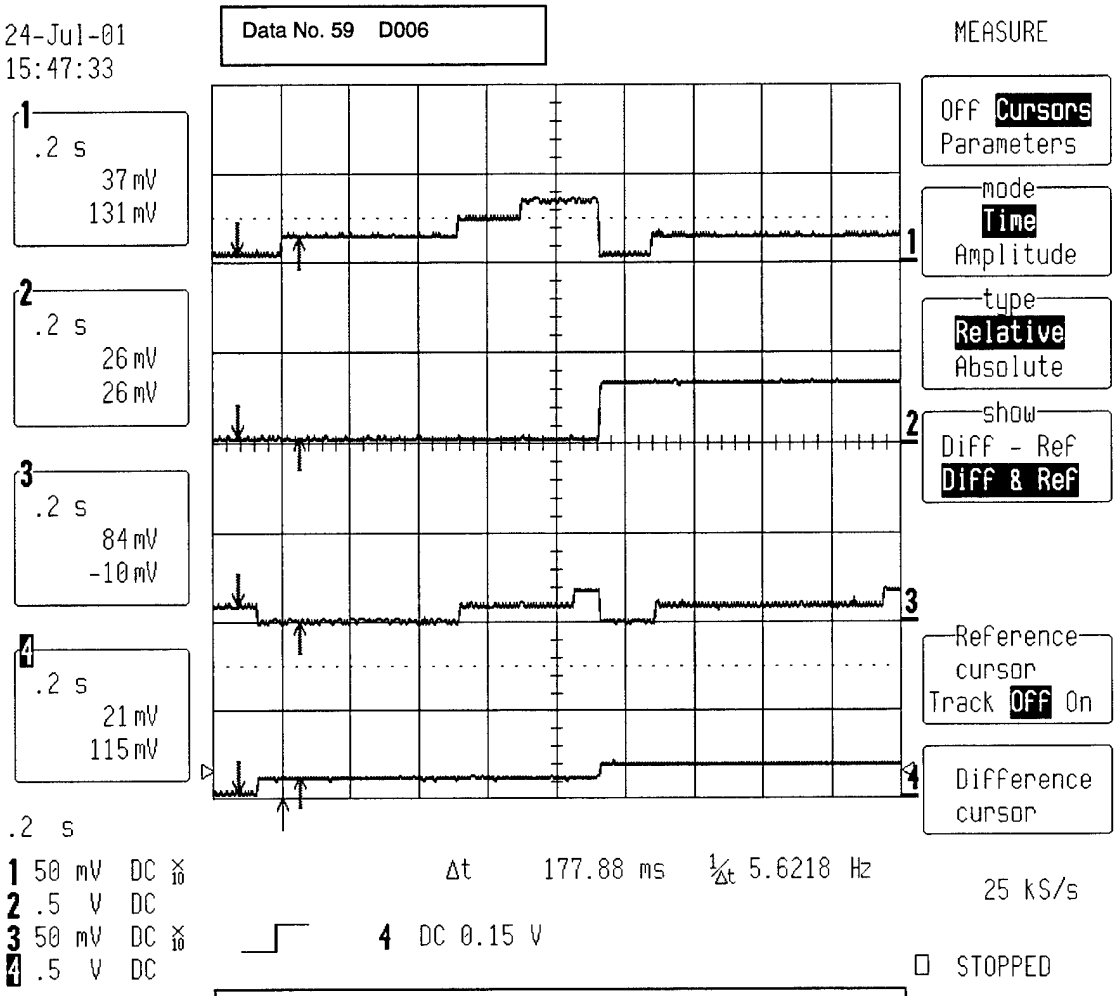

Ch1-Input (current pulses related) to the One second Data Sample and Reset circuit box [9A].
Ch2-Output (current pulses related) from the One second Data Sample and Reset circuit box [9A].
Ch3-Input (acoustic pulses related) to the One second Data Sample and Reset circuit box [9A].
Ch4- Output (acoustic pulses related) from the One second Data Sample and Reset circuit box [9A].
Note: This is a special display where both cursors (before and after data transfer)on each channel are shown.
---Voltages corresponding to the cursor positions—

	Before transfer	After Transfer
Ch1-	37 mV	131 mV
Ch2-	26 mV	26 mV
Ch3-	84 mV	10 mV
Ch4-	21 mV	115 mV

Note: Compare with the next display.

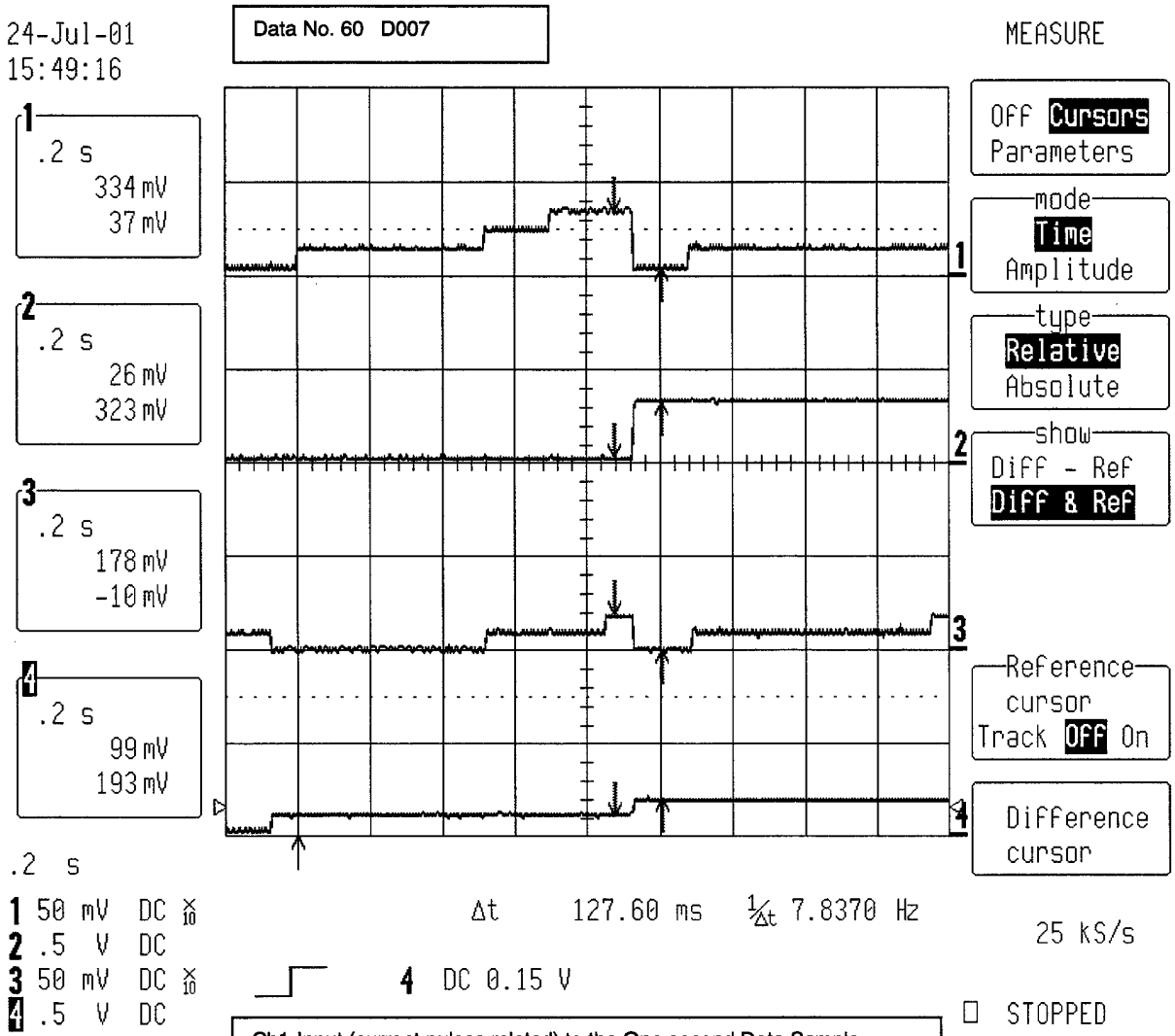

Ch1-Input (current pulses related) to the One second Data Sample and Reset circuit box [9A].
Ch2-Output (current pulses related) from the One second Data Sample and Reset circuit box [9A].
Ch3-Input (acoustic pulses related) to the One second Data Sample and Reset circuit box [9A].
Ch4- Output (acoustic pulses related) from the One second Data Sample and Reset circuit box [9A].
Note: Cursors are moved to the right to execute the data transfer.
---Voltages corresponding to the cursor positions—

Before transfer	After Transfer
Ch1-334 mV	37 mV
Ch2-26 mV	323 mV
Ch3-178 mV	10 mV
Ch4-99 mV	193 mV

Note: Compare with the previous displays.

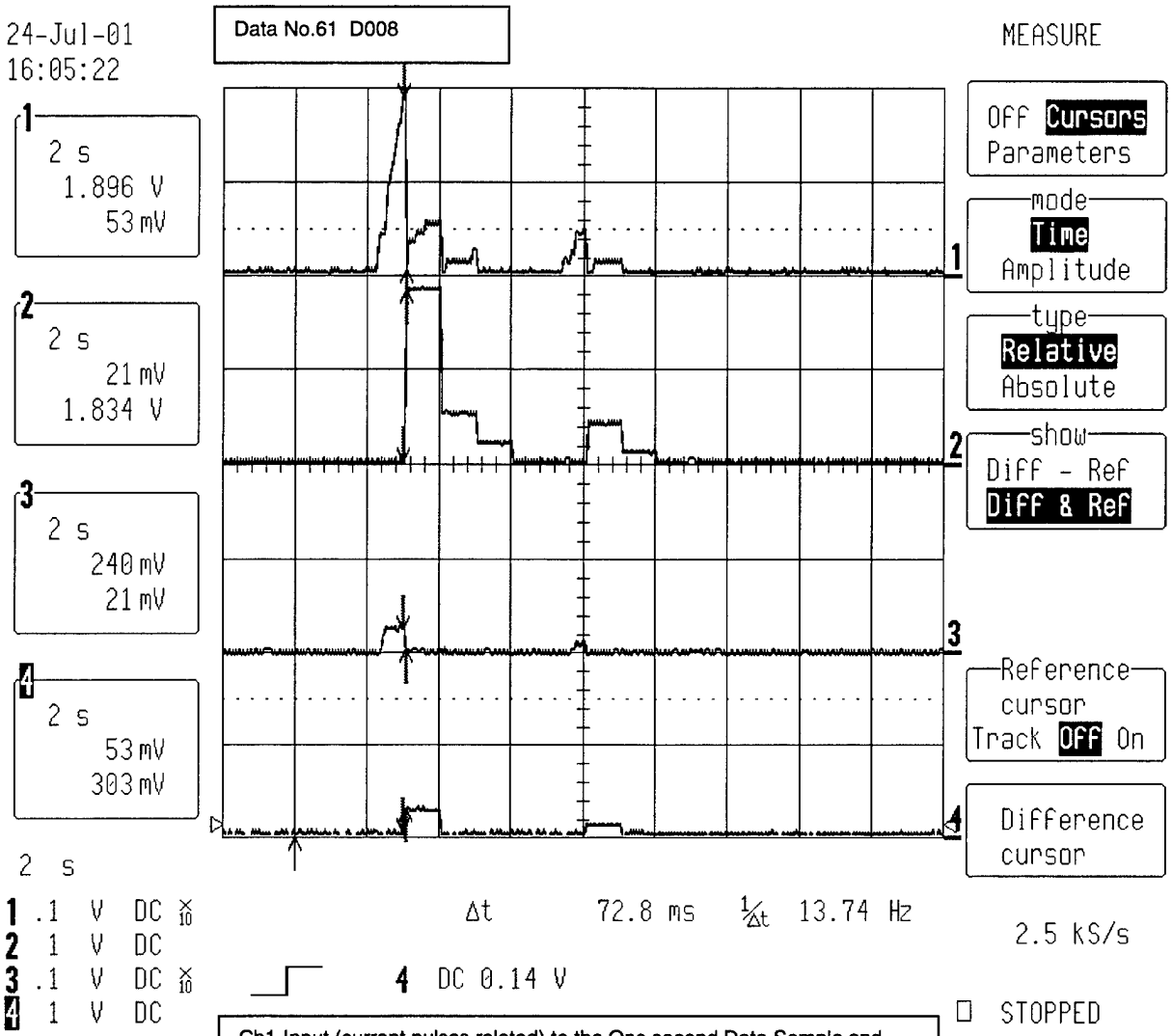

Ch1-Input (current pulses related) to the One second Data Sample and Reset circuit box [9A].
Ch2-Output (current pulses related) from the One second Data Sample and Reset circuit box [9A].
Ch3-Input (acoustic pulses related) to the One second Data Sample and Reset circuit box [9A].
Ch4- Output (acoustic pulses related) from the One second Data Sample and Reset circuit box [9A].
Note: This is a special display where both cursors (before and after data transfer)on each channel are shown.
---Voltages corresponding to the cursor positions—

Before transfer	After Transfer
Ch1-1.896 V	53 mV
Ch2- 21mV	1.834 mV
Ch3-240 mV	21 mV
Ch4- 53 mV	303 mV

Note: Compare with the next display.

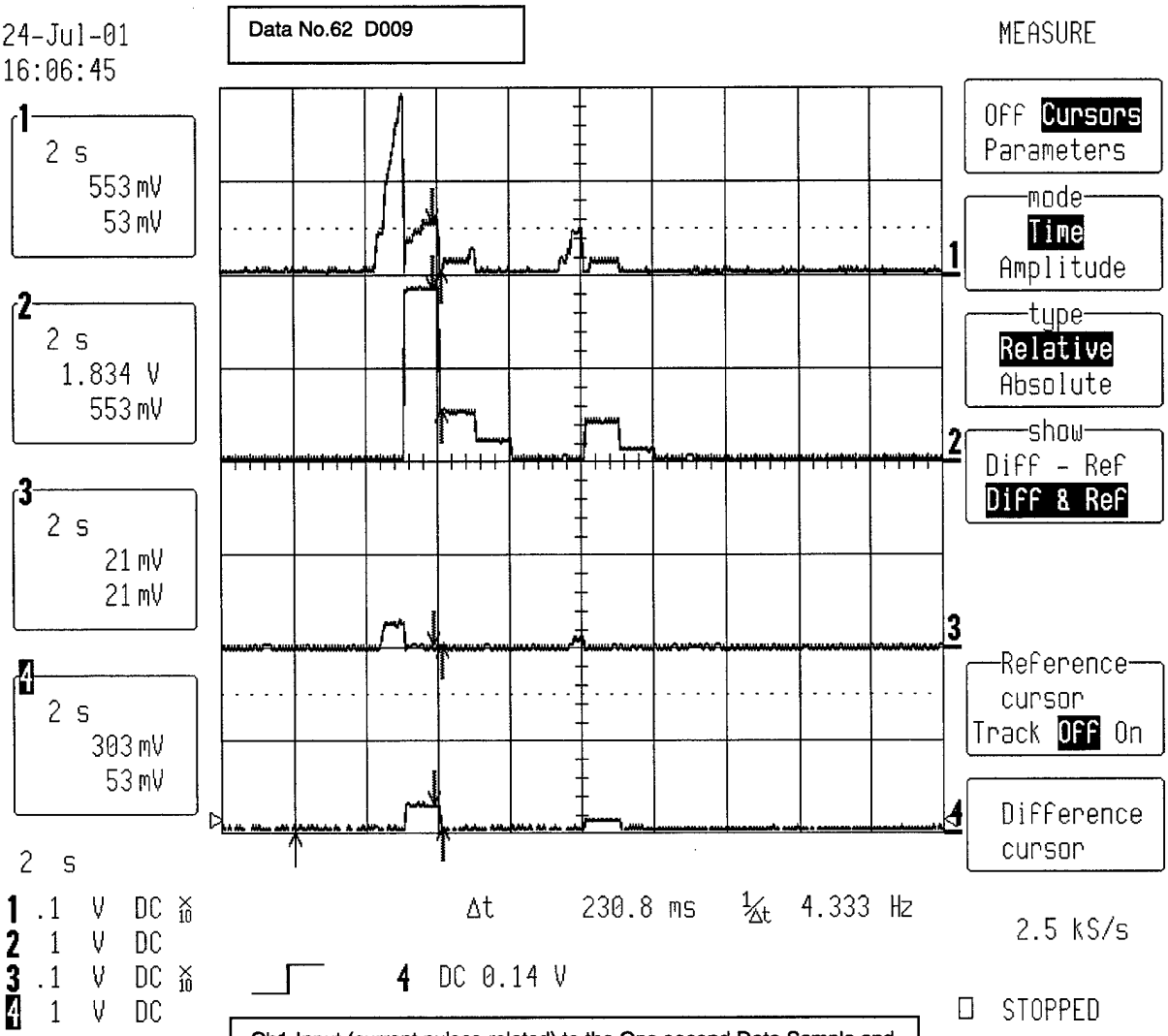

Ch1-Input (current pulses related) to the One second Data Sample and Reset circuit box [9A].
Ch2-Output (current pulses related) from the One second Data Sample and Reset circuit box [9A].
Ch3-Input (acoustic pulses related) to the One second Data Sample and Reset circuit box [9A].
Ch4- Output (acoustic pulses related) from the One second Data Sample and Reset circuit box [9A].
Note: Cursors are moved to the right to execute the data transfer.
---Voltages corresponding to the cursor positions—

Before transfer	After Transfer
Ch1-553 mV	53 mV
Ch2-1.834 mV	553 mV
Ch3-21 mV	21 mV
Ch4-303 mV	53 mV

Note: Compare with the previous display.

REPORT DOCUMENTATION PAGE

Form Approved
OMB No. 0704-01-0188

PLEASE DO NOT RETURN YOUR FORM TO THE ABOVE ADDRESS.

1. REPORT DATE *(DD-MM-YYYY)*	2. REPORT TYPE	3. DATES COVERED *(From - To)*
07–2002	Technical	

4. TITLE AND SUBTITLE

MONITORING OF HIGH-POWER MICROWAVE TUBE SYSTEMS USING THE INTEGRATED CONDITION ASSESSMENT SYSTEM (ICAS)

5a. CONTRACT NUMBER

5b. GRANT NUMBER

5c. PROGRAM ELEMENT NUMBER

6. AUTHORS

N. R. Joshi
North Harris College and
Prairie View A&M University

A. D. Ramirez
D. W. Brock
S. D. Russell
SSC San Diego

5d. PROJECT NUMBER

5e. TASK NUMBER

5f. WORK UNIT NUMBER

7. PERFORMING ORGANIZATION NAME(S) AND ADDRESS(ES)

SSC San Diego
San Diego, CA 92152–5001

8. PERFORMING ORGANIZATION REPORT NUMBER

TR 1885

9. SPONSORING/MONITORING AGENCY NAME(S) AND ADDRESS(ES)

Office of Naval Research
800 North Quincy Street
Arlington, VA 22217–5660

10. SPONSOR/MONITOR'S ACRONYM(S)

ONR

11. SPONSOR/MONITOR'S REPORT NUMBER(S)

12. DISTRIBUTION/AVAILABILITY STATEMENT

Approved for public release; distribution is unlimited.

13. SUPPLEMENTARY NOTES

14. ABSTRACT

In the earlier phases of the Microwave Tube Built-In Test (MTBIT) program (1999–2001), a new advanced nondestructive testing technique was demonstrated using acoustic emission (AE) for in-situ monitoring of normal and abnormal performance of high-power radar tubes such as magnetrons, traveling wave tubes (TWTs), and klystrons. This report details the next step in transitioning the laboratory MTBIT system into a system that is compatible with condition-based maintenance systems employing the Integrated Condition Assessment System (ICAS) used by the Fleet. This report identifies the interface requirements for the sensors and ICAS, as well as accommodating limitations of the ICAS software, which currently is not configured to accommodate the sensor data rates and data sets required. Ten new electronic circuits were designed, built, and tested to interface the outputs of the current sensor and acoustic emission sensor attached to a magnetron through an OPTO22 digital and analog input/output (I/O) hardware along with its Optomux protocol, and the ICAS software (Version 4.11). The complete computerized system to monitor the in-situ performance of the high-power microwave tube was developed, tested, and reported here. The system could be extended to achieve the same goal with other microwave tubes such as TWTs and klystrons with minor modifications.

15. SUBJECT TERMS

Mission Area: Communications
High-power microwave tube
radar
Integrated Condition Assessment System (ICAS)

16. SECURITY CLASSIFICATION OF:			17. LIMITATION OF ABSTRACT	18. NUMBER OF PAGES	19a. NAME OF RESPONSIBLE PERSON
a. REPORT	b. ABSTRACT	c. THIS PAGE			Stephen Russell
U	U	U	UU	130	19B. TELEPHONE NUMBER *(Include area code)* (619) 553–5502

INITIAL DISTRIBUTION

20012	Patent Counsel	(1)
20271	Archive/Stock	(6)
20274	Library	(2)
2027	M. E. Cathcart	(1)
20271	E. R. Ratliff	(1)
20271	D. Richter	(1)
273K	D. W. Brock	(5)
2853	A. D. Ramirez	(5)
2853	S. D. Russell	(10)

Defense Technical Information Center
Fort Belvoir, VA 22060–6218 (4)

SSC San Diego Liaison Office
C/O PEO-SCS
Arlington, VA 22202–4804

Center for Naval Analyses
Alexandria, VA 22311–1850

Office of Naval Research
ATTN: NARDIC (Code 362)
Arlington, VA 22217–5660

Government-Industry Data Exchange
Program Operations Center
Corona, CA 91718–8000

Office of Naval Research
ATTN: Code 332
Arlington, VA 22217-5660

Dr. Narayan Joshi
Beaumont, TX 77706 (10)

Naval Surface Warfare Center
Carderock Division
Philadelphia, PA 19112